Fall 12-15-2017

Defining the Role of Neuropilin-2 in Macrophages: Implications in Tumor Associated Macrophages in Pancreatic Cancer

Sohini Roy
University of Nebraska Medical Center

DEFINING THE ROLE OF NEUROPILIN-2 IN MACROPHAGES: IMPLICATIONS IN TUMOR ASSOCIATED MACROPHAGES IN PANCREATIC CANCER

by

SOHINI ROY

A DISSERTATION

Presented to the Faculty of the
University of Nebraska Graduate College
in Partial Fulfillment of the Requirements
for the Degree of Doctor of Philosophy

BIOCHEMISTRY AND MOLECULAR BIOLOGY GRADUATE PROGRAM

Under the supervision of Professor **Kaustubh Datta**

University of Nebraska Medical Center
Omaha, Nebraska
November 2017

Supervisory Committee Members:
Surinder K. Batra, PhD.
Rakesh K. Singh, PhD.
Michael A. Hollingsworth, PhD.

Table of Contents

ABSTRACT

DEFINING THE ROLE OF NEUROPILIN-2 IN TUMOR ASSOCIATED MACROPHAGES: IMPLICATIONS IN PANCREATIC CANCER

SOHINI ROY

University of Nebraska Medical Center, 2017

Advisor: Kaustubh Datta, PhD.

Macrophages are extremely heterogeneous and highly plastic hematopoietic cells that reside in all tissues and act as a bridge between the innate and adaptive arms of the immune responses. Besides, they undertake a wide array of housekeeping functions like, clearance of cellular debris that arise due to regular turnover in tissues, iron homeostasis, immune surveillance as well as tissue repair processes post inflammation. They are also causally associated with several clinical conditions, including cancer where the infiltration of macrophages contribute to disease progression, metastasis and therapy resistance, and thereby poor clinical outcome.

Neuropilins (NRPs) are non-tyrosine kinase cell surface glycoproteins expressed in all vertebrates and widely conserved across species. The two isoforms, NRP1 and NRP2 are mainly known for their role as co-receptors for class III Semaphorins and for members of the vascular endothelial growth factor (VEGF) family of molecules. Both NRP1 and NRP2 are overexpressed in many cancers, exert pleiotropic effects in various aspects of cancer pathobiology and correlate with the stage and grade of the disease and poor survival. Intriguingly, additional immunoregulatory roles for NRPs have been reported in myeloid and lymphoid cells, in normal physiological as well as different pathological conditions, including cancer, various immunological disorders, and bone diseases. In comparison to NRP1, the overall comprehensive function of NRP2 in macrophages and factors that govern those functions is not well known. Therefore, the enveloping goal of this dissertation is to comprehensively understand the role and function of NRP2 in macrophages and their implication in tumor associated macrophages in solid tumor.

In the first part of the dissertation, we primarily investigated the expression pattern of NRP2 during the differentiation of macrophages under inflammatory (M1) and immunosuppressive (M2) polarizing conditions. We observed although NRP2 is not expressed at a detectable level in monocytes, its expression is upregulated during the differentiation of monocytes precursors to either M1 or M2 type mature macrophages. We identified a novel function of NRP2 in regulating phagocytosis in macrophages by modulating the levels of $Rab5^{+}$ early phagosomes and $Rab7^{+}$ late phagosomes. In NRP2 depleted macrophages clearance of bacteria or yeast components was delayed and these cells exhibited elevated number or early phagosomes and decreased number of late phagosomes.

Since pancreatic cancer (PC) typifies the complex architecture of a tumor stroma and tumor associated macrophages are abundantly present here, the second part of the dissertation is aimed at elucidating the implication of NRP2 regulated phagocytosis in TAMs in this lethal disease. The expression NRP2 in TAMs in human and mouse PC tissues was assessed. Due to nutrient limiting conditions and rapid proliferation of tumor cells in the TME, many of the cancer cells undergo apoptosis. TAMs efferocytose these dying tumor cells, an event that polarizes them further to pro-tumoral type and contribute to relapse and therapy resistance. We observed that in the absence of NRP2, clearance of apoptotic cells was delayed. The implication of this observation in PC progression was tested using a subcutaneous tumor model. Upon depletion of NRP2 in TAMs, tumors were smaller. Of note, NRP2 depletion did not affect TAM recruitment to, or angiogenesis but recruited and activated anti-tumor CD8 cells into the TME. Further, RNA-Seq analysis of CD11b+ TAMs isolated from tumors indicated that many genes associated with either endosomal/phagosomal maturation, recycling and exocytosis, immune modulation and leukocyte recruitment and activation are deregulated following NRP2 depletion. Further, NRP2 depletion downregulated many of the immunosuppressive genes and cytokines in macrophages that may be important for either suppression of T cell response or induce Treg formation. The data further suggested that NRP2 is important for efferocytosis and maintaining TAM-like phenotype in intratumoral macrophages, thus helping to create a tumorigenic immunosuppressive environment in the TME.

Taken together, studies in this dissertation document a requirement for NRP2 in macrophage phagocytosis. Further, regulation of efferocytosis in TAMs by NRP2 have implications in TAM functions and tumor progression. Hence, targeting NRP2 axis in TAMs may help re-engineer the immunosuppressive stroma in the TME and emerge as potential therapy in combination with chemotherapy or other adjuvant therapies.

I dedicate this entire dissertation to my father, Mr. Gour Roy, my father-in-law Mr. Amitava Bhattacharjee, my mother, Mrs. Shelly Roy, my mother-in-law, Mrs. Jharna Bhattacharjee, my husband, Mr. Rahul Bhattacharjee and my closest friend and family, Dr. Arup K. Bag.

Acknowledgement

First and foremost, I want to express my heartfelt gratitude towards my mentor, Dr. Kaustubh Datta, who is one of my greatest inspirations. I cannot thank him enough for keeping faith in me and for believing that I can successfully complete my project. Training under his mentorship and learning to critically analyze and evaluate experiments under his guidance was one of the best things that happened in my scientific career. He also instilled in me the qualities to become a humble and polite human being. I hope all the training and qualities imbibed from him will help me go a long way in my life and I can become a passionate scientist and a fine human being like him.

I would like to extend my gratitude to all my current and former lab members, for being so patient and supportive. I thoroughly enjoyed the scientific discussions that I often had with my lab members, and they helped me hone my scientific aptitude. I consider myself fortunate to be able to spend five years in a lab that felt like my second home. I want to thank Navatha for being a great friend and confidante. We have survived the highs and lows of graduate student life together and it helped make our bond stronger. I would also like to thank the former members of our neighboring lab, Dr. Michael Upchurch and Jana Opavska for being great friends.

I want to specially thank all my supervisory committee members, Dr. Surinder K Batra, Dr. Rakesh Singh and Dr. Michael A. Hollingsworth. I am indebted to them for their precious time, constructive criticisms and positive inputs during my entire graduate studies. They have always motivated me to remain enthusiastic about my work and encouraged my ideas and opinions. It has been a privilege to train

under fine scientific minds as them. I want to specially thank Dr. Singh for teaching us how to perform orthotopic pancreatic surgery in mouse. He was always available for scientific discussions and I learnt a great deal about animal experiments from him. Words are not enough to express my gratitude to Dr. James E. Talmadge. He introduced me to the intricacies of immunology and helped me with all the aspects of my projects. I also want to extend my thanks to my comprehensive examination committee members, Dr. Justin Mott, Dr. Parminder Mehta and Dr. Jixin Dong. They helped me improve my scientific writing skills and thinking. It was a great learning experience for me.

I want to thank my family for their love, constant support and motivation. I want to start by thanking my husband. Mr. Rahul Bhattacharjee, who is also pursuing his PhD, in Kent State University, Ohio. He was always by my side during my professional and personal challenges. He always motivated me by saying that PhD is my dream and I must make it come true, no matter what challenges come our way. All the sacrifices he made, and all the little things he did for me, brought me closer to my goal. I want to thank him for being a part of this journey with me. Words are not enough to express my gratitude to my former lab member and my best friend and family, Dr. Arup K. Bag, for being a rock in my life. He has given unconditional support to me during all the tough times I encountered. He constantly pushed me to bring out the best in me. I want to thank him deeply for training and teaching me scientific skills and how to think critically. I thoroughly enjoyed the numerous though provoking scientific discussions I had with him. I never realized science could be so much fun until I worked with him. He has instilled in me a great

sense of professionalism and other qualities that helped me become a better human being. I want to thank my close friend and sister-in-law, Suranjana Goswami, for her unreserved love and support to me and my family. I want to thank my parents, Mr. Gour Roy and Mrs. Shelly Roy, for their unconditional love and support. This journey would not have been possible without their sacrifice, to provide me higher education, so that I can fulfil my dreams. I sincerely thank them for all the little things they have done for me. I hope I can continue to make them proud. I also want to express my gratitude towards my father-in-law, Mr. Amitava Bhattacharjee, and my mother-in-law, Mrs. Jharna Bhattacharjee, for their constant love and support. They have never failed to be my side in testing times, always infusing in me positive attitude and praying for my well-being. A special thank you to my sister-in-law, Oindrila Bhattacharjee, for being more than a sister and bringing comic relief in our lives. All of them have made unconditional sacrifices to help make my dream come true and see me smile. I thank them with all my heart and soul; they are the reason I could finish my dissertation. I owe them for what I am today and it is only right that I share this credit with everyone who were a part of my journey.

Last, but not the least, I want to thank one of my closest friends here, in Omaha, Dr. Kriti Bahl and her husband, Dr. Suprit Gupta. Kriti and I started our graduate life together, here, at UNMC. She could relate to all the highs and lows I went through and was always there whenever I needed her. I want to deeply thank her for giving me so many warm and fond memories, and that I am going to cherish all

of them forever. This journey would not have been possible without her positive attitude and pep-talks.

List of Figures

Chapter III

Chapter IV

Chapter I
Introduction

*A part of this chapter has been published under the title "**Multifaceted Role of Neuropilins in the immune System: Potential Targets for immunotherapy"** in collaboration with *Sohini Roy, Arup K. Bag, Rakesh K. Singh, James E. Talmadge, Surinder K. Batra and Kaustubh Datta* in Frontiers in Immunology. (https://doi.org/10.3389/fimmu.2017.01228).

1.1.1. Macrophages: A brief summary

Macrophages belong to the mononuclear phagocytic system. They are the most plastic cell type among the hematopoietic family and extremely diverse in functions. Macrophages bridge the innate and adaptive arms of the immune response. They are also endowed with a variety of house-keeping functions, like clearance of cellular debris through phagocytosis, immune sentinel in tissues and priming adaptive responses as well as developmental processes, metabolism and homeostasis. Macrophages are also causally associated with various diseases, like diabetes, multiple sclerosis, autoimmunity, rheumatoid arthritis, asthma, atherosclerosis, as well as cancer. In the following sections, we will briefly summarize and discuss the development, different polarization states of macrophages and their role and function in normal physiology as well as some clinical conditions.

1.1.2. Origin and different monocyte subsets

Myelopoiesis starts in the yolk sac 3-4 weeks into gestation in human and embryonic day 8 in mice. Myeloid progenitors developing from the primitive ectoderm give rise to the embryonic macrophages. The first hematopoietic stem cell (HSC) seeds the fetal liver around 5weeks of gestation and expand and mature to erythroid, lymphoid and myeloid cells. Extra embryonic hematopoiesis stops at around 10-12 weeks into gestation in human and E12 in mice. The liver remains the primary site of hematopoiesis until birth in mice and week 20-24 of gestation in humans. The HSC from liver gradually colonize the thymus and spleen and finally the bone marrow just before birth in mice (and second trimester in human). The

HSC gives rise to monocytes through the granulocyte-macrophage progenitor (GMP), the macrophage-dendritic cell precursor (MDP) and common monocyte progenitor (CMP) intermediates, in a sequential manner (1). There are different monocyte populations in both mouse and human. In humans, monocytes can be divided into the following groups: a major population called the classical monocytes ($CD14^{++}CD16^{-}$), intermediate monocytes ($CD14^{++}CD16^{+}$) and a minor population called the non-classical monocytes ($CD14^{+}CD16^{++}$) (2). The classical monocytes express significant levels of CCR2 and CD62L, and low levels of CX3CR1 whereas the non-classical type expresses a high level of CX3CR1. Extensive transcript enrichment analyses have shown homology between $Ly6C^{hi}CX3CR1^{lo}CCR2^{hi}$ (in mouse) and $CD14^{++}CD16^{-}$ monocytes (in human) and between $Ly6C^{lo}CX3CR1^{hi}CCR2^{lo}$ (in mouse) and $CD16^{+}$ monocytes (in human) (3-5). During infection or injury, chemokines and pro-inflammatory cytokines released from the inflamed tissue induce the egress of monocytes from the bone marrow. The classical monocytes are targeted towards the site of infection where they differentiate to mature macrophages and either exhibit cell mediated cytotoxicity towards infected cells or can even migrate to the lymph nodes to prime DC or naïve T cells for adaptive immune responses (6). The non-classical monocytes which mainly patrol the endothelium, can also be recruited to sites of infection where they secrete TNF and other inflammatory cytokines (7).

The tissue resident macrophages are heterogeneous, seed different tissues and are maintained by self-renewal. They can origin atleast from three different

sources: yolk sac derived macrophages, fetal liver monocytes or bone marrow, depending on the tissue and the stage of development (8).

1.1.3. Macrophage polarization states

Macrophage polarization refers to the activation state of the cells at a given point of time under a certain condition. As mentioned earlier, macrophages are highly plastic in nature and respond rapidly to the cues they receive from their surroundings. Tissue resident macrophages act as immune sentinels. Following a pathogen insult or inflammatory reaction, they get skewed into an activated state. Additional monocytes from circulation as are recruited which further differentiate to activated inflammatory macrophages. These activated cells, called **M1** macrophages are robust inducers of T cell response and are cytotoxic. They secrete a wide variety of inflammatory cytokines and other molecules to eliminate the infection. Post infection or inflammation, these cells engage in a tissue repair program. At this stage, they are polarized towards an anti-inflammatory or alternatively activated state (**M2**). These M2 macrophages are inducers of regulatory T cells, release angiogenic growth factors and molecules and enzymes to remodel and repair the damaged tissue. Finally, most of the infiltrating macrophages either egress from the site of infection or die at the end of the resolution phase.

Agents for M1 type polarization: Macrophages exposed to G-MCSF and TLR agonists, like LPS and IFN-ɣ and Tumor Necrosis Factor (TNF) are polarized to the inflammatory M1 type. Once activated, they produce M1 associated hallmark molecules like IL-12, inducible Nitric Oxide Synthase (iNOS), IL-6, IL-1β and

reactive oxygen and nitrogen species (ROS and RNS respectively). They also activate the helper CD4+ T cells and cytotoxic CD8+ T cells.

G-MCSF, upon binding to its receptor, triggers JAK2/STAT5 signaling, resulting in the activation of ERK and AKT pathways as well as the nuclear translocation of NF-κβ and IRF5 (9). G-MCSF stimulates the macrophages to produce inflammatory cytokines like, IL-6, IL-8, G-CSF, M-CSF, TNF, and IL-1β. TLR agonists like LPS trigger MyD88 and MaL/Tirap (Toll-interleukin 1 receptor domain containing adaptor protein)-dependent pathways that subsequently activate the NF-κB, activator protein 1 (AP-1), IRFs, STAT1, and EGR (early growth response) family members. LPS induced macrophages produce robust inflammatory cytokines like IFN-β, IL-12, TNF, IL-6, IL-1β, chemokines, antigen presentation molecules and several co-stimulatory molecules. IFN-Y signals through the receptors, IFNGR-1 and IFNGR-2. Following ligand binding, the receptors activate the JAK1 and JAK2 proteins which then recruit molecules like STAT1, IRF-1 and IRF-8 (10). Although a combination of LPS and IFN-Y is used to polarize M1 macrophages in vitro, the gene signature profiles of the combination is different from that of macrophages treated with either LPS or IFN-Y alone. This highlights the heterogeneity of the macrophage population existing in *vivo* and cautions us to carefully extrapolate our *in vivo* or *in vitro* findings.

Agents for M2 type polarization: M2 macrophages are further classified into three groups, based on the polarizing cytokine they are exposed to and the signaling pathways that get triggered thereafter. Alternative activation triggered by IL-4 or IL-13 was termed as M2a, cells exposed to and polarized by Fc receptors

and immune complexes belong to M2b and that by IL-10 and glucocorticoid receptors was named M2c subgroup. M-CSF alone can also skew the cells towards an anti-inflammatory M2 phenotype. However, in a tissue environment, macrophages form a mixed population and it is impossible to distinguish them as either M2a or M2b or M2c type. These cells are a potent source of immunosuppressive cytokines like IL-10, TGF-β, angiogenic molecules like VEGF family of members and tissue remodeling factors like MMPs. They also suppress the activation of helper and cytotoxic T cells and induce the formation of T_{regs}.

M2 inducers like M-CSF when binds to the cognate receptor, induces the dimerization and autophosphorylation of the receptor and subsequent activation of ERK, phosphatidylinositol 3-kinase, phospholipase C and finally the nuclear translocation of Sp1. IL-4 activates JAK1 and JAK3 which results in the activation of STAT6. IL-4 can act through different receptor pairs: IL-4Rα1 can pair with the common gamma chain, Yc; or it can heterodimerize with the IL-13Rα1 chain that can bind both IL-4 and IL-13. Additionally, IL-13 can signal through a third receptor, IL-13Rα2. IL-4 and IL-13-treated macrophages, although similar, exhibit different gene signature profiles. In case of M2b macrophages, FcYR represses IL-12, one of the hallmark cytokines for M1 state, and induces the production of IL-10 and promotes a Th2 response (11, 12). The M2c inducers, IL-10 and glucocorticoids signal through entirely different pathways. For example, macrophages metabolize glucocorticoids that are secreted by the adrenal glands. These hormones bind to the glucocorticoid receptor alpha (GCR) and results in its nuclear transcription, where it either alone or by interacting with other transcription factors regulate the

expression of genes like, complement component 1 subunit A (C1QA), TSC22 domain family, member 3 (DSIPI), MRC1, thrombospondin 1 (THBS1), IL-10, IL1R2, and CD163 (13). IL-10 on the other hand, signals through the STAT3 pathway and regulate the expression of several genes like, selected Fc receptors, the chemoattractants CXCL13 and CXCL4, the recognition receptors formyl peptide receptor 1 (FPR1), TLR1, TLR8, MARCO (14).

Of note, macrophage polarization is not an absolutely ON/OFF phenomenon. For example, both the M1 and M2 types express Arg1, albeit in different amounts. Another such pervasive misconception is about IL-10, a robust anti-inflammatory cytokine. Although known as a marker for M2 polarized macrophages, IL-10 is also secreted by M1 type cells. Surprisingly, macrophages stimulated with immune complexes and that are signaling through Fc receptors produce significant amount of IL-10. This may be a result of negative feedback regulation to avoid excess inflammatory response. Another major concern is that most of the studies on macrophages done *in vitro* use simple polarization techniques. This clearly does not mimic the complex overlapping and pleiotropic signals that a macrophage is exposed to in a tissue where M1 and M2 signals cannot possibly exist alone. Also, the polarization technique varies among different laboratories and hence there is a lot of inconsistency in the markers used for each subtype. However, some of the classical markers used to identify either M1 or M2 polarized macrophages is listed in Fig. 1.6 and 1.7.

The above-mentioned M1/M2 classification of macrophages is over-simplified and vague. Especially, under conditions of non-resolving inflammation,

like cancer, chronic infection or autoimmune disorders, macrophages exhibit much more complex molecular profile and gene signatures of M2 as well as M1 type macrophages. In the above cases, there is an increased output of monocytes from the bone marrow to maintain sustained recruitment to the site of chronic inflammation. Also, a non-resolving inflammation like cancer takes years to decades to develop, allowing the monocytes/macrophages a lot of time to adapt to the wide array of signals they receive. Once inside the tumor, they are exposed to inflammatory as well as immunosuppressive factors, as a result of which they show a mixed phenotype resembling more of M2 macrophages, but also express some genes characteristic of the M1 type cells.

1.1.4. Functions of macrophages in normal physiology and clinical conditions

Macrophages are indispensable for normal developmental processes. On the other hand, they are also causally related to several clinical conditions, like autoimmunity, rheumatoid arthritis, atherosclerosis, cancer to name a few. Few of these aspects of are discussed briefly below:

Development: In absence of macrophages, several developmental defects have been reported. For example, *Csf1* null mice, which lacks macrophages, develops osteopetrosis due to loss of osteoclasts. The cavities in bones where hematopoiesis occurs are not formed in these mice. However, the mice survive till adulthood due to extramedullary hematopoiesis in spleen and liver. Macrophages are also important for angiogenesis, proper tissue architecture and patterning in

kidney, pancreas, mammary gland, brain as well as stem cell niche maintenance and deciding their fate (15).

Phagocytosis: The primary function of macrophages is phagocytosis. For example, during erythropoiesis, macrophages surround the maturing erythroblasts and engulf the extruded erythrocyte nuclei (16). Macrophages also phagocytose cells not expressing CD47 and hence are critical for deciding erythropoietic egress from bone marrow (17). They also maintain hematopoietic steady state by clearing neutrophils in spleen and liver (18). Macrophages are also central to clearing apoptotic cells arising as part of daily turnover in our body or apoptotic debris occurring during infection or injury. The importance of removal of apoptotic cells by macrophages is discussed later in the relevant sections.

Metabolic homeostasis: Macrophages are important for maintenance of systemic metabolic homeostasis. For example, in healthy lean individuals, macrophages are alternatively activated (express Arg-1, CD206) and comprise 10-15% of white adipose tissue, which acts as a long-term storage of nutrients. This is important for imparting insulin sensitivity in the white adipose tissue. However, in obesity, the white adipose tissue is under stress and releases macrophage chemoattractants like CCL2, CCL5 and CCL8 and macrophage content increases upto 45-60%. These macrophages are inflammatory in nature and contribute to insulin resistance in obesity (19-23). Further, high fat feeding causes inflammatory macrophage infiltration into the insulin producing islets and augments β-cell dysfunction (24, 25). Macrophages also phagocytose aged erythrocytes and contribute to iron recycling (26).

Thermogenesis: Brown adipose tissue or brown fat generates heat and maintains our body temperature. Alternative activation of macrophages by IL-4 and IL-13 induce the production of catecholamines in macrophages that contribute to thermogenesis in brown fat.

Infections: In case of pathogenic infection or inflammation, circulating monocytes are rapidly recruited to the site of injury where they polarize to classically activated M1 type. These cells secrete pro-inflammatory and cytotoxic cytokines, anti-microbial mediators like ROS/NOS and mediate killing of infected cells. They also directly or indirectly alert the adaptive immune responses for eradicating the invading pathogen. Post injury, macrophages adopt a reparative phenotype where they phagocytose and clean up the apoptotic debris that arose due to infection or injury and plays a vital role in tissue remodeling, regeneration and wound healing process by secreting growth factors, angiogenic molecules, and matrix metalloproteinases. However, in cases where the repair process is impaired, it results in aberrant healing and fibrosis (scarring).

Inflammatory diseases: Macrophages are also causally associated with several chronic sterile inflammation related diseases, like rheumatoid arthritis (RA), inflammatory bowel disease (IBD), asthma, atherosclerosis and fibrosis. For example, in RA, IBD and multiple sclerosis, macrophages secrete pro-inflammatory cytokines like IL-12, IL-18, IL-23, TNF-α and contribute to disease pathogenesis and severity. On the other hand, allergic asthma, which arises due to airway obstruction and inflammation and lung remodeling, is characterized by the abundance of macrophages that secrete Th2 like cytokines and molecules that

degrade the tissue and remodel the airway. Macrophages also secrete molecules that result in the recruitment of eosinophils, basophils and Th2 type T cells that worsen the disease.

1.2. Neuropilins: A brief introduction

Neuropilins (NRPs) are multifunctional, transmembrane surface glycoproteins that are expressed in all vertebrates and are highly conserved across species. They were originally identified for their role in axonal guidance. NRPs are well known for their function as co-receptors for Vascular Endothelial Growth Factor (VEGF) members and Class III Semaphorins by interacting with VEGF receptors and Plexins respectively. However, work over the past decade have identified additional role of NRPs in a wide array of physiological processes, like development, angiogenesis, immunity as well as clinical conditions like cancer. The two isoforms, NRP1 and NRP2 are often over-expressed in different cancers and their expression correlates with poor clinical outcome. NRPs are known to aid cancer progression by promoting cell survival under therapeutic stress, inducing tumor associated angiogenesis and therapy resistance. They are also expressed in a variety of immune cells, like, macrophages, dendritic cells, and different T cell subsets where they take part in the development, migration and immune responses under physiological as well as pathological conditions. NRPs are also expressed in bone compartment, namely osteoclast and osteoblast where they regulate bone homeostasis. Of the two isoforms, NRP1 is well characterized in different T cell subsets and to some extent in myeloid cells (dendritic cells and macrophages). NRP2, on the other hand, is poorly characterized in the immune

cell subpopulations, and details of its ligands and pathways governing its functions not well understood.

1.2.1. Genomic organization, protein structure and splice variants of Neuropilins

There are two isoforms of NRPs, NRP1 and NRP2. They are encoded by distinct genes located on different chromosomes, 10p12 for NRP1 and 2q34 for NRP2. The two isoforms arose because of gene duplication and share homology in their structure and overlapping sets of ligands and functions. Each gene contains 17 exons and 16 exons and similarity in exon-intron junctions (27). The general domain structure of the NRPs comprises of an N-terminal extracellular region, a single pass transmembrane domain followed by a short C-terminal cytosolic part (43-44 amino acids). The extracellular portion comprises of two CUB (complement binding factors C1r/C1s, Uegf, Bone Morphogenetic protein 1)(a1/a2) domain, two Factor V/VIII coagulation factor homology (b1/b2) domain, a b-c linker, followed by a MAM (homologous to meprin protease, A5 antigen, receptor tyrosine phosphatase μ and κ). The CUB domain interacts with Semaphorin group of ligands, the b1/b2 domain is important for binding anionic phospholipids and thus mediate cell-cell adhesion. This is also the site for interaction with VEGF ligands. The MAM domain is required for homo or heterodimerization with other receptors. Several splice variants have been identified for each of NRP1 and NRP2. Both NRP1 and NRP2 can exist as membrane bound or soluble splice forms. The latter often act as decoy molecules and antagonize the function of the full-length receptors. For instance, two such splice forms, $_{12}$sNRP1 and $_{11}$sNRP1 arise due

to pre-mRNA splicing at intron 12 and 11 respectively (27). $_{12}$sNRP1 acts as a decoy receptor for $VEGF_{165}$. When $_{12}$sNRP1 was overexpressed in rat prostate carcinoma cells, this resulted in tumors with increased number of hemorrhaged and damaged blood vessels and higher number of apoptotic tumor cells (28). Two additional soluble splice forms have been reported for NRP1, namely, sIIINRP1 and sIVNRP1 and their expression detected in normal condition as well as tumor tissues. Both these isoforms act as a ligand trap and regulated breast cancer cell migration (29). Another splice variant for NRP1 is reported; it lacks a stretch of 7 amino acids, two residues downstream of the O-glycosylation site and hence undergoes less glycosylation. When overexpressed in prostate cancer cells, it reduced tumor cell proliferation and migration and hence slowed tumor growth (30).

Two membrane bound splice variants are known for NRP2, namely NRP2a and NRP2b. They differ at the last 100 amino acids in the cytoplasmic tail. NRP2a is 44% homologous to NRP1 and may exhibit redundant functions. The extracellular domain of NRP2a and NRP2b are identical, but share only 11% homology in their transmembrane and cytosolic domains, indicating activation of divergent downstream signaling cascades and functions. Indeed, a recent study reported opposite function of these two splice variants in non-small cell lung carcinoma. NRP2b showed pro-metastatic role whereas NRP2a antagonized tumor progression and metastatic burden (31). In humans, two splice variants for NRP2a have been identified, namely NRP2a(17) and NRP2a(22). The former arises as a result of insertion of insertion of 17 amino acids after position 809,

located between the MAM and transmembrane domains. On the other hand, NRP2a(22) has an insertion of additional 5 amino acids within the 17 amino acid stretch as in NRP2a(17) as a result of alternate splicing. Similarly, NRP2b can also exist as two splice forms, NRP2b(0) and NRP2b(5) that is generated by alternate splicing between exon 15 and 16b and insertion of 0 or 5 amino acids after residue 808. NRP2b(0) is more abundantly expressed than NRP2b(5) (27). Of note, NRP2a and NRP2b have divergent C terminus, indicating they probably can activate distinct signaling pathways and exert non-redundant functions. Therefore, to successfully target NRPs, it is crucial to clearly understand why the different isoforms or splice variants are expressed, sometime one preferentially over another, under different conditions and the differences in their cellular signaling.

In mice, NRP2 undergoes alternative splicing and gives rise to four splice variants; these differ in the insertion of 0, 5, 17 or 22 amino acids after residue 809. The fact that these differential insertions occur in the b-c linker and transmembrane domain, it may alter the ability of the splice variants to homo or heterodimerize with other surface receptors. Hence the splice forms may potentially regulate distinct downstream cellular signaling pathways (27).

A soluble isoform for NRP2 is known, $_{9}$sNRP2 (62.5 kDa). Alternate splicing results in the inclusion of an intron in the b2 domain of the mRNA and an in frame stop codon results in the termination of the translation of the protein. Hence this soluble isoform has the a1/a2 domain, the b1 domain but only a part of the b2 domain, but not the last 48 amino acids of the b2 domain, the b-c linker, the transmembrane domain and the cytosolic tail (27). Intriguingly, $_{9}$sNRP2 acts as a

ligand trap and sequesters VEGFC, impairing the oncogenic VEGFC/NRP2 signaling axis and growth of prostatospheres *in vitro (32)*.

1.2.2. Post translational modifications of NRPs

Both NRP1 and NRP2 undergo various post translational modifications with different functional consequences. NRP1 is often modified by the covalent addition of Glycosaminoglycan (GAG) to a conserved Serine residue (Ser^{612}) in the b-c linker region (33). Structurally, GAGs are a repeating disaccharide unit containing N-acetylglucosamine (GlcNac) or N-acetylgalactoseamine (GalNac) and a uronic acid or galactose. GAGs can be either Heparan sulfate (HS-GAG) or Chondroitin sulfate (CS-GAG), keratin sulfate or hyaluronic acid. In several human tumor cell lines, NRP1 exists as N-glycosylated as well as CS-GAG modified fractions. Surprisingly, the latter negatively regulated tumor cell invasion (34). CS GAG NRP1 is predominantly expressed in the vascular smooth muscle (SMC) cells. In HUVEC cells, NRP1 expressed equivalent amount of CS GAG and HS GAG. GAG modification on NRP1 enhances its binding to VEGF, however, CS-GAG NRP1 may act as a decoy receptor under certain circumstances. On the other hand, HS-GAG NRP1 may bind multiple NRP1 molecules and promote NRP1 clustering. Such a cluster can bind VEGFR2 in presence of VEGF and stabilize the complex, prevent internalization of VEGFR2, resulting in enhanced signaling (33). In contrast, there are no reports for such modification on NRP2. In DCs, NRP2 undergoes post translational modification by the addition of polysialic acid (PSA) chains to mucin type O-linked glycans between the b2 and c domains(35, 36)(35, 36)(35, 36)(35, 36)(35, 36)(35, 36)(35, 36)(35, 36)(35, 36)(35, 36)(35, 36)(35,

36)(35, 36. NRP2 polysialylation regulates CCL21 driven trafficking of DCs to the secondary lymphoid organs and modulates interactions between DCs and T lymphocytes (37). NRP1 has also been recently reported to undergo polysialylation at a level 50% of that of NRP2, although the exact biological implication of this remains unknown (38).

1.2.3. Ligands for the NRPs

NRP1 and NRP2 are most well known for their role as co-receptors to VEGF family members and Class III Semaphorins. Semaphorins comprise a large family of proteins and can be sub-categorized into seven classes. They bind with Plexins on the cell surface and activate cellular signaling to affect different aspects of developmental biology, immune responses, as well as clinical disorders. Class III Semaphorins are secreted from cells and can interact with either NRP1 or NRP2 at the a1/a2/b1 domain. Together with Plexin A1 or A2, they form a holoreceptor

complex. NRP1 and NRP2 exhibit some selectivity in binding to the Semaphorins. For instance, the major ligand for NRP1 is Sema3A, although it can also bind Sema3F, albeit with lower affinity. NRP2, on the other hand, binds mainly Sema3C and Sema3F, but not Sema3A. NRPs also bind VEGF family members with differential specificities. For example, NRP1 binds VEGFA, classically $VEGFA_{165}$ (39). NRP2 preferentially binds with proteolytically cleaved and activated VEGFC, although it can also bind other VEGFA isoforms. Structural studies have delved into explaining how NRPs exhibit selectivity in binding different VEGF isoforms. It has been shown that a surface groove in the b1 domain binds with linear epitopes containing a C-terminal arginine, present in the VEGFA isoforms and proteolytically cleaved VEGFC. However, the interactions can be fine-tuned by additional side chain interactions in the b1 domain region.

NRPs are also known to bind several other ligands, where they mainly act as co-receptors to enhance the signal. For example, NRPs can bind with Transforming Growth Factor beta 1 (TGF-β1) and signal through the canonical Smad2/3 pathway to trigger anti-apoptotic and anti-proliferative pathways. They also bind to c-Met and platelet derived growth factor (PDGF) and contribute to cancer pathogenesis. It is now well established that miRNAs circulate either in encapsulated form or bound to protein Argonaute-2 (AGO2) and travel to distant sites where they crosstalk with target cells. A recent study showed that NRP1 binds AGO2/miRNA complexes and facilitates their cellular internalization process (40). miRNAs have now been proven to be causally associated with several clinical

disorders, including cancer. miRNA/NRP1 interaction may have impact in different pathological conditions.

1.2.4. Phenotypes of genetically engineered mouse models for NRPs

The crucial roles of NRP1 and NRP2 in developmental biology began to emerge from different genetically engineered mouse models. NRP1 depletion is embryonically lethal at E10.5-E13.5. The embryos die of severe cardiac and vascular defects (41-43). Transgenic mice with NRP1 overexpression also die in utero at E12.5 owing to extensive hemorrhage and had developmental defects in the nervous system (44). In contrast, NRP2 knock out mice are viable and proceed to adulthood. However, they have smaller lymphatic vessels and proper development of cranial nerves, spinal sensory axons is impaired (45-47). NRP2 also plays an important role in bone homeostasis. This was evident from the significantly lower bone mass of NRP2 knock out mice. The bone loss was attributed to reduced number of osteoblasts and increased number of osteoclasts in absence of NRP2 (48). Simultaneous depletion of NRP1 and NRP2 is embryonic lethal at E8.5; the embryos die due to severe vascular defects (49).

1.2.5. Role of NRPs in macrophages

Both NRP1 and NRP2 expression have been reported in macrophages under various conditions (50). NRP1 is expressed on tissue resident macrophages, like alveolar, bronchial, intravascular, decidual as well as microglia/macrophages in the brain. For example, $TIE2^{+}$ yolk sac derived microglia/macrophages that express NRP1 are important during brain vascularization. These macrophages are present near the endothelial cells and

promote vessel fusion. However, NRP1 has been shown to be dispensable for normal vessel growth in brain (51-53). Recently, there have been a lot of focus on tumor infiltrating macrophages (TAMs). As discussed later, TAMs comprise a unique population of myeloid derived cells in the tumor core and their infiltration correlates with disease progression and clinical outcome in many cancers. TAMs have been causally associated with various aspects of cancer, like cancer cell survival, EMT, migration and invasion, angiogenesis and suppression of immune response against the malignant cells (54-57). Recently, it has been shown that recruitment of TAMs to the hypoxic core of the tumor is crucial for their attainment of pro-tumorigenic properties. Once recruited to the tumor site, NRP1 regulates the migration of TAMs to the hypoxic core and its ablation arrests the TAMs in the peripheral normoxic region of the tumor, activates anti-tumor immune response and reduces tumor burden (58, 59). NRP1 is also expressed in glioma associated macrophages (GAM) and promotes their tumorigenic activities. Indeed, depletion of NRP1 in GAMs reduced the burden of glioma tumors (60). An immunoregulatory role for NRP1 has been documented in several other studies as well.

NRP2 on the other hand, is not well characterized in the myeloid cell compartment. Previous literature as well as work in the current dissertation show that NRP2 is not expressed at a detectable level in the monocytes, but its expression is induced in inflammatory M1 as well as alternatively activated M2 macrophages. NRP2 is also detected in tissue macrophages, including alveolar, bronchial, peritoneal as well as intravascular macrophages in mice (50). A recent study reported that polysialylation is progressively lost in monocytes as the cells

migrate towards pulmonary and peritoneal sites of inflammation. Interestingly, peritoneal macrophages do not express polysia themselves, however NRP2 is modified post-translationally by polysialylation when maintained in culture. Further, removal of polysia increased the phagocytosis of bacteria in macrophages. However, it is still not clear if this observation could be attributed to polysialylated NRP2 (61). It is possible that macrophages lose polysia during bacterial infection to enhance phagocytosis, following which it is re-expressed and probably plays a part in the interaction with T cells. Polysialylated NRP2 has also been reported in microglia, where they mainly remain confined in the golgi compartment. Following LPS stimulation, it gets quickly mobilized to the cell surface and is eventually lost. Interestingly, polysialylated NRP2 was detected in the cell culture supernatant, indicating metalloproteinase mediated cleavage of the protein. Exogenous addition of polysia blunted the production of pro-inflammatory cytokines in microglia in response to LPS challenge. This indicated a possible role for polysialylated NRP2 in negative feedback regulation of inflammatory response in macrophages (62, 63). However, the main concern in this finding is since the addition of exogenous polysia abrogated the production of inflammatory cytokines in microglia in response to LPS, this effect does not necessarily depend on the polysia carrier. Also, it is not clearly known why polysialylated NRP2 is mobilized to the cell surface following LPS challenge.

Expression pattern of NRP2 in TAMs is not well characterized, nor is its function in cancer associated macrophages known. Two previous studies have reported NRP2 expressing macrophages in patients with lung cancer as well in

mouse mammary tumors (50, 64). However, no data exists till date that correlates NRP2 expression in TAM with disease progression or clinical outcome and patient survival. We have detected NRP2 expression in TAMs in pancreatic cancer. Expression of NRP2 in TAMs in pancreatic cancer and its functions and implications in tumor progression will be discussed in more detail in the relevant sections.

Fig 1.1. Neuropilin (NRP) domain structure and splice variants. The general domain structure of NRP1 and NRP2 is shown. There is an N-terminal extracellular domain for ligand binding, followed by a single pass transmembrane domain and a short cytosolic tail. The extracellular domain comprises of two CUB, two b1/b2 and one MAM domain. The sites for binding different ligands are indicated. Both NRP1 and NRP2 can exist as multiple splice variants. Soluble isoforms (sNRP1 and sNRP2) contain truncated extracellular domain but lack the transmembrane and cytosolic regions and can act as decoy receptors to blunt NRP function. NRP2 can exist as two splice forms, NRP2a and NRP2b, which share only 11% homology in their C terminus, therefore, being capable of regulating different signaling pathways. The percentage of sequence homology in the different extracellular and cytosolic domains of NRP1 and NRP2 as well as between NRP2a and NRP2b are indicated. The C termini of both NRP1 and NRP2a contain a PDZ binding motif (SEA) that can act as docking site for interacting partners. Red arrowheads indicate insertion at residue 808 in NRP2 of five amino acids GENFK giving rise to different splice variants of NRP2a and NRP2b.The percentage amino acid homologies between the domains of full length NRP1 and NRP2 isoforms and between the NRP1 and NRP2a/NRP2b isoforms are indicated. The figure has been adapted from Roy *et al*. “Multifaceted Role of Neuropilins in the Immune System: Potential Targets for Immunotherapy”. Front Immunol. 2017. doi: 10.3389/fimmu.2017.01228 with permission.

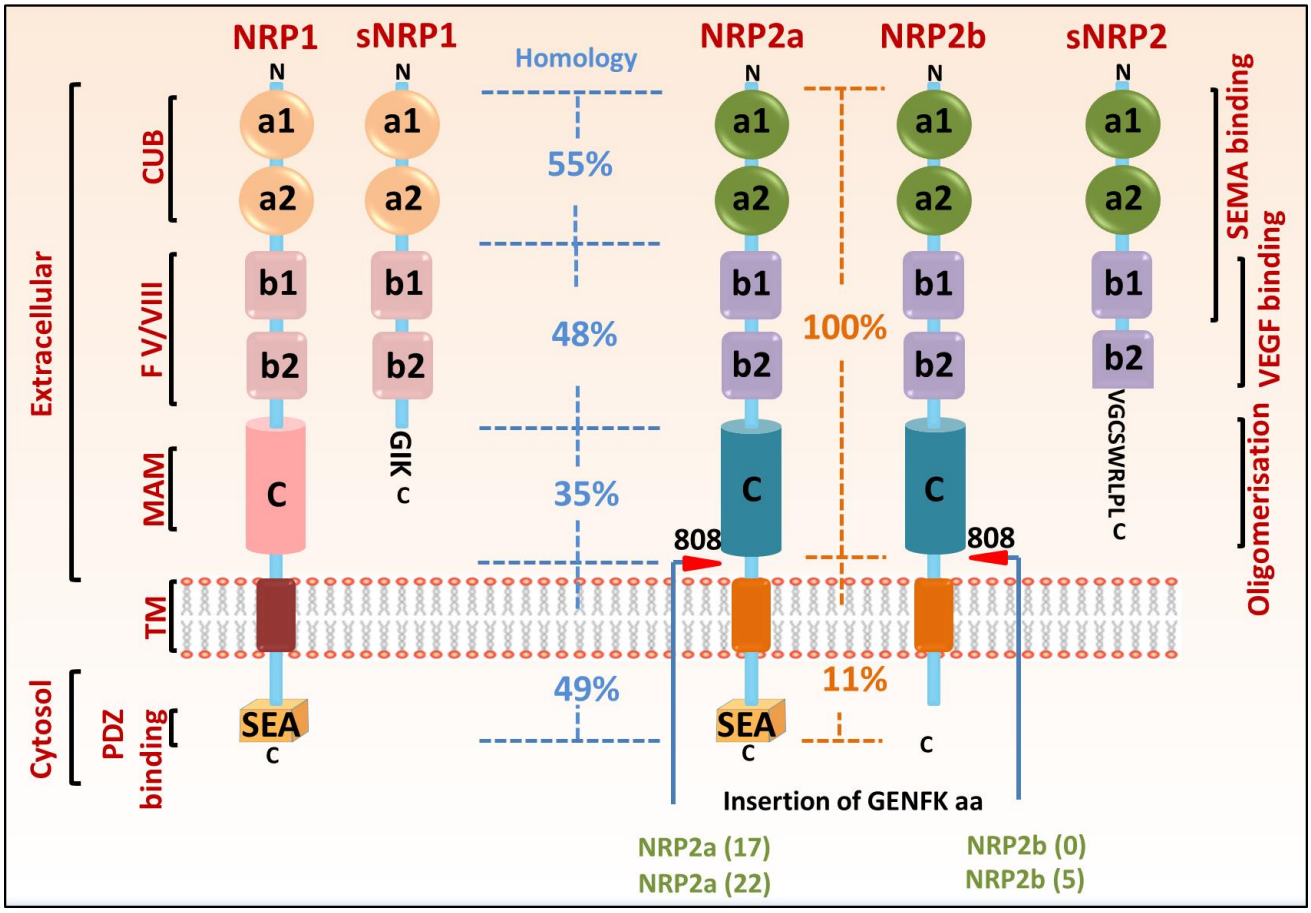
NRP1
sNRP1
Homology
NRP2a
NRP2b
sNRP2
N
a1
a2
b1
b2
C
GIK C
VGCSWRLPL C
808
SEA
C
55%
48%
35%
49%
100%
11%
Insertion of GENFK aa
NRP2a (17)
NRP2a (22)
NRP2b (0)
NRP2b (5)
Extracellular
CUB
F V/VIII
MAM
TM
Cytosol
PDZ binding
SEMA binding
VEGF binding
Oligomerisation

Fig. 1.2. Origin of monocytes in the bone marrow. Hematopoietic stem cells (HSC) in the bone marrow continuously giving rise to monocytes through sequential generation of Granulocyte-Myeloid Progenitor (GMP), Monocyte-Dendritic Cell Precursor (MDP) and Common Myeloid Progenitor (cMOP) intermediates. Monocytes exit bone marrow to enter circulation. The two classes of monocyte subsets are shown: classical monocytes and non-classical monocytes; in the steady state, the two subsets form a developmental continuum, but are functionally distinct. This figure has been adapted from Ginhoux *et al*. "Monocytes and macrophages: developmental pathways and tissue homeostasis." Nat Rev Immunol. 2014. doi: 10.1038/nri3671 with permission.

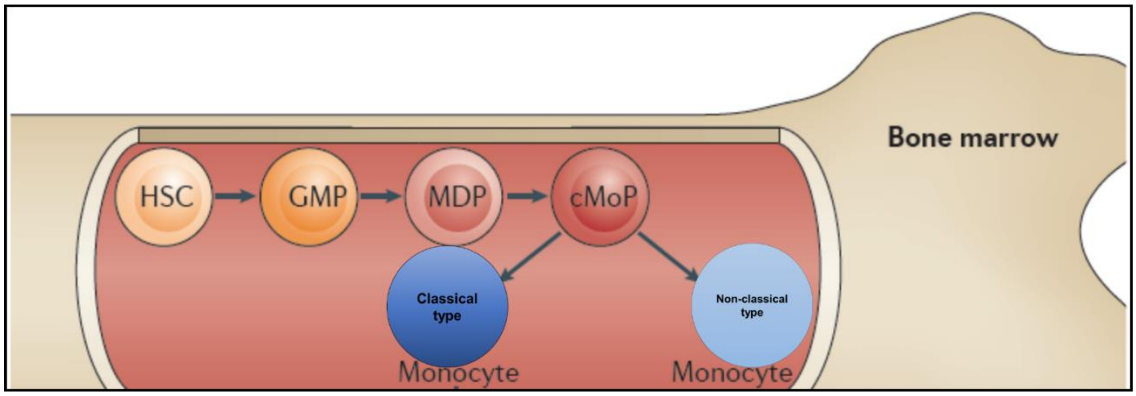
Bone marrow
HSC
GMP
MDP
cMoP
Classical type
Non-classical type
Monocyte
Monocyte

Fig. 1.3. Human monocyte subsets and their functions. Three different human monocyte subsets are indicated: classical ($CD14^{+++}CD16^{-}$), intermediate ($CD14^{++}CD16^{+}$) and non-classical ($CD14^{+}CD16^{++}$). In the steady state, the different subsets comprise a developmental continuum, although the classical type can switch to the intermediate and non-classical types in circulation. Classical monocytes display efficient antimicrobial capability due to their enhanced phagocytic activity, and secrete ROS/NOS upon LPS stimulus, whereas intermediate and non-classical MCs secrete inflammatory cytokines, TNFα and IL-1β. During inflammation, classical and intermediate subsets infiltrate target tissue, mature to M1Mϕ and present self-antigen via MHC-I/II to prime naïve T cells. In steady state, non-classical monocytes patrol the endothelium and become M2Mϕ. They express CD206, IL-10 and are involved in tissue remodeling, wound healing, immunosuppression and are pro-tumorigenic. During the resolution phase of inflammation, M1 Mϕ can repolarize to M2Mϕ. This figure has been adapted from Yang *et al*. “Monocyte and macrophage differentiation: circulation inflammatory monocyte as biomarker for inflammatory diseases.” Biomarker Research. 2014. doi.org/10.1186/2050-7771-2-1 with permission.

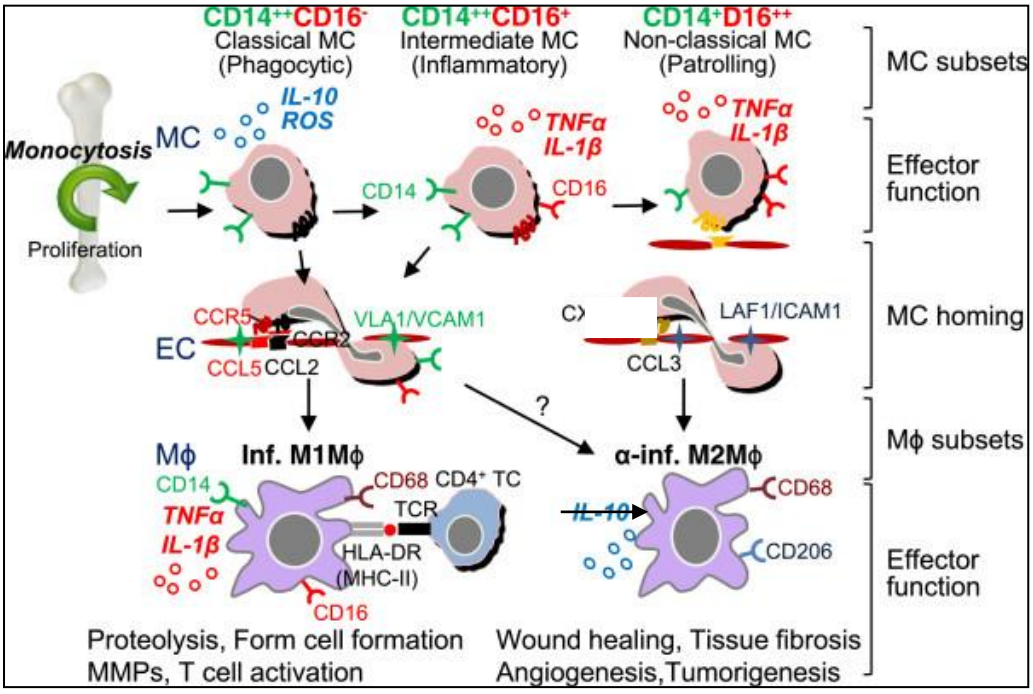
CD14++CD16-
Classical MC
(Phagocytic)
CD14++CD16+
Intermediate MC
(Inflammatory)
CD14+D16++
Non-classical MC
(Patrolling)
MC subsets
Monocytosis
Proliferation
MC
IL-10
ROS
CD14
TNFα
IL-1β
CD16
TNFα
IL-1β
Effector
function
CCR5
CCR2
CCL5
CCL2
EC
VLA1/VCAM1
LAF1/ICAM1
CCL3
MC homing
?
Mϕ
Inf. M1Mϕ
α-inf. M2Mϕ
Mϕ subsets
CD14
TNFα
IL-1β
CD68
CD4+ TC
TCR
HLA-DR
(MHC-II)
CD16
IL-10
CD68
CD206
Effector
function
Proteolysis, Form cell formation
MMPs, T cell activation
Wound healing, Tissue fibrosis
Angiogenesis,Tumorigenesis

Fig.1.4. Mouse monocyte subsets and their functions. Different monocyte subsets in mouse are indicated: classical ($Ly6c^+$) and non-classical ($Ly6c^-$). $Ly6C^+$ monocytes leave the bone marrow in a CC-chemokine receptor 2 (CCR2)-dependent manner. In the steady state, both the subtypes form a developmental continuum, and $Ly6C^+$cells can differentiate into $Ly6C^-$ type. $Ly6C^-$ MCs patrol the endothelium are recruited into normal tissue to become tissue resident Mϕ/DCs where they clear apoptotic debris and perform other housekeeping functions. $Ly6C^+$MCs rapidly respond to inflammation or pathogen invasion, become M1Mϕ and exhibit antimicrobial capability, enhanced phagocytosis and secrete ROS, TNFα, and IL-1β, present antigens and activate T cells; they are anti-tumorigenic. $Ly6C^-$ MCs are recruited to tissue and differentiate into M2Mϕ, which secrete anti-inflammatory cytokine and contribute to tissue repair and are reparative and immunosuppressive in nature and are protumorigenic. During the resolution phase of inflammation or injury, M1 type can re-polarize to M2 type macrophages. This figure has been adapted from Yang *et al*. “Monocyte and macrophage differentiation: circulation inflammatory monocyte as biomarker for inflammatory diseases.” Biomarker Research. 2014. doi.org/10.1186/2050-7771-2-1 with permission.

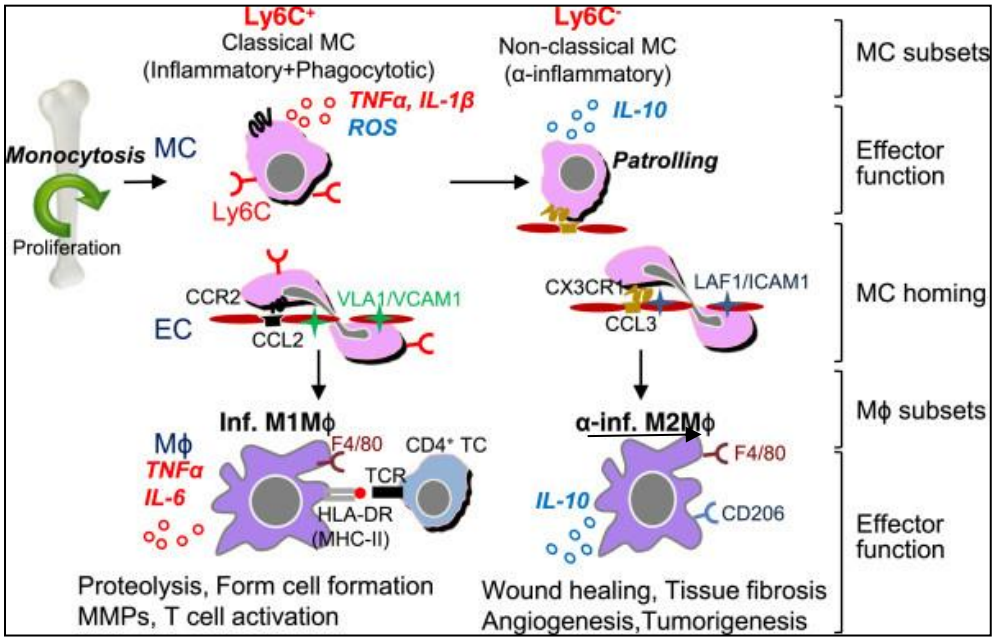
Ly6C+
Classical MC
(Inflammatory+Phagocytotic)
Ly6C-
Non-classical MC
(α-inflammatory)
MC subsets
Monocytosis
MC
Proliferation
TNFα, IL-1β
ROS
Ly6C
IL-10
Patrolling
Effector function
CCR2
VLA1/VCAM1
EC
CCL2
CX3CR1
LAF1/ICAM1
CCL3
MC homing
Inf. M1Mϕ
α-inf. M2Mϕ
Mϕ subsets
Mϕ
TNFα
IL-6
F4/80
CD4+ TC
TCR
HLA-DR
(MHC-II)
F4/80
IL-10
CD206
Effector function
Proteolysis, Form cell formation
MMPs, T cell activation
Wound healing, Tissue fibrosis
Angiogenesis, Tumorigenesis

Fig.1.5. Stimuli for M1/M2 type polarization of macrophages and the pathways associated. A. M1-M2 macrophage model, in which M1 is generated following exposure to interferon-gamma (IFN-g) + lipopolysaccharide (LPS) or tumor necrosis factor (TNF); M1 macrophages are characterized by secretion of IL-12, IL-1, IL-23, TNF, IL-6 and MHC-II and low levels of IL-10 and are anti-microbial, cytotoxic and anti-tumoral. M2 type is further subdivided to M2a (IL-4/IL-13 induced), M2b (immune complex+ Toll-like receptor (TLR) ligands induced), and M2c (IL-10 and glucocorticoids induced). (B) The key signaling pathways and downstream mediators behind the M1 and M2 stimuli in macrophages are highlighted. The diagram includes granulocyte macrophage colony-stimulating factor (GM-CSF) and macrophage colony-stimulating factor (M-CSF) as M1 and M2 stimuli respectively, in addition to other cytokines mentioned. This figure has been adapted from Martinez et al. “The M1 and M2 paradigm of macrophage activation: time for reassessment.” F1000Prime Rep. 2014. doi: 10.12703/P6-13 with permission.

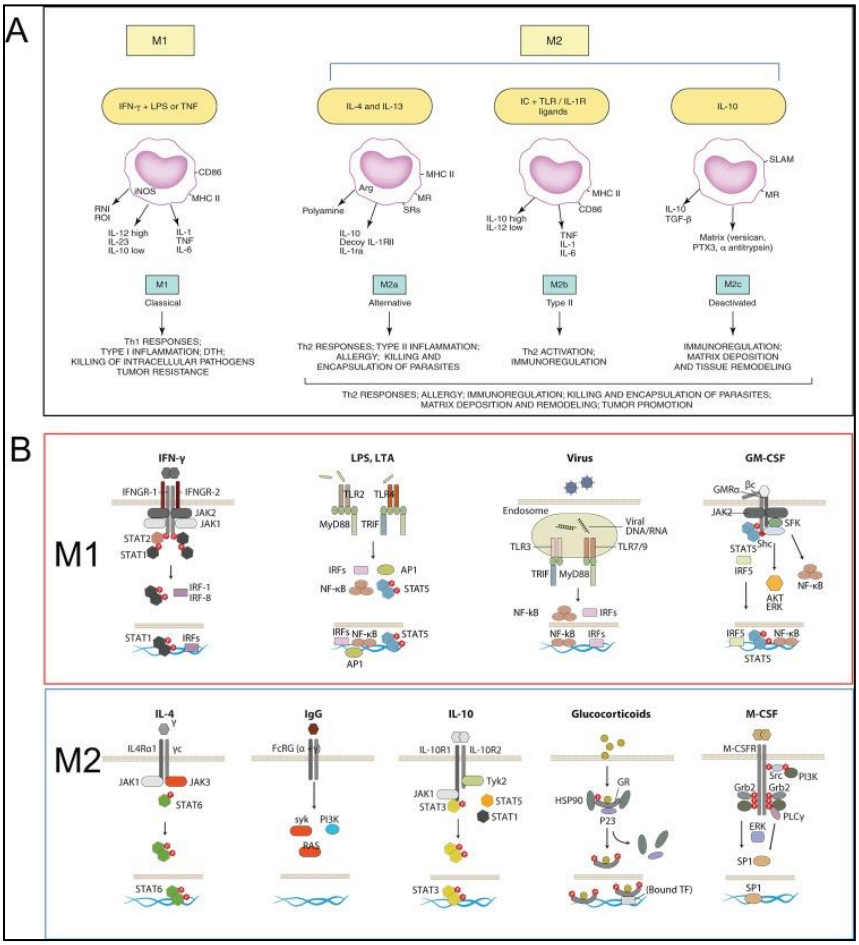
A
M1
M2
IFN-γ + LPS or TNF
IL-4 and IL-13
IC + TLR / IL-1R ligands
IL-10
CD86
iNOS
MHC II
RNI
ROI
IL-12 high
IL-23
IL-10 low
IL-1
TNF
IL-6
MHC II
Arg
MR
Polyamine
SRs
IL-10
Decoy IL-1RII
IL-1ra
MHC II
IL-10 high
IL-12 low
CD86
TNF
IL-1
IL-6
SLAM
MR
IL-10
TGF-β
Matrix (versican, PTX3, α antitrypsin)
M1
Classical
M2a
Alternative
M2b
Type II
M2c
Deactivated
Th1 RESPONSES; TYPE I INFLAMMATION; DTH; KILLING OF INTRACELLULAR PATHOGENS TUMOR RESISTANCE
Th2 RESPONSES; TYPE II INFLAMMATION; ALLERGY; KILLING AND ENCAPSULATION OF PARASITES
Th2 ACTIVATION; IMMUNOREGULATION
IMMUNOREGULATION; MATRIX DEPOSITION AND TISSUE REMODELING
Th2 RESPONSES; ALLERGY; IMMUNOREGULATION; KILLING AND ENCAPSULATION OF PARASITES; MATRIX DEPOSITION AND REMODELING; TUMOR PROMOTION
B
M1
IFN-γ
IFNGR-1
IFNGR-2
JAK2
JAK1
STAT2
STAT1
IRF-1
IRF-8
STAT1
IRFs
LPS, LTA
TLR2
TLR4
MyD88
TRIF
IRFs
AP1
NF-κB
STAT5
IRFs
NF-κB
STAT5
AP1
Virus
Endosome
Viral DNA/RNA
TLR3
TLR7/9
TRIF
MyD88
NF-kB
IRFs
NF-kB
IRFs
GM-CSF
GMRα
βc
JAK2
SFK
STAT5
Shc
IRF5
NF-κB
AKT
ERK
IRF5
NF-κB
STAT5
M2
IL-4
γ
IL4Rα1
γc
JAK1
JAK3
STAT6
STAT6
IgG
FcRG (α γ)
syk
PI3K
RAS
IL-10
IL-10R1
IL-10R2
Tyk2
JAK1
STAT3
STAT5
STAT1
STAT3
Glucocorticoids
GR
HSP90
P23
(Bound TF)
M-CSF
M-CSFR
Src
PI3K
Grb2
Grb2
PLCγ
ERK
SP1
SP1

Fig.1.6. Marker panel for M2 macrophages. This figure has been adapted from Murray et al. “Macrophage Polarization.” Annual Review of Physiology. 2016. DOI:10.1146/annurev-physiol-022516-034339 with permission.

Gene name	Common name	Knockout described in first research paper	Tested in macrophage polarization
M2 marker panel			
Retnla	FIZZ1, RELMα	Yes	Immunoregulatory against excessive T_H2 responses
Clec10a	Mgl2	Yes	ND
Ccl17	Ccl17	Yes	ND
Ccl24	Eotaxin-2	No	ND
Irf4	Irf4	Yes	Required for M2 macrophage development
Chil3[b]	Chitinase 3, Chi3l3, Ym1	No	ND
Mrc1	Mannose receptor	No	ND
Arg1[a]	Arginase-1	Yes	Immunoregulatory against excessive T_H2 responses
RNase2a[c]	Ear11	No	ND
Ear2	Ear2	No	ND
Ccl8	Ccl8	No	ND
Mela[d]	Mela	No	ND
Clec7a	Dectin-1	No	Important antifungal mechanism
Pdcd1lg2	PD-L2	Yes	Partly; required for M2 propagation of $Foxp3^+$ Treg
Socs2	Socs2	Yes	ND
Cdh1	Cadherin 1	No	Not required
Ppard	PPARδ	Yes	Required for M2 macrophage development
Pparg	PPARγ	Yes	Required for M2 macrophage development
Ccl22	Ccl22	No	ND

Fig.1.7. Marker panel for M1 macrophages. This figure has been adapted from Murray et al. “Macrophage Polarization.” Annual Review of Physiology. 2016. DOI:10.1146/annurev-physiol-022516-034339 with permission.

Gene name	Common name	Knockout described in first research paper	Tested in macrophage polarization
M1 marker panel			
Il1a	Il1a	Yes	Defects in normal M1 type inflammation in the absence of IL-1R signaling
Il1b	Il1b	Yes	Defects in normal M1 type inflammation in the absence of IL-1R signaling
IL6	IL6	Yes	Unknown. Increases IL-4Rα expression (same pathway as mediated by IL-10)
IL12a	IL12a	Yes	Indirect defects in TH1 responses (and hence IFN-γ production)
Il12b	Il12b	Yes	Indirect defects in TH1 responses (and hence IFN-γ production)
Il23a	Il23a	Yes	ND
IL27	IL27	Yes	ND
Tnf	Tnf	Yes	Required to suppress M2 macrophages; required for normal M1 macrophages
Csf3	G-CSF	Yes	ND
Csf2	GM-CSF	Yes	Required in part for macrophage viability and expansion
Nfkbiz	IκBζ	Yes	Selective defects in macrophage inflammatory signaling
Ccl1	Ccl1	Yes	ND
Cxcl13	Cxcl13	Yes	ND
Ccl11	Eotaxin	Yes	ND
Cxcl2	Cxcl2	No	ND
Tnfaip3	A20	Yes	Unknown; prediction of increased M1 associated with increased inflammation
Socs3	Socs3	Yes	Research of the role of SOCS proteins in polarization is controversial (126)
Peli1	Pellino 1	Yes (E3 ligase-deficient knockin	ND
Nos2	iNOS	Yes	Key antimicrobial defense and signaling pathway
Marco	Marco	Yes	ND

Fig.1.8. Physiological roles of macrophages. Macrophage heterogeneity arises from their different origins (either yolk sac or bone marrow derived) and their ability to detect and rapidly adopt to complex signals in the tissue microenvironment (shown on the *left*). The vast range of physiological roles undertaken by macrophages, e.g. erythropoiesis, metabolic homeostasis (insulin resistance), iron recycling, development, tissue regeneration and thermogenesis (shown on the *right*). Macrophages respond to external stimuli through “sensor systems” in the form of *(a)* cell surface and intracellular pattern recognition receptors for detecting invading pathogens and damage-associated molecular patterns; *(b)* receptors for recognizing and engulfing apoptotic cells; *(c)* receptors that promote M1/M2-like activation; *(d)* receptors for neurotransmitters *(e)* cell surface receptors that regulate macrophage activation, e.g. the inhibitory receptors SIRP1-α and CD200R. Integrins *(f)* mediate interaction with macrophages and ECM. Macrophages produce numerous molecules that contribute to tissue remodelling and inflammation and mediate clearance of apoptotic bodies, cell debris. Macrophages rely heavily on efficient phagocytosis and endocytosis for maintenance of homeostasis as well as other functions. This figure has been adapted from Gordon et al. “Physiological roles of macrophages.” Pflügers Archiv - European Journal of Physiology. 2017 with permission.

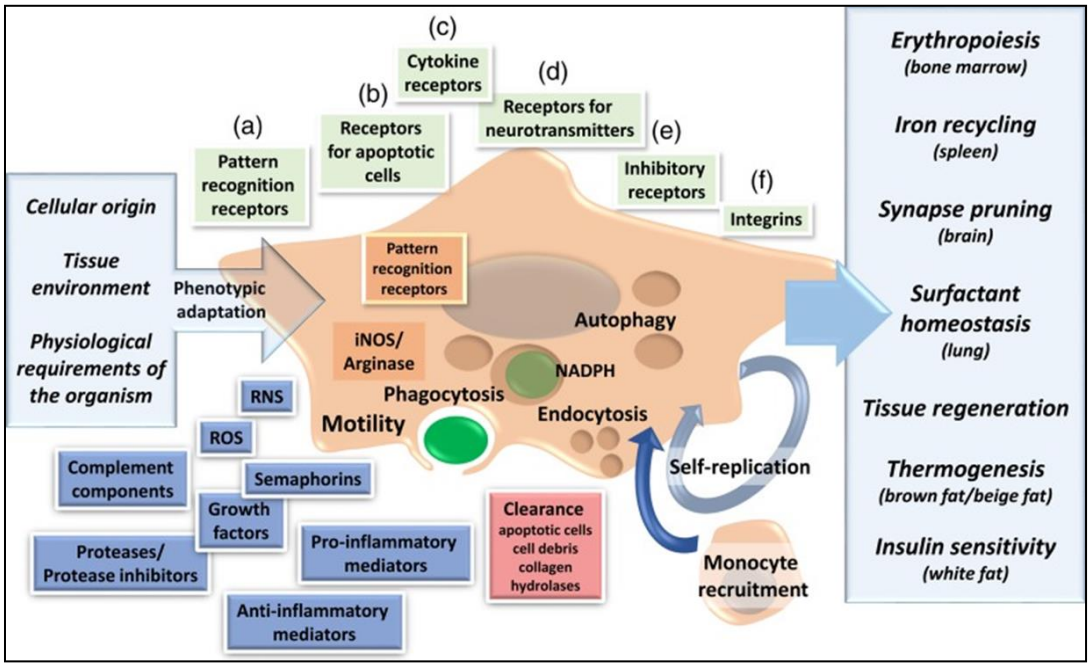
(a)
(b)
(c)
(d)
(e)
(f)
Pattern recognition receptors
Receptors for apoptotic cells
Cytokine receptors
Receptors for neurotransmitters
Inhibitory receptors
Integrins
Cellular origin
Tissue environment
Physiological requirements of the organism
Phenotypic adaptation
Pattern recognition receptors
iNOS/ Arginase
RNS
ROS
Complement components
Semaphorins
Growth factors
Proteases/ Protease inhibitors
Pro-inflammatory mediators
Anti-inflammatory mediators
Motility
Phagocytosis
Autophagy
NADPH
Endocytosis
Clearance
apoptotic cells
cell debris
collagen
hydrolases
Self-replication
Monocyte recruitment
Erythropoiesis
(bone marrow)
Iron recycling
(spleen)
Synapse pruning
(brain)
Surfactant homeostasis
(lung)
Tissue regeneration
Thermogenesis
(brown fat/beige fat)
Insulin sensitivity
(white fat)

Fig.1.9. Role of NRP2 in macrophages. NRP2 is expressed in microglia, tissue resident (M2) and inflammatory M1 type macrophages as well as TAMs. In peritoneal macrophages, NRP2 is involved in phagocytosis. In microglia, NRP2 is polysialylated and remains confined in the golgi compartment. Following LPS challenge, it rapidly translocates to the cell surface and is shed from the cells. The role of NRP2 in TAMs is not reported. This figure has been adapted from Roy *et al*. "Multifaceted Role of Neuropilins in the Immune System: Potential Targets for Immunotherapy". Front Immunol. 2017. doi: 10.3389/fimmu.2017.01228 with permission.

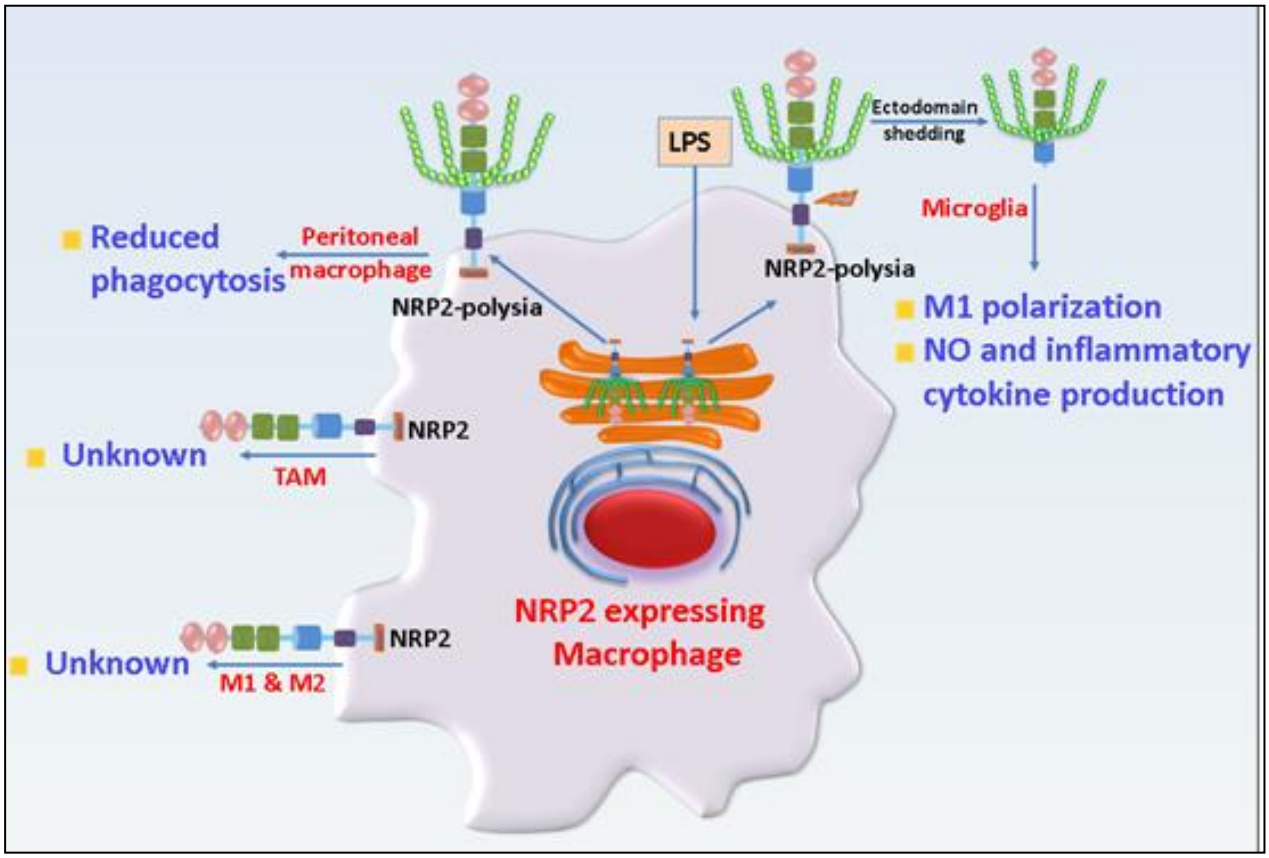
LPS
Ectodomain shedding
Microglia
Reduced phagocytosis
Peritoneal macrophage
NRP2-polysia
NRP2-polysia
M1 polarization
NO and inflammatory cytokine production
NRP2
Unknown
TAM
NRP2 expressing Macrophage
NRP2
Unknown
M1 & M2

2.1. Tumor Associated Macrophages: An overview

The tumor microenvironment (TME) is now considered a complex ecosystem, comprising not only of cancer cells, but also other cell types, like immune cell infiltrates, stromal cells, endothelial cells and fibroblasts. It is now well established that this ecology of cells evolves with and engages in a complex cross talk with one another, thereby providing support to the growing tumor. Suppression of antitumor adaptive immune response and non-resolving tumor-promoting inflammation have now become known as hallmarks of cancer. Of the inflammatory immune cell infiltrates, macrophages are the most abundant in the ecological niche of cancer and orchestrate the non-resolving cancer related inflammation (CRI). There is now substantial evidence to suggest that tumor associated macrophages (TAMs) engage in dynamic interplay with cancer cells, and other immune and non-immune cells in the TME, adopt a pro-tumoral phenotype, both in the primary and metastatic sites and most often correlate with poor clinical outcome. Therefore, understanding the ontogeny of TAMs, and the molecular pathways that govern their differentiation and functional phenotypes will emerge as an important prong in developing effective therapeutic strategies in combination with chemotherapy and other immunotherapies in the future.

2.1.1. Origins of TAMs and their recruitment to the TME

In neoplastic tissues, cues from malignant cells or other cells of the TME that govern the TAM differentiation and functional phenotypes are diverse in nature and vary between tumors, or even various parts of the same tumor. Therefore, there are varied TAM populations within a single tumor. Of note, most of the time

TAMs do not fit into the oversimplified M1/M2 classification mentioned earlier and exhibit complex molecular signatures. However, despite the varied intra-tumoral and intertumoral phenotypes of TAMs, they are in general polarized towards an immunosuppressed type in all cancers. As mentioned earlier, macrophages can originate from either yolk-sac derived or bone marrow derived precursors. However, the precise ontogeny of TAMs is still not entirely clear. Work over the past few decades indicate that TAMs can arise either from circulating blood monocytes, monocytic myeloid derived suppressor cells (M-MDSCs) that get recruited to the TME or from local resident tissue macrophages of embryonic origin (65). For example, in mouse gliomas, TAMs can originate from either blood monocytes or tissue resident microglial cells (66). Using genetically engineered mouse models, there have been attempts to assess the relative contribution of TAMs arising from these various sources in tumor progression. Many recent studies have documented that most TAM sub-populations in the TME arise from the $Ly6C^+$ circulating blood monocytes that invade the growing tumor in response to recruitment cues from the TME, at least in grafted tumors (67), primary mouse mammary tumors (68) and in lung metastases (57). Indeed, in mouse glioma, the $Ly6C^+$ circulating monocytes that differentiated to TAMs were causally associated with increased rate of tumor incidence and shorter disease-free survival. Interestingly, there was no significant contribution of TAMs that arose from the resident microglial cells (66). Cortez-Retamozo *et al*. proposed that circulating monocytes that give rise to TAMs originate from extramedullary hematopoiesis that allows a rapidly mobilizable reservoir of TAMs for the tumor. However, recent

lineage tracing studies have shown that bone marrow is the primary source of monocytes that differentiate to TAMs, with minimal contribution from the spleen (69).In addition, there are conflicting studies to suggest that TAMs arise from the non-classical subset of circulating monocytes (70). Hence, it is possible that the origin of TAMs depends on the tumor type and the tumor microenvironment. Additionally, their origin may also dictate their functions in the tumor (71). Some of these aspects have been discussed in more details elsewhere (72).

The tumor bed secretes a wide array of cytokines and chemokines that act as a gradient for recruiting circulating monocytes and differentiate them towards TAMs. Among these, CD62L, CX3CL1, CCL2, VEGF-A, CSF-1 are widely implicated in TAM recruitment to the TME. For instance, in solid tumors, the inflamed endothelium secretes molecules like CD34, podocalyxin, endomucin, nepmucin, MAdCAM-1, endoglycan, GlyCAM-1, Spg2000 etc., which act as ligands for CD62L expressed on circulating monocytes to recruit them to the TME. Also, tumor cells produce CX3CL1, CCL2 and VEGF-A which bind to and act through their cognate receptors, CX3CR1, CCR2 and VEGFR1 respectively to promote monocyte migration to the TME (73). Additionally, CCL2/3/4/5/22, CXCL8, Endothelin, PDGF have also been showed to promote monocyte recruitment (74).

2.1.2. Pro-tumoral role of TAMs

Tumor infiltrating macrophages assist in tumor progression in many ways. It is now well accepted that in addition to mutations acquired in the tumor cells, a persistent inflammatory micro-environment can provide necessary support to

cancer initiation (75). For example, chronic inflammation caused by Helicobacter pylori in the stomach, Crohn's disease, chronic pancreatitis have all been causally associated with cancer initiation (76-78). Macrophages significantly contribute to this process by producing molecules like IL-6, TNF-α, IFN-Y (78, 79). For example, genetically depleting STAT3 in macrophages results in chronic inflammation in the colon and subsequent invasive adenocarcinoma (80). This persistent inflammation supports a mutagenic microenvironment for the tumor cells to acquire additional mutations (78). Macrophages also produce reactive oxygen and nitrogen species which further add to the genetic instability of the cancer cells. The mutated cells recruit more inflammatory cells in a vicious cycle which further facilitates tumor formation (57, 75, 76).

During the proliferation phase of the tumor, one of the most well-known and well-characterized functions of macrophages is regulation of the 'angiogenic switch'. Macrophage secreted factors induce endothelial cells to produce VEGFA resulting in the **angiogenic switch** (81, 82). Further, $TIE2^{+}$ macrophages physically associate with endothelial cells of blood vessels through ANG2 and blockade of this association reduced angiogenesis in several tumor models (83, 84). Intriguingly, recent reports indicate macrophages can transdifferentiate to lymphatic endothelial cell precursors and contribute to lymphangiogenesis (85). Metastatic cancers, before spreading to distant sites, first colonize the draining lymph nodes. Thus, by inducing lymphangiogenesis, macrophages facilitate cancer cell metastasis. Another important criterion for cancer cell metastasis is acquirement of EMT phenotype (86). With the advancement of cancer, tumor cells

suppress the epithelial markers like E-Cadherin and upregulate mesenchymal markers like Snail and Slug. Macrophages can **induce EMT** in cancer cells in multiple cancers, including pancreatic, lung, hepatocellular and breast cancers (87-89). Macrophages also release a variety of molecules like Osteonectin, MMPs, cathepsin proteases that help remodel the surrounding extra cellular matrix and facilitate cancer cell invasion and migration (90, 91). $TIE2^{+}$ macrophages can further facilitate tumor cell **intravasation** into blood vessels (92). Recently. an anatomical structure comprising tumor cell, macrophages and endothelial cells in histological sections of primary human breast cancers has been reported. These "Tumor microenvironment for metastasis (TMEM)" structures are predictive of metastasis. Macrophages and tumor cells engage in a paracrine interaction and get aligned along blood vessels in 'lock step' fashion with the former eventually facilitating the escape of the latter into circulation (92-94).

One of the most principal factors contributing to tumor advancement and therapy failure is **suppression of the adaptive immune response** against the malignant cells in the TME. Once the recruited monocytes enter the TME, tumor cell derived factors efficiently re-educate them towards an immunosuppressive TAM phenotype. The latter, in addition to the myriad functions described earlier, potentially suppress helper T effector cell activation against the tumor by secreting elevated levels of immunosuppressive molecules like TGF-β and IL-10 and skew them towards Th2 phenotype. These molecules not only blunt helper and cytotoxic T cell response against the tumor, but also **induce the development of Tregs** (56, 95, 96). Also, in the TME, TAMs undergo metabolic reprograming. They

produce Arginase-1 and other metabolites via the indoleamine 2,3-dioxygenase (IDO) pathway which results in the starvation of T cells and their inactivation. L-Arginine is metabolized by inducible Nitric Oxide Synthase (iNOS) or Arginase-1, depending upon the M1 or M2 state of macrophages (95). TAMs secrete Arginase-1 and hence consumes L-Arginine from the TME to produce urea and L-ornithine (97, 98). Non-availability of L-Arginine restricts T cell activation (99). The Th2 cells, eosinophils and basophils in the TME also produce ample amount of IL-4, IL-10, IL-13 which elicit TAM polarization of macrophages (100-102). Tumor cells themselves secrete molecules like M-CSF and TGF-β to cause a phenotypic shift in the infiltrating macrophages (103). Most importantly, intratumoral macrophages are known to express **immune checkpoint inhibitor** molecules like PDL-1, PDL-2 and ligands for CTLA-4 in various cancers. Upon binding with their cognate ligands, these molecules potentially restrict T cell receptor (TCR) and B cell receptor (BCR) signaling and restricts their activation and proliferation (56). Enhanced expression of these checkpoint inhibitors on TAMs is one of the key factors why most of the therapies fail in the clinic or show poor benefit. Another important function of TAMs is to remove cellular debris to maintain growth permissive environment for cancer cells. In the TME, apoptotic index is usually high, either due to nutrient limitation or rapid proliferation of cancer cells. TAMs phagocytose the cellular debris and facilitate their clearance. This process of efferocytosis skews the macrophages more towards TAMs and establishes further immunosuppression in the microenvironment (104). This aspect will be discussed in more details in the relevant section.

Finally, macrophages are essential for the formation of pre-metastatic niche where disseminated cancer cells seed and colonize. Once tumor cells arrive at the target tissue, they form micro-clots with associated platelets and get arrested in tissue vessels (105). Tumor cells then secrete CCL2 and recruit circulating monocytes via CCR2 (56, 106, 107). These recruited monocytes, called metastasis associated macrophages (MAM) facilitate extravasation of cancer cells by increasing vascular permeability.

2.1.3. Approaches to target TAMs

Immunotherapy has gained a lot of focus in the treatment of several cancers lately. With increasing amount of evidences establishing a crucial role for TAMs in tumor progression, metastasis and recurrence post therapy, several macrophage centered strategies to target TAMs are currently being explored. The approaches mostly aim at either inhibiting the recruitment of macrophages and thus dampening their protumorigenic activities, or re-educate TAMs and activate them towards an inflammatory phenotype that can trigger cytotoxic responses towards cancer cells or activate T cells. A few of the various strategies employed are listed below:

Inhibiting the CSF-1/CSF-1R axis: CSF-1 is one of the most crucial molecules for myeloid cell differentiation. The ligand is overexpressed by many cancer cells, as a means to recruit and differentiate TAMs (56, 108) and their expression correlates with poor prognosis (109, 110). A number of small molecule inhibitors or antibody antagonists have been tested in multiple preclinical models (111-114). For instance, emactuzumab (RG7155), a humanized monoclonal antibody against CSF-1R decreased

TAM densities and increased CD8+ T cells in the tumor (114). It showed similar results in patients with several solid tumors enrolled in a phase I clinical trial, as part of the same study. Another similar inhibitor, Pexidartinib (PLX3397) induced regression in patients with tenosynovial giant cell tumors (115), but did not increase 6-month progression free survival in a phase II clinical trial with patients diagnosed with recurrent glioblastoma (116). In addition to this, few other CSF-1R inhibitors, namely, BZL945, GW2580 have shown positive results in mouse preclinical models, either alone or when used in combination with gemcitabine or paclitaxel based chemotherapy or other inhibitors (111, 117-119).

Re-educating TAMs towards an activated phenotype: Many of the studies aimed at depleting monocyte/macrophage recruitment into the tumor bed resulted in failure and eventual disease relapse. This is primarily because macrophages are crucial for eliciting antitumor adaptive responses. One of the most important strategies currently being explored is to re-educate the immunosuppressed TAMs and activate them towards an inflammatory M1 phenotype and prime them for triggering cytotoxicity or recruiting and activating cytotoxic T cells. IFN-γ has been tested in advanced ovarian cancer patients for its ability to induce macrophage driven cytotoxicity (120, 121). One of the most important molecules in this regard is CD40 agonist. This when administered, resulted in a shift towards M1 type macrophages, upregulated their antigen presentation ability and activated T cell responses (122). Based on these findings, a fully humanized

CD40 agonist, CP-870,893, was tested in a phase I trial in combination with chemotherapy to treat advanced stage pancreatic cancer patients. The combination therapy showed partial responses in 4 out of 22 patients and correlated with improved survival (123). Another strategy that is currently under clinical evaluation is ibrutinib, in combination with gemcitabine-nab-paclitaxel in advanced stage pancreatic cancer patients. This drug prevents the crosstalk between M2-like TAMs and B cells via the PI3Kγ-BTK pathway and re-polarized TAMs towards M1 type and triggered T cell responses (124).

Blocking recruitment of monocytes/macrophages: Cancer cells secrete a wide variety of cytokines to attract and recruit circulating monocyte and polarize them towards TAMs. Hence, many strategies have attempted to block the recruitment of monocytes/macrophages to the tumor microenvironment. Among these, treatment with anti-CCL2 antibodies in combination with chemotherapy, reduced tumor growth and metastasis in several tumor models (125-128). CCL2 antibodies have also been tested in several Phase I and Phase II clinical trials (129-131), with variable results. Another chemokine, CCL5, when targeted with antibodies (Maraviroc), also associated with clinical response in a small cohort of patients with advanced stage colorectal cancer (132). Other strategies like, bisphosphonates (which induce apoptosis in bone macrophages, osteoclasts and tissue macrophages) and trabectedin (which deplete MDSCs and also TAM

population to some extent) have also yielded positive responses in bone metastatic cancers, like breast and prostate cancers (133, 134)

Different strategies to target TAMs and the different clinical trials that are either completed or ongoing, have been discussed in more details elsewhere (65). Several studies over the past few years have attempted at investigating the biomarker potential of TAMs in several cancers. In most cases, either CD68, a pan macrophage marker or CD163 (a M2 type marker), CD204 (macrophage scavenger receptor A) or CD206 (induced by IL-4) have been used to identify tumor infiltrating macrophages. A high degree of TAM infiltration correlated with tumor grade, more advanced stage of the disease and poor clinical outcome in most of the cancers studied, including breast, bladder and pancreatic cancers. In stark contrast, a negative correlation between TAM infiltration and disease stage was observed in gastric cancers (135). Further, in some cancers, like non-small-cell-lung-cancer and colorectal cancer, a high degree of TAM infiltration correlated with a favorable patient prognosis (136, 137). Interestingly, chemotherapy/radiotherapy can significantly alter the TAM phenotype, as a result affect the overall clinical outcome and the potential of TAMs as a predictive biomarker. In many preclinical models using either chemotherapy or radiotherapy, M2-like macrophages localized in the perivascular regions of the tumor and promoted disease relapse post therapy. This can be attributed to extensive tissue damage due to therapy which results in the recruitment of myeloid cells and triggering of repair mechanisms by immunosuppressive macrophages (111, 138). For instance, in patients with Hodgkin’s Lymphoma and follicular lymphoma who

underwent chemotherapy, a high degree of $CD68^{+}$ TAMs correlated with decreased survival compared to patients who did not receive chemotherapy (139, 140). However, in follicular lymphoma patients undergoing R-CHOP regimen, increased CD163+ TAM infiltration was associated with favorable outcome (141). This indicated that TAM function largely depends on the type of treatment used and they can either hamper or bolster anti-tumor immune response. Similarly, in case of radiotherapy, it augments macrophage infiltration into irradiated tissues. TAMs then either promote tissue repair mechanisms and thereby contribute to disease recurrence by adopting an immunosuppressive phenotype or activate anti-tumor immune response in the host and decreasing metastatic burden (103, 142, 143). For example, post radiotherapy, there is an increased expression of CSF-1 and hence increased macrophage infiltration in a preclinical xenograft mouse model of human intracranial glioblastoma. However, combination therapy with radiation and Pexidartinib (CSF-1R antagonist) potentiated the therapeutic benefits of radiotherapy. One of the clever ploys deployed by cancer cells is to overexpress ‘don’t eat me’ signals like CD47, to avoid phagocytosis by macrophages or other antigen presenting cells. As expected, antibody targeting CD47 resulted in antibody dependent cellular phagocytosis (ADCP) and yielded beneficial results in several preclinical mouse studies and have entered clinical trials. Moreover, targeting CD47 which is expressed by cancer stem cells at large, enabled the phagocytosis and removal of the latter by macrophages. Further, targeting CD47 in combination with chemotherapy showed beneficial results in patient derived xenograft models (144). Also, blocking CD47 in combination with

PDL1 blockade resulted in enhanced antitumor responses (145). However, tumor cell phagocytosis is a contentious topic. Increased phagocytosis of tumor cells by macrophages although beneficial at first, however, it skews the TAMs more towards protumorigenic type. The latter associates with recurrence and metastasis by creating an immunosuppressive microenvironment (104). Further, conventional anti-angiogenic therapies mostly fail because of increased infiltration of myeloid cells. Hypoxia resulting from vasculature destruction by anti-angiogenic drugs induces enhanced infiltration of macrophages that can then trigger angiogenic responses. Moreover, macrophages often overexpress immune checkpoint inhibitor molecules, like PDL-1, PDL-2, ligands for CTLA-4 among others. These are often further upregulated on macrophages in response to hypoxia (146). Antibody mediated targeting of CTLA-4 resulted in the removal of Tregs by the FcγR+ macrophages (147, 148). Therefore, synergistically targeting TAMs with anti-checkpoint inhibitor antibodies may be clinically beneficial and are currently undergoing early clinical assessment. Overall, these suggest that even though macrophage centered therapeutic strategies are currently being explored, they will probably yield best results when used in combination with other standard of care therapies or to complement other immunotherapies.

Fig. 2.1. Origin of tumor associated macrophages. Blood monocytes and monocyte derived suppressor cells (MDSCs) get recruited to the tumor tissue in response to a wide array of chemokines and cytokines released from the tumor. Once they infiltrate the tumor tissue, the monocytes and MDSCs differentiate to TAMs following exposure to tumor microenvironment derived factors. In some cancers, tissue resident macrophages can proliferate *in situ* and give rise to TAMs. This figure has been adapted from Mantovani et al. “Tumour-associated macrophages as treatment targets in oncology.” Nat Rev Clin Oncol. 2017. doi: 10.1038/nrclinonc.2016.217. with permission.

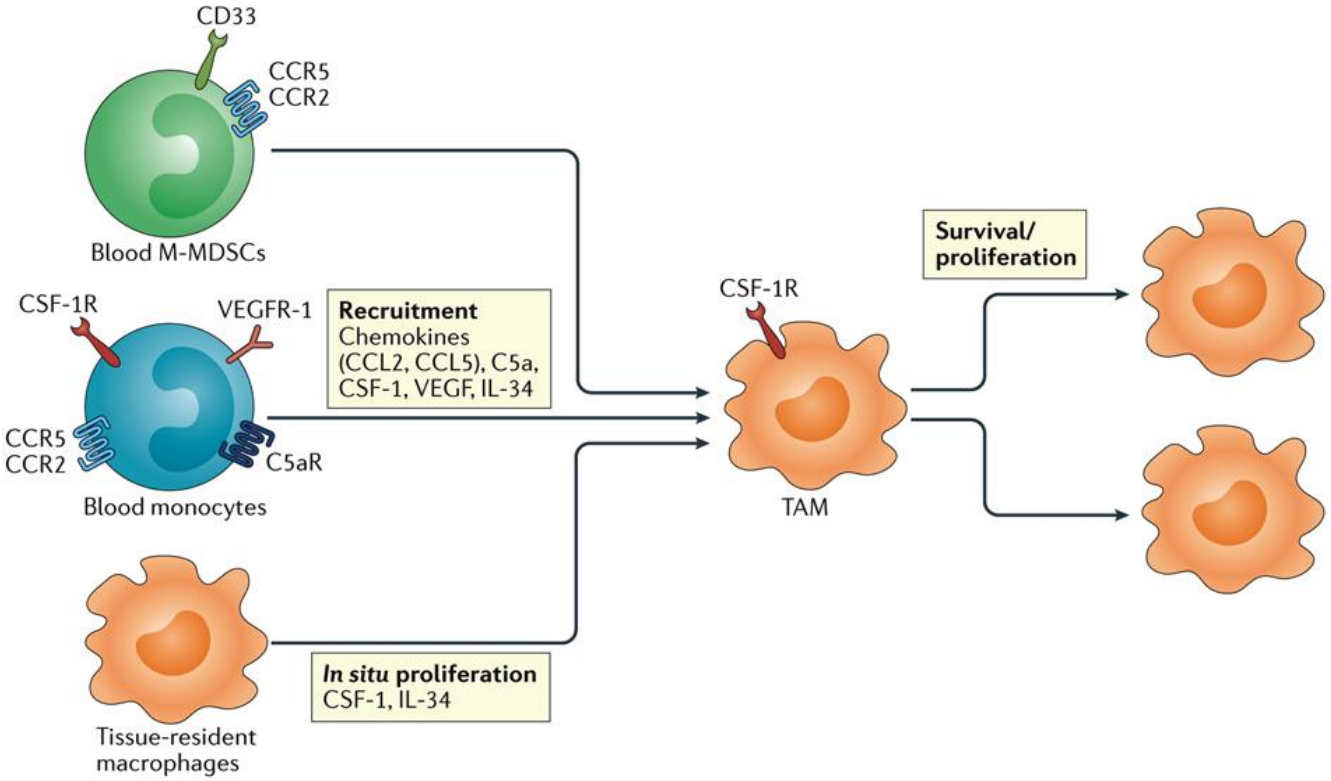
CD33
CCR5
CCR2
Blood M-MDSCs
CSF-1R
VEGFR-1
CCR5
CCR2
C5aR
Blood monocytes
Recruitment
Chemokines
(CCL2, CCL5), C5a,
CSF-1, VEGF, IL-34
CSF-1R
TAM
Survival/
proliferation
In situ proliferation
CSF-1, IL-34
Tissue-resident
macrophages

Fig. 2.2. TAMs promote immune suppression in the tumor microenvironment. TAMs engage in cross-talk with other immune cell types in the microenvironment to suppress anti-tumor immune response. TAMs secrete immunosuppressive cytokines like IL-10, TGF-β which promote T_{reg} cell formation and inhibit dendritic cell maturation. Metabolic reprogramming of TAMs result in metabolic starvation of T cells and inhibit their activation and effector functions. They also upregulate checkpoint inhibitor molecules like PDL-2 to further inhibit T cell activation. This figure has been adapted from Mantovani et al. “Tumour-associated macrophages as treatment targets in oncology.” Nat Rev Clin Oncol. 2017. doi: 10.1038/nrclinonc.2016.217. with permission.

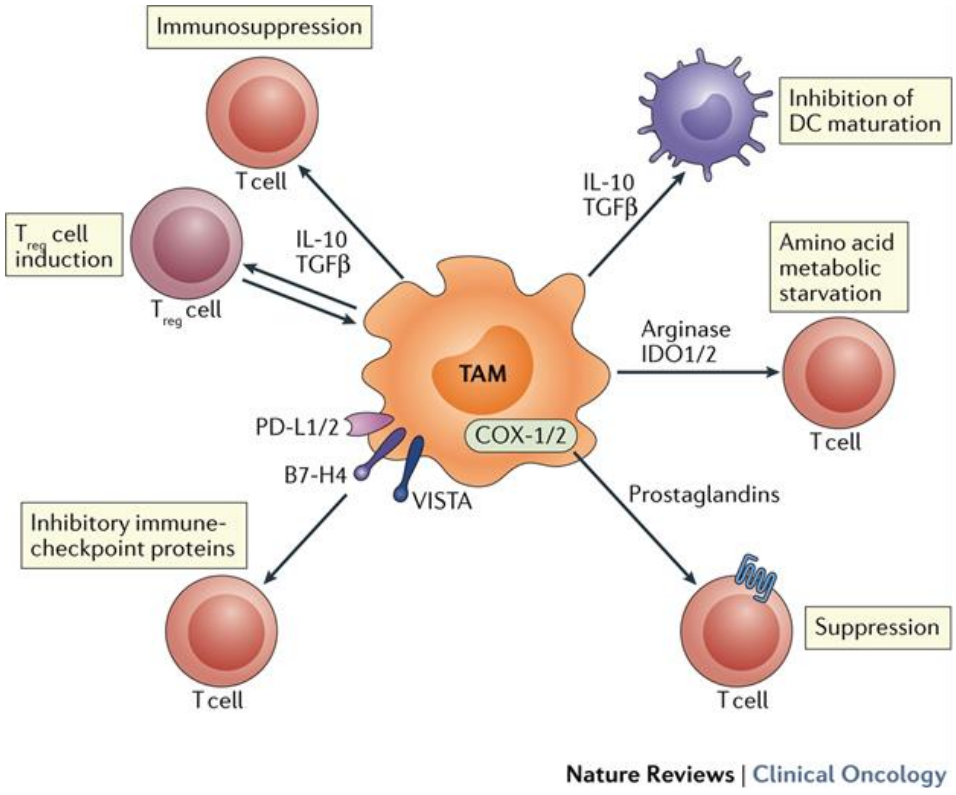
Immunosuppression
T cell
Inhibition of DC maturation
IL-10
TGFβ
T reg cell induction
IL-10
TGFβ
T reg cell
Amino acid metabolic starvation
Arginase
IDO1/2
TAM
T cell
PD-L1/2
COX-1/2
B7-H4
VISTA
Prostaglandins
Inhibitory immune-checkpoint proteins
T cell
Suppression
T cell
Nature Reviews | Clinical Oncology

Fig. 2.3. TAMs promote tumor cell intravasation. TAMs engage in a bi-directional cross-talk with tumor cells and promote tumor cell invasion. TAMs produce TGF-β that induce EMT in cancer cells and facilitate their migration and matrix remodeling and adhesion to matrix proteins. CSF-1 from tumor cells and EGF from cancer cells potentially results in their 'lock-step' conformation and the two cell types migrate together along the collagen fibers towards blood vessels. The cancer cells then pile up on the blood vessels and the macrophages help them intravasate through a structure known as ""Tumor Microenvironment of Metastasis" (TMEN). This figure has been adapted from Noy et al. "Tumor-Associated Macrophages: From Mechanisms to Therapy." Immunity. 2014. doi.org/10.1016/j.immuni.2014.09.021. with permission.

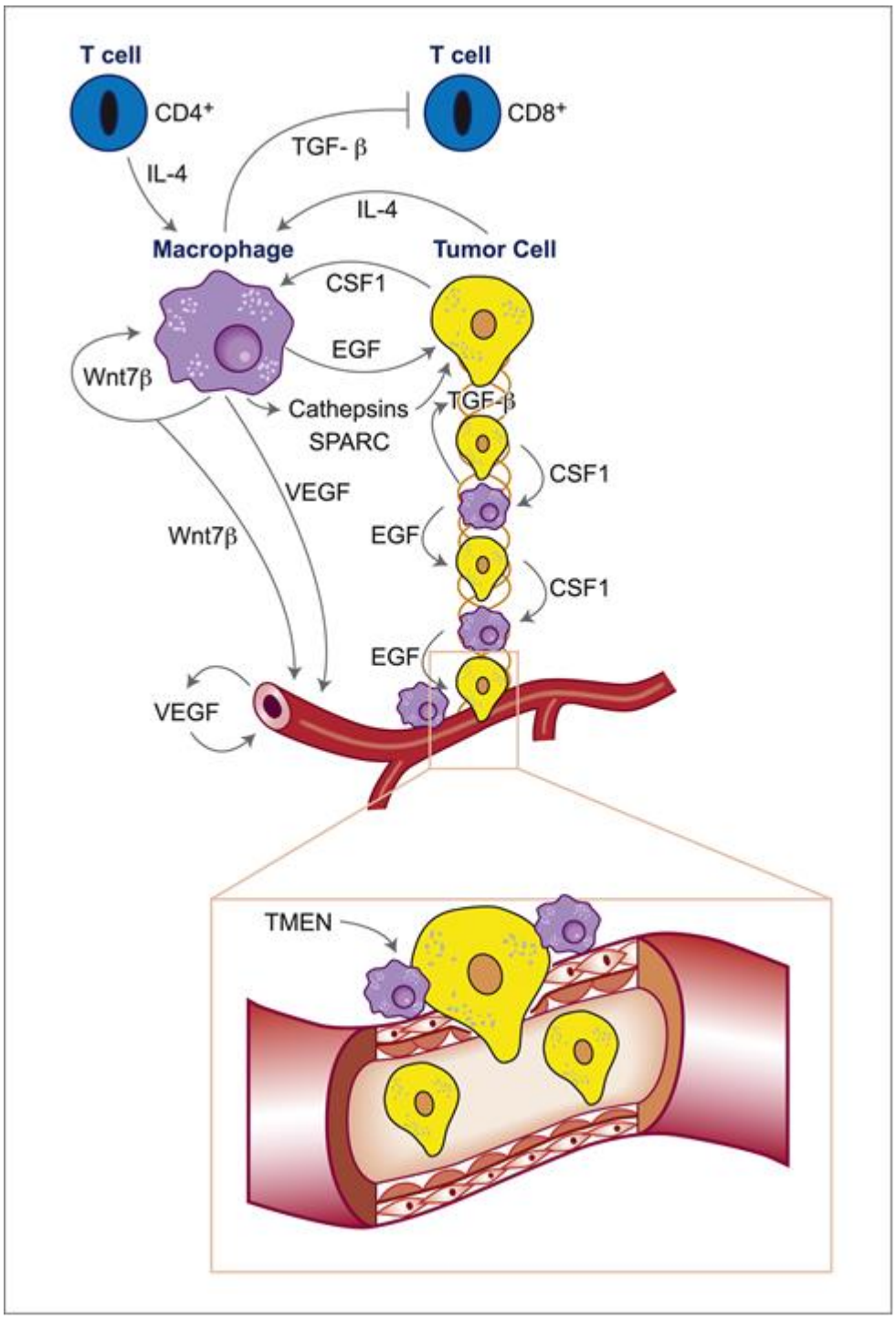
T cell
CD4+
T cell
CD8+
TGF- β
IL-4
IL-4
Macrophage
Tumor Cell
CSF1
EGF
Wnt7β
Cathepsins
SPARC
TGF-β
CSF1
VEGF
Wnt7β
EGF
CSF1
EGF
VEGF
TMEN

Fig. 2.4. TAMs promote tumor metastasis. Once the tumor cells are arrested in the blood vessels of target seeding organs, macrophages facilitate their extravasation into the tissue by increasing the vascular permeability. Also, TAMs promote survival of the tumor cells in the new metastatic site and suppress immune cell activation. This figure has been adapted from Noy et al. “Tumor-Associated Macrophages: From Mechanisms to Therapy.” Immunity. 2014. doi.org/10.1016/j.immuni.2014.09.021. with permission.

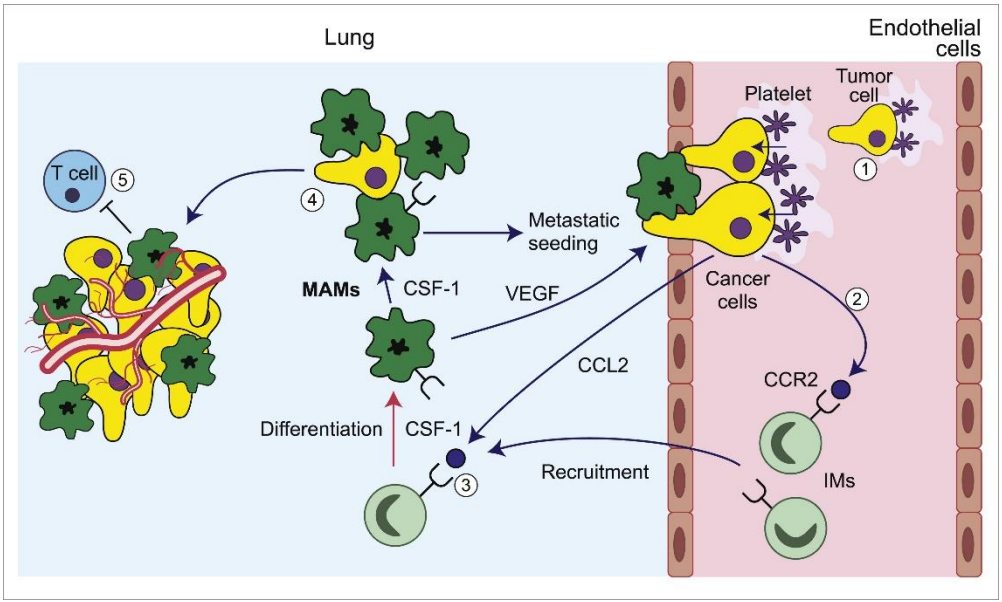
Lung
Endothelial cells
Platelet
Tumor cell
T cell
5
4
1
Metastatic seeding
MAMs
CSF-1
VEGF
Cancer cells
2
CCL2
CCR2
Differentiation
CSF-1
Recruitment
IMs
3

Fig. 2.5. Brief summary of different clinical trials to target TAMs. This figure has been adapted from Mantovani et al. “Tumour-associated macrophages as treatment targets in oncology.” Nat Rev Clin Oncol. 2017. doi: 10.1038/nrclinonc.2016.217. with permission.

Table 2 | **Clinical trials of agents targeted at macrophages in tumours**

Compound (sponsor)	Clinical phase (status)	Tumour type	Combination partner(s)	ClinicalTrial.gov reference
CSF-1R inhibitors				
Pexidartinib (PLX3397; Plexxikon)	Phase I/II (ongoing)	Sarcoma, nerve-sheath tumours	Sirolimus	NCT02584647
	Phase II (ongoing)	Melanoma	NA	NCT02071940
	Phase I (ongoing)	Prostate cancer	Radiotherapy and ADT	NCT02472275
	Phase I/II (ongoing)	Solid tumours	Pembrolizumab (anti-PD-1 antibody)	NCT02452424
	Phase I (ongoing)	Advanced-stage pancreatic cancer or CRC	Durvalumab (anti-PD-L1 antibody)	NCT02777710
	Phase III (ongoing)[180]	PVNS or GCT-TS	NA	NCT02371369
	Phase III (ongoing)	Breast cancer	Eribulin	NCT01596751
	Phase Ib/II (ongoing)	Leukaemia, sarcoma, or neurofibroma	NA	NCT02390752
	Phase I/II (ongoing)	Acute myeloid leukaemia	NA	NCT01349049
	Phase I/II (ongoing)	Glioblastoma	Radiotherapy and temozolomide	NCT01790503
	Phase I (ongoing)	Advanced-stage solid tumours	Paclitaxel	NCT01525602
	Phase I/II (ongoing)	Breast cancer	Standard neoadjuvant chemotherapy*	NCT01042379
PLX7486 (Plexxikon)	Phase I (ongoing)	Advanced-stage solid tumours	NA	NCT01804530
Anti-CSF-1R antibodies				
LY3022855 (IMC-CS4; Eli Lilly)	Phase I (ongoing)	Solid tumours	Durvalumab (anti-PD-L1 antibody) and tremelimumab (anti-CTLA-4 antibody)	NCT02718911
	Phase I (ongoing)	Breast or prostate cancer	NA	NCT02265536
	Phase I (ongoing)	Solid tumours	NA	NCT01346358
Emactuzumab (RO5509554/ RG7155; Roche)	Phase I (ongoing)	Solid tumours	Atezolizumab (anti-PD-L1 antibody)	NCT02323191
	Phase I (ongoing)[158,159]	Solid tumours	± Paclitaxel	NCT01494688
AMG820 (Amgen)	Phase I/II (ongoing)	Pancreatic cancer, CRC, or non-small-cell lung cancer	Pembrolizumab (anti-PD-1 antibody)	NCT02713529
	Phase I (completed)	Solid tumors	NA	NCT01444404
Anti-CD47 antibodies				
Hu5F9-G4 (Stanford University)	Phase I (ongoing)	Myeloid leukaemia	NA	NCT02678338
CC-90002 (Celgene)	Phase I (ongoing)	Myeloid leukaemia or myelodysplastic syndrome	NA	NCT02641002
	Phase I (ongoing)	Advanced-stage solid or haematological malignancies	NA	NCT02367196
CD47–Fc fusion protein				
TTI-621 (Trillium)	Phase I (ongoing)	Haematological malignancies	NA	NCT02663518
Agonistic anti-CD40 antibodies				
CP-870,893 (Pfizer, UPenn)	Phase I (completed)	Melanoma	NA	NCT02225002
	Phase I (completed)	Solid tumours	Paclitaxel and carboplatin	NCT00607048
	Phase I (completed)[181]	Pancreatic adenocarcinoma	Gemcitabine	NCT01456585
RO7009789 (Roche)	Phase I (ongoing)	Solid tumours	Vanucizumab (anti-ANG-2–VEGF bispecific antibody)	NCT02665416
	Phase I (ongoing)	Pancreatic adenocarcinoma	Nab-paclitaxel and gemcitabine	NCT02588443
Anti-IL-1α antibody				
Xilonix (XBiotech)	Phase III (ongoing)	CRC	NA	NCT01767857
Anti-CCL2 antibodies				
Carlumab (CNTO 888; Centocor)	Phase II (completed)[147]	Prostate cancer	NA	NCT00992186
	Phase I (completed)[144,149]	Solid tumours	Gemcitabine, paclitaxel and carboplatin	NCT01204996
CCR2 antagonist				
PF-04136309 (Pfizer)	Phase I (completed)[150]	Advanced-stage pancreatic adenocarcinoma	FOLFIRINOX	NCT01413022
Bruton kinase inhibitor				
Ibrutinib	Phase II/III (ongoing)	Pancreatic adenocarcinoma	Gemcitabine and nab-paclitaxel	NCT02436668
Modified vitamin-D-binding protein (macrophage-activating factor)				
EF-022 (Efranat)	Phase I (ongoing)	Solid tumours	NA	NCT02052492

Data were obtained from http://clinicaltrials.gov. ADT, androgen-deprivation therapy; ANG-2, angiopoietin-2; CRC, colorectal cancer; CTLA-4, cytotoxic T-lymphocyte-associated protein 4; FOLFIRINOX, 5-fluorouracil, folinic acid, irinotecan, and oxaliplatin; GCT-TS, giant-cell tumour of the tendon sheath; NA, not applicable; PD-1, programmed cell-death protein 1; PD-L1, programmed cell death 1 ligand 1; PVNS, pigmented villonodular synovitis; UPenn, University of Pennsylvania; VEGF, vascular endothelial growth factor. *In this trial, I-SPY 2, various experimental agents are being added to standard neoadjuvant therapy (with paclitaxel, doxorubicin, cyclophosphamide and trastuzumab (anti-HER2 antibody), depending on molecular subtype), including: pexidartinib; trebananib (AMG 386; angiopoietin-1/2-neutralizing 'peptibody') with or with trastuzumab; ganitumab (AMG 479; anti-IGF-1R) plus metformin; MK-2206 (AKT inhibitor) with or without trastuzumab; T-DM1 (trastuzumab emtansine) and pertuzumab (anti-HER2 antibody); pertuzumab and trastuzumab; ganetespib (heat shock protein 90 inhibitor); veliparib (ABT-888; poly[ADP-ribose] polymerase inhibitor); neratinib (HER2 tyrosine kinase inhibitor); and pembrolizumab (anti-PD-1 antibody).

Fig. 2.6. TAMs are double-edged swords in cancer therapies. TAMs can either increase or dampen the therapeutic efficacy for anti-cancer treatments. Some conventional therapies (like doxorubicin, gemcitabine) can either promote the formation of antigen presenting cells or skew TAMs towards inflammatory M1 type. On the other hand, cytotoxic therapies or radiation therapies cause cell death and tissue damage which recruit fresh myeloid cells. The latter trigger a misdirected tissue repair response, re-vascularization, protection of cancer stem cell niche and suppression of adaptive immune response. This figure has been adapted from Mantovani et al. “Tumour-associated macrophages as treatment targets in oncology.” Nat Rev Clin Oncol. 2017. doi: 10.1038/nrclinonc.2016.217. with permission.

Nature Reviews | Clinical Oncology

Fig. 2.7. TAMs after chemotherapy as predictor for patient outcome. TAMs can either foster or dampen therapeutic efficacy of anti-cancer treatments and hence can act as predictor for clinical outcome following therapy. This figure has been adapted from Mantovani et al. “Tumour-associated macrophages as treatment targets in oncology.” Nat Rev Clin Oncol. 2017. doi: 10.1038/nrclinonc.2016.217. with permission.

Table 1 | **High density of TAMs as a predictor of patient outcomes after chemotherapy for neoplasia**

Study (year of publication)	Tumour type	Therapy	TAM markers	High TAM density	Outcome prediction
Farinha *et al.*[68] (2005)	Follicular lymphoma	BP–VACOP followed by involved region radiation	CD68	>15 macrophages/HPF (×1,000)	Negatively correlated with DFS and OS (≤0.001)
Taskinen *et al.*[70] (2007)	Follicular lymphoma	CHOP	CD68	Highest decile	Negative correlated with DFS ($P = 0.026$)
		CHOP + rituximab	CD68	Highest tertile	Positively correlated with DFS ($P = 0.006$)
Steidl *et al.*[66] (2010)	Classic Hodgkin lymphoma	ABVD*	CD68	>25–50% positive cells	Negatively correlated with DSS ($P = 0.003$)
E2496 Intergroup trial; Tan *et al.*[67] (2012)	Classic Hodgkin lymphoma (locally advanced and advanced stage)	ABVD	CD68	>12.7% of positive pixels	Negatively correlated with DFS and OS (both $P < 0.01$)
			CD163	>16.8% of positive pixels	Negatively correlated with DFS ($P = 0.03$) and OS ($P = 0.04$)
		Stanford V	CD68	>12.7% of positive pixels	Negatively correlated with DFS ($P < 0.01$) and OS ($P = 0.02$)
			CD163	>16.8% of positive pixels	Negatively correlated with DFS and OS (both $P < 0.01$)
Kridel *et al.*[71] (2015)	Follicular lymphoma	CVP + rituximab	CD163	>3.97% of positive pixels	Negatively correlated with DFS ($P = 0.004$)
		CHOP + rituximab	CD163	>0.16% of positive pixels	Positively correlated with DFS ($P = 0.01$ training, $P = 0.03$ validation)
Algars *et al.*[55] (2012)	Colorectal cancer (stage III)	Unspecified‡	CLEVER-1/ stabilin-1§	>10 peritumoral/0.0625 mm^2 (×400)	Positively correlated with DSS ($P = 0.05$)
			CD68	>30 peritumoral/0.0625 mm^2 (×400)	Positively correlated with DSS on univariate analysis, but not significantly ($P = 0.09$)
Di Caro *et al.*[45] (2016)	Pancreatic cancer	No adjuvant chemotherapy	CD68	Highest quartile	Negatively correlated with DFS ($P = 0.02$)
		Gemcitabine-based adjuvant chemotherapy	CD68	Highest quartile	Positively correlated with DSS ($P = 0.05$)
Malesci *et al.* (unpublished data)	Colorectal cancer (stage III)	No adjuvant chemotherapy	CD68	>8% of cells in immune-reactive area (tumour border)	None
		5-FU-based adjuvant chemotherapy	CD68	>8% of cells in immune-reactive area (tumour border)	Positively correlated with DFS ($P < 0.001$)

5-FU, 5-fluorouracil; ABVD, doxorubicin, bleomycin, vinblastine, and dacarbazine; BP–VACOP, bleomycin, cisplatin, etoposide, doxorubicin, cyclophosphamide, vincristine, and prednisone; CHOP, cyclophosphamide, doxorubicin, vincristine, and prednisone; CVP, cyclophosphamide, vincristine, and prednisone; CVPP, cyclophosphamide, vinblastine, procarbazine, and prednisone; DFS, disease-free survival; DSS, disease-specific survival; GDP, gemcitabine, dexamethasone, and cisplatin; HPF, high-power field; OS, overall survival; TAM, tumour-associated macrophage. *Or ABVD-like, with or without radiation therapy. Second-line therapy comprised autologous stem-cell transplantation, CVPP or GDP chemotherapy, and/or field radiation. ‡5-FU and folinic acid plus oxaliplatin (FOLFOX) adjuvant chemotherapy is the standard-of-care for stage III colorectal cancer. §CLEVER-1 and stabilin-1 were used as a marker of alternatively activated M2 macrophages.

Fig. 2.8. Different approaches to target TAMs. Various approaches are being tried to either promote the cytotoxicity of TAMs by re-programing them to M1-type, activation of adaptive responses or inhibit their recruitment, survival or immunosuppression caused by them. This figure has been adapted from Mantovani et al. “Tumour-associated macrophages as treatment targets in oncology.” Nat Rev Clin Oncol. 2017. doi: 10.1038/nrclinonc.2016.217. with permission.

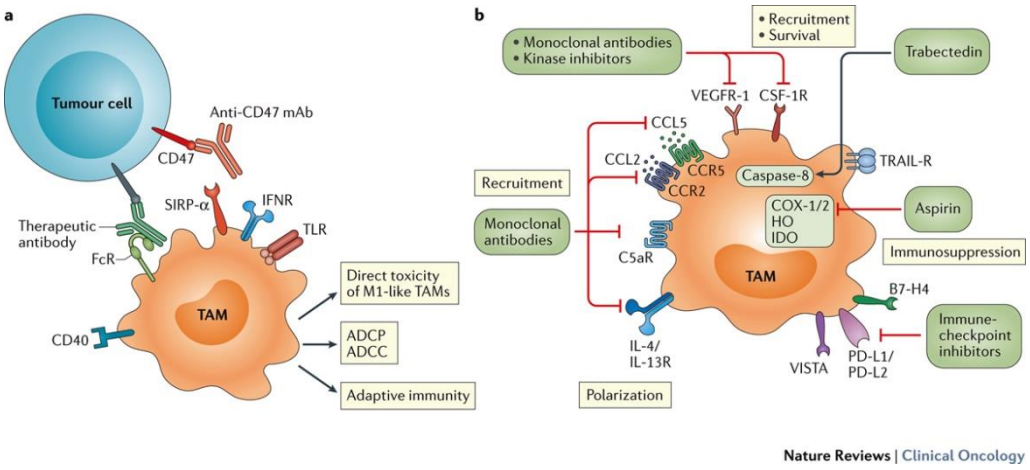

Nature Reviews | Clinical Oncology

2.2. A brief overview of Pancreatic Cancer

2.2.1. Epidemiology

Pancreatic Cancer is one of the most lethal type of cancers and accounts for 3% of all cancers and 7% of all cancer related deaths in the United States. The American Cancer Society predicts 53,670 people will be diagnosed with pancreatic cancer in 2017. The mortality rate due to the disease is estimated at 43,090 in the United States alone in 2017 (2017 Cancer Facts and Figures of American Cancer Society). It is the 3rd leading cause of cancer related deaths in the US. By 2020, it is estimated to become the 2nd leading cause of cancer related deaths in the US, surpassing colorectal cancer. Early stages of Pancreatic Cancer are asymptomatic, however, for patients diagnosed with symptoms, the disease has already metastasized where less than 15% cases are suitable for surgical resection (149). Hence, chemotherapy presents the standard and only line of care for most of the patients, but gemcitabine provides only modest regression of the cancer. Almost all the patients undergoing therapy rapidly develop chemoresistance. Pancreatic cancer is one of the few cancers for which the 5-year survival rate has not improved significantly in the last 40years with 74% of patients dying within the first year of diagnosis and only 9% of the patients surviving more than 5 years. Despite extensive research, we are still desperately searching for the ‘magic bullet’ that can cure pancreatic cancer. There are several risk factors that have been associated with the disease. For example, obesity and inactivity, use of tobacco, exposure to certain chemicals, Type 2 diabetes, chronic pancreatitis, Cirrhosis of the liver, diets rich in fat have all been causally associated

with pancreatic cancer. In addition, genetic alterations or familial predisposition can also cause pancreatic cancer. For example, hereditary breast and ovarian cancer syndrome caused by BRCA1/2 gene mutation, familial atypical multiple mole melanoma (FAMMM) syndrome caused by mutations in the *p16/CDKN2A* gene, *hereditary non-polyposis colorectal cancer* (HNPCC) caused by a defect in MLH1 or MSH2 gene, familial pancreatitis caused by mutations in PRSS1 gene, Peutz-Jeghers syndrome, caused by defects in the *STK11* gene, Von Hippel-Lindau syndrome, caused by mutations in the *VHL* gene can all increase the risk of exocrine pancreatic cancer. (Detailed information regarding the causes, risk factors and prevention of pancreatic cancer is available in the official webpage of American Cancer Society). Pancreatic cancer stage and grade is measured using the standard TNM system, where T stands for the primary tumor size, N means whether the cancer has spread to nearby lymph nodes and finally M, indicating if the disease has metastasized to distant organs (more detailed information about the TNM grading can be found on the webpage https://www.cancer.org/cancer/pancreatic-cancer/detection-diagnosis-staging/staging.html).

2.2.2. Pathology

The pancreas is a unique organ comprising of both exocrine and endocrine glands. The exocrine gland secretes digestive enzymes like chymotrypsinogen, trypsinogen amylase and pancreatic lipase. The endocrine gland, more commonly known as the Islets of Langerhans, produce 3 types of hormones into the blood stream, namely, glucagon, insulin and somatostatin. Pancreatic cancer can

broadly be of two main types, exocrine neoplasia and endocrine neoplasia, as described below in details:

Exocrine cancer is most common type of pancreatic malignancy. About 95% of pancreatic tumors are adenocarcinomas (pancreatic ductal adenocarcinoma, PDAC). PDAC appears as a white yellow mass with the surrounding normal pancreatic tissue showing signs of atrophy, fibrosis and dilated ducts (150). The neoplasms can either present as well differentiated glands (carcinoma) or poorly differentiated sarcomatoid carcinomas (151). PDAC evolves from either of three types of pre-neoplastic lesions, namely, microscopic pancreatic intraepithelial neoplasia (PanIN), macroscopic cysts, namely, the intraductal papillary mucinous neoplasm (IPMN) and mucinous cystic neoplasm.

The most well characterized and by far the most common precursor lesions for PDAC development are PanINs. Based on their cytological and architectural irregularities, PanINs were categorized as: PanIN-1A (flat lesion) and PanIN-1B (micropapillary type) that show low-grade dysplasia; PanIN-2 lesions that develop features like, additional loss of cell polarity, nuclear crowding, cell enlargement, and hyperchromasia with frequent papillary formation; PanIN-3 is the most advanced lesions clinically and exhibit severe nuclear atypia, luminal necrosis, and epithelial cell budding into the ductal lumen (152-154). However, recently, this three-tier classification has been replaced by a revised two-tier low grade (PanIN-1 and PanIN-2) and high grade (PaniN-3) classification system. As per this system, the high-grade lesions have the most potential to generate PDAC (155). Indeed, low grade lesions are common in adult normal pancreas or patients suffering from

chronic pancreatitis. But PanIN-3 lesions are exclusively detected in invasive PDAC (154).

IPMNs are less ordinary form of precursor lesion for PDAC. They arise in the main pancreatic duct or its major branches and are characterized by papillary like elongation of ductal epithelium and production of mucin (151, 152). Although they present better prognosis, there have been multiple incidences where IPMNs advanced to malignancy. Previously they were classified as villous dark cell type, papillary clear cell type, and compact cell type, in combination of mucin expression profiles. Later, based on morphology and mucin expression profiles, they were re-classified into gastric type (=papillary clear cell type), intestinal type (=villous dark cel type), pancreatobiliary type, and oncocytic type (=compact cell type, =intraductal oncocytic papillary neoplasm (IOPN) (156, 157). Benign, borderline, and malignant lesions are detected in gastric and intestinal types, however, progression of IPMNs into carcinoma usually occurs from the intestinal type (158). The pancreatobiliary type and oncocytic type are mostly malignant lesions (156, 157). Mucinous cystic neoplasms (MCNs) are rare and slow growing pre-neoplastic lesions. They are found only in women, and are characterized by the development of epithelial cysts that are lined by mucin producing cuboidal or columnar cells and remain surrounded by ovarian stroma. Given their larger size, MCNs are easily distinguished from PanINs. Further, they can be categorized as either adenoma, borderline or malignant non-invasive or invasive neoplasia (152). Several other pancreatic cancers, relatively less common, of exocrine origin are known, for example, adenosquamous carcinomas, squamous cell carcinomas,

signet ring cell carcinomas, undifferentiated carcinomas, and undifferentiated carcinomas with giant cells (https://www.cancer.org/cancer/pancreatic-cancer/about/what-is-pancreatic-cancer.html).

Acinar cell carcinoma is a rare exocrine pancreatic neoplasia and accounts for less than 2% of exocrine pancreatic cancers. The malignant cells produce elevated levels of pancreatic enzymes like lipases and appear granular under the microscope. This is because they contain excess amount of zymogen in their cytosol. In ACC, the malignant cells can be arranged in two fashions: acinar, where the cells form a thin lumen with basal nuclei and moderate amount of eosinophilic cytosol in the apical portion of the cells, or solid, where the cells are arranged as sheets or nests with no apparent lumen. Basally palisaded nuclei can be detected at the interface of solid nests of malignant cells and stroma (152). Adenosquamous carcinoma, another rare variety, forms glands as adenocarcinoma but cells undergo squamous differentiation with disease progression. Colloid carcinoma is another form of exocrine pancreatic cancer where nests of cancer cells appear to be floating in extracellular mucin. This form of the disease is comparatively less aggressive. Hepatoid carcinoma is a very rare disease where the cancer cells appear like liver cells. Mucinous cystic neoplasm is more commonly found in women, where malignant cysts containing mucin forms at the tail of the pancreas and can become invasive over time. Pancreatoblastomas, more commonly known as pancreatic cancer of infancy, is found in children. The cancer cells look like nests of squamoid cells floating in a pool of more uniform looking cells, but can undergo acinar and neuroendocrine differentiation. Serous Cystadenomas is a

benign cystic tumor that can be surgically removed. Signet Ring cell carcinoma, another rare variety of pancreatic cancer, is characterized by the presence of large mucin globule in the cells that pushes the nucleus to the side of the cell, giving it a signet ring like appearance. Solid-Pseudopapillary Neoplasms are found in women in their 30's. Some parts of the tumors can be solid or produce finger like projections. Although less harmless, it can metastasize if not removed. Undifferentiated carcinomas are extremely aggressive in nature and the malignant cells do not resemble any cell type in the body. Undifferentiated Carcinoma with Osteoclast-like Giant Cells is another extremely rare type of exocrine pancreatic cancer where the individual malignant cells become gigantic and resemble osteoclasts in the bone (http://pathology.jhu.edu/pc/BasicTypes2.php?area=ba).

Pancreatic endocrine tumor (PNET) is more commonly known as Islet cell tumor. 1 in every 100,000 people is diagnosed with this rare type of disease and accounts for less than 2% of all pancreatic tumors (159). It is less aggressive than pancreatic exocrine tumors and grows more slowly. Although the exact molecular mechanism of PNET is not clearly determined, people with four types of inherited disorders, namely, Multiple Endocrine Neoplasia Type I (caused by a mutation in *MEN1* gene on chromosome 11q13), von Hippel-Lindau disease (arises due to mutation in *VHL* gene on chromosome 3), von Recklinhausen's disease (caused by NF1 gene on chromosome 17) and tuberous sclerosis complex (caused by mutation in TSC1 and TSC2 genes on chromosome 8) have been reported to have higher incidence of PNET. Intriguingly, PNET encompasses a broad range of neoplasms of the pancreatic endocrine cells and can either be insulinomas (insulin

secreting tumors), gastrinomas (gastrin secreting tumor), glucagonomas (glucagon secreting tumors), VIPomas (vasoactive intestinal polypeptide secreting tumor), somatostatinomas (somatostatinoma secreting tumor) and GRFomas (growth hormone releasing factor, GRF secreting tumor). PNET can also be non-functional, meaning these tumors do not produce any hormone and therefore hard to detect at early stages of development and are only diagnosed when the disease has advanced into late stages (https://www.pancan.org/facing-pancreatic-cancer/learn/types-of-pancreatic-cancer/endocrine-pancreatic-neuroendocrine-tumors/).

2.2.3. Role of the Tumor Micro-environment in PDAC: current therapies and challenges

A key distinguishing feature of PDAC is the strong desmoplastic stroma that constitutes the bulk of the tumor. The robust desmoplastic reaction comprises of cancer associated fibroblasts, pericytes, endothelial cells, various immune cell infiltrates, pancreatic stellate cells and several cytokines and growth factors that remain in a complex extra cellular matrix (ECM) and contribute to disease pathogenesis and clinical outcome. The complex stroma in PDAC can be separated into the following compartments: the tumor cells, the hematopoietic compartment, the mesenchymal compartment and the ECM. The pancreatic tumor cells secrete cytokines and chemokines to recruit the immune cells and arrest them in a dysfunctional stage. For example, the tumor cells secrete G-MCSF to induce the generation of MDSCs. They also express inhibitory ligands like PDL-1, TGF-β, IL-10 and IDO that can directly suppress the activity of CD8 T cells. The stroma

acts as a physical barrier and restricts successful delivery of therapeutic drugs. For example, in the PDAC TME, there is extensive secretion from tumor cells and deposition of the glycosaminoglycan hyaluronan or hyaluronic acid (HA) (160). HA is negatively charged and therefore can imbibe large amount of water, expand and exert stress on the collagen fibers. The latter contract under the tensile stress, increase the interstitial fluid pressure (IFP) which ultimately results in vascular collapse and hence the hypoperfusion (161) and limited access of drugs to the tumor interior. Indeed, treatment with pegylated hyalurinidase (PEGPH20) degraded HA, decreased IFP and improved drug delivery by increasing intratumoral vessel patency (161, 162). Administration of PEGPH20 in combination with gemcitabine decreased the metastatic burden and increased the objective response rate (161). A recent phase III clinical trial in combination with gemcitabine improved survival in metastatic PDAC patients (163). Other potential targets include cancer associated collagen, decorin, fibronectin, versican, and connective tissue growth factor (CTGF), all of which have been reported to correlate with PDAC progression (164). A monoclonal antibody against CTGF in combination with gemcitabine is currently used in clinical investigation in PDAC patients (NCT01181245). The pancreatic stellate cells (PSC) also play a significant role in stromal resistance in PDAC. Pancreatic tumor cells stimulate the PSCs become activated to myofibroblasts and secrete ECM components and promote fibrogenesis (165). Olive *et al.* showed that inhibition of Sonic Hedgehog pathway (Shh) can deplete the stroma and improve drug delivery by increasing vascularity (166). However, it was accompanied with rapid development of therapy resistance

and more aggressive disease features. Additionally, a phase I and phase II clinical trial launched by Infinity Pharmaceuticals was stopped owing to poor clinical performance of the drug.

Intriguingly, the significance of the hematopoietic compartment in PDAC can be understood from the fact that they constitute 50% of the total cells in the PDAC tissue. As in the case of most tumors, in PDAC, the infiltrating macrophages (TAMs), MDSCs, and T cells engage in complex paracrine signaling that eventually results in suppression of T cell response and generation of Tregs and MDSCs. In human PDAC, the frequency of MDSCs in circulation correlates with the stage of the disease (167). Frequency of Granulocyte MDSC (Gr-MDSC) correlates with more advanced stage of the disease (168). Depletion of MDSC in autochthonous PDAC model resulted in activation and infiltration of T cells (169). However, depletion of Gr-MDSC increased the population of monocytic MDSC (Mo-MDSC). Additionally, a recent phase I study aimed at depleting Gr-MDSCs did not work in patients (170). This creates an immune privileged TME that aids and abets the tumor progression. Tregs comprise another significant factor for therapy failure. They accumulate as early as in pre-invasive lesions, thereby dampening T cell response from the earliest stages of disease progression (169) and abundantly present in the blood, lymph nodes and primary lesion in PDAC patients (171, 172) and correlated with poor survival (173). Currently, several strategies are being tested to target Tregs (174). For example, two approved antibodies against the immune checkpoint inhibitor CTLA-4, namely Ipilimumab and Tremelimumab are currently being tested in several clinical trials in PDAC. Although Ipilimumab failed

to show significant benefit in a phase II clinical trial of locally advanced or metastatic disease, it has shown promise when used in combination with GVAX, a G-MCSF gene transfected vaccine aimed at activating immune cell response (175). Currently several other clinical trials are ongoing where patients are being treated with a combination of Ipilimumab and GVAX or Ipilimumab and gemcitabinehydrochloride (https://clinicaltrials.gov/ct2/show/study/NCT01896869,https://clinicaltrials.gov/ct2/show/NCT01473940). Another potential immunotherapeutic method is genetically modifying autologous T cells and adoptively transfer them back to the patients to equip them to mount immune response against the tumor associated antigens (TAA). This is achieved by using modified T cell receptor (TCR) or chimeric antigen receptors (CAR). Several CAR based preclinical studies performed in mice yielded promising results with tumor regression and increased disease free survival (176-178).

Among the myeloid cells, dendritic cells (DC) are the most potent antigen presenting cells (APC) that can potentially present antigen to activate adaptive T cell response (koski 2008 immunol rev). However, like most cancers, in pancreatic cancer DC function is compromised by secretion of factors that interfere with DC recruitment, activation and survival (179). In pancreatic cancer, DCs are mainly located at the tumor edge and their recruitment to the microenvironment compromised. Fewer DC in circulation correlated with poor outcome in PDAC and increased number of circulator DCs correlated with better survival in both resectable and non-resectable tumor (180-182). Therefore, strategies to activate

DC can in turn result in alerting the adaptive immune response against the tumor cells. In PDAC patients treated with gemcitabine or cisplatin, DC functions were restored and showed synergistic effect with chemotherapeutic drugs (183, 184).

TAMs are the major constituent of pancreatic tumor stroma. Macrophages can secrete inflammatory cytokines and molecules to promote acinar-ductal metaplasia, a dedifferentiated state that can potentially become malignant (185). Not only are macrophages abundantly present in the preinvasive lesions (169), but they also are a rich source of cytokines, chemokines, proteases, angiogenic molecules and growth factors that can remodel the ECM, induce EMT in cancer cells and facilitate metastasis as well as suppress anti-tumor T cell responses. Like most solid tumors, CD163+ or CD204+ macrophages are associated with shorter survival in PDAC, whereas increased infiltration of M1-type macrophages is a predictor of longer survival in patients (173). Distinct aspects of TAM in PDAC are discussed in detail in the following sections.

2.2.4. Role of macrophages in the progression of Pancreatic Cancer

As mentioned earlier, the hallmark of Pancreatic Cancer is its rich desmoplastic microenvironment, which is some cases can account for up to 80% of the tumor mass. The stroma comprises tumor infiltrating immune cells including macrophages, Tregs, endothelial cells, myofibroblasts and extracellular matrix components (186). Infiltrating immune cells are one of the major concerns for development of therapy resistance in Pancreatic Cancer. Macrophages are the most abundantly found immune cell type in the pancreatic cancer TME and

contribute to various aspects of pancreatic cancer progression, therapy resistance and disease relapse, as described below in details:

Macrophages and prognosis in pancreatic cancer: It is now well established that TAMs promote tumor progression by inducing tumor associated angiogenesis, facilitating EMT and invasion, increasing the stemness of cancer stem cells and suppressing the anti-tumor immune response. CD163+ TAMs were detected in primary lesions of pancreatic cancer, compared to adjacent normal tissues and chronic pancreatitis and positively correlated with tumors in the tail and body of the pancreas (187). Further, elevated TAM infiltration could be causally associated with lymph node metastasis, neural invasion of the tumor, therapy resistance and poor survival in pancreatic cancer (188, 189). However, it is important to note that macrophage phenotype can be stage dependent and evolves with advancement of the disease. For example, in the initial stages of PDAC, macrophages are more M1-type but get skewed more towards M2-like TAMs with progression of cancer (96).

Factors important for the recruitment and polarization of macrophages in pancreatic cancer: Tumor cell derived chemokines, cytokines and other growth factors recruit circulating monocytes and polarize them towards pro-tumoral TAMs as the monocytes infiltrate the TME. One of the most potent chemokines in this regard is C-C chemokine ligand 2 (CCL2) that acts via its receptor CCR2 (68, 107). Several cytokines, like macrophage colony stimulating factor (M-CSF) and endothelial monocyte-activating polypeptide II (EMAPII) have been shown to recruit monocytes to tumor site. However, M-CSF is not frequently expressed by

pancreatic cancer cells (190). The latter on the other hand, express significantly higher level of granulocyte macrophage (GM-CSF) that can potentially generate MDSCs (191). Additionally, pancreatic cancer cell derived GM-CSF is sufficient for the development of CD11b+ TAMs and suppression of immune response against the tumor (191). Once inside the TME, tumor cell and other stromal cell derived factors hijack the monocytes and re-educate them towards TAM phenotype. In Pancreatic cancer, several factors have been identified in this context. For example, Heparanase, which cleaves heparan sulfate glycosaminoglycans, can potentially augment STAT3 signaling in TAMs and contribute to their pro-tumorigenic activity (192).

Role of macrophages in various aspects of pancreatic cancer pathogenesis:

As in other types of cancers, TAMs in pancreatic cancer have been causally associated with various aspects of the disease, such as angiogenic and hypoxic responses, silencing of the adaptive immune response against cancer cells, EMT and cancer invasion, stem cell survival and metastasis. TAMs are known to induce angiogenesis by releasing well characterized panel of pro-angiogenic molecules, such as, VEGFA, TNF-α, basic fibroblast growth factor (bFGF) and thymidine phosphorylase (TP). Inside the TME, TAMs are known as the most potent source of VEGFA. They also secrete other molecules and enzymes, like, MMP-2, MMP-7, MMP-9, MMP-12, COX-2, CCL2, CXCL12, CXCL8, CXCL13 and CCL5, all of which can act as angiogenesis modulators. However, pancreatic cancer is strikingly less dependent on angiogenesis, showing substantially lesser number of microvessels compared to normal pancreas and hence is hypovascular (193). In

contrast, there are reports which have correlated the expression of VEGFA with high vessel density in pancreatic cancer, increased risk for metastasis and poor disease outcome. Further, TAMs can express TIE-2 and localize in the hypoxic region of the tumor in response to Angiopoietin-2 (Ang-2) secreted from the hypoxic vascular cells and contribute to angiogenic switch (194). M-CSF secreted into the TME can also upregulate the expression of TIE-2 on TAMs (195). TAMs have been shown to promote the self-renewal and tumorigenic and metastatic propensity of CSCs in various cancers (196). In PDAC, pharmacologically targeting CSF-1R or CCR2 and thereby inhibiting TAM recruitment significantly reduced the number of pancreatic cells expressing the CSC marker ALDH (197).

EMT is a hallmark feature of cancer cells prior to metastasis. Pancreatic cancer cell lines like, Panc-1 and BXPC3 when cultured in the presence of TAMs, upregulate mesenchymal markers and suppress the expression of E-Cadherin. Cytokines like IL-10, macrophage migration inhibitory factor (MIF) and CCL-18 have been reported to contribute to EMT (198). It is thus likely that these molecules secreted from TAMs act in concert to promote EMT in pancreatic cancer. It is well-known that TAMs secrete molecules and enzymes to remodel the matrix for cancer cell invasion and migration. In PDAC, TAMs produce macrophage inhibitory protein-3 alpha (MIP-3α) that can regulate cancer cell invasion through the production of MMP-9. Another important function of TAMs is facilitating lymphangiogenesis, a crucial factor for metastasis. Studies have shown strong correlation between infiltration of CD163+ and CD206+ TAMs and

lymphangiogenesis (199) and poor prognosis resulting from lymph node metastasis.

One of the main challenges for treating PDAC is the desmoplastic reaction associated with it. PDAC stroma is essentially immunosuppressive in nature. TAMs, which are abundantly present in the PDAC TME, constitute one of the key factors responsible for suppression of adaptive immune response against the cancer cells. As mentioned earlier, TAMs successfully suppress immune activation in the TME by inducing the formation of Tregs and secreting immunosuppressive cytokines like, IL-10, TGF-β which potentially blunt the activation and function of helper and cytotoxic T cells and arresting them in an immature stage. TAMs can also secrete factors like IL-4, IL-13, IL-1β and G-MSCF which can potentially generate MDSCs and further cause immunosuppression (200). Of note, TAMs, Tregs, MDSCs all express several immune checkpoint inhibitor molecules like PDL-1, CTLA-4 etc. It is thus likely that all these immunosuppressive immune cells work synergistically in PDAC TME and contribute to disease progression and therapy resistance.

2.2.5. Probable Strategies for Targeting TAMs in Pancreatic Cancer

TAMs are indispensable for cancer progression. Hence, extensive research is currently ongoing to develop potential therapies and target intratumoral TAMs. In the TME, the life span of a macrophage can be divided into three stages: mobilization from bone marrow and recruitment to target tissue, transformation depending on local cues derived from the microenvironment and pro-tumoral activities. Therefore, anti-macrophage therapies attempt at targeting either the

recruitment step, survival of TAMs or re-educating and re-polarizing them towards anti-tumor type. For example, CCL-2/CCR2 axis is important for the recruitment of circulating monocytes to tumor site in PDAC and blocking this axis inhibits the mobilization of bone marrow monocytes and their subsequent recruitment to tumor site and has shown promising results in several clinical trials in various neoplasms. PF-04136309, a small molecule inhibitor for CCR2 (developed by Pfizer) depleted CCR2+ CD14+ monocytes and macrophages from primary pancreatic cancer and pre-metastastic liver. This also activated anti-tumor immune response and reduced tumor growth and metastasis in mice (201).

M-CSF and CSF-1R signaling axis is very important for macrophage functioning. Targeting this axis has yielded promising results in various cancers (202). Despite the fact that PDAC TME produces more G-MCSF compared to M-CSF, several reports have documented the benefit of targeting CSF-1R axis in reducing CSCs and improving therapeutic response *in vivo* (197*)*. Also targeting this axis depletes the CD206+ TAMs and re-polarize the remaining macrophages towards an activated phenotype (203). Another attractive approach of targeting TAMs is to re-educate them towards an inflammatory and activated M1-like phenotype, which will then support the activation of anti-tumor adaptive immune response. One of the prominent studies in this regard was done by administering CD40 agonist antibody. CD40 is a cell surface receptor expressed in various APCs like monocytes, macrophages, DCs. Its ligand CD40L is expressed on activated T cells. Binding of the ligand with CD40 results in the proliferation and activation of CD4+ and CD8+ T cells (204). Preclinical studies using CD40 agonist induced

infiltration of CD40+ macrophages into the tumor and induced elevated levels of M1-type markers in intratumoral macrophages (MHC class II, CD86) and mounted robust anti-tumor response (122). Further, CD40 agonists (CP-870, 893) in combination with gemcitabine significantly increased treatment efficacy in a small cohort of 22 patients with surgically incurable pancreatic cancer (123). Using RECIST criteria, 4 patients showed partial response, 11 patients with stable disease with PET demonstrating 25% reduction in FDG uptake in the primary tumor. 1 patient with partial response also showed complete regression of 7.6cm liver mass and 47% regression in second liver metastasis. Also, the level of inflammatory cytokines increased in the patients.

There are several other reports that have attempted at targeting TAM survival in the TME using mouse models and have observed moderate to promising results. However, anti-TAM therapy in pancreatic cancer is still in its infancy. One important caveat is that most of the therapeutic strategies proposed in the current section have been validated in mouse tumor models. Also, many therapies that have shown promising results in other cancers have not yet been validated in PDAC. Hence, more extensive research is required to successfully target TAMs in PDAC in the future.

Fig. 2.9. Anatomy of the pancreas. a: Gross anatomy of the pancreas. b: The exocrine pancreas. c: A single acinus. d: A pancreatic islet embedded in exocrine tissue. The pancreas consists of separate functional units for performing two major functions: secretion of digestive juices and glucose metabolism. The acinar cells that produce the digestive enzymes form the bulk of the pancreatic tissue and are organized into grape-like clusters. The ducts produce mucus and bicarbonate to the enzyme mixture and terminate in main and accessory pancreatic ducts and empty into the duodenum. The endocrine pancreas secretes hormones into the bloodstream. The α- and β-cells produce glucagon and insulin, respectively. Pancreatic polypeptide and somatostatin are produced in the PP and δ-cells and regulate the secretory properties of other pancreatic cells. This figure has been adapted from Bardeesy et al. “Pancreatic cancer biology and genetics.” Nat Rev Cancer 2002. doi:10.1038/nrc949 with permission.

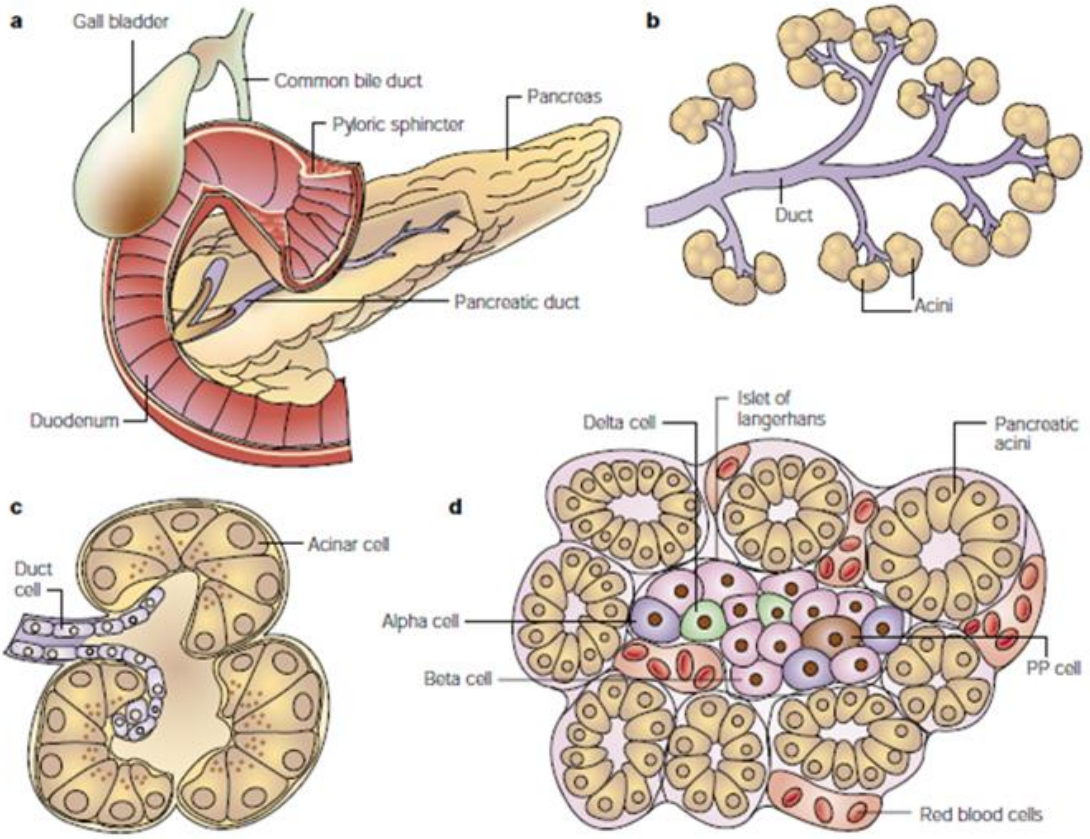
a
Gall bladder
Common bile duct
Pancreas
Pyloric sphincter
Pancreatic duct
Duodenum
b
Duct
Acini
c
Acinar cell
Duct cell
d
Islet of langerhans
Delta cell
Pancreatic acini
Alpha cell
Beta cell
PP cell
Red blood cells

Fig. 2.10. Progression of PanIN lesions to Pancreatic Ductal Adenocarcinoma. Pancreatic Cancer progresses sequentially through the formation of PanIN lesions (low grade to high grade) to invasive carcinoma, acquiring mutations in stages. The hallmark mutations occur in the genes K-RAS and the tumor suppressors CDKN2, TP53, SMAD4/DPC4 and BRCA2. The figure has been adapted from http://2010.igem.org/Team:ESBS-Strasbourg/proteolux/application/cancer.

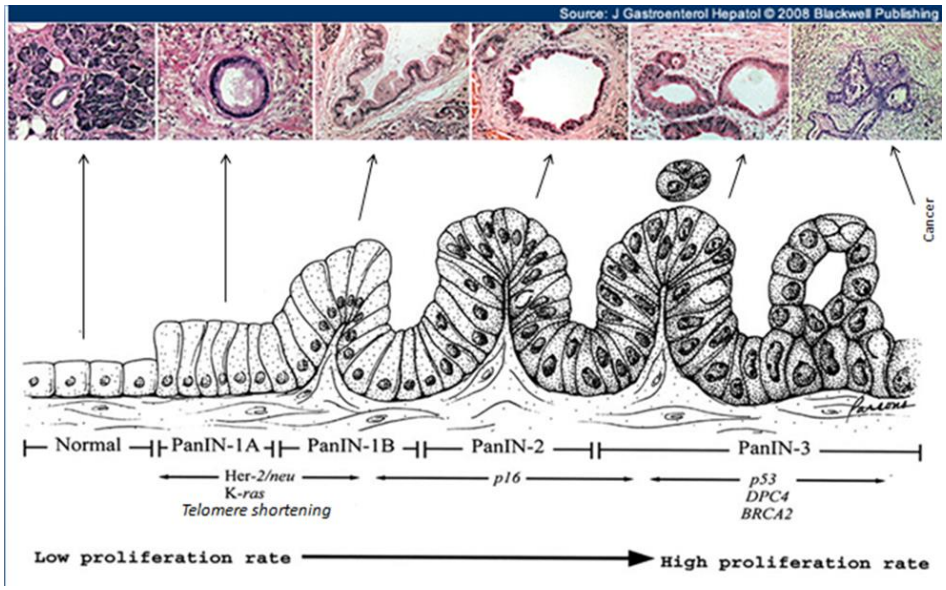
Source: J Gastroenterol Hepatol © 2008 Blackwell Publishing
Cancer
Normal
PanIN-1A
PanIN-1B
PanIN-2
PanIN-3
Her-2/neu
K-ras
Telomere shortening
p16
p53
DPC4
BRCA2
Low proliferation rate
High proliferation rate

Fig. 2.11. Different components of the desmoplasia associated with PDAC. PDAC TME is comprised of cancer associated fibroblasts, TAMs, T_{reg}s, other immune cells, endothelial cells, and matrix proteins and contribute to the dense desmoplasia that is the hallmark feature of PDAC. Cancer associated fibroblasts deposit matrix which creates solid stress and compresses the vasculature for limited diffusion into the tumor. TAMs, T_{reg}s are mainly responsible for suppression of the immune responses against the tumor cells. The figure has been adapted from Carr *et al*. “Pancreatic cancer microenvironment, to target or not to target?”. Embo Mol Med 2016. doi: 10.15252/emmm.201505948 with permission.

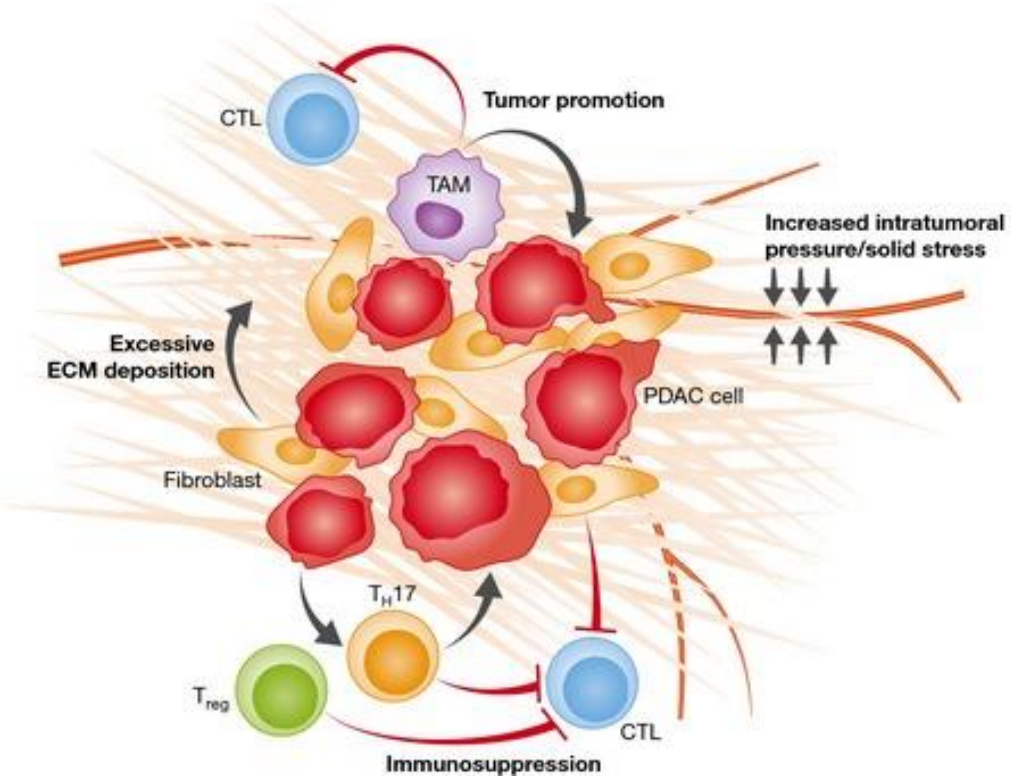
CTL
Tumor promotion
TAM
Increased intratumoral
pressure/solid stress
Excessive
ECM deposition
PDAC cell
Fibroblast
T_H17
T_{reg}
CTL
Immunosuppression

Fig. 2.13. Therapeutic agents and strategies to target TAMs at different stages of pancreatic cancer pathogenesis. The figure has been adapted from Cui *et al*. “Targeting tumor-associated macrophages to combat pancreatic cancer.” Oncotarget 2016. doi: 10.18632/oncotarget.9383 with permission.

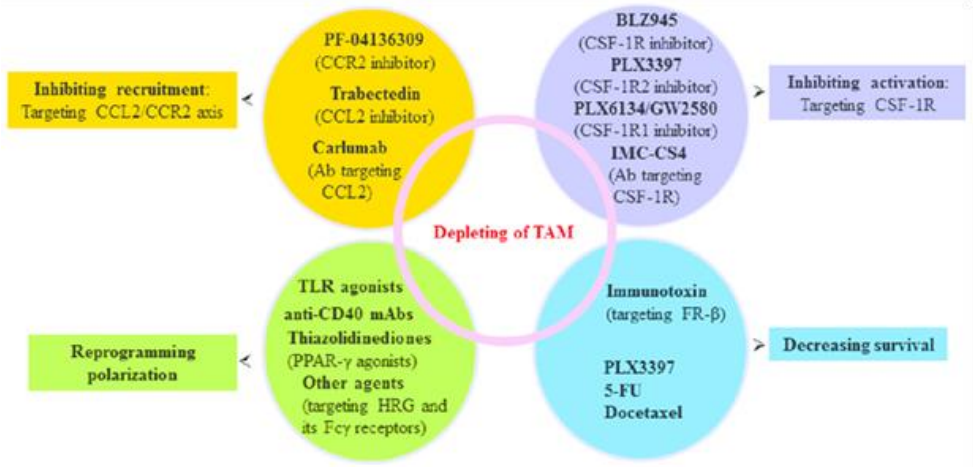
Inhibiting recruitment:
Targeting CCL2/CCR2 axis
PF-04136309
(CCR2 inhibitor)
Trabectedin
(CCL2 inhibitor)
Carlumab
(Ab targeting
CCL2)
BLZ945
(CSF-1R inhibitor)
PLX3397
(CSF-1R2 inhibitor)
PLX6134/GW2580
(CSF-1R1 inhibitor)
IMC-CS4
(Ab targeting
CSF-1R)
Inhibiting activation:
Targeting CSF-1R
Depleting of TAM
Reprogramming
polarization
TLR agonists
anti-CD40 mAbs
Thiazolidinediones
(PPAR-γ agonists)
Other agents
(targeting HRG and
its Fcγ receptors)
Immunotoxin
(targeting FR-β)
PLX3397
5-FU
Docetaxel
Decreasing survival

3.1. Efferocytosis: A Brief Overview

Efferocytosis is a strictly orchestrated process where phagocytes, such as macrophages recognize and engulf apoptotic cells and remove them from the system in an immunologically silent manner. Programmed cell death, such as apoptosis is an indispensable process, starting from early developmental stages and lasting over an organism's lifetime, for the maintenance of physiological homeostasis. In adult humans, one million cells undergo apoptosis per second as part of the regular turnover process (205, 206). However, under normal homeostatic conditions, we rarely observe any apoptotic cell. This is because the apoptotic cellular debris is as efficiently removed through the process of efferocytosis as it is generated, to avoid inappropriately evoking the adaptive immune responses. If apoptotic cells are not engulfed, they leak out their cellular contents as secondary necrosis and this result in aberrant immune responses by exposure to self-antigens and a break in tolerance. Indeed, in absence of clearance of apoptotic cells, lethal developmental defects, autoimmune disorders or even cancers can occur. Also, components leaked out as secondary necrosis can be recognized by IgG autoantibodies which in turn can activate the inflammatory immune response. All these events thereby underscore the importance of efferocytosis in maintaining normal human physiology.

In the tissues, the task of recognizing, engulfing and clearing the apoptotic cells have been endowed upon professional phagocytes, like macrophages as well as nonprofessional phagocytes, such as epithelial cells or fibroblasts. Tissue Resident Macrophages are the most well characterized cell population that

efficiently clear dying cells in different tissues. However, in the absence of professional phagocytes, nonprofessional phagocytes can fill up the niche. For example, in the mammary gland or the intestinal epithelium, where macrophages are scarce, the tissue epithelial cells and fibroblasts play a leading role in clearing the apoptotic cellular debris. In addition to the alveolar macrophages, bronchial epithelial cells can also clear the cellular debris resulting from airway epithelial cells undergoing apoptosis (207).

3.1.1. Stages of efferocytosis

The process of efferocytosis occurs in 4 stages:

1. **Release of 'find me' signals from dying cells to recruit phagocytes to the site of cellular corpses:** In most of the cases, phagocytes are not proximal to the site of cell death. Therefore, to recruit phagocytes to the location of cell death, the dying cells express a variety of 'find me' molecules that act as chemotactic signals for the phagocytes e.g. ATP, Sphingosine-1-Phosphate (S1P), Lysophosphatidylcholine (LPC), CX3CL1 and a wide variety of other molecules. ATP released from dying cells in a caspase dependent manner via the activation of pannexin-1 channels is recognized by purinergic receptors, like P2Y2 on phagocytes (208). Fractalkine or CX3CL1 released from dying cells bind to CX3CR1 expressed on phagocytes and mediates their migration to site of cell death (209).

2. **Phagocyte recognition of apoptotic cells and activation of 'eat me' molecules on the dying cells:** Once the phagocytes reach the site of cell

death, the apoptotic cells upregulate various molecules that serve as ‘eat me’ signals to the former. Also, these molecules help the phagocytes to distinguish between apoptotic cells from neighboring healthy cells. Among others, Phosphatidyl Serine (PtdSer) is arguably the most well-known ‘eat me’ molecule expressed on the surface of apoptotic cells. This is then recognized by several molecules like, T-cell immunoglobulin mucin receptor 4 (TIM4), brain-specific angiogenesis inhibitor 1 (BAI1), and stabilin-2 as well as several bridging molecules, like milk fat globule-EGF factor 8 (MFG-E8) and Gas6. These then engage integrin $\alpha_v\beta_3$, $\alpha_v\beta_5$, or Tryo3-Axl-Mer (TAM) receptors on the surface of the phagocytes to begin the uptake process. There are several other molecules like ICAM3, Calreticulin, Oxidized LDL-like moieties and glycosylated surface proteins that have been reported to further enhance this process by acting as ‘eat me’ molecules. Of note, healthy cells express several ‘don’t eat me’ molecules on their surface, like CD47 which is recognized by cognate receptor SIRPα on phagocyte, that impairs phagocytosis of living cells even in the presence of externalized PtdSer (210). Indeed, constitutive expression of CD47 is a clever ploy used by cancer cells to avoid being phagocytosed (17). Administration of neutralizing antibodies against CD47 has shown promising results in mouse tumor models (211) and extensive research is ongoing to develop effective neutralizing antibodies against CD47 to treat lethal malignancies. CD31 and CD300a are two additional ‘don’t eat me’ molecules, albeit less well characterized in comparison with CD47.

3. **Uptake of the apoptotic corpse:** Once the phagocyte captures the dying cell, the next step in the process of efferocytosis is internalization of the apoptotic cell by the phagocyte. This process is similar to macropinocytosis and requires active membrane ruffling. Once the 'eat me' molecules engage the cognate receptors on the phagocyte, there occurs extensive cytoskeleton rearrangement in the latter to facilitate the uptake process. This is mediated by the Rho family of small GTPases like RhoA, ROCK, Rac and Cdc42. RhoA negatively regulates efferocytosis and its depletion enhances the uptake process (210). Its effect is mainly mediated by increasing the kinase activity of ROCK, which in turn phosphorylates Myosin Light Chain and increases the contractility of the cell (212), thereby inhibiting the formation of pseudopods and phagocytic cup formation. However, RhoA activation at later stages may aid the digestion process by enhancing phagosome acidification (213). Different pathways have been proposed so far, that can regulate the uptake process. All pathways ultimately lead to the evolutionarily conserved Rac1. GTP-bound active Rac1 promotes Arp2/3 activation and cytoskeleton rearrangement through Scar/WAVE pathway for phagocytic cup formation (214, 215).

4. **Processing, degradation and clearance of engulfed cell:** Once the apoptotic cell is inside the phagocyte, the latter begins the process termed as phagosome maturation that eventually leads to degradation of the cargo. In fact, recent studies indicate the events downstream of uptake, that is proper digestion and clearance affects the phagocyte's ability to engulf

additional targets (216-218). For efficient clearance, phagosomes containing the cellular corpse undergoes acidification and ultimately fuse with the lysosomes (219, 220). The process of efferosome (phagosome containing apoptotic cell debris) maturation and degradation of apoptotic cells in professional phagocytes proceeds very rapidly, thus making it technically challenging for researchers to investigate the process. The maturation of early phagosomes to mature late phagosomes and eventual fusion with the lysosomes is similar as in classical endocytosis. First, Dynamin, a GTPase is recruited to the phagocyte-apoptotic cell interface. This then interacts with Vps34 on the nascent phagosome, and recruits GDP-bound GTPase Rab5. Rab5 is then activated by GEFs like Gapex-5 (221) which then promotes Vps34 activation and generation of PtdIns(3)P on the surface of the phagosome. Next, Mon1 and its partner Ccz-1 form a complex and act as Rab5 effector and recruit Rab7 and its activation (222)an event that is crucial for phagosome maturation. Indeed, in Mon1 depletion conditions, phagosomes were arrested at Rab5+ stage and failed to transit to Rab7+ late phagosomes. Next, the HOPS complex gets activated and the phagosome fuses with the lysosome. Inside the mature phagolysosomes, the apoptotic cells are then degraded by the acidic proteases and nucleases.

Recently, another pathway has been proposed that can contribute significantly to the overall degradation and clearance process. This pathway, named LC3-associated autophagy (LAP) is at the interface of

autophagy and phagocytosis. LAP gets activated once a phagocyte internalizes a cargo using surface receptors, like Toll like receptors 1/2 (TLR 1/2), TLR4, TLR 2/6, FcR, and TIM4 (recognizes PtdSer on apoptotic cells) and play a vital role in regulating the immune response. Interestingly, it has been reported that bacterial viability is needed to initiate LAP, however this is not the case for zymosan bioparticles or efferocytosis of apoptotic cells. Despite sharing several common molecular players, there are certain fundamental differences between canonical autophagy and LAP. For example, the latter recruits LC3 to the phagosomes as early as within 5-10minutes of phagocytosis whereas in canonical autophagy, LC3 recruitment can take up to several hours. In brief, following engulfment, the Class III PI3K complex, comprising of Beclin 1, VPS34, UVRAG and Rubicon are recruited to the phagosome (here LAPosome) containing the apoptotic debris. The PI(3)P generated by VPS34 is important for the recruitment of the downstream LAP components (such as, ATG5, ATG12, ATG16L, and ATG7). PI(3)P and Rubicon stabilize NOX2, the predominant NADPH oxidase in phagocytes, for the production of ROS at the phagosome. Both PI(3)P and ROS help recruit LC3 to the LAPosome surface which then fuses with the lysosome for degradation of the cargo (223, 224).

3.1.2. What happens to the efferocyte: Efferocytosis a fate-determining event for macrophages?

As mentioned earlier, inappropriate inflammation or aberrant activation of the immune response needs to be kept in check for the maintenance of physiological homeostasis. Hence, the hallmark feature of efferocytosis is the lack of immunogenic response. Several clinical conditions have been identified where defective clearance of dying cells contribute to the pathogenesis. Indeed, defects in the efferocytosis receptors like, MerTK, CD36 or MFG-E8, give rise to autoimmunity in mice and humans, especially systemic lupus erythematosus (SLE) (225).

The effects of efferocytosis can vary depending on the type of the efferocyte. For example, the rate of digestion of engulfed apoptotic cells is much slower in DCs than in macrophages (226), thereby allowing the dying cell derived antigens to associate with the MHC molecules for presentation to the adaptive immune system. Further, DCs have been reported to exhibit selectivity in their ability to engulf and digest cellular corpses. $CD8a^+$ and $CD103^+$ DCs that express the transcription factor Batf3 are much more efferocytic than $CD11b^+$ DCs that are dependant on the transcription factor IRF4 (227). Also, the more efferocytic DCs ($CD8^+$ and $CD103^+$) can then migrate to the lymph nodes where they can cross-present the antigens to the cytotoxic T cells for their cross-priming. Apoptotic cell derived immunogens can also escape the efferosomes and associate with MHC1 molecules for cross-presentation. Presence of elevated levels of TLR3/7 in the endosomes can facilitate this process and subsequent activation of CD8+ T cells. The effect of efferocytosis on non-professional phagocytes like, epithelial cells or stromal cells is not clearly understood and needs further investigation. In case of

macrophages, efferocytosis reprograms phagocytes to an anti-inflammatory phenotype. Following engulfment of apoptotic cells, phagocytes suppress the production of inflammatory cytokines like, IL-12, TNF-α and lL-1 and upregulate the production of immunosuppressive cytokines like, TGF-β and lL-10 (225). Both TGF-β and lL-10 are potent in dampening effector helper T cell response by stimulating regulatory T cells and T helper 2 cells. Also, in case of any inflammatory condition, like microbial infection, the infiltrating inflammatory cells (such as neutrophils) are cleared through efferocytosis by macrophages during the resolution phase. In macrophages with impaired LAP, phagosome acidification does not occur resulting in defective degradation of apoptotic debris. These LAP deficient macrophages produce considerable amounts of inflammatory cytokines like IL-6 and IL-1β, but not anti-inflammatory cytokines like IL-10. The exact molecular mechanism that couples the two processes of efferocytosis and immune suppression is not clearly understood and is under extensive investigation. However, recent studies have identified several nuclear receptor (NR) family members for their role in the regulation of inflammatory response during efferocytosis. For example, depletion of LXR-α/β in macrophages fail to produce TGF-β and lL-10 but secrete copious amount of IL-1β and lL-12 (228). However, the molecules that trigger these nuclear receptors or bridge the various stages of efferocytosis with gene regulation is still not clearly known.

Finally, the efferocytic macrophages must also be removed from to establish tissue homeostasis. Three possibilities have been proposed: either the efferocytic macrophages exit the body through mucosa or emigrate to the blood or

lymph or they undergo programmed cell death and are removed locally by tissue resident macrophages (225). Contrary to the idea that macrophages lack the imigratory property to lymphatics in comparison with DCs, it was documented that following efferocytosis, $CD11B^{high}$ macrophages convert to $CD11B^{low}$ satiated phagocytes with enhanced pro-resolving properties and display propensity to migrate from the site of inflammation to the lymphoid organs (229). This is crucial for the return of homeostasis in the tissue. However, the satiated macrophages can also release chemoattractants to recruit new monocytes for continued clearance of cellular debris.

3.1.3. Efferocytosis in different conditons

The impact of effecrocytosis has been studied under different conditions. A few are discussed in detail below.

Efferocytosis in microbial clearance: Efferocytosis plays a vital role in microbial clearance (230). Many of the pathogens that infect cells deploy mechanisms to hijack the cellular machinery in order to persist inside the host cell. The infected cell activates the apoptosis pathway to get rid of the pathogen. Cytotoxic T cells can also extrinsically induce apoptosis in the infected cell by secreting perforins or granzymes or via the Fas/FasL pathway. The apoptotic cell with its load of infectious particles is next engulfed by macrophages through efferocytosis. This can potentially have two possible outcomes: either the pathogen will be destroyed along with the engulfed dying cell or the pathogen can use the process of efferocytosis as a “Trojan Horse” mechanism to disperse into and infect new host cells. For example, during the infection of *Leishmaniasis major*, infected

neutrophils undergo apoptosis. These dying neutrophils with their intracellular load of pathogen are then efferocytosed by macrophages and this is a crucial step for establishment of the disease. Strikingly, infection of macrophages with *Mycobacterium tuberculosis* usually induces necrosis to allow dispersion to new cells (231). However, it does induce apoptosis in some of the infected macrophages. These apoptotic macrophages are next efferocytosed by uninfected macrophages that then destroy the pathogen along with the dying cell corpse using phagolysosomal fusion machinery (232). What is intriguing, in many cases the infection with bacterial pathogen circumvents the phagolysosomal fusion and degradation. This can be attributed to the ability of many pathogens to arrest phagosome maturation and prevent phagolysosomal fusion. For example, Mycobacterium tuberculosis have several bioactive lipids on their surface that interfere with the recruitment of endosome and lysosome and hence phagosome maturation (233, 234). However, when the apoptotic cell containing the pathogen is efferocytosed by uninfected macrophages, it results in clearance of the pathogen. This may be possible because the pathogen, when infected along with the dying cell, remains in the efferosome and hence may not have access to the host cell efferocytosis machinery. Also, despite the fact that many of the molecular components are similar in the processes of classical phagocytosis and efferocytosis, a different subset of effector molecules are involved in efferosome maturation than a phagosome (219, 220). For example, canonical Rab5 GEF, Rabex5 is involved in phagosome maturation but not in efferosome maturation. Instead, Gapex5 may potentially act as Rab5 GEF during maturation of

efferosomes. Hence, it is possible that the pathogen is not equipped with remodeling or interfering with these family of proteins and hence efferosome maturation proceeds resulting in the eventual pathogen clearance. Of note, molecular players associated with autophagy are also known to be involved in efferocytosis mediated pathogen clearance (223). As mentioned earlier, efferocytosis of apoptotic cells induce the secretion of anti-inflammatory molecules and cytokines in macrophages. However, when a macrophage ingests an apoptotic cell infected with pathogen, two possible conflicting signals are expected: pathogen associated molecular patterns (PAMPs) that drive inflammatory signaling pathways, and apoptotic cell that triggers the anti-inflammatory responses. Currently, the unique signal elicited by a macrophage following efferocytosis of pathogen-infected cell is still not clearly understood.

Efferocytosis in atherosclerosis: Atherosclerosis is a clinical condition where plaques form inside arteries due to deposition of fatty materials, like, cholesterol, fatty substances, cellular waste products, calcium and fibrin. As plaques continue to accumulate, it narrows the artery wall, gradually slowing down blood flow and decreasing oxygen availability to cells. Atherosclerosis can result in clinical conditions like a heart attack, angina, stroke and gangrene. Macrophages play crucial role in all stages of atherosclerosis (235). They are recruited to clean up the plaque and their ability of efferocytosis correlates with disease stage and plaque stability. The conventional M1/M2 phenotype of macrophages depends on the stage of the lesion in atherosclerosis and is dynamic and complex, and probably undergoes conversion depending on a variety of factors (236). As the

fatty materials get deposited on the artery wall, it recruits circulating monocytes and differentiate them to macrophages. The latter engulf the lipoproteins and store the lipids in droplets, becoming foam cells in the process. The foam cells secrete inflammatory cytokines and finally undergo apoptosis. They are then cleared by efferocytosis by freshly recruited macrophages, which results in resolution of inflammation in the early lesions and thus reduction in lesion cellularity and size. However, in the more advanced lesions, the process of apoptosis exceeds efferocytosis and hence clearance of apoptotic macrophages is impaired. This results in the accumulation of apoptotic macrophages and subsequent secondary necrosis. Gradually a necrotic core builds up which leads to further inflammation and formation of vulnerable plaque and acute thrombosis.

3.1.4. Efferocytosis in cancer: TAMs paving a pro-metastatic niche?

The exact role of phagocytosis of cancer cells by phagocytes is a contentious topic. As mentioned earlier, cancer cells upregulate the expression of ‘don’t eat me’ signals e.g. CD47 to escape being phagocytosed. Treatment with neutralizing antibodies against CD47 have shown promising results in various mouse tumor models and extensive research is currently ongoing to develop anti CD47 therapies for clinical trials. Recently, Gordon *et al*. has shown that TAMs express PD-1, a well-known checkpoint inhibitor for T cell activation and its expression negatively regulates the ability of the macrophages to phagocytose cancer cells. Blockade of PD-1-PDL-1 increased the phagocytic ability of TAMs and resulted in reduced tumor burden and increased survival in mice (237). However, efferocytosis of dying cancer cells can act as a double-edged sword.

The non-immunogenic properties of efferocytosis that prevails under normal homeostasis conditions can be mimicked by malignant cells to create an environment of immunosuppression in the TME. For example, in their recent elegant study, Stanford *et al*. reported an immunosuppressive role of cancer cell phagocytosis (104). Within the TME, apoptosis of cancer cells is a common feature, arising because of nutrient limitation and rapid proliferation of malignant cells. These dying tumor cells are then efficiently phagocytosed and cleared by the TAMs. Interestingly, using mouse model for postpartum breast cancer (ppBC), Stanford *et al*. showed efferocytosis of dying tumor cells increased the production of Th-2 like cytokines (IL-4, IL-10, IL-13, TGF-β) in TAMs and increased the risk of metastasis by 10-fold. Additionally, tumor associated tissue repair processes, expansion of regulatory T cell population (Treg) and production of immunosuppressive cytokines by phagocytes were all dependent on efferocytosis induced TGF-β signaling. Further, pharmacologically blocking efferocytosis of dying cancer cells significantly reduced the risk for metastasis in ppBC. Of note, evasion of phagocytosis by upregulation of ‘don’t eat me’ signals is a hallmark of cancer cells and several studies have indicated towards a therapeutically beneficial effect of enhancing cancer cell clearance by phagocytes. Additionally, although treatment with cytotoxic therapies in cases provide partial response, eventually result in relapse of the disease with more aggressive features. These cases are characterized by an initial activation of the immune cells followed by their subsequent impairment to mount a robust antitumor immune response. Stanford *et al*. showed in their elegant study that this could be attributed to

efferocytosis mediated enhanced pro-tumorigenic polarization of TAMs. Administration of cytotoxic therapy resulted in significant death of tumor cells in the TME. Intriguingly, the TAMs that phagocytosed these dying tumor cells became more pro-tumoral and showed increased tissue healing, production of Th-2 like immunosuppressive cytokines and more Treg induction in the TME, as well significantly increased risk for distant metastasis. Indeed, treatment with a combination of chemotherapy and efferocytosis blocker not only reduced the risk for therapy-enhanced metastasis but also limited the number of TAMs and immunosuppression in the TME. This study raised the attractive possibility that inducing cell death using chemotherapeutic agents as well as inhibiting their clearance by phagocytes can activate the adaptive immune response against the tumor and can emerge as potential therapy in the future.

In addition to this, depletion of the efferocytosis receptor, MERTK, dampened tumor growth and metastasis in syngeneic breast, melanoma and colon cancer models (238). Bone marrow transplantation of $MERTK^{-/-}$ cells into lethally irradiated MMTV-PyVMT mice slowed tumor progression. Additionally, $MERTK^{-/-}$ CD11b+ macrophages isolated from $MERTK^{-/-}$ tumors produced significantly higher amount of IL-6 and IL-12p40, hallmarks of immune activation. In line with this, there was increased infiltration of cytotoxic CD8 cells into the tumor.

The expression of PtdSer, the well-known ‘eat me’ signal is deregulated in cancer. In the TME, PtdSer is expressed by tumor cells, immature vasculature as well as tumor cell derived exosomes. Tumor associated dendritic cells that engulf PtdSer expressing tumor cells remain arrested in an impaired functional state,

incapable of expressing the costimulatory molecules required for optimum antigen presentation to the T cells. Following chemotherapy or radiotherapy, the apoptotic index in the TME is increased which correlates with increased PtdSer expression. This eventually results in further immunosuppression. Moreover, the cognate receptors and other bridging molecules expressed on TAMs interact with PtdSer on tumor cells and hinder tumor recovery by creating an immunosuppressive local environment. All these studies indicated that molecules associated with efferocytosis of dying tumor cells probably act as critical immune checkpoint inhibitors and targeting these molecules can work akin PDL-1 and CTLA-4. Indeed, pre-clinical studies showed that administration of PtdSer blocker resulted in immune activation in the TME, marked by increase in M1 macrophages, reduction in the number of MDSCs and infiltration of cytotoxic T cells (239). Currently Bavituximab, a PtdSer targeting antibody is being tested in multiple clinical trials, either as monotherapy or in combination with other therapies and has so far shown signs of activity (240).

These studies taken together, raise an important question, if cancer cells are targeted using chemotherapy or radiotherapy, and the phagocytosis of the apoptotic cells are blocked pharmacologically by immunomodulating TAMs, will the defective efferocytosis activate anti-tumor immune response in the host?

Fig. 3.1. Find me and Eat me signals during efferocytosis. Interaction between different molecules that mediate recognition and uptake of apoptotic cells. The figure has been adapted from Hochreiter-Hufford *et al*. “Clearing the Dead: Apoptotic Cell Sensing, Recognition, Engulfment, and Digestion.” Cold Spring Harbor Perspectives in Biology. 2013. doi: 10.1101/cshperspect.a008748

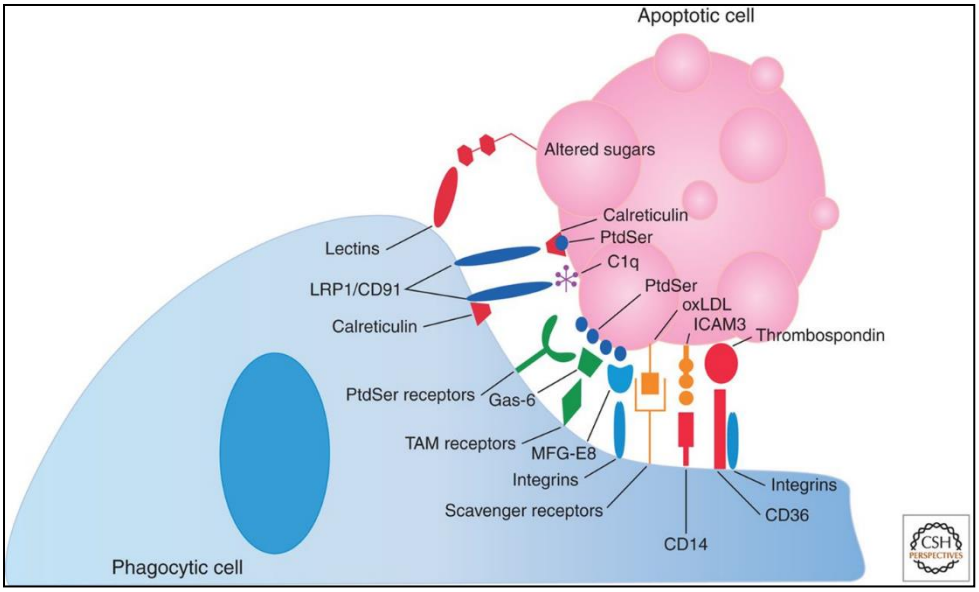
Apoptotic cell
Altered sugars
Calreticulin
PtdSer
C1q
Lectins
LRP1/CD91
Calreticulin
PtdSer
oxLDL
ICAM3
Thrombospondin
PtdSer receptors
Gas-6
TAM receptors
MFG-E8
Integrins
Scavenger receptors
Integrins
CD36
CD14
Phagocytic cell

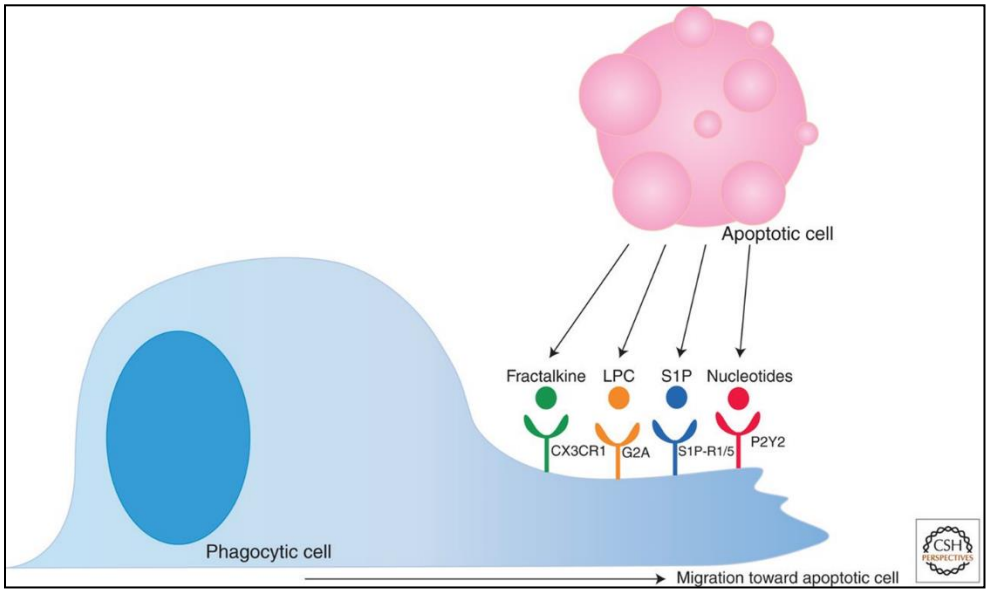
Apoptotic cell
Fractalkine
LPC
S1P
Nucleotides
CX3CR1
G2A
S1P-R1/5
P2Y2
Phagocytic cell
Migration toward apoptotic cell

Fig.3.2. Phagosomal maturation during efferocytosis. During efferocytosis, Dynamin is first recruited to the apoptotic cell/phagocyte interface. Dynamin then interacts with Vps34, resulting in Rab5 recruitment and activation. Activated Rab5 further activates Vps34, resulting in the formation of PI(3)P on the phagosome surface. In the next step, Mon1-CCz complex recruits Rab7 recruitment to the phagosome. Finally, the HOPS complex is recruited, Rab7 is activated and eventually the phagosome containing the apoptotic cell fuses with with the lysosome for degradation of the cargo. The figure has been adapted from Hochreiter-Hufford *et al*. “Clearing the Dead: Apoptotic Cell Sensing, Recognition, Engulfment, and Digestion.” Cold Spring Harbor Perspectives in Biology. 2013. doi: 10.1101/cshperspect.a008748

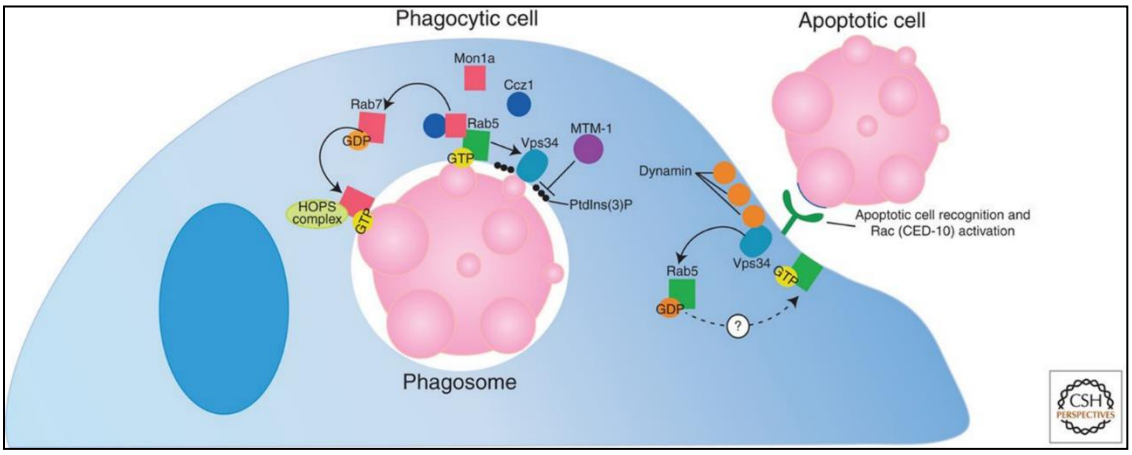
Phagocytic cell
Apoptotic cell
Mon1a
Ccz1
Rab7
GDP
Rab5
GTP
Vps34
MTM-1
PtdIns(3)P
HOPS complex
GTP
Phagosome
Dynamin
Apoptotic cell recognition and Rac (CED-10) activation
Rab5
GDP
?
Vps34
GTP
CSH PERSPECTIVES

Fig.3.3. LC3 associated autophagy (LAP) during efferocytosis. Following engulfment of apoptotic cell corpse, the Class III PI3K complex, comprising of Beclin 1, VPS34, UVRAG and Rubicon are recruited to the LAPosome containing the apoptotic debris. The PI(3)P generated by VPS34 recruits the downstream LAP components (such as, ATG5, ATG12, ATG16L, and ATG7). PI(3)P and Rubicon stabilize NOX2 for the production of ROS at the phagosome. Finally, PI(3)P and ROS help recruit LC3 to the LAPosome surface which then fuses with the lysosome for degradation of the cargo. LAP mediated efferocytosis results in decreased production of IL-12, TNF-α, IL-1β and IL-6 and enhanced secretion of IL-10 and TGF-β, thereby dampening the inflammatory immune activation. The figure has been adapted from Green *et al*. “The clearance of dying cells: table for two.” Cell Death Differ 2016 doi: 10.1038/cdd.2015.172 with permission.

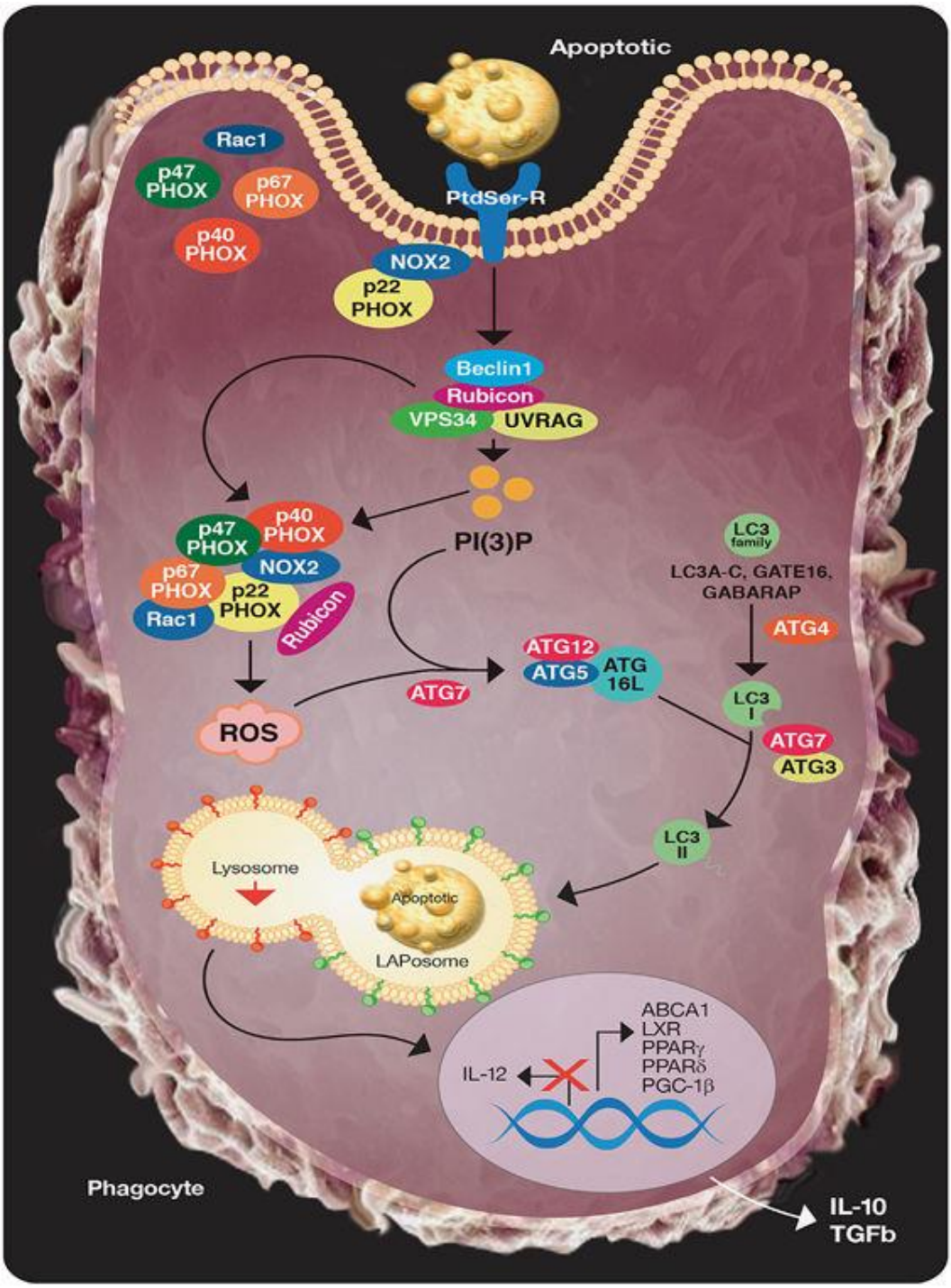
Apoptotic
Rac1
p47 PHOX
p67 PHOX
p40 PHOX
PtdSer-R
NOX2
p22 PHOX
Beclin1
Rubicon
VPS34
UVRAG
PI(3)P
p47 PHOX
p40 PHOX
NOX2
p67 PHOX
p22 PHOX
Rac1
Rubicon
ROS
ATG7
ATG12
ATG5
ATG 16L
LC3 family
LC3A-C, GATE16, GABARAP
ATG4
LC3 I
ATG7
ATG3
LC3 II
Lysosome
Apoptotic
LAPosome
ABCA1
LXR
PPARγ
PPARδ
PGC-1β
IL-12
Phagocyte
IL-10
TGFb

Fig.3.4. Efferocytosis in cancer. Efferocytosis of apoptotic cells by TAMs in TME resulting in increased pro-tumorigenic polarization of TAMs. Enhanced production of immunosuppressive cytokines stimulates regulatory T cells and dampens effector T helper and cytotoxic T cell response against tumor, resulting in increased risk for relapse post therapy and distant metastasis. This figure is adapted from Stanford *et al*. “Efferocytosis produces a prometastatic landscape during postpartum mammary gland involution.” JCI 2014 doi:10.1172/JCI76375 with permission.

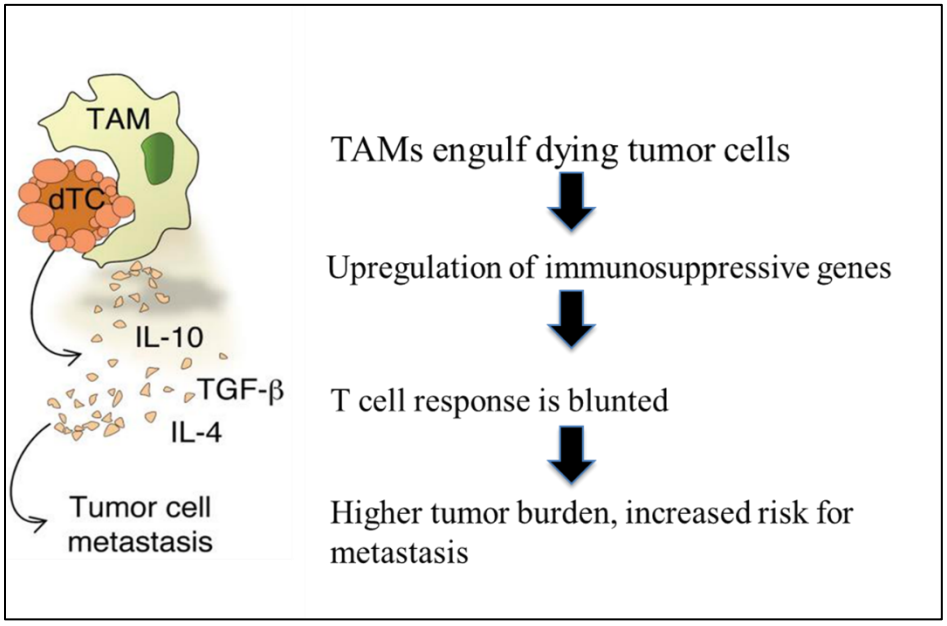
TAM
dTC
IL-10
TGF-β
IL-4
Tumor cell metastasis
TAMs engulf dying tumor cells
Upregulation of immunosuppressive genes
T cell response is blunted
Higher tumor burden, increased risk for metastasis

Concluding remarks and dissertation hypothesis

Macrophages comprise a heterogenous population of innate immune cells and are highly plastic in nature. They are endowed with diverse functions, ranging from maintenance of homeostasis by phagocytosing and clearing apoptotic debris in tissues, metabolic homeostasis, development of organs, angiogenesis to combating inflammations or pathogenic infections. They can also bridge the innate and adaptive arms of the immune system by their ability to prime naïve T cells. Depending on the milieu of cytokines and chemokines they are exposed to in the tissue microenvironment, macrophages can exist as classically activated or M1 type or alternatively activated or M2 type. M1 type macrophages are cytotoxic and release pro-inflammatory cytokines to eliminate infected or injured cells. However, post infection or injury, M1 type cells polarize towards a reparative M2 type, that secrete angiogenic growth factors, tissue remodeling matrix metalloproteases and other immunosuppressive cytokines for suppressing T cell responses, that augment the wound healing and tissue repair processes. Intriguingly, macrophages comprise a substantial population of many solid tumors, including breast, prostate, and pancreatic cancers. In most of the cancers studied so far, the intratumoral infiltration of macrophages correlate with disease stage and severity and is causally associated with poor clinical outcome. Tumor associated macrophages (TAMs) comprise a complex population of cells. Although their gene expression profiles are characteristic of the M2 type, they also express several M1 type genes. Extensive studies over the past few years have shown that TAMs are indispensable for tumor progression. They have been associated with several

stages of neoplastic development, like, attainment of epithelial to mesenchymal transformation (EMT), survival and proliferation of cancer cells, maintenance of cancer stem cell niche, tumor associated angiogenesis and lymphangiogenesis, suppression of anti-tumor immune responses and distant metastases. Research is currently ongoing to discover strategies to re-educate TAMs towards a classically activated M1 type. Several clinical trials targeting various aspects of TAMs either alone or in combination with other therapies have been reported (54, 56, 65).

Neuropilins (NRPs) are non-tyrosine kinase, cell surface glycoproteins that are widely characterized for their roles in development, migration and angiogenesis. Two isoforms are known till date, NRP1 and NRP2. They are endowed with unique as well as redundant functions. NRPs have been implicated in several neoplasms where they are often overexpressed and correlate with cancer cell survival under stress, proliferation, metastasis and poor patient survival. Research over the past few years have focused on the role and function of NRPs in different immune cell compartments. For example, NRP1 is a marker for mouse regulatory T cells and is associated with immunosuppression. It is also expressed in macrophages and is important for their protumoral activities (241). In contrast, NRP2 is less characterized in the immune subsets. Although previous studies detected NRP2 expression in macrophages, its function and the molecular pathways that govern these functions are still not clearly known. Our lab has previously reported a novel role for NRP2 in regulating endocytic maturation in cancer cells. NRP2 positively regulates the maturation of early to late endosomes.

This is important for cancer cells that heavily rely on endocytic machinery for their oncogenic activities (242). The primary role of macrophages is phagocytosis. This function is indispensable for clearance of pathogens, pathogen infected cells as well as for maintenance of physiological homeostasis. Following internalization of cargo, nascent phagosomes in macrophages mature to late phagosome and phagolysosome, recruiting and fusing with the classical endocytic compartments and gradually becoming more and more acidic in the process (219-222). Since the processes of endosomal and phagosomal maturation are similar, and involve several common downstream effectors, *we hypothesize that NRP2 regulates phagosome maturation in macrophages; hence NRP2 depletion will affect pathogen clearance in macrophages.* Our study aims to fully understand the role of NRP2 in macrophage biology and how this may affect macrophage function in normal physiology as well as clinical settings.

One of the essential functions of TAMs in the TME is efferocytosis of apoptotic cancer cells. In the TME, the apoptotic index is high owing to either nutrient limited growth condition or rapid proliferation of cancer cells or any therapeutic stress. The dying cell corpses need to be removed as efficiently as they are generated and impairment of their clearance results in the leakage of cellular contents into the surrounding milieu as secondary necrosis. This can potentially activate anti-tumor immune responses. Intriguingly, efferocytosis of dying tumor cells makes TAMs more tumorigenic and immunosuppressive, and significantly increases the risk for metastasis. Blockade of efferocytosis can potentially reduce the risk for metastatic cancer and disease recurrence (104). *We*

hypothesize that NRP2 in TAMs regulates clearance of apoptotic tumor cells and maintains an immunosuppressive environment in the TME; hence NRP2 ablation in macrophages will slow down tumor progression and activate anti-tumor immune response. The goal of this study is to understand the role of NRP2 in macrophages and how this NRP2 driven function may affect TAMs and tumor progression. Pancreatic Ductal Adenocarcinoma (PDAC) is one of the most lethal types of cancers with high incidence and low survival rates. One of the hallmarks of PDAC is the dense desmoplastic reaction that acts as a physical barrier to therapeutics. TAMs are abundantly present in PDAC and have been causally associated with distinct stages of disease progression, metastasis, therapy resistance and correlate with poor outcome (243-245). Despite the exciting potential of a targeted immunotherapy for treating PDAC, it is a clinical reality that tumors relapse, often with more aggressive features. Our goal is to identify the function of NRP2 in TAMs and how targeting this axis may affect PDAC progression. Collectively, the outcome of the study will address the requirement for developing strategies to target NRP2 in TAMs either alone or as combination therapy in the effective treatment of PDAC.

Chapter II

Materials and Methods:

2.1 Antibodies used

NRP2 (CST 3366 for mouse, R&D AF2215 for human), CD8 (CST 98941), CD4 (ab183685), CD68 (ebioscience 14-0681-82), F4/80 (ebioscience 14-4801-82), CD31 (ab28364), α-SMA (ab5694, kind gift from Dr. Maneesh Jain, University of Nebraska Medical Center), Granzyme B (ab4059), Rab5 (ab13253), Rab7 (ab50533), Rho GDI (Santa Cruz Biotechnology sc373724), β-actin (Cell Signaling Technology, 4970), Hsc 70 (Santa Cruz Biotechlogy, sc 7298), α,β tubulin (Cell signaling technology 2148).

2.2 Cell culture and generation of human PBMC and murine bone marrow derived macrophages:

Monocytes isolated from the peripheral blood of healthy human donors were obtained from the elutriation core facility at the University of Nebraska Medical Center. Cells obtained were >97% pure. PBMCs were then cultured at 37ºC with 5% CO_2 in RPMI 1640 containing 10% fetal bovine serum, 2mM glutamine, 100 µg/mL streptomycin and 100U/mL penicillin for the indicated time points. M1 macrophages were obtained by maintaining PBMCs in culture for 6 days with 100 ng/mL G-MCSF; fresh media containing G-MCSF was added to the cells every alternate day. On day 7, cells were stimulated with 1 µg/mL LPS and 10 ng/mL human recombinant IFN-Y for 24 hours. M2 macrophages were obtained by similarly maintaining PBMCs in culture for 6days with 100 µg/mL human

recombinant M-CSF and activated with IL-4, IL-10, IL-13 (10 ng/mL each) for 24 hours on day 7.

For generation of murine macrophages, mice were first euthanized by CO_2 asphyxiation, and the animal surface sprayed with 70% ethanol. tibia and femur were harvested from mice, cleaned of all muscle and connective tissue. Intact bones were then transferred to tissue culture dish containing Dulbecco's Phosphate Buffered Saline (PBS) on ice. Bone marrow was flushed from both the ends of the bone shafts with ice cold PBS using a 25-gauge needle and 30cc needle, and collected into 50mL falcon tubes on ice. Cells were centrifuged at 2000rpm for 10minutes. The cell pellet was resuspended in RPMI and filtered through a 70µm Nylon mesh filter to remove muscle and connective tissue. Cells were centrifuged again and 1mL Erythrocyte Lysis Buffer added to the pellet for lysing the red blood cells and allowed to stand for 1minute at room temperature. To neutralize, 1omL of RPMI media was added, homogenized by pipetting thoroughly with a 10mL pipette and centrifuged again at 2000 rpm for 10minutes. The cell pellet was resuspended α-MEM media containing 10% fetal bovine serum, 2mM glutamine, 100 µg/mL streptomycin and 100U/mL penicillin and the number of cells counted using a hemocytometer. Trypan Blue staining was performed to analyze the cell viability. Based on the experiment, the required number of cells were plated in either tissue culture dishes, two well chambers, or 6-well plates and cultured at 37ºC with 5% CO_2 in the above-mentioned media for the indicated periods of time. For the generation of M1 macrophages, 50 ng/mL murine recombinant G-MCSF was added into the culture for 7days; on day 2, the non-

macrophage lineage cells were removed by replacing the supernatant with fresh media containing G-MCSF. Repeated boosts of G-MCSF was added to the cells every alternate day. Finally, on day7, the old media was replaced with new media containing 1µg/mL LPS and 10ng/mL murine recombinant IFN-Y and kept for 24 hours. M2 macrophages were obtained by similarly adding murine M-CSF into the culture for 7days. Cells were activated by the addition of 10ng/mL IL-4 for 24 hours. For some experiments, to knock out NRP2, 4-HydroxyTamoxifen (1mM stock in methanol) was added into the culture media at a concentration of 0.3 µM every alternate day for 3-5days.

For isolation of peritoneal macrophages, mice were euthanized as mentioned earlier and sprayed with 70% ethanol and mounted on a Styrofoam block. The outer skin of the peritoneum was cut using scissors and forceps and gently pulled back to reveal the inner lining of the peritoneum. Using a 27gauge needle, 5mL ice cold PBS was injected into the peritoneal cavity carefully so that no organs were punctured. The peritoneum was gently massaged for 5mins to dislodge any attached cells into the cavity. Using a 25gauge needle, as much fluid was collected from the cavity as possible. Care was taken so that no fat or connective tissue or blood contamination occurred. The fluid containing peritoneal macrophages were collected into 15mL falcon tubes on ice. They were centrifuged at 2000rpm for 10mins, resuspended in complete α-MEM media mentioned earlier. The cell number was counted using a hemocytometer and plated for experiments. Peritoneal macrophages were maintained in M-CSF containing media for 3 days, following which they were subjected to different assays. (Z)-4-HydroxyTamoxifen

was added into the cell culture medium (dose as mentioned earlier in this section) for 3 consecutive days to knock out NRP2.

Panc-1 cells were purchased from ATCC. UN-KC-6141 and KPC cells were generated by Dr. Surinder K. Batra, University of Nebraska Medical Center and were a kind gift to us from his laboratory. All these cell lines were maintained in Dulbecco's Modified Eagle's Medium (DMEM) media containing 10% fetal bovine serum, 2mM glutamine, 100 µg/mL streptomycin and 100U/mL penicillin at 37ºC with 5% CO_2. For generation of conditioned media, cells were plated in 75mm^2 tissue culture flasks and allowed to grow till 75% confluency. The complete media was then removed and cells washed twice with PBS without Calcium or Magnesium and replaced with only DMEM for 48hours. The conditioned media was then collected, centrifuged at 100rpm for 5minutes, strained through 0.22µm filter and kept at -80ºC until use.

Jurkat cells were purchased from ATCC and cultured in RPMI-1640 medium containing 2 mM L-glutamine, 10 mM HEPES, 1 mM sodium pyruvate, 4500 mg/L glucose, and 1500 mg/L sodium bicarbonate, 10% FBS, 100 µg/mL streptomycin and 100U/mL penicillin at 37ºC and 5% CO_2.

2.3 Generation of human and murine Tumors Associated Macrophages (TAMs) *ex vivo*:

To generate tumor associated macrophages ex vivo, PBMCs and BMDMs were treated with conditioned media (50% v/v) collected from pancreatic cancer cell line

Panc-1 (ATCC) and UN-KC-6141 or KPC cell lines respectively for the indicated periods of time.

2.4 Generation of mouse model:

The NRP2$^{flox/flox}$ mouse was developed by Peter Mombaerts, Max Planck Research Unit for Neurogenetics. The Nrp2 targeted mutation was generated in 129P2/OlaHsd derived E14 ES cells and has a *loxP*-tauGFP-pA^{+}-FNF cassette inserted into the first intron and a corresponding loxP site inserted upstream of the start codon. The FRT-flanked neomycin resistance sequence (FNF) was excised by crossing to mice with the Tg(ACTB-flp)4917Dym transgene insertion, which was generated in a mixed B6;SJL background, yielding the *Nrp2$^{tm1.1Mom}$* targeted mutation on a mixed background that is predominantly 129P2 and C57BL/6. These mice were bred to pure C57BL/6 background and were a kind gift to us from our collaborator, Dr. Michael Muders, Germany. The FVB- Tg(Csf1r-Mer-iCre-Mer)1Jwp/J mice (developed by Dr. Jeffrey W Pollard, Albert Einstein College of Medicine) were purchased from Jackson Laboratories. These Tg(Csf1r-Mer-iCre-Mer)1Jwp transgenic mice express a Cre recombinase/mutant murine estrogen receptor double-fusion protein under the direction of the mouse Csf1r, colony stimulating factor 1 receptor, promoter. Tamoxifen-inducible cre activity is detected in bone-marrow-derived macrophages and yolk sac macrophages. When these Tg(Csf1r-Mer-iCre-Mer)1Jwp mice are bred with mice containing a loxP-flanked sequence of interest, tamoxifen-inducible, Cre-mediated recombination will result in deletion of the flanked sequences in Csf1r-expressing cells; making them useful for studying inflammation, metastasis and tracking myeloid lineage cells.

The MerCreMer double fusion protein consists of Cre recombinase flanked on each end with a mutated murine estrogen receptor (mer) ligand binding domain (amino acids 281-599, G525R); which does not bind its natural ligand (17'-estradiol) at physiological concentrations but will bind the synthetic estrogen receptor ligands 4-hydroxytamoxifen (OHT or tamoxifen) and, with lesser sensitivity, ICI 182780. Restricted to the cytoplasm, MerCreMer can only gain access to the nuclear compartment after exposure to tamoxifen. A transgenic construct containing tandem copies of icre/Esr1*, or Mer-icre-Mer, under the control of the mouse *Csf1r*, colony stimulating factor 1 receptor, promoter, was injected into fertilized FVB/N mouse eggs. Founder line 1 was subsequently established. Upon arrival at The Jackson Laboratory, the mice were crossed to FVB/NJ at least once to establish the colony. For our experimental purpose, the FVB-Tg(Csf1r-Mer-iCre-Mer)1Jwp/J (henceforth called CSF1R-Cre) mouse was first bred with C57BL/6 mice for one generation (n1). Cre^{+} mice from this n1 generation was then crossed with $NRP2^{flox/flox}$ mice to generate $NRP2f^{lox/flox}$CSF1R-Cre compound mice. Following administration of intraperitoneal injection of Tamoxifen (75mg/kg body weight from 20mg/mL stock in corn oil, every day for 5-7days) or (Z)-4-hydroxytamoxifen into cell culture medium specifically and selectively knocks out NRP2 from myeloid cells expressing CSF1R, like monocytes, macrophages and dendritic cells in an inducible manner.

2.5 Mouse genotype analysis:

Approximately, 0.5cm piece tails of 3-4 weeks old mice were snipped and digested using the tail extraction buffer and thermostable protease from Kapa Hotstart Genotyping kit (Kapa Biosystems). Each reaction mixture contained 88µL of PCR grade water, 10µL of 10X KAPA Express extract buffer (final concentration 1X) and 2µL (1U/µL) of KAPA Express enzyme. Lysis was performed for 15min at 75ºC and then stopped at 95ºC for 5mins. The digested samples were centrifuged at 13000rpm for 5mins and supernatants were transferred to clean tubes without disturbing the cell pellet. Following manufacturer's protocol, the genomic DNA was diluted 10-fold in 10 mM Tris-HCl (pH 8.0–8.5) and then used for PCR. Each PCR reaction mix consisted of 0.5µM final concentration of each of forward and reverse genotyping primers, 2X KAPA2G Fast (HotStart) Genotyping Mix with dye, 1µL of crude DNA extract (diluted) and 10.25 µL of PCR grade water. KAPA2G Fast Genotyping Mix (2X) is a ready-to-use master mix containing all components for fast PCR, except primers and template. The 2X ReadyMix contains KAPA2G Fast DNA Polymerase (with or without antibody-mediated HotStart), KAPA2G Buffer A, dNTPs (0.2 mM each at 1X), $MgCl_2$ (1.5 mM at 1X) and stabilizers. The ReadyMix also contains two inert dyes, allowing for the analysis of PCR reaction products by agarose gel electrophoresis without the need to add a DNA loading solution. After PCR amplifications, the amplicons were run on a 2% agarose gel containing 3% v/v Ethydium Bromide prepared in 1X TAE buffer, and visualized using BioDoc-It Imaging system.

2.6 Nucleofection:

siRNA transfection in PBMCs was performed using Human Monocyte Nucleofection kit (Lonza, VPA-1007) following manufacturer's protocol. 25nM siNRP2 or Scrambled antisense RNA was used. Cells were analyzed or subjected to any assay 48-72 hours after siRNA transfection.

2.7 Immunoblot Analyses:

Briefly, cells were washed with ice cold PBS followed by lysis with CHAPS lysis buffer (150mM KCl, 50mM HEPES (pH 7.4), 0.1% CHAPS, 2mM EDTA, 20µg/mL Leupeptin, 10µg/mL Aprotinin, 5mM DTT, 1mM PMSF and Halt protease and phosphatase inhibitor cocktail) on ice. Cells were gently scraped using cell scraper and sonicated on ice. Supernatant was separated by cold centrifugation (13000 rpm for 5 mins) and total protein was estimated using Bradford method (Biorad, Hercules, CA). SDS sample buffer was added and the sampled were heated at 95ºC for 8mins. The whole cell extracts were next run on 4–20% Mini-PROTEAN® TGX™ Gel (BioRad) and transferred to polyvinylidene difluoride (PVDF) membrane (Life Technologies, Carlsbad, CA). Protein transfer was to PVDF membrane was checked regularly by Ponceau stain. The membrane was then blocked in either 5% non-fat dry milk or 5% Bovine Albumin Serum (BSA) in 1X TBST (1X Tris Buffered Saline, 0.1% Tween-20) for atleast 1hour. The blocked membrane was then incubated overnight in 1X PBS containing appropriate dilution of primary antibodies overnight at 4ºC with continuous shaking at low speed. The next day, membrane was washed with 1X TBST for 5min (x5) and then incubated for 1hr in 1X TBST containing appropriate dilution of horseradish peroxidase-conjugated secondary antibody (Santa Cruz Biotechnology, Dallas, TX) with

continuous shaking at low speed. The membranes were washed in 1X TBST for 5min (x5). The protein bands were detected using SuperSignal™ West Femto Maximum Sensitivity Substrate. For successive immunoblots, membranes were stripped in Stripping Buffer (Thermo Fisher Scientific) for 20mins, re-blocked in 1X TBST containing either 5% BSA or 5% non-fat dry milk and probed as mentioned before.

2.8 RNA isolation using Trizol:

Cells were harvested and washed twice with PBS. 1mL of TRI ReagentTM (Invitrogen, CA) was added per 10million cells (if the cells were more and appeared cloudy, more trizol was added accordingly). They were gently scraped using cell scraper and collected in 2mL eppendorfs and kept for 5mins at room temperature. 300µL of Chloroform was added into each tube and mixed well by inverting the tubes for 15-20seconds. The tubes were allowed to stand for 5mins at room temperature following which they were centrifuged at 12000 rpm for 15mins at 4ºC. The clear upper supernatant was extracted without disturbing the cellular layer and collected into fresh eppendorfs. To this, we added 500µL isopropanol and 1µL of Glycogen (RNA graded from Invitrogen) and samples were allowed to stand for 5mins at room temperature. The samples were then centrifuged at 12000rpm for 15min at 4ºC. The supernatant was decanted and 1mL of 75% ethanol was added, mixed and spun at 7500rpm for 5mins at 4ºC. The supernatant was decanted and tubes air-dried for 10mins. The pellet was resuspended in 25µL DEPC water. The concentration and quality of the RNA was analyzed using Nanodrop

Spectrophotometer. The RNA was either stored at -80ºC until use or processed immediately for cDNA synthesis.

2.9 Quantitative Real-Time PCR (qRT-PCR):

Total RNA was extracted using TRIzol reagent as mentioned above. 1µg of RNA was used to synthesize cDNA by Transcriptor First Strand Synthesis kit (Roche, Indiapolis, IN, 04379012001). Quantitative real time PCR (qRT-PCR) was then carried out using Power SYBRGreen master mix (Life Technologies, Grand Island, NY, 4368706) as described using Applied Biosystems (ABI) 7500 Real Time PCR machine. The acidic ribosomal phosphoprotein, 36B4 gene was used to normalize and calculate the relative levels of mRNA expression of genes of interest, using the $2^{-\Delta\Delta Ct}$ methods and expressed as arbitrary units. The sample analysis was performed in duplicates. Data is represented as ±SEM.

2.10 Continuous *E.coli* phagocytosis and clearance assay:

(i) continuous phagocytosis to demonstrate phagosome maturation defect: The pHrodo™ Red *E. coli* BioParticles™ Conjugate suspension was prepared following manufacturer's protocol. The particles are non-fluorescent outside the cell, but fluoresce red in the phagosomes. The intensity of red fluorescence increases with increasing acidity of cellular compartment where the particles are localized. An optimized dose of 65µg/mL bioparticles were used for phagocytosis.

For continuous phagocytosis assay, either human PBMC derived macrophages or murine BMDM were grown in two welled chambers as described in 2.2. Human

PBMC derived macrophages were subjected to nucleofection on day5 to knock down NRP2 and the assay was performed on day7. Before the assay, cells were washed twice with 1X DPBS. The fluorescent *E.coli* particles were then added at a concentration of 65µg/mL and incubated at 37ºC for the indicated periods of time to allow adequate particle internalization. Different time points were used depending upon the objective of the experiment. Phagocytosis was arrested by placing the cells on ice and washing vigorously 3-5 times with 1X DPBS to remove the excess particles. Cells were then fixed with 4% paraformaldehyde at 4ºC for 20 minutes and washed with DPBS to remove the excess fixative. Nuclei were stained using the nuclear dye Hoechst in PBS for 5 minutes, washed twice with 1X PBS and analyzed by either Zeiss LSM 800 with Airyscan or Zeiss 710 Confocal Laser Scanning Microscope at UNMC confocal core facility, and data were analyzed and processed with the Zeiss Zen 2010 software. All confocal data were quantified using ImageJ software and graphical illustrations made using GraphPad Prism software as mentioned later.

(ii) E.coli uptake assay: Human macrophages or mouse BMDMs were grown in two well chambers as mentioned in 2.10 (i). Before the assay, cells were washed twice with 1X DPBS and added 65µg/mL red fluorescent E.coli particles for 1hr at 37ºC to allow the cells to phagocytose the particles. Uptake was arrested by adding ice cold DPBS. Cells were thoroughly rinsed with DPBS to remove excess bioparticles from the supernatant. Cells were next fixed with 4% PFA for 20mins at 4ºC, washed thrice with DPBS to remove excess fixative and nuclei stained with

Hoechst. Cells were then analyzed by confocal microscopy as described in 2.10 (i).

(iii) *in vitro* E.coli clearance assay: BMDMs or mouse peritoneal macrophages were grown in two well chambers as described earlier. On day of the experiment, cells were washed twice with 1X DPBS and added 500 µL of Opti-MEM media per well. pHrodo red E.coli bioparticles were added at a concentration of 65 µg/mL for 15mins (pulse) to allow the cells to uptake the bioparticles. Immediately after 15mins, uptake was stopped by adding ice cold DPBS. Cells were washed vigorously with DPBS (x3) to remove any E.coli particle that was not taken up or loosely adhered to cell surface. Fresh complete α-MEM media was added and the gradual maturation and clearance (breakdown) of the E.coli particles was monitored at different time points (chase). At each time point, chambers were taken out, cells vigorously washed with DPBS (x5) and fixed with 4% PFA for 20mins at 4ºC, nuclei stained with Hoechst and analysed using confocal microscopy as described earlier.

Where mentioned, human macrophages grown for phagocytosis as described in 2.10 (i) were washed with 1X DPBS twice and added pHrodo red fluorescent tagged E.coli bioparticles (30 µg/mL) and allowed the cells to phagocytose the bioparticles for 45mins. Cells were then gently washed with DPBS to remove the excess pHrodo red bioparticles from the media, added fresh DPBS into which green fluorescent E.coli bioparticles were added (30 µg/mL) for another 45mins. This allowed us to monitor phagosome maturation by chasing the maturation of pHrodo E.coli bioparticles containing phagosomes as well as uptake of E.coli

particles using the green bioparticles. At the end of the experiment, cells were vigorously washed with ice cold DPBS to stop uptake and fixed with 4% PFA for 20mins at 4ºC. Cells were washed with DPBS (x3) to remove excess fixative, nuclei stained with Hoechst and analyzed by Confocal microscopy as described in 2.10 (i).

2.11 *In vitro* Apoptotic Cell Clearance Assay:

For this assay, Jurkat cells were grown as mentioned in 2.2. Prior to the assay, the cells were centrifuged at 1000rpm for 5mins, washed with 1X PBS (x2). They were resuspended in only RPMI and incubated in 50µM Etoposide (Abcam) overnight at 37ºC and 5% CO_2 for 12hrs. This treatment routinely yielded 80-90% apoptotic cells. The next day, cells were centrifuged at 2000 rpm for 10mins and the pellet was washed twice with PBS. The cells were incubated with pHrodo™ Red, succinimidyl ester (Thermo Scientific) following manufacturer's instructions. This dye enabled us to view the apoptotic cells in the phagosomes only after they are internalized. Cells were centrifuged at 2000rpm for 10mins. The cell pellet was washed twice with 1X DPBS and resuspended in Opti-MEM medium (Gibco). Mouse BMDMs or peritoneal macrophages were plated in two well chambers and grown in the presence of M-CSF as described earlier in 2.2. (Z)-4-HydroxyTamoxifen was added to knock out NRP2 as described earlier. On the day of the assay, the old medium was removed, cells were washed twice with 1X PBS and added 500µL Opti-MEM medium per well. Apoptotic Jurkat cells were added (1:5 macrophage : jurkat ratio) for either 15min or 30min (pulse) and allowed the cells to uptake at 37ºC. Following this, uptake was stopped by adding ice cold

DPBS; cells were vigorously washed with DPBS (x3) to remove any cell that was not phagocytosed or remained loosely bound to the cell surface. Fresh complete α-MEM media was added and the clearance of apoptotic cells were monitored over time (chase). At each time point, cells were vigorously washed with DPBS (x5), fixed with 4% PFA at 4ºC for 20mins and washed again with DPBS (x3) to remove excess fixative. Nuclei were counterstained using Hoechst for 5mins and analysed using confocal microscopy as mentioned earlier.

2.12 *In vitro* Zymosan Clearance Assay:

For this assay, BMDMs were grown in two well chambers as described earlier. On the day of the experiment, cells were washed twice with 1X DPBS and added 500 µL of Opti-MEM media per well. pHrodo red zymosan particles were added at a concentration of 65 µg/mL for 15mins (pulse) to allow the cells to uptake the particles. Immediately after 15mins, uptake was stopped by adding ice cold DPBS. Cells were washed vigorously with DPBS (x3) to remove any zymosan particle that was not taken up or remained loosely adhered to cell surface. Fresh complete α-MEM media was added and the gradual maturation and clearance (breakdown) of the zymosan particles was monitored at different time points (chase). At each time point, chambers were taken out, cells vigorously washed with DPBS (x5) and fixed with 4% PFA for 20mins at 4ºC, nuclei stained with Hoechst and analysed using confocal microscopy as described earlier.

2.13 Subcutaneous Tumor implantation:

UN-KC-6141 cells were maintained in culture as described earlier. For subcutaneous implantation, cells were allowed to grow until 50% confluency. The night before implantation, the old medium was replaced with fresh complete medium. The next day, the cells were washed with 1X DPBS, and then trypsin was added to the cells for 2mins, neutralized by adding equal volume of media containing FBS and centrifuged at 1000rpm for 5mins. Cells were washed twice with DPBS and resuspended in DPBS and cell number and viability counted using Trypan Blue. Cells with less than 90% viability were discarded. Cells were centrifuged again and resuspended in HBSS. For implantation, 500,000 cells in HBSS were mixed with equal volume of Matrigel (without growth factors) so that the total volume was 100µL and kept on ice.

The right dorsal flanks of mice were gently shaved using Veet hair removal crème and a spatula. Care was taken so as not to irritate or inflame the skin of the mice. The cell mixture was slowly pulled up using a 1mL syringe and 22gauge needle and kept on ice. The skin of the mouse around the dorsal right flank was gently pinched using the index and middle finger and pulled away from the body of the mouse, and the cells were slowly and carefully injected into the pocket created. For our studies, mice were divided into two groups (n=3 or 5 in each group). To deplete NRP2 from the macrophages, the test group was injected with Tamoxifen intraperitoneally (75mg/kg body weight from a 20mg/mL stock in corn oil) everyday till the end point of the experiment. The control group was injected with corn oil as vehicle control. The tumor growth was manually monitored regularly using digital slide calipers and weight of the mice recorded. Once the end point of the

experiment was reached, mice were euthanized by CO2 asphyxiation following IACUC protocol and tumors harvested. Harvested tumors were washed gently in ice cold DPBS, transferred to new tubes containing DPBS and kept on ice. Tumors were fixed in 10% formaldehyde overnight and transferred to 70% ethanol and given to Tissue Science Facility at UNMC for paraffin embedding, sectioning (4 µm) and Hematoxylin and Eosin (H&E) staining. Sections were subjected to staining for different proteins as described later.

2.14 Histology and Immunostaining:

Immunohistochemistry and immunofluorescence staining on histological sections were performed using the following procedure: slides containing tissue sections (4µm thick) were kept on heat block at 58ºC for 2hours. They were then rehydrated in a sequential passage of solutions starting with Xylene for 20mins, 100% ethanol for 15mins, 95%, 90%, 80%, 75%, 50% and 20% ethanol for 5mins each followed by immersion in double distilled water for 10mins. For IHC only, slides were next immersed in 3% Hydrogen Peroxide (H2O2) in methanol for 1hr at room temperature followed by incubation in double distilled water for 5mins. Antigen retrieval was performed using Dako antigen retrieval solution (either pH9 or pH6, depending on the antigen of interest). The antigen unmasking solution was first preheated at a high temperature in the microwave until boiling and then the slides were immersed into it and boiled on a 98ºC water bath for 45mins. Following this, the slides were gradually allowed to cool to room temperature for atleast 1hr and then washed with 1X PBS thrice, 5mins each. Slides were then blocked with 5% goat serum in 1XPBS containing 0.2% saponin at 4ºC for 1hr in a moist chamber.

Then the tissue sections were covered with 1X PBS containing 0.2% saponin and 3% BSA and the required concentration of primary antibodies, and incubated overnight in a moist chamber at 4ºC. The next morning, slides were washed in 1X Tris Buffered Saline (TBS) solution for 5mins (x5). Secondary antibodies were then diluted in in 1X PBS containing 0.2% saponin and 3% BSA at 1:200 concentration for biotinylated antibodies (IHC) or 1:500 for fluorophore conjugated antibodies (IF) and incubated for 1hr in dark in a moist chamber. For IHC staining, slides were next washed with 1X TBS for 5min (x6) and then incubated with Avidin-Biotin complex for 40mins at room temperature, following manufacturer's instructions. Slides were then rinsed with 1X TBS for 5mins (x3) and added diaminobenzidine solution containing 0.3% H2O2 as a substrate for peroxidase (Dako) until the desired staining intensity was developed. Slides were washed in double distilled water and hematoxylin added for counter staining. The slides were then rinsed under running tap water to remove excess counter staining, and the dehydrated by gradual passage of slides from double distilled water to xylene in a reverse order mentioned earlier for rehydration of slides. Slides were finally mounted with Permount and covered with glass cover slips. Clear nail polish was used to seal the sides of the cover slips. The whole slides were next digitally scanned at Tissue Science Facility, UNMC. For IF, following incubation with secondary antibody, slides were thoroughly washed with 1X TBS for 5mins (x5) and finally once with distilled water and then mounted with Vectashield mounting media containing DAPI (Vector Laboratories, Burlingame, CA). For monolayer culture, immunofluorescence staining was performed as described: briefly, cells were

grown on poly-DL-lysine–coated coverslips (BD Biosciences) for indicated periods of time before fixation and analysis by confocal microscopy. Cells were rinsed with Dulbecco's Phosphate-Buffered Saline (DPBS; Invitrogen)(x3), followed by fixation with ice cold 4% paraformaldehyde at 4ºC for 20 minutes. Cells were then washed with DPBS (x3). Finally, cells were blocked using 1% BSA and 0.2% saponin in PBS for 1hr at 4ºC in a moist chamber. The slides were then incubated overnight in the same blocking buffer containing appropriate concentration of primary antibodies at 4ºC in a moist chamber. The next day, the coverslips were carefully washed in 1X PBS (x5) and added fluorescent conjugated antibodies (1:200) in 1X PBS containing 1% BSA and 0.2% saponin for 2hrs at 4ºC in a moist chamber. The coverslips were finally washed in 1X PBS (x5) and mounted on glass slides with mounting media containing DAPI as mentioned above and sealed with clear nail polish. Slides were viewed using either Zeiss LSM 800 with Airyscan or Zeiss 710 Confocal Laser Scanning Microscope at UNMC confocal core facility, and data were analyzed and processed with the Zeiss Zen 2010 software. All confocal data were quantified using ImageJ software and graphical illustrations made using GraphPad Prism software as mentioned later.

The list of all the primary antibodies used have been listed earlier. For the purpose of Immunofluorescence staining, the secondary antibodies conjugated with fluorophores were purchased from Invitrogen Corporation, and DAPI from Vector laboratories was used for counter staining the nuclei. For IHC, biotinylated antibodies were purchased from Invitrogen. The ABC Peroxidase Standard Staining Kit was purchased from Thermo Fisher Scientific.

2.15: TUNEL staining

To assess the number of apoptotic or necrotic cells in the tumor tissues, TUNEL staining was performed following manufacturers' instructions (Roche *In Situ* Cell Death Detection Kit, TMR red, catalogue number 12156792910).

2.16 Isolation of TAMs from subcutaneous mouse tumors:

TAMs were isolated as described elsewhere (246). Subcutaneous mouse tumors were generated as mentioned above. The tumors from both control and test animals were harvested and kept in ice cold RPMI media on ice. Each tumor was cut into small pieces using scissors or scalpel and the digestion media was added (RPMI media containing the following: 10U/mL Collagenase I, 400U/mL Collagenase IV, 30U/mL DNAse I- all diluted in HBSS) and kept at 37ºC for 30mins. Following this, the tumor pieces were crushed with the plunger of a 10mL syringe, 5mL RPMI media was added and homogenized well using a 10mL pipette. The tumor suspension was filtered by passing through a 70µm nylon gauze and the collected into fresh tubes. The suspension was centrifuged at 450g for 6min at 4ºC; the supernatant was discarded and the pellet was resuspended in 2mL erythrocyte lysis buffer to remove the RBCs. The tubes were allowed to stand for 2mins at room temperature, neutralized by the addition of 12mL of RPMI media, passed through a sterile 70µm nylon gauze and centrifuged again at 450g for 6mins at 4ºC and the supernatant discarded. The pellet was resuspended in Lymphoprep solution at a concentration of 1-2X10^7 cells/mL and transferred to fresh tubes. To this was added 6mL RPMI media very cautiously to obtain a two-

phase gradient. The gradients were centrifuged at 800 *x g* for 30 min at room temperature without acceleration or break. The interphase (enriched in myeloid cells and lymphocytes as well as the upper layer containing the RPMI media were collected into fresh tubes without disturbing the lymphoprep layer. The cells were washed once with MACS buffer, centrifuged at 800g for 5mins at 4ºC and the supernatant discarded. The cell pellet was finally resuspended in MACS buffer at a concentration of 10^8 cell/mL. TAMs were isolated using CD11B magnetic beads and LS columns (both from Miltenyi Biotech) following manufacturer's instructions. The CD11B+ myeloid cells were arrested in the columns and the non-labelled cells, which were mainly the enriched T cells, were collected as flow-through in separate tubes. The TAMs thus collected were centrifuged and Trizol was added and kept in -80ºC for processing for RNA-Seq analysis.

2.17 Transcriptome analysis using RNA-Seq:

CD11b+ cells were isolated from subcutaneous PC tumors using magnetic beads as mentioned in 2.15. RNA was isolated from the control and test group with n=3 animals contributing to each pool. This was done in order to obtain sufficient amount of RNA. RNA-Seq service was obtained from Kelvin Chan and his team at Seqmatic. Extracted RNA was QC with Agilent TapeStation RNA screentape. The RIN value of the control sample was 9.1 and that of the test was 9.4. A paired end read 2x75bp sequencing run of RNA libraries were performed using the Illumina NextSeq 500 instrument. For analysis, raw reads were demultiplexed by barcode and output into FASTQ format. Cutadapt was used to filter out adapter sequences and low-quality bases. Filtered sequence reads were aligned to mouse reference

genome mm10 using HISAT2 aligner. Reads mapping to exon regions as defined by Ensembl gene annotations were counted using FeatureCounts. Data analysis was performed with the help of Seqmatic, California and the Bioinformatics and Systems Biology Core at UNMC. To address the limitation of number of samples, we chose to identify differentially expressed genes using $\log_2$ fold metric instead of p-value. Genes with a cutoff value $\log_2$ fold change1 were selected and those with zero counts in both control and test samples or in either of them were eliminated for stringency. The Ingenuity Pathway Knowledge Base (IPA) was used to identify the enriched canonical pathways and cellular and molecular functions among the differentially expressed genes in the two samples. In addition to the IPA, the Database for Annotation, Visualization and Integrated Discovery (DAVID), the Gene Ontology Project, Kegg Pathway and extensive literature curation was performed to identify functional terms associated with the differentially expressed genes. Among the enriched functional annotation clusters, we selected representative clusters (as mentioned in the Results section) to analyze the effect of NRP2 depletion on phagocytosis, macrophage phenotype and secretion of chemokines and cytokines as well as interaction between macrophages and leucocytes/lymphocytes.

2.18 Statistical Analyses:

All the graphical illustrations statistical tests were performed using Prism-6 software (GraphPad software, Inc., La Jolla, CA). All data reported in graphs are expressed as mean ± standard error of mean (SEM) unless otherwise mentioned and were compared using unpaired student *T*-test, p values were considered

statistically significant when less than 0.05. All experiments were repeated at least 3times unless specified.

Chapter III

NRP2 is expressed in M1 and M2 type macrophages and regulate phagocytosis by modulating early to late phagosomal maturation.

3. NRP2 is expressed in M1 and M2 type macrophages and regulate phagocytosis by modulating early to late phagosome maturation.

3.A. Introduction

Macrophages are highly plastic and functionally diverse cells of the immune system and undertake an array of functions, like maintenance of homeostasis by phagocytosing and clearing apoptotic debris in tissues, metabolic homeostasis, development of organs, angiogenesis to combating inflammations or microbial infections. They can also bridge the innate and adaptive arms of the immune system by their ability to prime naïve T cells. Briefly, macrophages can exist as classically activated or M1 type or alternatively activated or M2 type. M1 type macrophages are cytotoxic and release pro-inflammatory cytokines to eliminate infected or injured cells. However, post infection or injury, M1 type cells polarize towards a reparative M2 type, that secrete angiogenic growth factors, tissue remodeling matrix metalloproteases and other immunosuppressive cytokines for suppressing T cell responses, that augment the wound healing and tissue repair processes (15, 54, 56, 247).

Neuropilins (NRPs) are non-tyrosine kinase, cell surface glycoproteins that are widely characterized for their roles in development, migration and angiogenesis. Two isoforms are known till date, NRP1 and NRP2. NRPs are often overexpressed in several neoplasms and correlate with cancer cell survival under stress, proliferation, metastasis and poor patient survival. Research over the past few years have focused on the role and function of NRPs in different immune cell compartments. In comparison to NRP1, NRP2 is less characterized in the immune

subsets (241). Although previous studies detected NRP2 expression in macrophages, its function and the molecular pathways that govern these functions are still not clearly known. The primary role of macrophages is phagocytosis. This function is indispensable for microbial clearance. Following internalization of cargo, nascent phagosomes in macrophages mature to late phagosome and phagolysosome, recruiting and fusing with the classical endocytic compartments and gradually becoming more and more acidic in the process (219, 220). The processes of endosomal and phagosomal maturation are similar in many aspects, often recruiting identical effector molecules. Our previous report documented a requirement for NRP2 in endosomal maturation in cancer cells (242). However, its role in phagocytosis in macrophages is not well understood. Based on our previous observation that NRP2 positively regulates endosomal maturation in cancer cells and the similarity between endosomal and phagosomal maturation processes, we hypothesized that NRP2 regulates phagocytosis in macrophages.

In this chapter, we report the expression pattern of NRP2 in human and murine macrophages under M1 and M2 polarizing conditions. Using human macrophages and bone marrow derived macrophages isolated from transgenic mice generated in our lab, where NRP2 can be selectively depleted from the myeloid cells, we observed NRP2 regulates phagosomal maturation in macrophages and hence pathogen clearance *in vitro*. Further, NRP2 depletion does not significantly affect the uptake of phagocytic cargo. In agreement with the phagosomal maturation defect, we observed an increased accumulation of Rab5+ early phagosomes and a concomitant decrease in the number of Rab7+ late

phagosomes in absence of NRP2. Overall, our study documents a novel role of NRP2 in regulation of phagocytosis in macrophages.

3.B. Results

NRP2 is expressed in human and murine bone marrow derived M2 type macrophages: NRP2 is not expressed by monocytes or bone marrow precursor cells. To get M2 type macrophages, monocytes isolated using elutriation from the peripheral blood of healthy human donors were differentiated using M-CSF for 7days, following which they were exposed to M2 polarizing cytokines, like IL-4, IL-10 and IL-13 for 24hrs. A similar differentiation protocol was followed for differentiating mouse bone marrow derived precursor cells. NRP2 is not detected at protein level in either human monocytes or murine bone marrow derived precursor cells, but an enhanced mRNA (not shown) and protein expression was observed during the differentiation of the human monocytes to mature M2 type macrophages (**Fig. 3.1 A**). Interestingly, there was no further increase in the expression level of NRP2 following treatment with M2-polarizing cytokines, IL-4, IL-10 or IL-13. Further, the data suggested a post translational modification of NRP2 as the cells gradually differentiated to mature macrophages. Various post translational modifications have been reported for NRP2. For example, it undergoes polysialylation in microglia. The post translational modification of NRP2 in macrophages is beyond the scope of the current study.

A similar enhancement in the mRNA (not shown) and protein level of NRP2 was observed during the differentiation of murine bone marrow derived precursor cells to mature macrophages following treatment with mouse recombinant M-CSF for

7days, and then exposure to M2-polarizing cytokines, like IL-4, IL-10 or IL-13 for 24hrs (**Fig. 3.1 B**).

NRP2 is expressed in human and murine bone marrow derived M1 type macrophages: To generate inflammatory M1 type macrophages, monocytes isolated from the peripheral blood of healthy human donors using elutriation was differentiated using G-MCSF for 7days, following which the cells were treated with a combination of LPS and IFN-γ for 24hrs. As mentioned in 3.B.1, NRP2 is not detected at protein level in the human monocytes. However, an upregulation in the expression of NRP2 mRNA (not shown) and protein was observed as the cells differentiated towards M1 type macrophages. There was further enhancement in the expression of NRP2 following stimulation of the cells with a combination of LPS and IFN-γ (**Fig. 3.2 A**). Similarly, in murine bone marrow derived precursor cells, NRP2 expression was not observed at a detectable level. However, an enhancement in NRP2 protein level was observed as the precursor cells differentiated to M1 type macrophages. Here also, following stimulation with a combination of LPS and IFN-γ for 24hrs, further upregulation in the protein level of NRP2 was observed (**Fig. 3.2 B**).

NRP2 regulates phagocytosis in human macrophages: Phagocytosis is one of the key functions of macrophages and important for maintenance of physiological homeostasis as well as microbial clearance during infections. Phagocytosis, a special form of endocytosis, recruits similar downstream effector molecules and the two pathways eventually converge onto each other. Because we previously observed that NRP2 regulates endocytosis in cancer cells, therefore, we wanted

to investigate whether NRP2 regulates phagocytosis in macrophages. To confirm if NRP2 plays a role in phagocytosis in human macrophages, we differentiated human PBMCs on M-CSF for 7days. NRP2 was depleted using siRNA approach. We incubated the macrophages with pHrodo red and pH insensitive green *E.coli* bioparticles at an optimized concentration of 65µg/mL for 1.5hrs. The pHrodo *E.coli* bioparticles are non-fluorescent at neutral pH, however their fluorescence intensity increases with an increase in acidity of the vesicle they are localized in. Following engulfment, phagocytic cargo remains in nascent early phagosomes of higher pH, which sequentially mature to late phagosomes, becoming more and more acidic and finally fuse with the lysosomes. Therefore, a bright red fluorescence dot in the cell indicates a mature phagocytic vesicle containing the *E.coli*, which has or is going to be fused with lysosomes and thus can indicate an active phagocytic process. On the other hand, the pH insensitive *E.coli* particle (green) uniformly fluoresces irrespective of the pH of the phagosome or phagolysosome it is delivered to. This experimental approach enabled us to test the ability of the macrophages to mature the phagosomes (red) as well as their uptake efficiency (green) in the presence and absence of NRP2. A schematic for the experimental design is shown in **Fig. 3.3 A**. Quantification of the average total cell fluorescence revealed a significant decrease in the intensity of red puncta in siNRP2 treated macrophages. This indicated that as compared to control where phagosomes containing *E.coli* bioparticles matured to acidic late phagosomes or fused with lysosomes, in NRP2 depleted macrophages, the maturation of early phagosome to more acidic less phagosome or the formation of phagolysosome was delayed.

However, the uptake efficiency in mock and siNRP2 treated macrophages were similar, as evident from the intensity of the green puncta **(Fig. 3.3 B)**. **Fig. 3.3 C and D** represent the quantification of the result and knockdown efficiency of NRP2 following electroporation with siNRP2. This data suggested that NRP2 regulates phagosomal maturation in macrophages, without significantly affecting the uptake process. NRP1 and NRP2 share structural homology and can have redundant functions. To test if NRP1 regulates phagosomal maturation in macrophages, phagocytosis assay was repeated using pHrodo *E.coli* bioparticles following NRP1 depletion. However, we did not observe any difference in the maturation of phagosomes when NRP1 was knocked down in macrophages (**Fig. 3.4 A**). **Fig. 3.4 B and C** respectively show the graphical representation of the result and the knockdown efficiency for NRP1. This indicates NRP2 uniquely regulates phagocytosis in macrophages.

Because during any type of infection or injury, GM-CSF induced M1-type macrophages are predominantly found in tissues and phagocytose pathogens, we tested the role of NRP2 in phagocytosis in GM-CSF treated human macrophages. For this, we repeated the phagocytosis assay using pHrodo *E.coli* bioparticles following NRP2 depletion by siRNA approach. Our results indicated a similar maturation delay in absence of NRP2 (**Fig. 3.5 A**). **Fig. 3.5 B and C** respectively show the graphical representation and the knockdown efficiency of NRP2. Next, to assess if NRP2 regulates the uptake of phagocytic cargo in GM-CSF treated macrophages, phagocytosis assay was repeated using pH insensitive *E.coli* bioparticles (red) following NRP2 depletion. We did not observe any significant

change in the uptake efficiency of macrophages depleted of NRP2 (**Fig. 3.6 A**). **Fig. 3.6 B and C** show the quantification of the phagocytic uptake and the knockdown of NRP2 respectively. Overall, these data suggest that NRP2 regulates phagocytosis in macrophages through modulation of phagosomal maturation.

NRP2 regulates phagocytosis in murine macrophages: We validated our observations made in human macrophages using a transgenic mouse model that we have developed in our lab. We have developed a compound mouse by crossing $NFP2^{fl/fl}$ mice with Tg (Csf1r-Mer-iCre-Mer)1Jwp mice for selective and inducible knockout of NRP2 in myeloid lineages following intraperitoneal administration of Tamoxifen (75mg/kg body weight from 20mg/mL stock in corn oil) for 3-5days or addition of (Z)-4-Hydroxytamoxifen to the cell culture medium at a concentration of 0.3µM for 3-5days (**Fig. 3.7 A**). We optimized NRP2 knockout using different concentrations of (Z)-4-HydroxyTamoxifen (**Fig. 3.7 B**). For future experiments, 0.3 µM concentration was used.

For phagocytosis assay, bone marrow derived precursors were differentiated to M2 type macrophages with M-CSF for 7days. (Z)-4-HydroxyTamoxifen was added to the cell culture medium at a concentration of 0.3µM every alternate day to knock out NRP2. Phagocytosis assay was performed using pHrodo red *E.coli* bioparticles at an optimized concentration of 65µg/mL for 1.5hrs. As in case of human macrophages, NRP2 depleted murine BMDMs had significantly less number of red visible puncta as compared to the control cells where bright red phagocytic vesicles were observed (**Fig. 3.8 A**). Reduction in the intensity of visible red fluorescence or number of bright red puncta indicated a

delay in the formation of acidic late phagosomes or phagolysosomes. **Fig. 3.8 B and C** show the graphical representation of the result and knock out efficiency for NRP2 respectively. NRP1 protein level remained unaffected following addition of HydroxyTamoxifen (**Fig. 3.8 C**), indicating that NRP2 uniquely regulates phagocytosis in macrophages.

Next, we wanted to test if NRP2 regulates uptake of phagocytic cargo in mouse macrophages. For this, mouse bone marrow derived macrophages were exposed to 65µg/mL pH insensitive *E.coli* bioparticles (red) for 1hr and uptake efficiency monitored using confocal microscopy. We did not observe any significant change in the uptake efficiency of macrophages following depletion of NRP2 (**Fig. 3.9 A**). **Fig. 3.9 B and C** show the graphical quantification of the result and the depletion of NRP2 respectively.

Since maturation of nascent phagosomes is a prerequisite for efficient degradation of engulfed cargo, next, we wanted to assess the effect of NRP2 depletion on macrophages to clear bacterial load *in vitro*. For this, we conducted a phagocytic pulse and chase experiment using pHrodo *E.coli* particles. A schematic diagram explaining the experimental design is shown in **Fig. 3.10 A**. First, bone marrow derived precursors were differentiated to M2 type macrophages as mentioned earlier and NRP2 knocked out using (Z)-4-HydroxyTamoxifen. pHrodo red *E.coli* bioparticles were added to the cells at a concentration of 65µg/mL for 15mins (pulse). Excess bacteria that either not engulfed or remained loosely adherent were removed by vigorous washing. Next, phagosomal maturation and degradation and clearance of the bacteria from the cells was monitored at chase

time points= 15mins, 45mins, 1.5hrs, 2hrs and 4hrs using confocal microscopy. In the control macrophages, starting from 0min up to 2hrs chase and 4hrs, there was a gradual increase in the intensity and number of red phagocytic vesicles indicating their maturation and probably fusion with lysosomes. Interestingly, at 4hrs chase, there was once again a decrease in the intensity of the visible red puncta, suggesting degradation of the *E.coli* bioparticles (**Fig. 3.10 B**). Compared to the control, NRP2 depleted macrophages had significantly less red intensity and less number of visible red puncta upto 2hrs chase **(Fig. 3.10 B)**. However, at 4hrs chase, higher value of total cellular fluorescence in the NRP2 depleted cells in comparison to the control macrophages indicated that phagosomes have probably started maturing in the former, whereas the bioparticles are almost degraded at that time in the control cells. This indicated that in control cells, phagosomes containing *E.coli* bioparticles matured and fused with lysosomes and degraded the phagocytic cargo, whereas in absence of NRP2, there was a delayed maturation of phagosomes. **Fig. 3.10 C and D** respectively show the quantification of the result and the knockout of NRP2. show the quantification of the result and the knock out efficiency for NRP2 respectively. Overall, these results further highlight the fact that NRP2 regulates phagocytic activity in macrophages. Cells infected with bacteria try to degrade the pathogen by phagosomal maturation and their subsequent lysosomal degradation. Based on our observations, it is thus conceivable that NRP2 depletion will impair the ability of professional phagocytes like macrophages to clear bacterial load following infection.

Following uptake of *E.coli* bioparticles, TLR4 pathway is activated. One major concern would be whether NRP2 selectively regulates TLR4 mediated phagosome maturation and degradation or whether NRP2 can regulate phagosome maturation or clearance of particles that recruit other pathways for their maturation and clearance. To test this, we performed phagocytic pulse and chase experiment using pHrodo red zymosan particles (that signal through TLR2 pathway) that are are non-fluorescent at neutral pH, but start fluorescing in the phagosomes. For this assay, murine BMDMs were cultured in the presence of M-CSF for 7days and NRP2 depleted by the addition of 0.3μM (Z)-4-HydroxyTamoxifen into the culture. Zymosan particles were added to the cells at a concentration of 65μg/mL for 15mins (pulse) following which the degradation was monitored at 6hrs, 10hrs, 14hrs and 18hrs (chase). A schematic diagram showing the experimental design is provided in **Fig. 3.11 A**. After 15mins pulse, both the control and NRP2 depleted macrophages showed similar number of zymosan containing phagosomes. At 6hrs, we observed a burst in the visible red fluorescence in both the control and NRP2 depleted cells. This indicated the beginning of the maturation process. However, at 10hrs, 14hrs and 18hrs, the control macrophages gradually matured the phagosomes and efficiently degraded and cleared the zymosan particles, as evident from the gradually decreasing intensity of visible red puncti structures of the zymosan particles. Interestingly, NRP2 depleted macrophages significantly delayed the degradation and clearance process. This was evident from the bright red fluorescence and bigger size of the zymosan particles that persisted within the cells, even at 18hrs, when the control cells had efficiently broken down individual

particles (**3.11 B**). This data confirms our hypothesis that NRP2 regulates phagocytic activity in macrophages and that its depletion significantly delays the clearance bacteria and zymosan particles *in vitro*. **Fig. 3.11 C and D** respectively show the graphical representation of the data and the knock out efficiency of NRP2.

NRP2 inhibits early to late phagosome maturation in macrophages: Our previous findings demonstrated that NRP2 regulates phagosomal maturation; depletion of NRP2 either genetically or by siRNA approach resulted in delayed maturation of *E.coli* containing phagosomes as well slowed down the clearance of E.coli and zymosan bioparticles in macrophages. Nascent phagosome maturation occurs in a step-wise manner through sequential recruitment of Rab5 to the early phagosomes followed by Rab7 to the late phagosomes. To test the effect of NRP2 depletion on phagosome maturation, we next assessed the $Rab5^{+}$ early phagosomes and $Rab7^{+}$ late phagosomes in NRP2 proficient and deficient cells. In NRP2 depleted human macrophages, there was an increased accumulation of Rab5+ early phagosomes and a concomitant decrease in the $Rab7^{+}$ late phagosomes (**Fig. 3.12 A**). Similar observations were made in mouse bone marrow derived macrophages following NRP2 knock out (**Fig. 3.13 A**). **Fig. 3.12 B and 3.13 B** show the graphical representations for changes in early and late phagosome maturation in human and mouse macrophages respectively. **Fig. 3.12 C and 3.13 C** respectively show that total cellular level of Rab5 and Rab7 remain unaffected following NRP2 depletion in human and mouse macrophages respectively. Knockdown or knockout for NRP2 is also shown in **Fig. 3.12 C and**

3.13 C respectively. Overall, these data suggest that NRP2 regulates phagosome maturation in macrophages. Depletion of NRP2 arrests maturing phagosomes in the early stages and impairs their maturation to late phagososomes or phagolysosomes.

3.C. Summary and Discussion

Limited information is currently available about the function of NRP2 in macrophages. Previous literature as well as our current data show NRP2 is not expressed at a detectable level in freshly isolated human monocytes or bone marrow derived precursor cells in mouse. Its expression is induced as the cells differentiate towards mature macrophages, under M1 as well as M2 polarizing conditions. This raises the important question what might be the potential function of NRP2 in macrophages under normal physiological conditions (for example, when macrophages predominantly exist as M-CSF induced M0/M2 type) or during infections or inflammations (where GM-CSF is abundant, and macrophages mainly polarize towards inflammatory M1 type) and whether it can be potentially targeted for therapeutic purposes in the future. Our current study has answered some of these questions. Earlier literature suggested that Neuropilins are required for cellular locomotion. The directional migration of neuronal and endothelial cells is regulated by Neuropilins and their co-receptors such as Plexins and VEGF receptors. Interestingly, recent report also indicated the presence of a specific polysialylated form of NRP2 in dendritic cells, which is required for their movement to lymph nodes (36). Although NRP2 may potentially promote the migration, studying other molecular pathways it can govern will be crucial for the comprehensive understanding of its role in macrophages under normal as well as pathological conditions.

We have previously reported a requirement for NRP2 in regulating endocytic activities in cancer cells, where it favors the maturation of early to late

endosome (242). Recognition of microbial pathogens and their phagocytosis is one of the most important functions of macrophages for maintenance of homeostasis. Following phagocytic engulfment, the internalized cargo initially remains in a nascent phagosome which needs to acquire the microbicidal enzymes and acidify its lumen for degradation of the cargo. For this maturation process, the phagosomes need to undergo a tightly co-ordinated sequence of fusion and fission with distinct compartments of the endocytic pathway (219, 220). Notably, the phagocytosis and classical endocytosis pathways are similar in many aspects, recruiting similar families of effector molecules for the maturation process. In their report, Stamatos *et al.* reported a progressive loss of polysialylation in monocytes and monocyte derived cells as they migrate to the pulmonary and peritoneal sites of inflammation. Removal of polysia enhanced macrophage phagocytosis of *Klebsiella pneumoniae*. However, it is not clear if this effect could be attributed to NRP2 alone (61). In the current study, we reveal a novel role of NRP2 in regulating phagocytosis in macrophages. NRP2 and NRP1 share structural homology and may have redundant functions. Importantly, the regulation of phagocytic activity is specific for NRP2 as NRP1 depletion did not influence the phagocytic activity of macrophages. To further assess how NRP2 regulates the phagocytic activity of macrophages, we tested whether NRP2 depletion leads to a defect in the uptake of phagocytic cargo or delays the maturation of phagocytic vesicles after the cargo has been engulfed. Our experiments with *E.coli* and zymosan particle conjugated with pH sensitive as well as pH insensitive fluorescent dye showed that NRP2 depletion did not result in a significant decrease in the uptake of phagocytic cargo.

However, it regulates the overall degradation and clearance of internalized cargo by affecting the maturation of early phagosomes to late phagosomes or phagolysosomes. We corroborated our observations in human peripheral blood derived as well as mouse bone marrow derived macrophages. Therefore, NRP2 mediated phagosomal maturation is a global phenomenon in human as well as mouse derived macrophages. A conclusive proof for the involvement of NRP2 in regulating the maturation process of phagosomes came when we observed an increase in $Rab5^+$ early phagocytic vesicles with a concomitant decrease in $Rab7^+$ late phagocytic vesicles, suggesting a defect during the exchange of Rab5 to Rab7 in phagosomes. Generation of $Rab7^+$ phagosomes is crucial for phagosome maturation, and is a prerequisite step for their fusion with lysosomes. Yet current knowledge on the detailed steps of phagosome maturation is limited. It is believed that the process begins with the recruitment of Dynamin (a large GTPase) which then interacts with Vps34 (a PI3 Kinase) and helps recruit Rab5 to the phagosome surface. Rab5, following its activation by Gapex-5 (Rab5 GEF), promotes Vps34 activation. Vps34 generates PtdIns(3)P on the phagosome surface where the vacuolar fusion protein complex, Mon1A-Ccz1, is recruited. Mon1A-Ccz1 helps the recruitment and activation of Rab7 in the membrane and also promotes the recruitment of the homotypic fusion and vacuole protein sorting (HOPS) complex. Rab7 then interacts with HOPS to facilitate the fusion of phagosome to lysosomes (219-222)In. Since NRP2 depletion in macrophages resulted in more $Rab5^+$ with a simultaneous decrease in $Rab7^+$ phagosomes, we concluded that the molecular effectors downstream of Rab5 are regulated by the NRP2 axis. Further studies are

warranted to identify and understand how NRP2 regulates the maturation defect in macrophages.

It is important to understand the clinical implications of NRP2 regulated phagocytosis in macrophages under different conditions. Since phagosome maturation is prerequisite for successful pathogen killing, many microbes have developed mechanisms to interfere with the phagosome maturation process. For example, *Mycobacterium tuberculosis* arrests phagosome maturation by preventing phagolysosomal fusion and the acquisition of lysosomal hydrolases (248). Interestingly, besides its role in pathogen killing, a phagosome also serves as a signaling platform for other related processes. The dynamics and molecular changes that a phagosome undergoes during the maturation phase enable other immune cells to respond to pathogen threat and maintain physiological homeostasis. Acceleration in phagosome maturation enhances pathogen killing. Whereas a delay in the maturation process preserves the antigenic peptides from degradative enzymes in the acidic mature phagosomes or phagolysosomes and favor presentation to T cells. This has been observed in case of macrophages and dendritic cells; macrophages acidify their phagosomes faster than dendritic cells. This enables the macrophages to rapidly degrade the internalized cargo whereas slow maturation in dendritic cells preserves antigen epitopes for longer period of time. Contrary to popular belief, it is now known that macrophages can also potentially present antigens to T cells and activate the immune responses (249). Additionally, MHC I complexes can be recruited to phagosomes through fusion of phagosomes and endosomal recycling vesicles and become accessible to the

antigenic peptides generated in the phagosomes (250). Next, they can be cross-presented to $CD8^+$ T cells and activate robust immune reaction. Also, macrophages may undergo apoptosis due to uncleared pathogen burden. Cellular contents leaked out can then be taken up by dendritic cells, resulting in enhanced T cell responses. This strategy is used for designing effective vaccines for various pathogens. Based on our observations, NRP2 favors phagosome maturation and hence aid in microbial clearance in macrophages. Although NRP2 depletion delays phagosome maturation, it is too early to assume if it will favor antigen presentation in macrophages and warrants further investigation. However, NRP2 may be useful for development of better vaccines in the future.

Fig. 3.1 Expression of NRP2 in M2 type macrophages. Immunoblot analyses showing expression pattern of NRP2 in M2 type human and mouse bone marrow derived macrophages. (A) Freshly isolated human monocytes were differentiated to mature macrophages with M-CSF for 7days to generate resting or M2 type macrophages. IL-4/10/13 was added on day7 for 24hrs to complete the M2 type polarization. NRP2 was not detected in the monocytes but expression increased as cells differentiated to mature macrophages. (B) Bone marrow cells isolated from WT C57/BL6 mice were differentiated to resting or M2 type type macrophages using M-CSF for 7days. Cells were exposed to IL-4/10/13 on day7 for 24hrs to complete the M2 type polarization. NRP2 was not detected in freshly isolated the bone marrow, but expression increased significantly during the differentiation to macrophages.

A

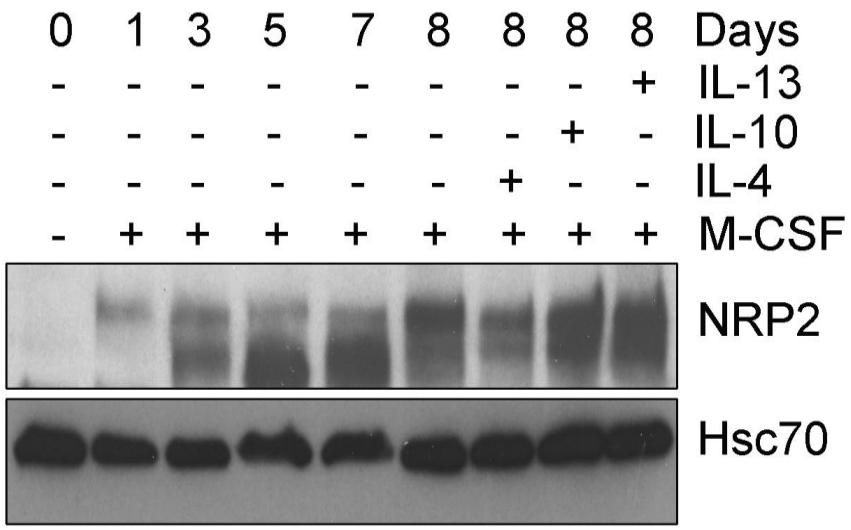
0 1 3 5 7 8 8 8 8 Days
- - - - - - - - + IL-13
- - - - - - - + - IL-10
- - - - - - + - - IL-4
- + + + + + + + + M-CSF
NRP2
Hsc70

B

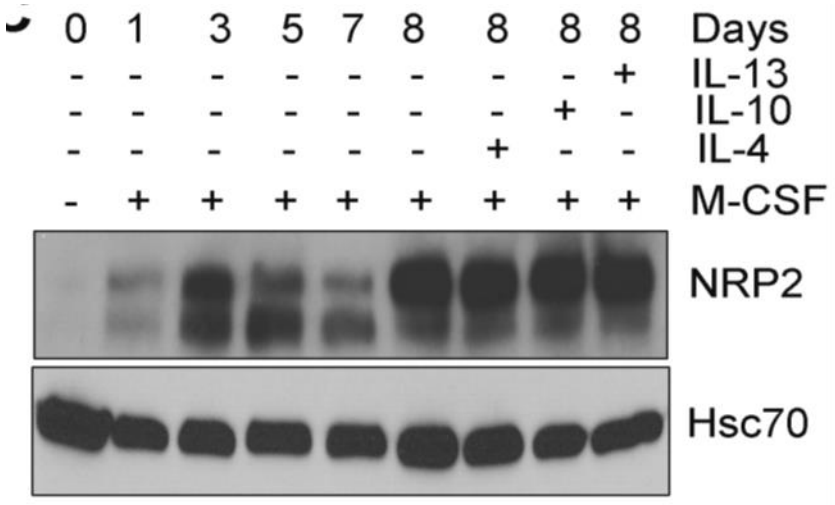
0 1 3 5 7 8 8 8 8 Days
- - - - - - - - + IL-13
- - - - - - - + - IL-10
- - - - - - + - - IL-4
- + + + + + + + + M-CSF
NRP2
Hsc70

Fig. 3.2 **Expression of NRP2 in M1 type macrophages.** Immunoblot analyses showing expression pattern of NRP2 in M1 type human and mouse bone marrow derived macrophages. (A) Freshly isolated human monocytes were differentiated to mature macrophages with GM-CSF for 7days to generate M1 type macrophages. A combination of LPS+IFNγ was added on day7 for 24hrs to complete the M1 type polarization. NRP2 was not detected in the monocytes but expression increased as cells differentiated to mature macrophages. (B) Bone marrow cells isolated from WT C57/BL6 mice were differentiated to M1 type macrophages using GM-CSF for 7days. Cells were exposed to a combination of LPS+ IFNγ on day7 for 24hrs to complete the M1 type polarization. NRP2 was not detected in freshly isolated the bone marrow, but expression increased significantly during the differentiation to macrophages.

A

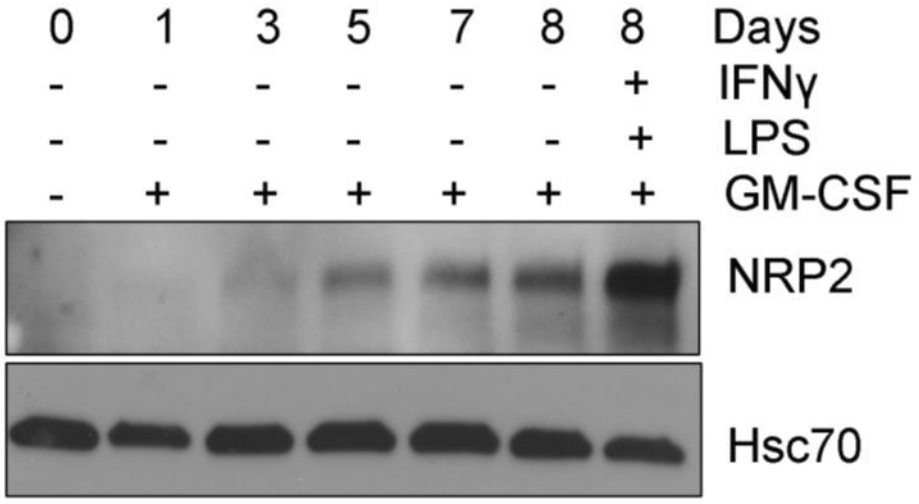
0 1 3 5 7 8 8 Days
- - - - - - + IFNγ
- - - - - - + LPS
- + + + + + + GM-CSF
NRP2
Hsc70

B

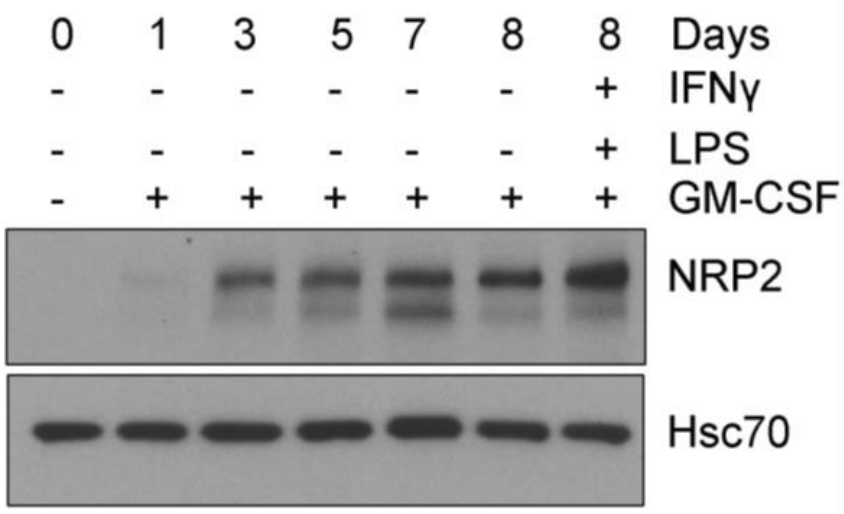
0 1 3 5 7 8 8 Days
- - - - - - + IFNγ
- - - - - - + LPS
- + + + + + + GM-CSF
NRP2
Hsc70

Fig. 3.3 NRP2 regulates phagosome maturation in macrophages without affecting uptake in human macrophages. (A) Schematic diagram for phagocytosis assay. (B) Phagocytosis assay for assessing the ability of M-CSF treated human macrophages to uptake *E.coli* bioparticles and phagosome maturation following NRP2 depletion by siRNA transfection. Cells were exposed to pH insensitive (green) and pHrodo *E.coli* (red) bioparticles for 1.5hr and analyzed microscopically. The first column shows the phagosome maturation (red puncta) in the scr (upper) and siNRP2 treated (bottom) cells. The second column shows the uptake efficiency (green puncta) in the scr (upper) and siNRP2 treated (bottom) cells. The third column represents merged images to show that NRP2 primarily affects phagosome maturation, but not phagocytic uotake in macrophages. Scale bars, 20μm. Single cell magnified within the boxed region to show green or red *E.coli* particle. (C) Uptake efficiency was measured as green cellular fluorescence whereas the intensity of red fluorescence was an indication for phagosome maturation. Results were represented as bar graph, values as mean ± SEM. Dapi was used for staining the nucleus in all the experiments. Student *t* test was used for comparison between 2 groups of cells. **P* < .05; ***P* < .005; ****P* < .0005. ns=not significant. (D) Immunoblot analysis shows knockdown efficiency for NRP2 following electroporation.

Fig. 3.3

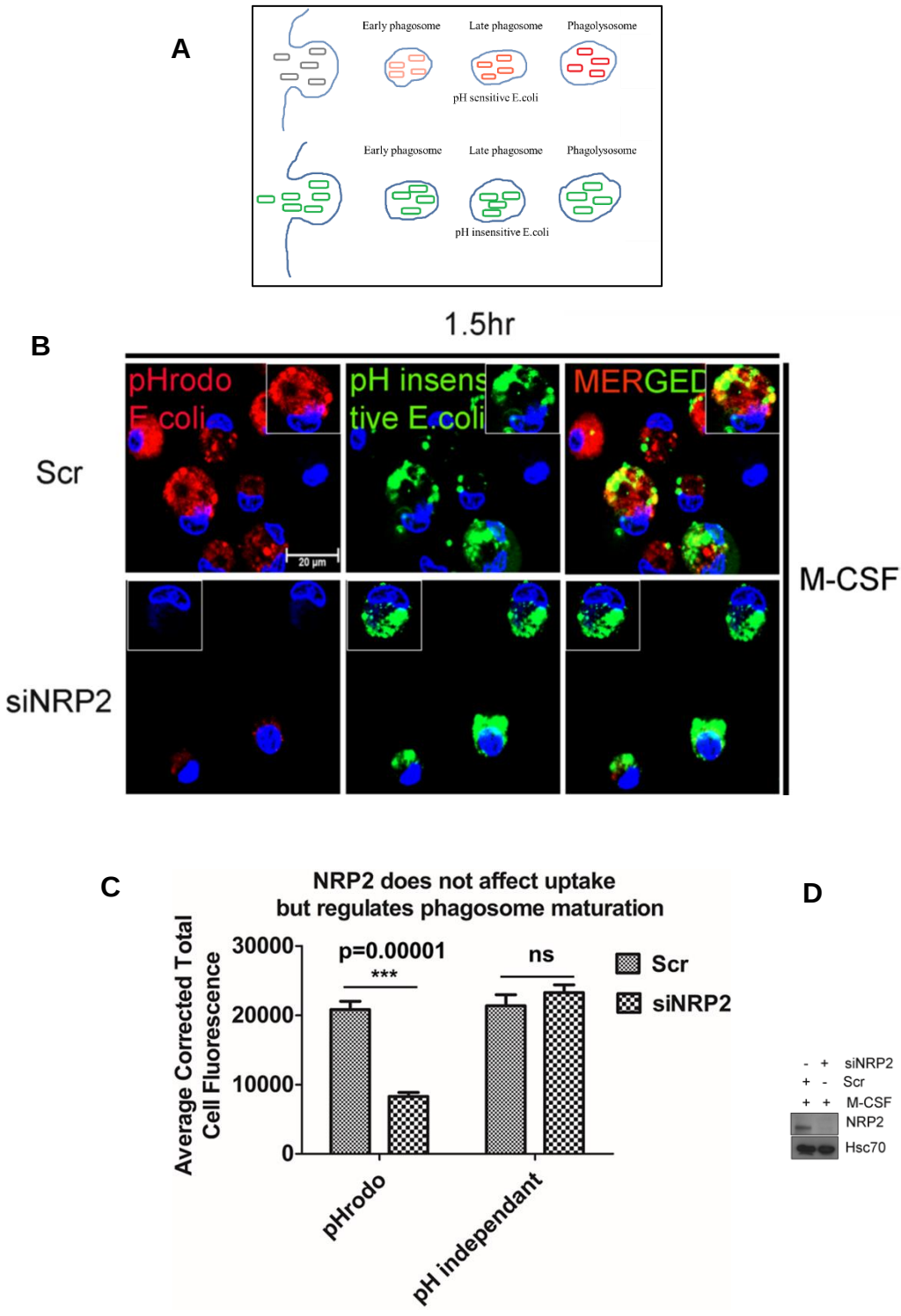
A
Early phagosome
Late phagosome
Phagolysosome
pH sensitive E.coli
Early phagosome
Late phagosome
Phagolysosome
pH insensitive E.coli
B
1.5hr
pHrodo E.coli
pH insensitive E.coli
MERGED
Scr
M-CSF
siNRP2
20 µm
C
NRP2 does not affect uptake
but regulates phagosome maturation
Average Corrected Total Cell Fluorescence
30000
20000
10000
0
p=0.00001
***
ns
Scr
siNRP2
pHrodo
pH independant
D
- + siNRP2
+ - Scr
+ + M-CSF
NRP2
Hsc70

Fig. 3.4 NRP1 does not regulate phagosome maturation in macrophages. (A) Phagocytosis assay to show NRP1 depletion does not have any effect on phagosome maturation in macrophages. Human macrophages were cultured for 7days with M-CSF. Phagocytosis assay was conducted with pHrodo *E.coli* bioparticles following NRP1 depletion by siRNA transfection. Phagosome maturation was microscopically assessed from the intensity of red fluorescent puncta. Insets show magnified image of cell containing bacteria. Scale bars 10µm. Dapi was used for nuclear staining. (B) Phagosome maturation in the presence and absence of NRP1 was quantified using Image J software and represented in bar graph as mean ± SEM. Student *t* test was used for comparison between 2 groups of cells. **P* < .05; ***P* < .005; ****P* < .0005. ns= non-significant. (C) Western blot shows knockdown of NRP1.

Fig. 3.4

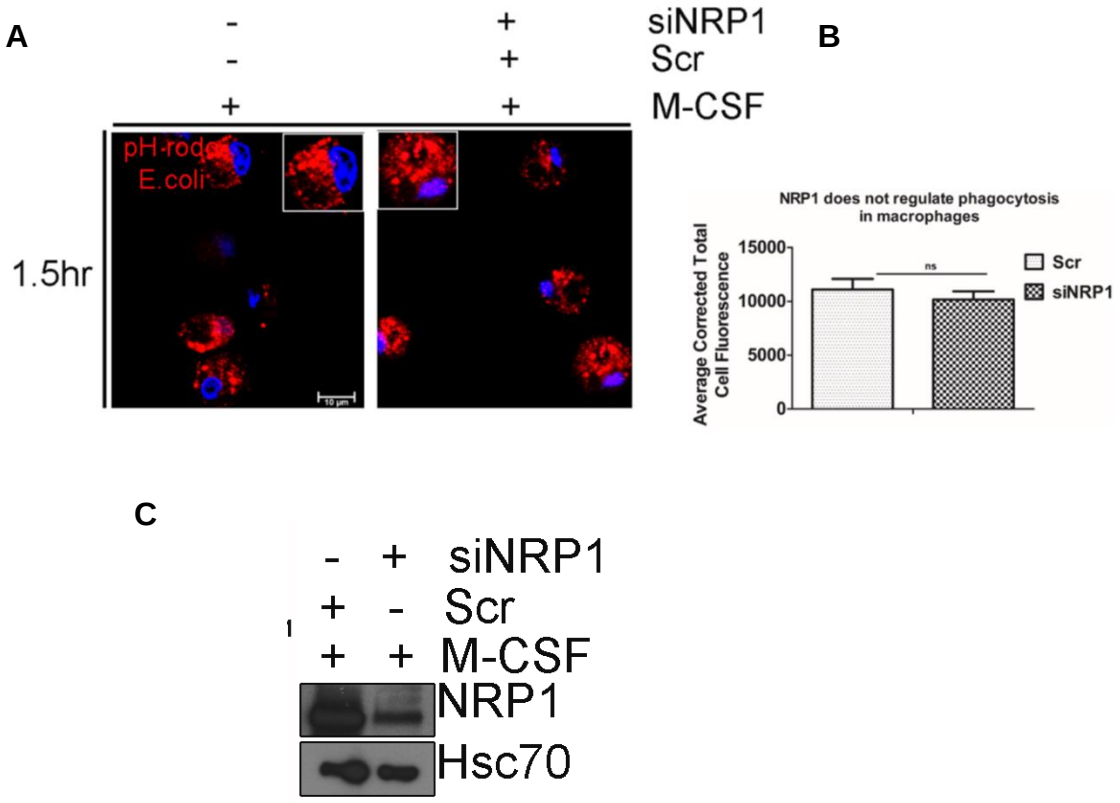
A
-
-
+
+
+
+
siNRP1
Scr
M-CSF
pH-rod
E.coli
1.5hr
B
NRP1 does not regulate phagocytosis in macrophages
Average Corrected Total Cell Fluorescence
15000
10000
5000
0
ns
Scr
siNRP1
C
- + siNRP1
+ - Scr
+ + M-CSF
NRP1
Hsc70

Fig. 3.5 NRP2 regulates phagosome maturation in GM-CSF treated macrophages. (A) Phagocytosis assay to assess the effect of NRP2 on phagosome maturation in GM-CSF treated human macrophages. Human monocytes were differentiated with GM-CSF for 7days and then exposed to pHrodo *E.coli* bioparticles for 1.5hr. Cells were fixed and analyzed by confocal microscopy. Phagosome maturation was scored from the intensity of red fluorescent puncta. Individual cell is magnified in the inset. Scale bars 10µm. Dapi was used for nuclear staining. (B) Bar graph showing quantification of phagosome maturation in GM-CSF treated macrophages following NRP2 depletion. Values are mean ± SEM. Student *t* test was used for comparison between 2 groups of cells. **P* < .05; ***P* < .005; ****P* < .0005. ns= non-significant. (C) Western blot shows knockdown for NRP2.

Fig. 3.5

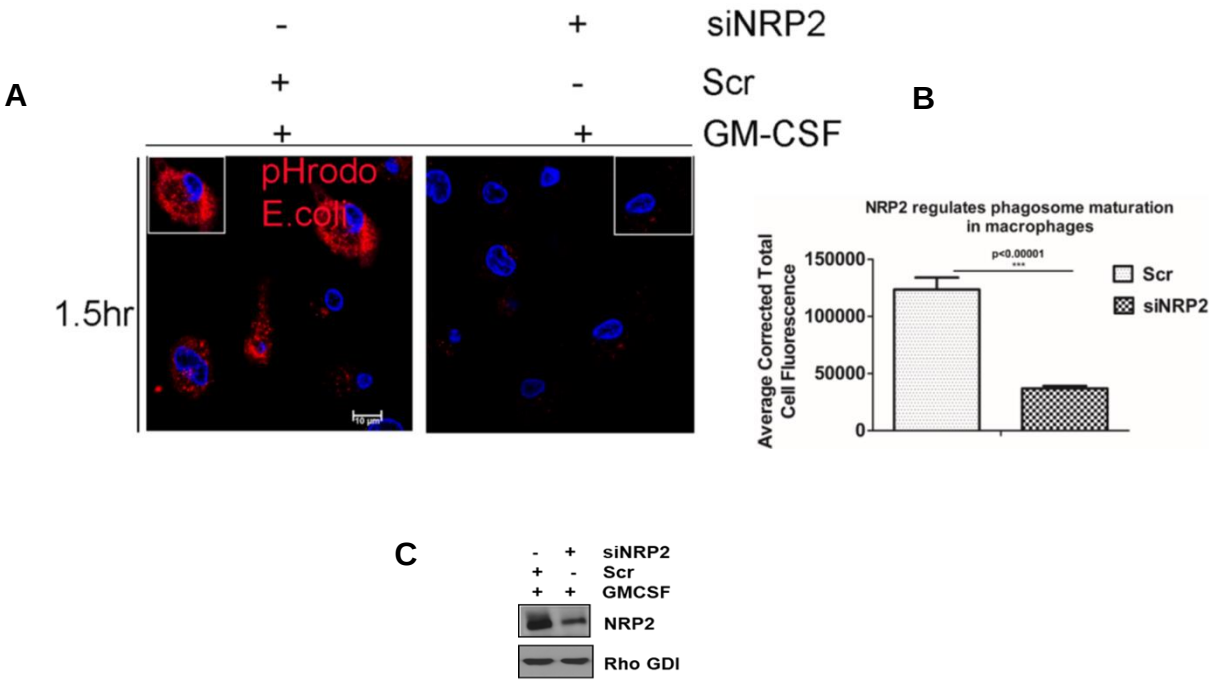
A
-
+
siNRP2
+
-
Scr
+
+
GM-CSF
pHrodo
E.coli
1.5hr
B
NRP2 regulates phagosome maturation in macrophages
p<0.00001
***
Average Corrected Total Cell Fluorescence
150000
100000
50000
0
Scr
siNRP2
C
- + siNRP2
+ - Scr
+ + GMCSF
NRP2
Rho GDI

Fig. 3.6 NRP2 does not affect uptake of phagocytic cargo in GM-CSF treated macrophages. (A) Phagocytosis assay to test the effect of NRP2 on phagocytic uptake in GM-CSF treated human macrophages. Cells were exposed to pH insensitive *E.coli* (red) for 1hr to allow the macrophages uptake the bacteria. Cells were then fixed and analyzed by confocal microscopy. The intensity of red fluorescent puncta was used as a measure for uptake efficiency of the cells. Individual cells are magnified in the insets. Scale bars 10μm. (B) Uptake efficiency of the macrophages was quantified using Image J software and represented as bar graph. Values are mean ± SEM. Dapi was used for nuclear staining. Student *t* test was used for comparison between 2 groups of cells. **P* < .05; ***P* < .005; ****P* < .0005. ns= non-significant. (C) Western Blot analysis showing knockdown efficiency of NRP2 following siRNA transfection.

Fig. 3.6

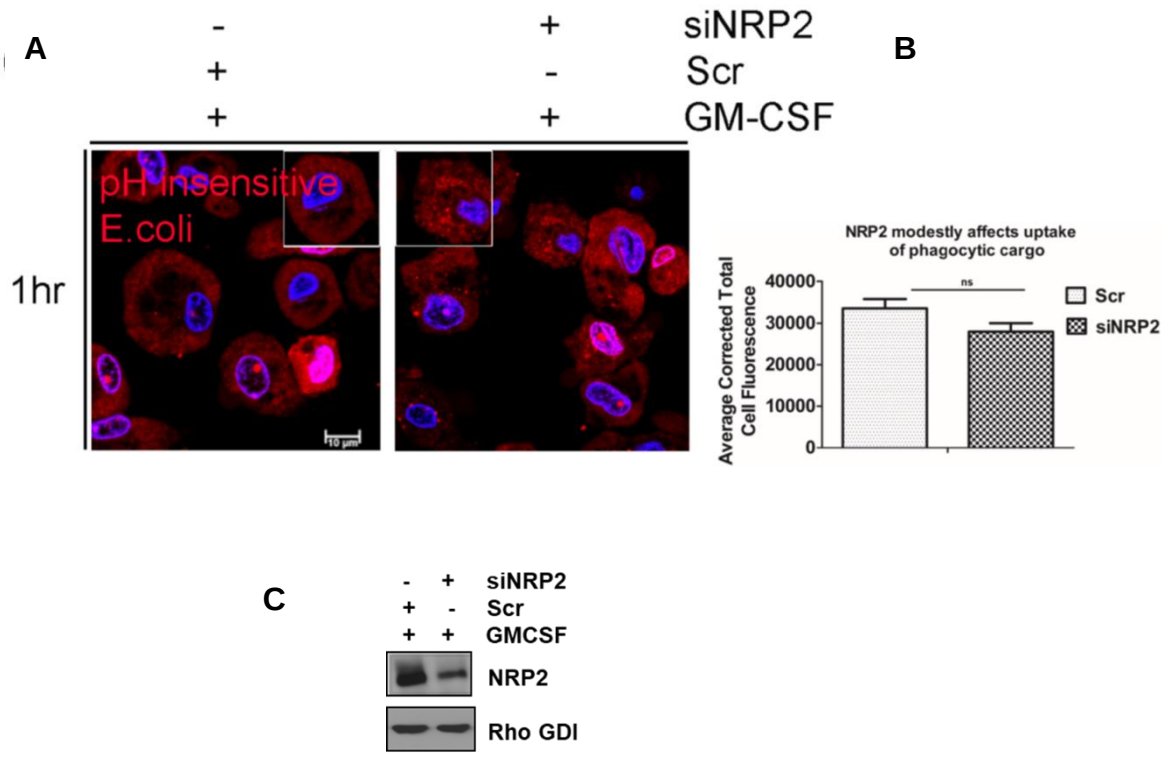
A
-
+
siNRP2
+
-
Scr
+
+
GM-CSF
pH insensitive
E.coli
1hr
10 μm
B
NRP2 modestly affects uptake
of phagocytic cargo
Average Corrected Total
Cell Fluorescence
40000
30000
20000
10000
0
ns
Scr
siNRP2
C
- + siNRP2
+ - Scr
+ + GMCSF
NRP2
Rho GDI

Fig. 3.7 Scheme for transgenic mouse generation and knock out of NRP2 from macrophages. (A) CSF1R-iCre mouse is bred with $NRP2^{f/f}$ mouse to get CSF1R-iCre;$NRP2^{f/f}$ mouse. NRP2 can be genetically knocked out from myeloid cells following intraperitoneal administration of Tamoxifen or adding (Z)-4-Hydroxy Tamoxifen into cell culture medium. (B) Western blot showing knock out of NRP2 from macrophages with different doses of Z)-4-Hydroxy Tamoxifen.

Fig. 3.7

A

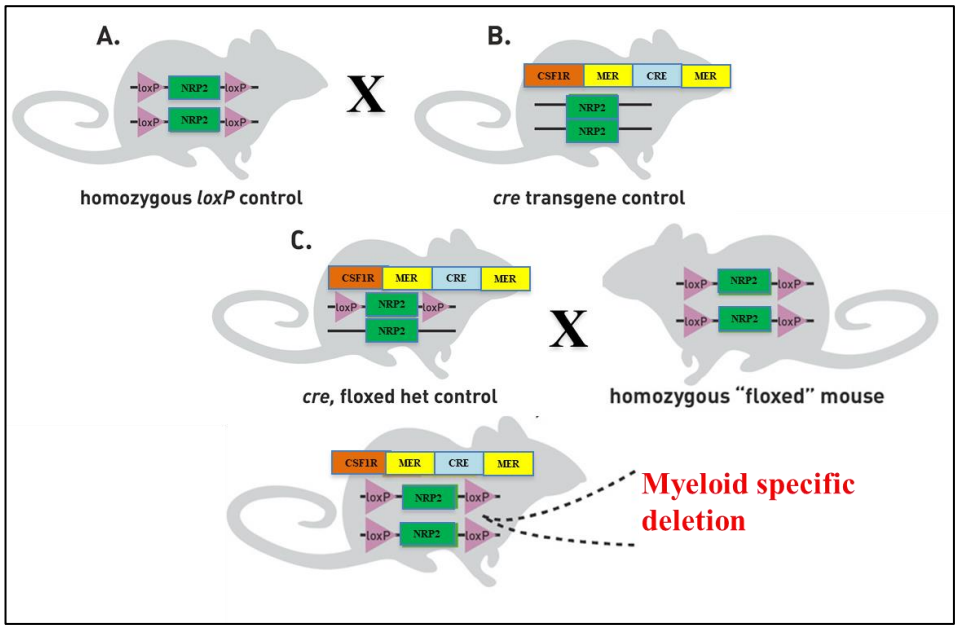
A.
B.
X
loxP
NRP2
CSF1R
MER
CRE
homozygous loxP control
cre transgene control
C.
cre, floxed het control
homozygous "floxed" mouse
Myeloid specific deletion

B

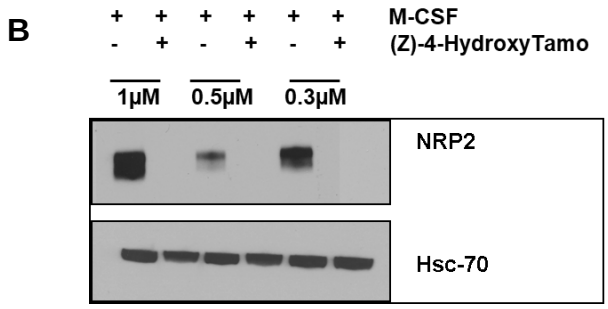
+ + + + + + M-CSF
- + - + - + (Z)-4-HydroxyTamo
1μM
0.5μM
0.3μM
NRP2
Hsc-70

Fig. 3.8 NRP2 regulates phagosome maturation in mouse macrophages. (A) Bone marrow cells isolated from CSF1R-iCre;NRP2$^{f/f}$ were cultured for 7days with M-CSF and NRP2 knocked out by adding (Z)-4-Hydroxy Tamoxifen to the culture medium. Cells were challenged with 65 µg/mL of pHrodo *E.coli* bioparticles for 1.5hrs. Cells were fixed and phagosome maturation was analysed by confocal microscopy. Dapi was used for nuclear staining. Inset shows magnified image of individual cell. Scale bar, 10µm. (B) Phagosome maturation was quantified as total cellular red fluorescence using Image J software and represented as bar graph. Values are mean ± SEM. Student *t* test was used for comparison between 2 groups of cells. **P* < .05; ***P* < .005; ****P* < .0005. ns= non-significant. (C) Western Blot analysis showing depletion of NRP2.

Fig. 3.8

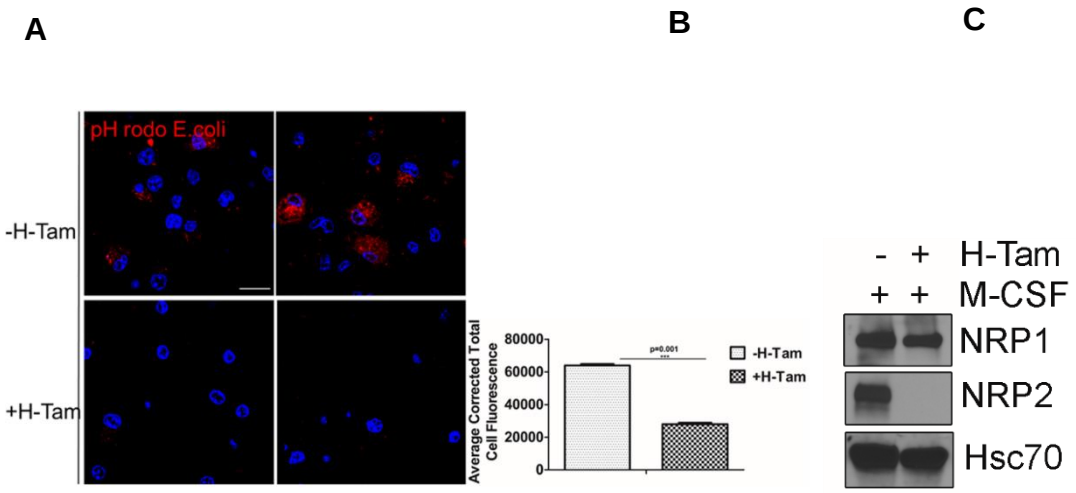
A
B
C
pH rodo E.coli
-H-Tam
+H-Tam
Average Corrected Total Cell Fluorescence
80000
60000
40000
20000
0
p=0.001
***
-H-Tam
+H-Tam
- + H-Tam
+ + M-CSF
NRP1
NRP2
Hsc70

Fig. 3.9 NRP2 does not significantly affect the uptake of phagocytic cargo in mouse macrophages. (A) Representative image for phagocytosis assay with bone marrow derived macrophages isolated from $NRP2^{fl/fl}$CSF1R-iCre mice to show the effect of NRP2 depletion on uptake phagocytic cargo. Cells were challenged with pH insensitive *E.coli* bioparticles for 1hr and analyzed by Confocal microscopy. Scale bars, 10µm. Magnified images within the inset show the phagosomes containing *E.coli* bioparticle. Dapi was used for staining the nuclei. (B) Quantification for uptake efficiency of macrophages (red puncta, measured as total cellular fuorescence using Image J software) in the presence and absence of NRP2, represented in bar graph as mean ± SEM. Student *t* test was used for comparison between 2 groups of cells. **P* < .05; ***P* < .005; ****P* < .0005. ns= non-significant. (C) Western Blot analysis showing depletion of NRP2.

Fig. 3.9

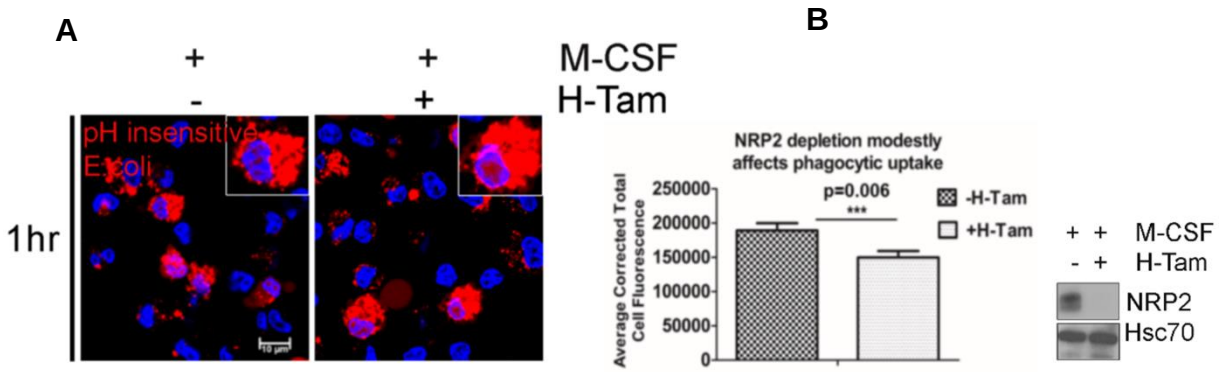
A
+
-
+
+
M-CSF
H-Tam
pH insensitive
E.coli
1hr
B
NRP2 depletion modestly affects phagocytic uptake
p=0.006
***
-H-Tam
+H-Tam
Average Corrected Total Cell Fluorescence
250000
200000
150000
100000
50000
0
+ + M-CSF
- + H-Tam
NRP2
Hsc70

Fig. 3.10 Effect of NRP2 depletion on bacterial clearance *in vitro* by macrophages. (A) Schematic diagram depicting bacterial clearance assay. (B) Bone marrow cells isolated from NRP2$^{fl/fl}$CSF1R-iCre mice were differentiated to macrophages for 7days using M-CSF. NRP2 was knocked out by the addition of (Z)-4-Hydroxy Tamoxifen to the cell culture medium. Macrophages were challenged with 65µg/mL pHrodo *E.coli* bioparticles for 15min (pulse time) and then assessed for their ability to mature the phagosomes and degrade the bacteria. Images were acquired at chase time = 0min, 15min, 45min, 90min, 120min and 240min using Confocal microscopy. Scale bars, 10 µm. Magnified images within the inset show the phagosomes containing *E.coli* particles. Dapi was used for nuclear staining. (C) Phagosome maturation and degradation of fluorescent bioparticles was assessed as corrected total cell fluorescence using Image J software. Cells were analyzed at times indicated at the graph abscissa and represented in bar graphs as mean ± SEM. Student *t* test was used for comparison between 2 groups of cells. *$P < .05$; **$P < .005$; ***$P < .0005$. ns= non-significant. (D) Western blot for NRP2 depletion is shown.

Fig. 3.10

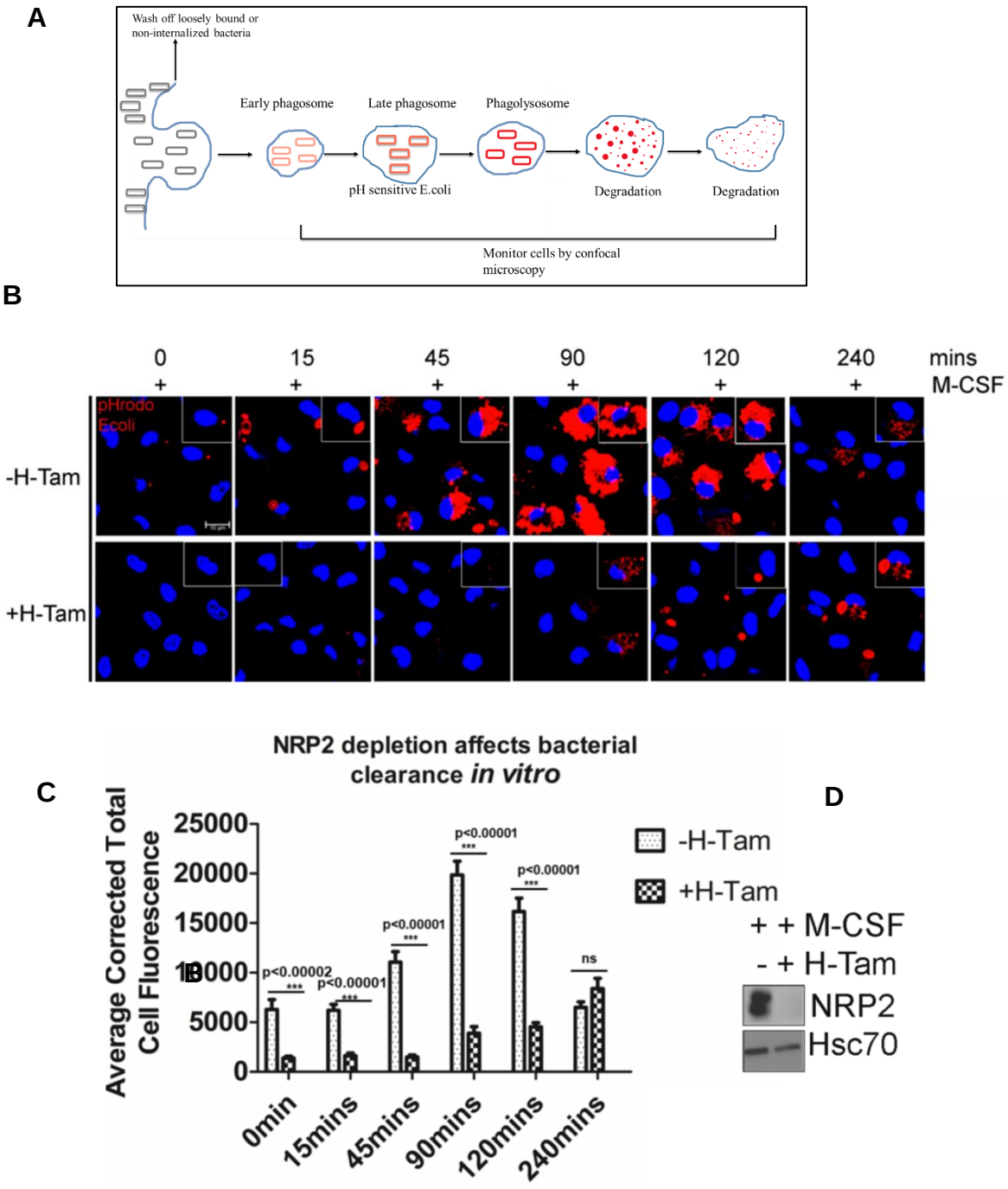
A
Wash off loosely bound or non-internalized bacteria
Early phagosome
Late phagosome
Phagolysosome
pH sensitive E.coli
Degradation
Degradation
Monitor cells by confocal microscopy
B
0
15
45
90
120
240
mins
+
+
+
+
+
+
M-CSF
pHrodo Ecoli
-H-Tam
+H-Tam
C
NRP2 depletion affects bacterial clearance in vitro
Average Corrected Total Cell Fluorescence
25000
20000
15000
10000
5000
0
p<0.00002
p<0.00001
p<0.00001
p<0.00001
ns
0min
15mins
45mins
90mins
120mins
240mins
D
-H-Tam
+H-Tam
+ + M-CSF
- + H-Tam
NRP2
Hsc70

Fig. 3.11 NRP2 affects zymosan clearance in vitro by macrophages. (A) Schematic diagram for zymosan clearance assay. (B) Bone marrow derived macrophages isolated from NRP2$^{fl/fl}$CSF1R-iCre mice were cultured for 7days with M-CSF. Cells were challenged with pHrodo zymosan particles for 15mins (pulse time) and then analyzed for phagosome maturation and degradation of zymosan particles following knocking out NRP2. Images were acquired at chase time= 0hr, 6hr, 10hr, 14hr and 18hr. Scale bars, 10µm. Magnified images within the inset show the phagosomes containing zymosan particles at each time point. Dapi was used to detect the nucleus. (C) Phagosome maturation and degradation of fluorescent zymosan particles was scored as corrected total cell fluorescence using Image J software. Cells were analyzed at times indicated at the graph abscissa and represented as bar graph. The values are mean ± SEM. Student *t* test was used for comparison between 2 groups of cells. **P* < .05; ***P* < .005; ****P* < .0005. ns= non-significant. (D) Western blot for NRP2 depletion is shown.

Fig. 3.11

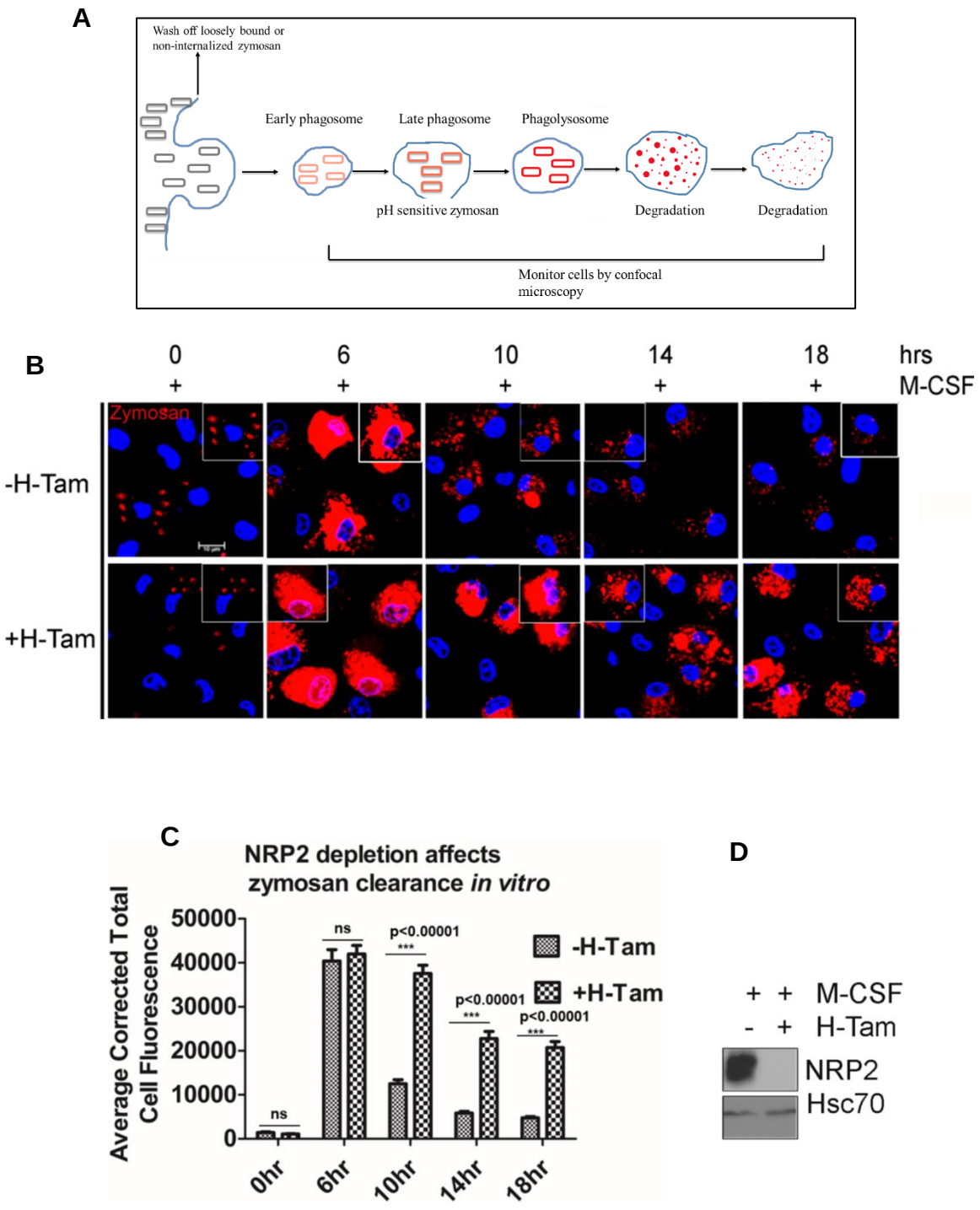
A
Wash off loosely bound or non-internalized zymosan
Early phagosome
Late phagosome
Phagolysosome
pH sensitive zymosan
Degradation
Degradation
Monitor cells by confocal microscopy
B
0
6
10
14
18
hrs
+
+
+
+
+
M-CSF
Zymosan
-H-Tam
+H-Tam
C
NRP2 depletion affects zymosan clearance in vitro
Average Corrected Total Cell Fluorescence
50000
40000
30000
20000
10000
0
ns
ns
p<0.00001
***
p<0.00001
***
p<0.00001
***
-H-Tam
+H-Tam
0hr
6hr
10hr
14hr
18hr
D
+ + M-CSF
- + H-Tam
NRP2
Hsc70

Fig. 3.12 NRP2 inhibits phagosome maturation in human macrophages. Depletion of NRP2 inhibits maturation of early to late phagosomes in macrophages. (A) Immunostaining of early and late phagosomal maturation markers in human macrophages following NRP2 depletion by siRNA transfection. The upper panel represents early phagosome marker Rab5 (green). Scale bars 10µm. The lower panel shows representative images for the late phagosomal marker Rab7 (green). Scale bars 20µm. Magnified images of individual cell is shown in the inset for each condition. Dapi was used for staining the nucleus. (B) Immunostaining data for Rab5 and Rab7 were quantified as cellular fluorescence using Image J software and represented as bar graph. The upper panel shows graphical representation of Rab5 in the presence and absence of NRP2. The lower panel shows bar graph representing the change in Rab7 following NRP2 depletion. All values are shown as mean ± SEM. Student *t* test was used for comparison between 2 groups of cells. **P* < .05; ***P* < .005; ****P* < .0005. (C) Western Blot analyses showing total cellular Rab5 and Rab7 and NRP2 depletion in whole cell lysates from human macrophages following knockdown of NRP2.

Fig. 3.12

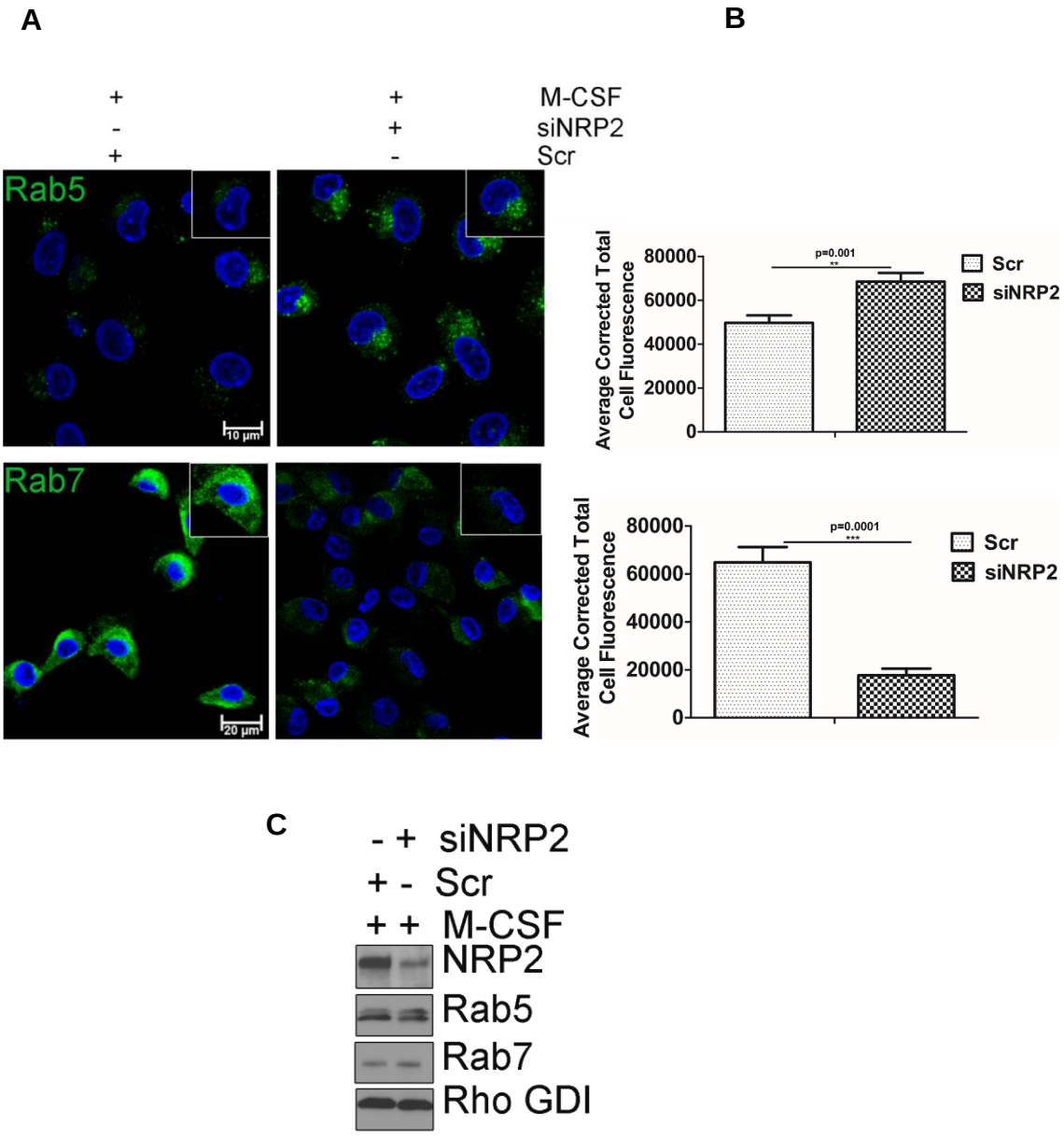
A
B
+ + M-CSF
- + siNRP2
+ - Scr
Rab5
Rab7
10 µm
20 µm
Average Corrected Total Cell Fluorescence
80000
60000
40000
20000
0
p=0.001
**
Scr
siNRP2
p=0.0001
***
C
- + siNRP2
+ - Scr
+ + M-CSF
NRP2
Rab5
Rab7
Rho GDI

Fig. 3.13 NRP2 inhibits phagosome maturation in mouse macrophages. (A) Immunostaining of early and late phagosomal maturation markers in mouse bone marrow derived macrophages following NRP2 depletion by addition of (Z)-4-Hydroxy Tamoxifen to cell culture media. The upper panel represents early phagosome marker Rab5 (red). The lower panel shows representative images for the late phagosomal marker Rab7 (red). Scale bars 10μm. The insets are magnified image of individual cell for each condition. (E) Representative bar graphs showing quantification of Rab5 and Rab7 using Image J software. The upper panel is the bar graph for change in Rab5 following NRP2 depletion. The lower panel is the graphical representation of change in Rab7 following NRP2 depletion. All values are shown as mean ± SEM. Dapi was used for staining the nucleus in all the experiments. Student t test was used for comparison between 2 groups of cells. *P < .05; **P < .005; ***P < .0005. (C) Western Blot analyses¬¬ showing total cellular Rab5 and Rab7 in whole cell lysates from mouse macrophages following knockdown of NRP2.

Fig. 3.13

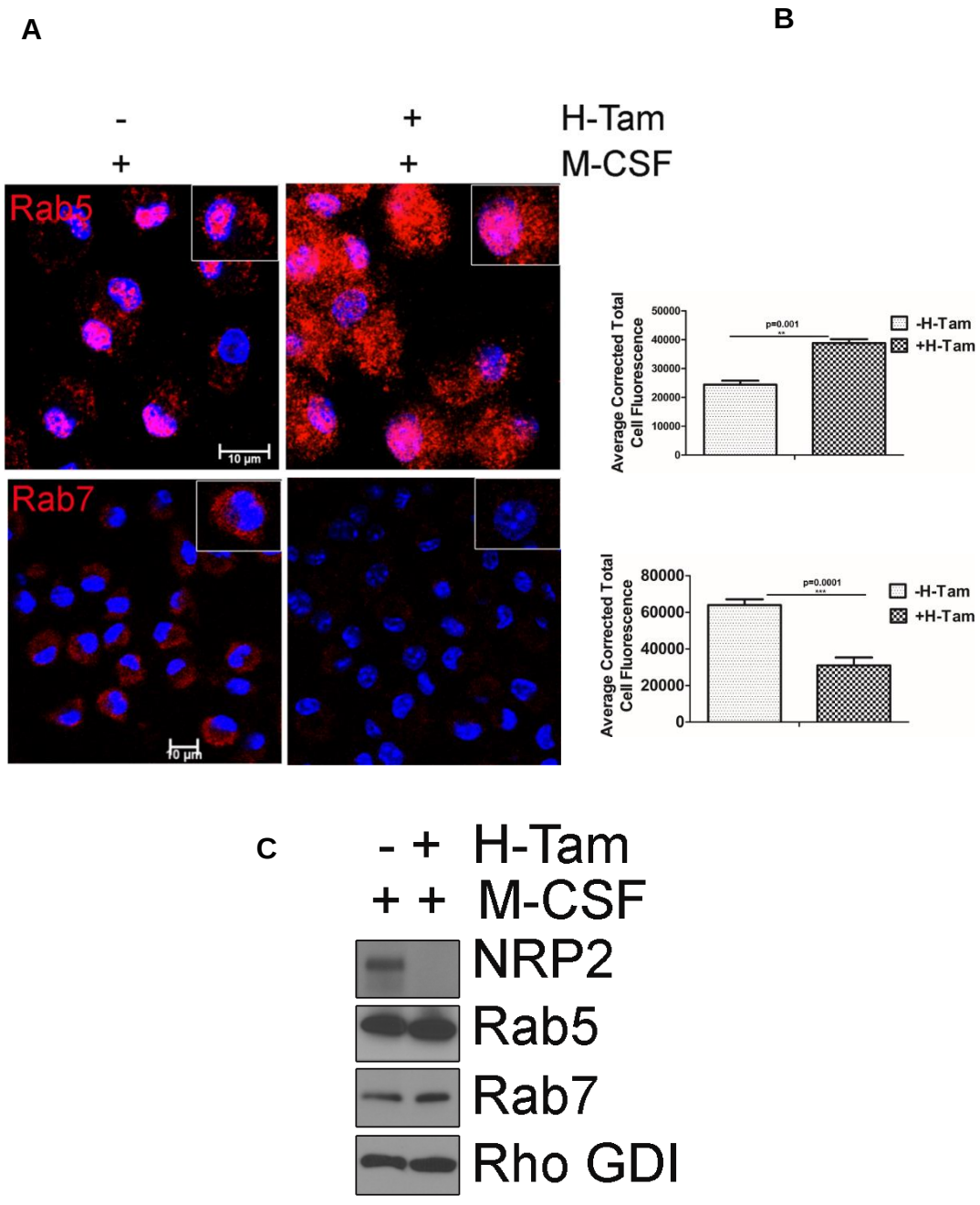
A
B
-
+
H-Tam
+
+
M-CSF
Rab5
10 µm
Rab7
10 µm
Average Corrected Total Cell Fluorescence
50000
40000
30000
20000
10000
0
p=0.001
**
-H-Tam
+H-Tam
Average Corrected Total Cell Fluorescence
80000
60000
40000
20000
0
p=0.0001
***
-H-Tam
+H-Tam
c
- + H-Tam
+ + M-CSF
NRP2
Rab5
Rab7
Rho GDI

Chapter IV

NRP2 is essential for clearance of dying cells and affects tumor progression and anti-tumor immune responses

4. NRP2 is essential for clearance of dying cells and affects tumor progression and anti-tumor immune responses

4.A Background, Hypothesis and Objectives

Macrophages are important component of the immune system and undertake a diverse array of functions like, clearance of cellular debris, development, metabolic homeostasis, microbial clearance and angiogenesis. Briefly, depending on the converging signals they are exposed to in the tissue microenvironment, macrophages can exist in two states: exposure to danger signals like bacteria or other infections skew them towards a classically activated or M1 type; these cells are cytotoxic and produce pro-inflammatory cytokines, ROS/NOS and robustly activate T cell responses. Post injury or infection, during the resolution phase, macrophages are polarized to alternatively activated or M2 state where they produce angiogenic and tissue remodeling factors that augment the wound healing process. Macrophages have been implicated in several clinical conditions, like RA, diabetes, atherosclerosis and cancer. Macrophages comprise a substantial population in the TME and have been causally associated with distinct stages of disease progression, including EMT, angiogenesis, stem cell niche maintenance, metastasis and therapy resistance. TAMs are complex cell population; although gene expression profiles suggest TAMs closely represent the conventional M2 type macrophages, they also express several genes characteristic of the M1 type. NRPs have been implicated in TAMs. NRP1 is expressed in TAMs and is important for their migration to the hypoxic core of the tumor and their protumoral activities. Although NRP2 expression has been briefly

reported in TAMs, knowledge about its function and the molecular pathways it governs is lacking.

Despite several targeted immunotherapies currently being explored pre-clinically or in clinical trials, most cancers relapse, with more aggressive features. One of the essential functions of TAMs in the TME is efferocytosis of apoptotic cancer cells. The role of efferocytosis in cancer has remained elusive. However, there are some evidences to indicate that the non-immunogenic properties of efferocytosis that prevails under normal homeostasis conditions can be mimicked by malignant cells to create an environment of immunosuppression in the TME. In a tumor, the apoptotic index is high because of the rapid growth of cancer cells in a nutrient limited hostile environment or because of treatment with chemotherapeutic drugs, and therefore mimic the environment of a non-resolving wound. TAMs show increased efferocytosis, which also facilitates immune tolerance by rendering the former more protumorigenic and increase the risk for metastasis. A protumoral role of efferocytosis was also observed where tumor progression was dampened following genetic depletion of the efferocytosis receptor MerTK (Cook 2013). $MerTK^{-/-}$ $CD11b^{+}$ cells isolated from the tumors showed signs of immune activation. Intriguingly, intratumoral dendritic cells engulfing tumor cells expressing the well-known ‘eat me’ signal, PtdSer remain arrested in an immature state of differentiation, incapable of expressing the co-stimulatory molecules required for optimum T cell activation (Bondanza A JEM 2004), resulting in further immunosuppression in the TME. However, the molecules

that couple the two pathways, viz. efferocytosis and immune modulation are still not well known.

The goal of this study is to understand the role of NRP2 in TAMs and how this may affect tumor progression. Pancreatic Ductal Adenocarcinoma (PDAC) is one of the most lethal types of cancers with high incidence and low survival rates. One of the hallmarks of PDAC is the dense desmoplastic reaction that acts as a physical barrier to therapeutics. TAMs are abundantly present in PDAC and have been causally associated with distinct stages of disease progression, metastasis, therapy resistance and correlate with poor outcome. Despite extensive research, therapeutic modalities are still not available to effectively treat PDAC. Our goal is to identify the function of NRP2 in TAMs and how targeting this axis may affect PDAC progression. Based on our previous reports and findings in Chapter 3, we hypothesized that NRP2 regulates efferocytosis of apoptotic cells in TME and maintains immune tolerance. In this chapter, we report that NRP2 is expressed in macrophages in human and mouse PDAC. We also observed that NRP2 in macrophages regulates efferocytosis and that its depletion significantly delays the clearance of apoptotic cells *in vitro*. Further, we investigated the effect of NRP2 mediated apoptotic cell clearance on pancreatic cancer progression, using a subcutaneous tumor model. NRP2 depletion resulted in a moderate decrease in tumor progression. Interestingly, NRP2 does not have any role in TAM recruitment into the tumors, however, NRP2 depletion significantly increased the intratumoral infiltration of cytotoxic CD8+ T cells. This could be attributed to the delayed clearance of apoptotic cancer cells in the TME and cross presentation to cytotoxic

T lymphocytes. CD11b+ TAMs from the tumors were isolated and Next Generation RNA-Sequencing analysis performed. Gene enrichment analysis showed deregulation of several genes associated with phagosomal maturation, exocytosis and recycling, immunosuppressive phenotype of TAMs as well as leucocyte migration and activation processes. In brief, our data strongly support our hypothesis that NRP2 regulates efferocytosis in macrophages and maintains immune tolerance in TME. Further, NRP2 depletion results in delayed apoptotic cell clearance and activates immune response against tumors and slows down tumor progression. Overall, the study strongly suggests the importance for the development of an adjuvant therapeutic strategy targeting the NRP2 axis in macrophages and to reduce pancreatic cancer recurrence and metastasis.

4.B Results

NRP2 is expressed in tumor associated macrophages (TAMs) in Pancreatic Cancer.

We obtained pancreatic cancer tissue sections (from the Rapid Autopsy Program at UNMC) from 10 PDAC patients who died with no history of treatment. We tested the presence of NRP2 expressing TAMs by co-staining with anti NRP2 and CD68 (a pan macrophage marker) antibodies. We observed that most of the macrophages in the tumor microenvironment were NRP2 positive (**Fig. 4.1 A**). However, we also detected the presence of few $NRP2^{lo}$ or $NRP2^{-}$ CD68+ macrophages in certain areas of 2 tissues. NRP2 expressing $F4/80^{+}$ macrophages were also detected in mouse pancreatic tumor tissue derived from KC mouse (**Fig. 4.1 B**). To generate TAMs in vitro, freshly isolated human monocytes or bone marrow cells from WT mice were differentiated for 7days with CM from either human PC Panc-1 or mouse PC UNKC-6141 and KPC cell lines respectively. In both the conditions, NRP2 expression increased as the cells differentiated to TAMs (**Fig. 4.2 A-C**). Overall, these results suggest that NRP2 is expressed by TAMs *in vivo* as well *in vitro*.

NRP2 regulates phagosomal maturation in TAMs *in vitro.*

Our previous findings indicated that NRP2 regulates phagosomal maturation in macrophages under M2 and M1 polarizing conditions, in human as well as in mice. Next, we wanted to test if NRP2 regulates phagosomal maturation in TAMs. To test this, we treated human monocytes with CM derived from Panc-1 cells for

7days to differentiate them to TAMs *in vitro*. Phagocytosis assay was performed with pH sensitive pHrodo *E.coli* particles and monitored under confocal microscope. Compared to the control, NRP2 deficient macrophages showed significantly lesser number of visible red puncta (**Fig. 4.3 A**). This suggests that phagsosomes containing *E.coli* particles matured into either late phagosomes or phagolysosomes and hence fluoresced bright red in the acidic vesicles. In contrast, in NRP2 depleted macrophages, the phagosomes did not mature to acidic late phagosomes or phagolysosomes and hence there was a significant decrease in the visible fluorescence intensity of the bioparticles. **Fig. 4.3 B and C** show the graphical representation of the result and the knockdown efficiency of NRP2 by siRNA approach.

The assay was repeated using bone marrow derived macrophages isolated from CSF-1R-iCRE;NRP2$^{f/f}$ mice. Cells were treated with CM derived from mouse pancreatic cancer cell lines UNKC-6141 and KPC. (Z)-4-HydroxyTamoxifen was added to cell culture medium to genetically delete NRP2 from the macrophages. Phagosomal maturation was assessed using the pH dependant pHrodo *E.coli* bioparticles. In the wild type cells, bright red puncta indicated phagosomal maturation to acidic late phagosomes or phagolysosomes. There was a significant reduction in the intensity as well number of bright red puncta in the NRP2 depleted cells, indicating a delay in the maturation process (**Fig. 4.3 D,G**). **Fig. 4.3 E,H and F,I** show the graphical representation of the results and the knock out efficiency of NRP2.

Overall, these results indicated that NRP2 regulates phagosomal maturation in TAMs (human and mice) and that its depletion results in a significant delay in the maturation process.

NRP2 in macrophages regulates efferocytosis of apoptotic cells.

Efferocytosis is a strictly orchestrated process where professional phagocytes, such as macrophages recognize and engulf apoptotic cells and remove them from the system in an immunologically silent manner. Maturation of nascent efferosome containing apoptotic debris and subsequent degradation and clearance share similarity with endosomal maturation and lysosomal fusion processes. Both the pathways often hire similar family of effector molecules. Based on our previous data that NRP2 regulates phagocytosis in macrophages, we wanted to investigate its role in the clearance of dying cells by macrophages. To test this, a pulse and chase experiment was performed where apoptosis was induced in Jurkat cells using 50µM Etoposide and added to M-CSF treated mouse bone marrow derived macrophages for 1hr (pulse). Non-engulfed or loosely bound cells were removed by vigorous washing and the macrophages were then monitored for their ability to degrade and clear the apoptotic cargo (chase). A schematic diagram showing the experimental design is depicted in **Fig. 4.4 A**. Phagosomes containing engulfed dead cells need to fuse with lysosomes to form phagolysosomes. During the course of degradation, the latter gradually decrease in size and finally disappear. Therefore, in the current experiment, ability of the macrophages to clear apoptotic cells was assessed from the breakdown of the apoptotic cells and loss of fluorescence (red). At 2hrs chase, there was significant increase in the red

fluorescence in both the control (-H-Tam) as well as NRP2 KO cells (+H-Tam). However, at 6hrs, there was a significant decrease in the red fluorescent intensity and disappearance of apoptotic cells in the control macrophages, indicating the apoptotic cells were broken down and degraded. In contrast, even after 12hrs, NRP2 KO cells exhibited significant delay in the clearance of apoptotic cell cargo (**Fig. 4.4 B**). This was apparent from larger size of the cargo and higher amount of fluorescence that persisted in the cells even after 12hours. **Fig. 4.4 C and D** respectively show the graphical representation of the result and the knock out efficiency in macrophages.

The assay was repeated using peritoneal macrophages isolated from CSF-1R-iCRE;NRP2$^{f/f}$ mice, and NRP2 knocked out by intraperitoneal administration of Tamoxifen. Here also, in NRP2 deficient cells, there was a significant delay in the degradation and clearance of apoptotic cells, compared to the NRP2 proficient control macrophages (**Fig. 4.5 A**). **Fig. 4.5 B and C** respectively show the graphical representation of the result and the knock out efficiency of NRP2 in macrophages following Tamoxifen treatment.

Overall, these data suggest that NRP2 in macrophages regulates the clearance of apoptotic cells and its depletion significantly increases the life time of the efferosome (phagosome containing the apoptotic cargo) and delays their clearance.

Efferocytosis of dying cancer cells in the TME is critical for the pro-tumoral behavior of TAMs and contributes to cancer progression and metastasis, and recurrence. Based on our previous data that NRP2 depletion affects the clearance

of apoptotic cells, we further wanted to test if NRP2 regulates the clearance of apopototic debris in TAMs. For this we repeated the efferocytosis pulse and chase assay using bone marrow precursor cells isolated from the transgenic mouse model (CSF-1R-iCre;NRP2$^{f/f}$). Cells were differentiated to TAMs using CM from the murine pancreatic cancer cell line UNKC-6141 for 7days. (Z)-4-HydroxyTamoxifen was added into the cell culture, every alternate day, for 7days, to genetically knock out NRP2 from the macrophages. Prior to the assay, as apoptosis was induced in Jurkat cells using Etoposide (as mentioned earlier). Apoptotic Jurkat cells were added to the macrophages for 1hr in 1:10 ratio (macrophage:Jurkat) and allowed the engulfment by macrophages. Following this, non-engulfed or loosely bound cells were washed away and macrophages monitored upto 12hrs for their ability to degrade and clear the apoptotic cells that were engulfed. At the beginning of chase, there was no significant difference in the intensity of red fluorescence in the control and NRP2 KO cells. At 2hr chase, the intensity increased in the control and NRP2 KO macrophages, indicating the efferosomes are maturing further and becoming acidic. However, at 6 and 12 hrs of chase, there was a significant decrease in the intensity of red fluorescence as well as size of the internalized apoptotic debris in the control macrophages. This suggests efficient degradation and clearance of apoptotic cells in the control macrophages. In contrast, the higher red fluorescent intensity and persistence of bigger cellular debris in the NRP2 KO macrophages at the above-mentioned time points indicated a delayed clearance of apoptotic cargo in the absence of NRP2

(**Fig. 4.6 A**). **Fig. 4.6 B and C** show the graphical representation of the result and genetic depletion of NRP2 in the macrophages respectively.

Overall, these results suggested that NRP2 regulates efferocytosis of apoptotic cells in macrophages, during physiological homeostasis (M-CSF) as well as TAM polarizing conditions (CM treatment). Further, NRP2 depletion in macrophages significantly delayed the degradation and clearance of the apoptotic cells.

NRP2 in macrophages regulates tumor growth

(1) NRP2 regulates apoptotic cell clearance in TME and affects tumor growth: Studies have shown that efferocytosis of apoptotic tumor cells by TAMs is an important factor for maintenance of pro-tumorigenic activities of TAMs. Further, blockade of efferocytosis relieves the tumor burden by activating anti-tumor immune responses. However, the molecular effectors that couple the processes of efferocytosis and immune silencing in phagocytes is still not clearly understood. Based on our previous findings that NRP2 regulates efferocytosis of dying cells by macrophages (**Fig. 4.4-4.6**), we sought to next test if NRP2 depletion in TAMs affects tumor growth. For this, we used a subcutaneous pancreatic cancer progression model. $2X10^6$ UNKC-6141 murine pancreatic cancer cells were mixed with Matrigel and subcutaneously implanted into the right flanks of animals. Once tumors became palpable, animals were randomly divided into two groups (n=5 each): Control and test. In the test animals, tamoxifen was administered intraperitoneally (75mg/kg body weight of the animals) to genetically deplete NRP2 from macrophages. Tumor growth was monitored for a period of 21days since day of implantation. The overall design of the study is shown in **Fig. 4.7**. NRP2

depletion in macrophages resulted in a decrease in tumor growth (**Fig. 4.8 A,B**). The tumors were excised and weighed and tumor volume measured. The average volume of the control tumors was 449.80 mm^3 and that of test tumor was 215.15 mm^3, indicating a 52.16% decrease in average tumor volume in the test group (**Fig. 4.8 C**). The average weight of the control and test tumors was 0.33 and 0.22 gm respectively, suggesting a 33.33% decrease in the average weight of the test tumors in comparison the control (**Fig. 4.8 D**). Importantly, weight of the mice did not alter significantly following Tamoxifen administration (**Fig. 4.8 F**). **Fig. 4.8 E** shows immunoblot for knock out efficiency of NRP2 from bone marrow macrophages following Tamoxifen administration intraperitoneally in the control and test animals. One concern was whether intraperitoneal administration of NRP2 could knock out NRP2 from macrophages inside the tumor. RNA-Seq analysis (**Fig. 4.11 H**) revealed a knock-out of NRP2 from the TAMs isolated from the tumors. Thus, it is conceivable that the effect on tumor progression and TME arises as a consequence of myeloid specific NRP2 depletion.

Interestingly, histological analysis of the tumor sections revealed a significant increase in the percentage of average necrotic area in the test tumors (32%) compared to the control (19.2%) (**Fig. 4.9 A and B**). This could be attributable to the impaired clearance of dying tumor cells by NRP2 deficient TAMs. Given that NRP2 has a known role in migration, we next tested if NRP2 depletion affected the migration of macrophages into the TME, using F4/80 as a macrophage marker. We did not observe any significant difference in the number of macrophages in the control and test tumors (**Fig. 4.10 A and B**). We did not observe any significant

difference in the CD8+ T cell infiltration or CD31+ vessel density in control versus test tumors (**Fig. 4.10 C-F**).

(2) NRP2 in macrophages affects tumor growth and suppresses anti-tumor immune responses: We repeated our subcutaneous tumor progression experiment (n=5). This time, we subcutaneously implanted 500,000 UNKC-6141 cells mixed with Matrigel into the right flank of CSF-1R-iCRE;NRP2$^{f/f}$ mice. Once the tumors became palpable, tamoxifen was administered as described earlier and tumor progression monitored for a period of 25days. We observed a decrease in tumor size in the test tumors where NRP2 was genetically knocked out from TAMs (**Fig. 4.11 A**). Tumor growth was regularly monitored, and tumor volume calculated using the formula v=0.5(LXBXB) where L=longest diameter and B=widest diameter of the tumor. **Fig. 4.11 B** shows the line plot for tumor growth in control and test animals over the indicated time point. Importantly, NRP2 depletion in macrophages showed a cytostatic effect on tumor growth after day 17 and the growth curve for test tumors reached a plateau after this time. In contrast, there was a steady increase in the average volume of the control tumors. The excised tumors were weighed and measured. The average volume of the control tumors was 325 mm^3 and that of test tumors was 132 mm^3, indicating there was a 59.38% reduction in average tumor volume following NRP2 depletion in TAMs (**Fig. 4.11 C**). The average weight of the control tumors was 0.42 gm compared to 0.21 gm in the test group, suggesting a 50% decrease in tumor weight following NRP2 depletion (**Fig. 4.11 D**). Importantly, TUNEL staining of the tumor sections revealed an increase in the necrotic area in the test tumors (**Fig. 4.11E**). We believe NRP2 depletion in

macrophages resulted in inefficient clearance of apoptotic tumor cells, which eventually underwent secondary necrosis and spilled their nuclear and cellular components. **Fig. 4.11 G** shows immunoblot for knock out efficiency of NRP2 in bone marrow derived macrophages in the test mice, following Tamoxifen administration. NRP2 is well known for its role in migration. We questioned if the increase in necrotic foci in test tumors were a consequence of impaired recruitment of macrophages to the site of the tumor or their delayed clearance stemming from downstream phagosomal maturation defect in absence of NRP2. Staining with anti F4/80 antibody revealed no notable change in macrophage migration and recruitment in control and test tumors (**Fig. 4.12 A and B**). This indicates that NRP2 probably is dispensable for the migration of macrophages to the site of tumor. Also, it suggests that recruited TAMs display dampened efferocytic ability in absence of NRP2 which resulted in increased accumulation of apoptotic or necrotic cells in the TME. Staining with anti CD31 antibody revealed no significant difference in average vessel density between the control and test tumors, suggesting there intratumoral angiogenesis was unaffected following NRP2 depletion in TAMs (**Fig. 4.12 C and D**). However, further tests are required to affirm if there is any difference in the level of vessel normalization in control versus test tumors. Expression of alpha smooth muscle actin (α SMA) has been shown to correlate with poor prognosis in many tumors. However, staining with anti- α SMA showed no significant difference between control and test tumors (**Fig. 4.14 E and F**). One drawback of the current work is that being a subcutaneous tumor progression model, it does not entirely mimic the natural tissue architecture or

tumor growth conditions as in an orthotopic model. Also, the presence of skin fibroblasts is unavoidable in the current model.

One of the major contributing factors to tumor growth is suppression of effector and cytotoxic T cell activation. Tumor cells as well as other immune and stromal cells in the TME secrete a wide array of chemokines, cytokines and other factors which interfere with recruitment and activation of effector and cytotoxic T cells. Interestingly, we observed a ~3-fold increase in intratumoral infiltration of cytotoxic CD8+ T cells in the test tumors following NRP2 depletion. This data suggests NRP2 in macrophages suppresses anti-tumor immune response and that its depletion in macrophages results in enhanced recruitment of CD8+ T cells into the tumor (**Fig. 4.13 A and B**). Staining with anti-Granzyme B (GrB) antibody revealed a mild increase in the average number of GrB+ cells in 3 out of 5 test tumors, however, this did not reach statistical significance (**Fig. 4.13 C and D**). Interestingly, staining with anti CD4 revealed an infiltration along the periphery in 3 of the 5 test tumors in comparison to control tumors (**Fig. 4.13 E and F**); however, this did not attain statistical significance.

Taken together, the results indicated a role for NRP2 in regulating tumor growth and immune response against the tumor, without affecting macrophage recruitment and intratumoral angiogenesis.

Transcriptome analysis of TAMs using next generation RNA-Sequencing.

To better understand how NRP2 in TAMs mechanistically regulates tumor growth and T cell responses, we monitored the growth of subcutaneous PC tumor (n=3)

for 15days, following which the animals were sacrificed, and tumors excised. **Fig. 4.14A** summarizes the experimental design. The average volume of the control tumors was 324.8mm^3 whereas that of the test tumors was 129.8mm^3, indicating a 60% decrease in the average volume of the test tumors (**Fig. 4.14 B**). The average weight of the control and test tumors were 0.27gm and 0.166gm respectively, indicating a decrease in the average weight of the test tumors by 38.51% (**Fig. 4.14 C**). CD11b+ TAMs isolated using magnetic beads. RNA was isolated and pooled from n=3 animals in either control or test group. This was done in order to obtain sufficient amount of RNA. RNA-Sequencing was performed as mentioned in the methods section. A paired end read 2x75bp sequencing run of RNA libraries were performed using the Illumina NextSeq 500 instrument. For analysis, raw reads were de-multiplexed by barcode and output into FASTQ format. Cutadapt was used to filter out adapter sequences and low-quality bases. Filtered sequence reads were aligned to mouse reference genome mm10 using HISAT2 aligner. Reads mapping to exon regions as defined by Ensembl gene annotations were counted using FeatureCounts. We analyzed our data on the basis of log fold change value. We considered transcripts which were differentially expressed more than 2 fold ($\log_2$ fold change 1) in either control or test sample and eliminated all transcripts with zero counts in either sample to maintain stringency. After applying the cutoff, we had 3616 genes whose expression was altered by atleast 2 fold following NRP2 depletion in macrophages. Out of these, 1567 genes were differentially up-regulated whereas 2049 genes were downregulated following NRP2 depletion (**Fig. 4.14 D**). These differentially expressed transcripts

were uploaded to the IPA database to identify the major enriched cellular and molecular functions in the absence of NRP2 in macrophages. We observed that pathways related to immune responses as well as phagosome formation were most significantly affected. The top 20 significantly pathways from IPA analysis included communication between innate and adaptive immune cells, altered T cell and B cell signaling, Th1 and Th2 activation pathway, Primary immunodeficiency signaling, Th1 pathway, autoimmune thyroid disease signaling and phagosome formation. Among other significantly altered pathways, we detected leucocyte extravasation signaling, inhibition of matrix metalloproteases, role of cytokines in mediating communication between immune cells, micropinocytosis signaling and caveolar mediated endocytosis. Representative IPA pathways related to immune responses and phagocytosis pathways with gene enrichment and statistical significance is shown in **Fig. 4.15 A**.

To gain a better understanding for the functional processes affected by NRP2 depletion, we determined the biological process gene ontological classification for each altered transcript using the DAVID and KEGG databases in combination with extensive review of published literature. As observed with IPA analysis, with DAVID, we observed that genes related to immune response and leucocyte/lymphocyte regulation were abundantly regulated. Also, clusters comprising of genes functionally annotated to cytokine and chemokine signaling, wounding response, endocytosis or vesicle mediated transport, microtubule organization were enriched. Since our *in vitro* and *in vivo* data indicated a role of NRP2 in the regulation of phagocytosis and efferocytosis as well as activation of

CTL response in tumors, we selected representative annotation clusters enriched for these functions. Genes from IPA, KEGG and DAVID clusters for T cell related immune response, cytokine/chemokine signaling pathways and phagocytosis and phagosome maturation were compiled and a unique gene list was created for each function and compared with our dataset of 3616 differentially regulated genes. Fig. **4.15 B** and **C** show representative functional annotation clusters for differentially expressed genes in TAMs following NRP2 depletion.

NRP2 depletion deregulates phagocytosis and endocytosis related pathways in TAMs

For assessing the effect of NRP2 depletion in the phagocytic activity of TAMs, we carefully analyzed the expression pattern of genes detected by IPA (canonical pathway: phagosome formation) and DAVID (annotation clusters 91 and 92) as well as additional genes from our dataset. We detected altered expression of several genes belonging to the Rab family of proteins. Genes like *Rab15, Rab3a, Rab6B, Rab34, Rab39, RabL3, Rab36, Rab13, Rab27B* were affected following NRP2 depletion in macrophages. Several other genes associated with phagocytosis or phagosome/endosome maturation like, *Tubb4a, TubA8, Rufy4a, Zap70* were deregulated. Interestingly, we detected elevated expression of genes encoding Rab7 GTPase activating proteins, *TBC domain 1 member 15* and *TBC domain 1 member 2*. Several Guanine Nucleotide Exchange Factors, like *Rho GEF 15, Cdc42 GEF 9, FYVE Rho GEF, RhoD* among others were also differentially expressed. These indicate that NRP2 is important for endocytosis and phagocytosis pathways in macrophages. Interestingly, we found one mircroRNA,

mir-24 to be significantly upregulated in NRP2 depleted TAMs. This mir has been reported to attenuate phagocytosis as well modulate inflammatory cytokines in macrophages and DCs (251). Interestingly, several molecules like *Elmo-3, Alox15, CD4, IgM, CD209 (DC-SIGN), OC-STAMP* involved in phagocytic uptake or clearance of apoptotic cells were downregulated, although other molecules like *Stabilin1, Marco* that too can bind to and are important for the clearance of apoptotic cells were upregulated. CX3CL1 secreted from apoptotic cells bind to CX3CR1 expressed on macrophages and induce chemotaxis for efficient clearance of the apoptotic cells. We observed a significant downregulation in the expression of CX3CR1 in NRP2 depleted TAMs. Downregulation of phagocytic cargo-uptake related receptors and molecules may be either a secondary effect of impairment of phagosome maturation following NRP2 depletion, as it has already been reported that a defect in phagosome maturation can dampen the internalization process. Also, it may be possible that downregulation of the efferocytosis related receptors may be a tumor microenvironment specific effect. Known representative genes whose expression altered following NRP2 depletion in macrophages are shown in **Fig. 4.16 A**. In conclusion, the gene expression data indicated the potential involvement of genes present in macrophages, which are important for NRP2-mediated efficient clearance of apoptotic cells. Intriguingly, phagosomes containing different cargo often recruit functionally similar but distinct molecules for phagosome maturation or phagolysosome biogenesis and often follow different maturation kinetics. The exact molecular mechanism of how these

NRP2-regulated genes involve in the phagosome maturation is currently unknown and merits further investigation.

NRP2 depletion alters genes in TAMs related to inflammation, immunosuppression, tissue remodeling, chemokines and cytokines

Our analysis from IPA software, DAVID and KEGG pathways revealed many of the immunosuppressive genes and those associated with EMT and metastasis, like, *IL-4, IL-10, TGF-α, IL-21R, IL-33, IL-34, IL-23a, IL-1β* were downregulated in TAMs following NRP2 depletion. Genes associated with ECM remodeling like *MMP9, MMP13, MMP11, MMP23, MMP25* were also downregulated. Among the inflammatory genes, we observed a mixed signature. There was an upregulation of *IFN-β1, IL-12a, Gr-K, Gr-F, IL-15Ra, IL-1RL2,* whereas *IFN-γ, IL-12b, Gr-A, Gr-B, Gr-C, IL23a* were downregulated among others. It is known that efferocytosis upregulates the immunosuppressive genes in macrophages. Inefficient clearance of apoptotic cells reduces the immunosuppressive genes and induces the expression of inflammatory genes. For instance, cytosolic DNA from dead cells can trigger the expression of IFNβ. *IL-12a* expression is induced under inflammatory conditions and due to its low abundance, its induction is considered to be the rate limiting step in the production of biologically active IL-12. Gr-K has been reported to be upregulated in sepsis and acute airway inflammation, and plays a role in inflammatory responses in macrophages. Further, it can get activated in conditions where Gr-A activity is compromised. Additionally, Gr-K and Gr-F both have cytolytic potential and can be tumoricidal. These observations are in support of our hypothesis and indicate that NRP2 depletion affects efferocytosis.

This in turn downregulates the expression of immunosuppressive genes and upregulates the inflammatory genes. IL-12b subunit can homodimerize and bind to IL-12 receptor but does not mediate signaling and it therefore a strong antagonist for biologically active IL-12. We speculate the decrease in *IL-12b* transcript may be an effort to avoid formation of the antagonist $(IL\text{-}12b)_2$ homodimer. IL-23 (heterodimer of IL-23a and IL-12b) can also promote tumor progression by suppressing T and NK cells effector functions (252). Therefore, downregulation of *IL-12a* transcript may possibly be an effort to decrease the biologically active form of IL-23. Also, mir-24 that was significantly upregulated in NRP2 depleted TAMs has been reported to affect the expression of TNF-α, IL-6 and IL-12b at the transcription level (251). These indicate an effect of NRP2 depletion on dampening phagocytosis and a complex interplay among various molecules to affect the phenotype TAMs.

Interestingly, several genes associated with the maintenance of stem cell niche and metastasis like *MUC1, WISP1, Angptl2, CXCR4* were downregulated in NRP2 depleted TAMs. TAMs are considered one of the important players in intratumoral vasculature. Interestingly, following NRP2 depletion, some of the genes associated with the endothelial cell like behavior, like, *SOX7, Angptl2, Angptl7* were downregulated. Angptl2 can regulate metastasis through CXCR4 signaling pathway and MMP13 mediated degradation of the collagen. It also has direct pro-angiogenic activity. However, we did not observe any change in average vessel density in tumors following NRP2 depletion in macrophages. We also analyzed the chemokine gene profile in control versus test tumors. We detected that

chemokines like *CXCL13, CCL25* that have been reported to promote migration of DC, activated T cells were upregulated in NRP2 depleted TAMs. Expression of *CCL22* (known for attracting Th2, Treg or Th17 cells) and *CXCL12* (may promote TAM differentiation) were downregulated in NRP2 deficient TAMs.

In brief, these indicate that in NRP2 depleted condition, TAMs suppress immunosuppressive genes and upregulates several inflammatory pathways. Known representative genes pertaining to macrophage polarization are shown in **Fig. 4.16 B.**

Effect of NRP2 depletion in macrophages on T cells

We observed that NRP2 depletion affects the clearance of apoptotic cells in macrophages as well as TAMs *in vitro*. Our *in vivo* observations suggested NRP2 depletion in macrophages resulted in an increased infiltration of cytotoxic $CD8^+$ and $CD4^+$ T cells (in 3 out of 5 tumors) into the tumor. We analyzed the transcriptome data in our quest to search for changes in expression of genes that could explain the increased infiltration of activated T cells into the tumors following NRP2 depletion in macrophages. As mentioned earlier, NRP2 depletion affected the expression pattern of several immunosuppressive genes, like *IL-4, IL-10, TGF-α, IL-21R, IL-33, IL-34.* IL-4, IL-10, TGF-α can potentially induce the formation of Treg cells. TGF-α can also interfere with T cell activation, proliferation and migration to the tumor tissue. Also, IL-12α and IFN-β1 were upregulated in the NRP2 depleted TAMs which can potentially activate T cell responses. Additionally, our analysis revealed an increased expression of *CXCL13* and *CCL25* that can recruit effector T cells whereas molecules like CCL22, Sema-7A and Sema-3E that

can either recruit Treg cells or interfere with T cell migration or their activation were downregulated in the NRP2 deficient TAMs. Additionally, molecules like Foxp3, PDL2, TIGIT that can either induce immunosuppression in macrophages and indirectly dampen T cell response or provide co-inhibitory signal to T cells were downregulated following NRP2 depletion (253-255). Therefore, we believe that NRP2 deletion in macrophages affects the expression of several immune response genes that act in consort and facilitates the infiltration of cytotoxic $CD8^+$ and $CD4^+$ T cells. Further, we observed inefficient clearance of dead cells in tumors where NRP2 was depleted from macrophages. Apoptotic cells if not removed, form secondary necrosis and the nuclear and cellular contents leak outside as a result of loss of membrane integrity. This was observed from TUNEL staining where we found an increase in the number of necrotic zones in the tumors following NRP2 depletion from macrophages. The leaked cellular contents from cells undergoing secondary necrosis can also potentially attract CD8+ T cells. Overall, we believe that the components of the necrotic cells and altered expression of several cytokines, chemokines and other signaling molecules following NRP2 depletion in macrophages act synergistically and result in robust infiltration of CD8+ T cells in to the tumors. Known representative genes that can potentially work in consort for T cell activation are shown in **Fig. 4.16 B**.

Summary and Discussions

Apoptosis is a highly orchestrated cell death modality and clearance of apoptotic cells by efferocytosis for removing aged or damaged cells in an immunologically silent manner is essential for maintenance of physiological

homeostasis. Impaired efferocytosis results in secondary necrosis and leakage of necrotic cell contents into the tissue milieu and can aberrantly activate adaptive immune responses. Efficient efferocytosis of cells infected with microbes (e.g. influenza virus, *Mycobacterium tuberculosis*) results in pathogen destruction. Cells infected with the pathogen can be taken up and degraded simultaneously by macrophages (230). Additionally, macrophages also efficiently remove the apoptotic or infected neutrophils that invade the site of injury or infection (256). This process of cleaning up further evokes non-inflammatory cascades, such as, production of IL-10, TGF-β in engulfing cells and polarizes the efferocytic macrophages towards an immunosuppressive phenotype and is important for resolution of inflammation and wound healing post infection or injury. Despite extensive research over the past decade, knowledge about the molecular pathways that link the processes of efferocytosis and immune suppression in macrophages is limited. Our data reveal a novel role of NRP2 in regulating efferocytosis in macrophages. We provide evidence to suggest that NRP2 promotes rapid and efficient clearance of engulfed apoptotic cells and its absence significantly delays the overall clearance process. NRP2 is a cell surface receptor. Hence, the question arises, does it interact with any of the ‘find me’ or ‘eat me’ molecules expressed on the surface of dying cells and affect the uptake process. However, after initial incubation with apoptotic cells (0 min chase), our data suggest that NRP2 does not affect the uptake process. Of note, NRP2 depletion does not block the clearance of apoptotic cellular debris, but delays the overall clearance process. Macrophages were monitored for upto 12 hrs for their ability to

clear engulfed apoptotic debris in the presence and absence of NRP2. We observed that in absence of NRP2, the degradation and clearance of apoptotic cells was significantly delayed in the macrophages. This suggested that NRP2 regulates the maturation of phagosomes containing apoptotic cells in macrophages. Our earlier data suggested that depletion of NRP2 resulted in an accumulation of Rab5+ vesicles and a concomitant decrease in the number of Rab7+ positive vesicles in the cells. Although it is now accepted that the processes of endocytosis, phagocytosis and efferocytosis share similarities, each of these processes are distinct and may recruit unique effector molecules at each stage. Therefore, it is possible that NRP2 may interact with different effector molecule for efferosome maturation and apoptotic cell clearance. Further studies are required to investigate the molecular players that interact with NRP2 in apoptotic cell clearance process. Another important question is whether efferosome maturation and autophagy share a common mechanism. Recently, LC3 associated phagocytosis (LAP) has been proposed as an alternative pathway for clearance of apoptotic cells. We have previously reported a role for NRP2 in regulating autophagy in cancer cells. Whether NRP2 regulates efferocytosis through LAP needs further studies. Also, it is important to know if LC3 overlaps with Rab5 or Rab7 in phagosomes containing apoptotic cells and interact with each other in the presence and absence of NRP2.

It is important to estimate the implications of our findings. Efficient efferocytosis and clearance of engulfed apoptotic cells are indispensable for the maintenance of cellular homeostasis. As mentioned earlier, defective efferocytosis

gives rise to pathological conditions like autoimmunity, systemic lupus erythematosus (SLE), atherosclerosis among others. Interestingly, delayed phagosome maturation arising either as a consequence of impaired fusion with lysosome or failure in the acquisition of degradative enzymes helps preserve antigenic epitopes and favors cross presentation. Since we observed that NRP2 depletion significantly delays apoptotic cell clearance, it is plausible that its depletion or deficiency will increase the chance for cross presenting the apoptotic cell derived peptide and activate CD8+ T cell responses and aggravate inflammation related clinical disorders.

Phagocytosis of cancer cells by APCs in the TME is a contentious topic. Cancer cells over-express ‘don’t eat me’ molecules to evade APC mediated uptake and presentation to the T cells. Additionally, TAMs have recently been shown to express PD-1 that negatively correlates with their phagocytic capacity of tumor cells. Further, blocking of interaction between PD-1 and PD-L1 increased phagocytosis and reduced tumor growth in a macrophage dependent manner. However, TAM mediated phagocytosis of tumor cells can act as a double-edged sword in tumor progression and metastasis. Most of the patients undergoing treatment for cancer, including Pancreatic Cancer receive either chemotherapy (CT) (such as Gemcitabine) or radiotherapy (RT). These conventional treatment modalities interact in a complex way with the dense stroma that is the hallmark feature of PC and can be detrimental. There are now evidences to show that there is increased infiltration of myeloid cells in to the TME following CT or RT that limits the anti-neoplastic efficacy and are associated with tumor protective function and

disease recurrence with more aggressive features. This can be attributed to increased apoptotic index in the TME following therapy and increased efferocytosis by the freshly recruited TAMs. This triggers anti-inflammatory cascades and elicit a misdirected tissue repair response, eventually resulting in further immunosuppression and tumor relapse. Blocking efferocytosis holds promise by increasing anti-tumor immune response. For example, Bavituximab, a PS targeting antibody is currently being assessed in multiple clinical trials and has shown considerable benefit (https://clinicaltrials.gov/ct2/show/NCT03139916)(http://www.peregrineinc.com/clinical-trials.html) (240, 257). We previously observed a role for NRP2 in regulating efferocytosis of apoptotic cells. Previous studies have briefly reported the presence of NRP2 expressing macrophages in lung carcinoma (human) and mouse tumor. In the current study, we detected NRP2 expressing TAMs in primary lesions of PDAC patients as well as in mouse PC tissue. We further observed that treatment of macrophages with conditioned media from human and mouse PC cell lines exhibited phagosomal maturation defect when challenged with *E.coli* in absence of NRP2, indicating a requirement for NRP2 in phagocytosis in TAMs. Next, in our assessment of the ability of TAMs to efficiently clear apoptotic debris in presence and absence of NRP2, we observed that in comparison to the WT TAMs, NRP2 depleted macrophages failed to completely degrade and clear apoptotic cells even after 12 hrs. Interestingly, the effect was more robust in the presence of tumor cell derived conditioned media compared to MCSF treatment. Of note, we did not notice any uptake defect in NRP2 deficient TAMs. These results indicated that NRP2 is important for

phagosome maturation in TAMs and regulates the clearance of apoptotic cells by TAMs.

To test how delayed clearance of apoptotic tumor cells may affect PC growth, we used a subcutaneous tumor progression model. Genetic ablation of NRP2 in TAMs reduced tumor growth. However, we did not notice any changes in intratumoral macrophages following NRP2 depletion, indicating NRP2 is dispensable for TAM recruitment. Interestingly, when we implanted $2X10^6$ cells, we observed a significant increase in the percentage of necrotic area in tumors where NRP2 was depleted in TAMs. This could be attributed to a rapid growth of the tumor cells and high apoptotic index and impaired efferocytosis by NRP2 depleted TAMs and secondary necrosis resulting from the dying tumor cells. Macrophages are the major source of intratumoral angiogenesis. However, NRP2 depletion in TAMs did not significantly affect intratumoral angiogenesis. Also, we did not see any increase in CD8+ T cells infiltration in test tumors. We do not know if this was because the time period we monitored the tumor progression was not optimal for noticing a change in CD8+ T cell infiltration.

Interestingly, when we repeated the experiment using 500,000 cells and monitored tumor growth, we once again observed a decrease in tumor growth rate following NRP2 depletion in TAMs. More importantly, growth curve for test group reached a plateau after day 17, indicating a cytostatic effect of NRP2 deletion in macrophages. Hence, it is conceivable that NRP2 depletion in macrophages can potentially harness tumor growth. TUNEL staining revealed an increased number of necrotic foci in tumors following NRP2 depletion in macrophages. We believe

the increase in the number of necrotic foci resulted from inefficient clearance of apoptotic tumor cells and eventual secondary necrosis that led to leakage of nuclear and cellular contents. NRP2 depletion did not affect macrophage recruitment to the site of the tumor, hence we conclude that the increase in the necrotic area is a consequence of inefficient apoptotic cell clearance in the TME. It is known that accumulation of apoptotic cells that eventually result in leakage of cellular contents due to secondary necrosis can potentially activate CD8+ T cells. Indeed, NRP2 depletion in TAMs significantly increased the infiltration of cytotoxic CD8+ T cells in test tumors (~3 fold). Interestingly, we did not observe any change any intratumoral angiogenesis following NRP2 depletion in TAMs. Stromal desmoplasia is a hallmark feature of PC and it has been shown to act as a physical barrier to therapy efficacy. High α-SMA has been associated with worse prognosis in PC. Although we did not observe any notable change in the α-SMA in test tumors, one must note that the subcutaneous tumor microenvironment does not mimic that of the natural PDAC (as found in orthotopic tumors). Further, pericytes often express α-SMA that can interfere with the conclusion.

We have concluded from our earlier experiments that NRP2 regulates the clearance of *E.coli*, zymosan and apoptotic cells by modulating the phagosome maturation process. Whole transcriptome sequencing of TAMs in conjunction with pathway analysis revealed an altered expression of several Rab family proteins. For instance, *Rab15, Rab3a, Rab6B, Rab34, Rab39, RabL3, Rab36, Rab13, Rab27B* were affected following NRP2 depletion in macrophages. Some of these like, Rab36, Rab13, Rab27B have potent roles in retrograde transport, recycling

or exocytosis pathways. Several other genes associated with phagocytosis or phagosome/endosome maturation like, *Tubb4a, TubA8, Rufy4a, Zap70* were deregulated suggesting a phagosomal maturation defect. Proteins like Rufy have a C-terminal FYVE domain for interaction with PI3P on the early phagosomes or endosomes and can interact with GTP-bound Rab5 and hence maybe a potential candidate for regulating the recruitment of downstream effector molecules for phagosome maturation. Interestingly, we detected elevated expression of genes encoding Rab7 GTPase activating proteins, *TBC domain 1 member 15* and *TBC domain 1 member 2*. Increased expression of these proteins can potentially inactivate GTP-bound Rab7 recruited to the phagosome membrane and interfere with phagosomal maturation. Several Guanine Nucleotide Exchange Factors, that may be involved in actin cytoskeleton reorganization, like *Rho GEF 15, Cdc42 GEF 9, FYVE Rho GEF, RhoD* among others were also differentially expressed. These indicate that NRP2 is important for endocytosis and phagocytosis pathways in macrophages. Interestingly, several molecules like *Elmo-3, Alox15, CD4, IgM*, *CD209 (DC-SIGN), OC-STAMP* involved in either phagocytosis or clearance of apoptotic cells were downregulated, although *Stabilin1, Marco,* two of the molecules involved in binding and recognizing apoptotic cells, were upregulated. Downregulation of efferocytosis related receptors and molecules may be either a secondary effect of impairment of phagosome maturation following NRP2 depletion. It has already been reported that a defect in phagosome maturation can dampen the internalization process, although we did not observe any internalization defect in NRP2 depleted macrophages *in vitro*. However, it may be

possible that downregulation of the efferocytosis related receptors may be a tumor microenvironment specific effect. Taken together, this supports our observations that NRP2 is important for the efficient clearance of apoptotic cells by macrophages by favoring phagosome maturation and also indicates that apoptotic tumor cells were inefficiently removed by NRP2 depleted TAMs owing to either dampened uptake (may arise as a secondary effect) or a defect in the downstream events of phagosome maturation. Intriguingly, phagosomes containing different cargo often recruit functionally similar but distinct molecules for phagosome maturation or phagolysosome biogenesis and often follow different maturation kinetics. Enrichment and identification of differential recruitment of proteins during maturation is best observed following isolation of phagosome membranes. It may be possible that NRP2 interacts with a common adapter molecule and regulates the recruitment of several effector molecules at various stages of phagosome maturation. The exact molecular mechanism how NRP2 regulates the phagosome maturation is currently unknown; the differentially expressed genes from our RNA-Seq data does not readily indicate how NRP2 regulates phagosome maturation at the molecular level and merits further investigation.

The hallmark feature of efferocytosis is that it is immunologically silent and induces the expression of immunosuppressive genes in macrophages. Blockade of efferocytosis or inefficient clearance of apoptotic cells removes that suppressive effect and activates the inflammatory pathway. Our RNA sequencing analysis identified suppression of several immunosuppressive genes, for example, *IL-4, IL-10, TGFα, CCL22* were downregulated whereas inflammatory genes like *IFN-β1,*

IL-12a, Gr-K, Gr-F were upregulated. Additionally, we observed some chemokines or chemokine receptors like CCL25 or CXCL13 that can potentially recruit cytotoxic CD8+ or effector CD4+ T cells were upregulated in NRP2 depleted condition. Also, increase in IFN-β1, Il-12a may act to activate T cell response. A lot of effort is currently being given to harness checkpoint inhibitor molecules like CTLA-4, PDL-2, PDL-1, PDL-1 which interfere with T cell activation and help maintain a local environment of immunosuppression in the TME. Interestingly, PDL-2 was downregulated in TAMs following NRP2 depletion. Additionally, molecules that can either activate T cell death, like FasL or indirectly interfere with T cell activity by promoting immunosuppression in macrophages (like TIGIT, Foxp3) were also downregulated. However, some of the altered genes showed a mixed signature. It is important to remember that TAMs are a complex population and often show a mixed phenotype, highlighting their plasticity. Taken together, we conclude that NRP2 depletion affects a wide array of molecules associated with the immune response that act in consort and result in $CD8^+$ T cell activation. It is important to remember that the time point selected for RNA-seq (15 days post tumor implantation) provides us a snapshot of the changes occurring in TAM during that time point. Many important changes in gene profile that may reflect further deregulation of efferocytosis and therefore activation of M1-type inflammatory pathways in TAMs may have either happened before or would take place at later time points.

Tumors manipulate the immune system in multiple ways, eventually shaping it to promote tumor growth and metastasis. One of the key mechanisms

by which this is achieved is through suppression of effector and cytotoxic T cell recruitment to the tumor bed and their activation, and through recruitment of suppressor T cells. In summary, based on our current findings that NRP2 depletion in macrophages suppresses the immunosuppressive genes robustly increases $CD8^+$ T cell infiltration, we propose NRP2 may be a potential candidate for therapeutic intervention in treating solid tumors, including PC. However, considering targeting NRP2 in TAMs to dampen efferocytosis and activate anti-tumor immune response as a potential strategy for treating cancer, one must weigh the risks associated with necrotic cell death and leakage of necrotic cellular components, hyper activation of T cells, autoimmunity and tissue damage. For example, impaired efferocytosis of apoptotic cells in post-partum condition results in tissue scarring and inflammation and interferes with lactation ability. Also, inflammation resulting from blockade of NRP2 mediated efferocytosis may adversely promote tumor associated inflammation and aid in tumor progression. Therefore, it is important to identify the optimal therapeutic window for targeting efferocytosis in cancer.

Fig. 4.1 NRP2 is expressed by tumor infiltrating macrophages in pancreatic cancer. (A) Representative confocal image showing the presence of NRP2 expressing TAM in human PDAC tissue. The first panel shows only NRP2 positive cells in the tumor section (red). The second panel shows CD68+ macrophages (green). The third panel represents merged image showing NRP2+CD68+ macrophage in the tumor tissue. Scale bar, 50µm. Inset shows magnified image of a single macrophage. Arrows indicate NRP2+CD68+ macrophage while * indicate NRP2 expressing non-macrophage type cells. Dapi was used to stain the nucleus. (B) Representative confocal image showing the presence of NRP2 expressing F4/80+ macrophages in mouse pancreatic tumor. The first panel shows cells that stained positive for NRP2 (green). The second panel represents F4/80+ cells (red). The third panel represents merged image showing NRP2+F4/80+ macrophages in the tumor section. Scale bars, 20µm. Inset showing magnified image of an individual NRP2+ macrophage. Arrows indicate NRP2+F4/80+ cells while * indicate NRP2 expressing other cell types in the tumor section.

Fig. 4.1

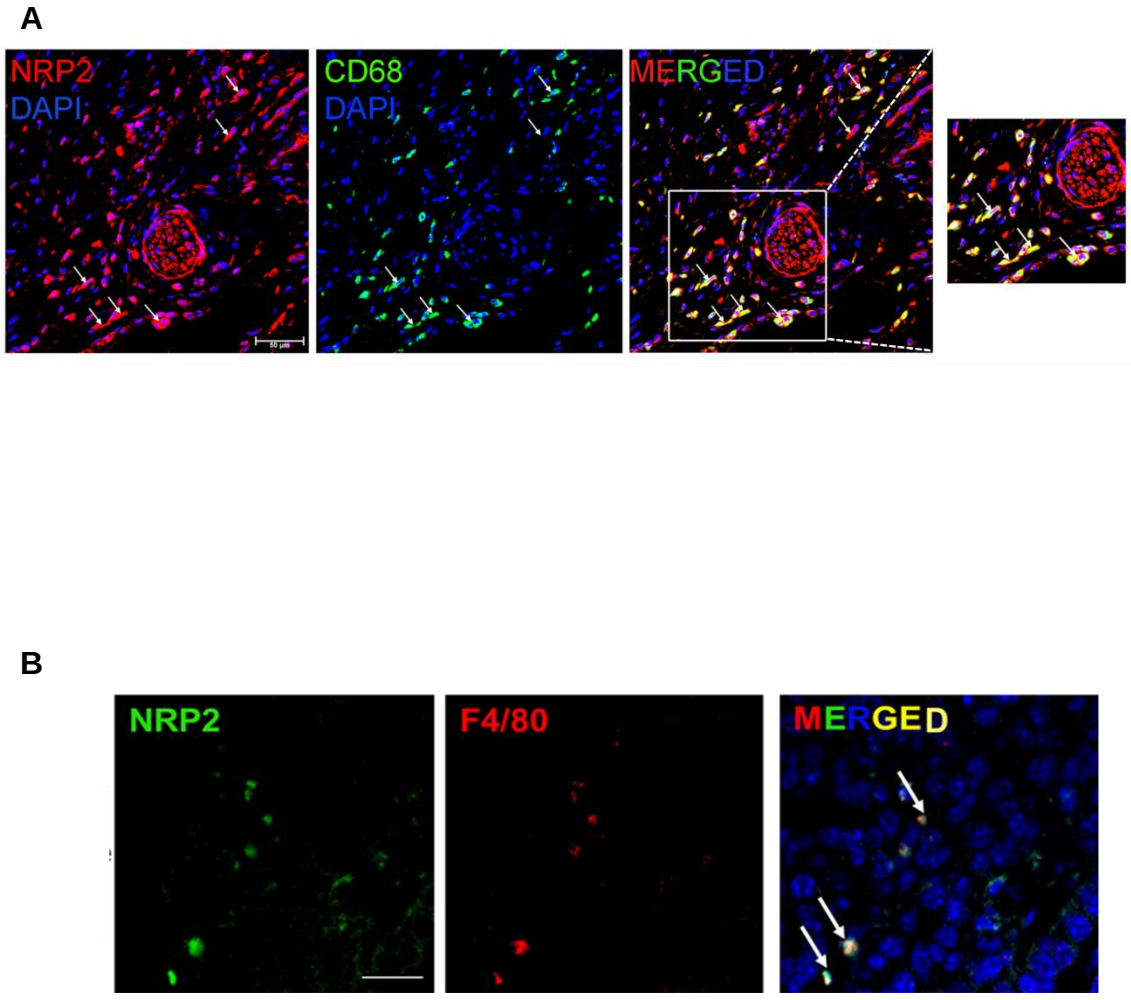

Fig. 4.2 Expression of NRP2 in human and mouse TAMs generated in vitro. (A-C) Immunoblot analyses showing NRP2 expression in TAMs generated *in vitro*. Freshly isolated human monocytes or bone marrow cells from WT mice were differentiated to TAMs with CM from Panc-1 (human) or UNKC-6141 or KPC cells (mouse) for 7days. Significant NRP2 expression was observed in both human and mouse TAMs generated *in vitro*.

Fig. 4.2

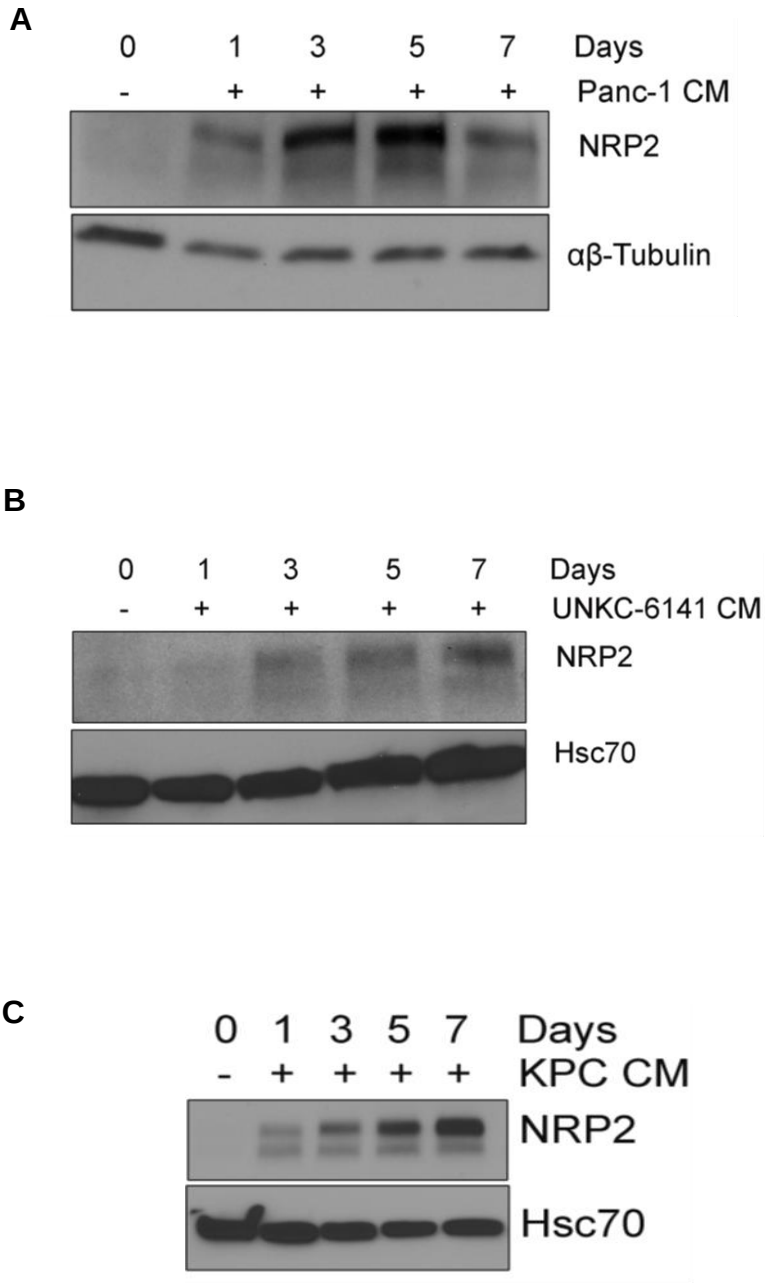
A
0 1 3 5 7 Days
- + + + + Panc-1 CM
NRP2
αβ-Tubulin
B
0 1 3 5 7 Days
- + + + + UNKC-6141 CM
NRP2
Hsc70
C
0 1 3 5 7 Days
- + + + + KPC CM
NRP2
Hsc70

Fig. 4.3 NRP2 regulates phagosome maturation in TAMs in vitro. Human macrophages treated with CM from Panc-1 cells were used for phagocytosis assay with pHrodo *E.coli* bioparticles. Phagosome maturation was scored from visible red puncta under the microscope. (A) Representative confocal microscopy image showing NRP2 depletion impaired phagosome maturation in Panc-1 CM treated macrophages. Inset shows magnified image of an individual cell. Scale bar, 10µm. (B) Phagosome maturation was quantified as total cellular fluorescence using Image J software and represented in a bar graph. (C) western blot showing NRP2 depletion. (D,G) Mouse bone marrow derived macrophages treated with CM from UNKC-6141 or KPC cells were exposed to pHrodo *E.coli* bioparticles. Phagosome maturation was assessed from the intensity of visible red puncta under the microscope. Representative confocal microscopy image is shown. Inset shows magnified image of an individual cell. Scale bar, 20µm. (E,H) Phagosome maturation was quantified as total cellular fluorescence using Image J software and represented in a bar graph. All values as mean ± SEM. Dapi was used for staining the nucleus in all the experiments. Student *t* test was used for comparison between 2 groups of cells. **P* < .05; ***P* < .005; ****P* < .0005. ns=not significant. (C,F, I) Western Blots for NRP2 depletion for each experiment is shown.

Fig. 4.3

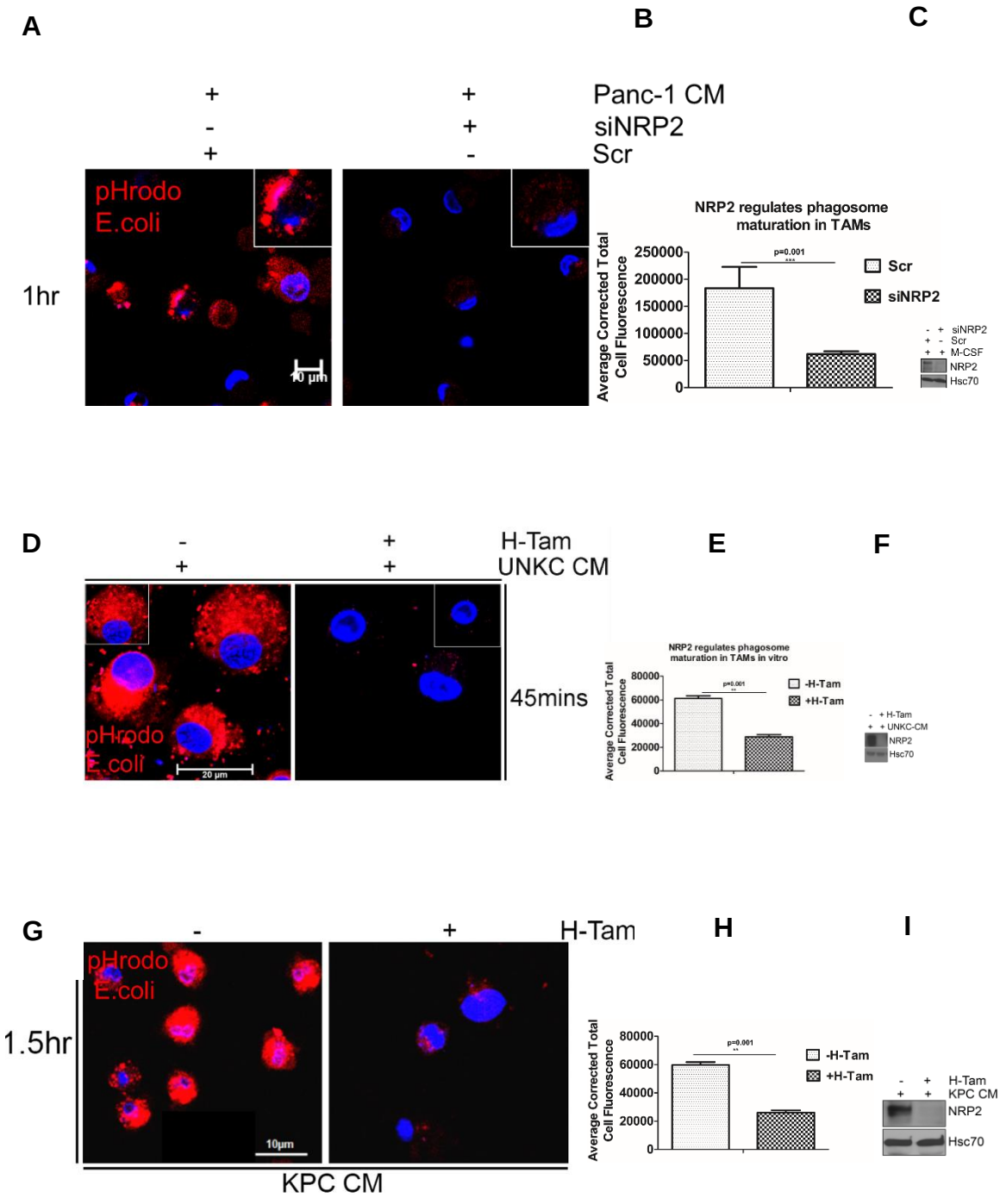
A
B
C
+
-
+
+
+
-
Panc-1 CM
siNRP2
Scr
pHrodo
E.coli
1hr
10 µm
NRP2 regulates phagosome maturation in TAMs
Average Corrected Total Cell Fluorescence
250000
200000
150000
100000
50000
0
p=0.001
Scr
siNRP2
- + siNRP2
+ - Scr
+ + M-CSF
NRP2
Hsc70
D
E
F
-
+
+
+
H-Tam
UNKC CM
pHrodo
E.coli
20 µm
45mins
NRP2 regulates phagosome maturation in TAMs in vitro
80000
60000
40000
20000
0
-H-Tam
+H-Tam
- + H-Tam
+ + UNKC-CM
NRP2
Hsc70
G
H
I
-
+
H-Tam
pHrodo
E.coli
1.5hr
10µm
KPC CM
80000
60000
40000
20000
0
p=0.001
-H-Tam
+H-Tam
- + H-Tam
+ + KPC CM
NRP2
Hsc70

Fig. 4.4 NRP2 regulates efferocytosis of apoptotic cells in bone marrow derived macrophages. Efferocytosis assay to assess the effect of NRP2 depletion on the ability of macrophages to mature the efferosomes and degrade the apoptotic cells. (A) A schematic diagram showing the experimental design. (B) Bone marrow cells isolated from $NRP2^{fl/fl}$CSF1R-iCre mice were cultured for 7days with M-CSF. Macrophages were then challenged with apoptotic Jurkat cells for 1hr (pulse). Non-engulfed or loosely adherent apoptotic cells were removed and macrophages were then microscopically assessed for their ability to degrade the apoptotic cell cargo for the chase time points= 0hr, 2hr, 6hr, 12hr. Scale bars, 10µm. Magnified images within the insets show single cell containing apoptotic body at each indicated time point for the panels. (C) Intensity of cellular fluorescence (red) was analyzed using Image J software and used as a measure for the ability of the macrophages for efferosome maturation and to degrade the apoptotic cargo. Cells were analyzed at the time points indicated in the graph abscissa and results represented as bar graphs. Values are mean ± SEM. (D) Immunoblot to show knock out of NRP2 following addition of (Z)-4-Hydroxy Tamoxifen. Dapi was used for staining the nucleus in all experiments. Student *t* test was used for comparison between 2 groups of cells. **P* < .05; ***P* < .005; ****P* < .0005. ns=non-significant.

Fig. 4.4

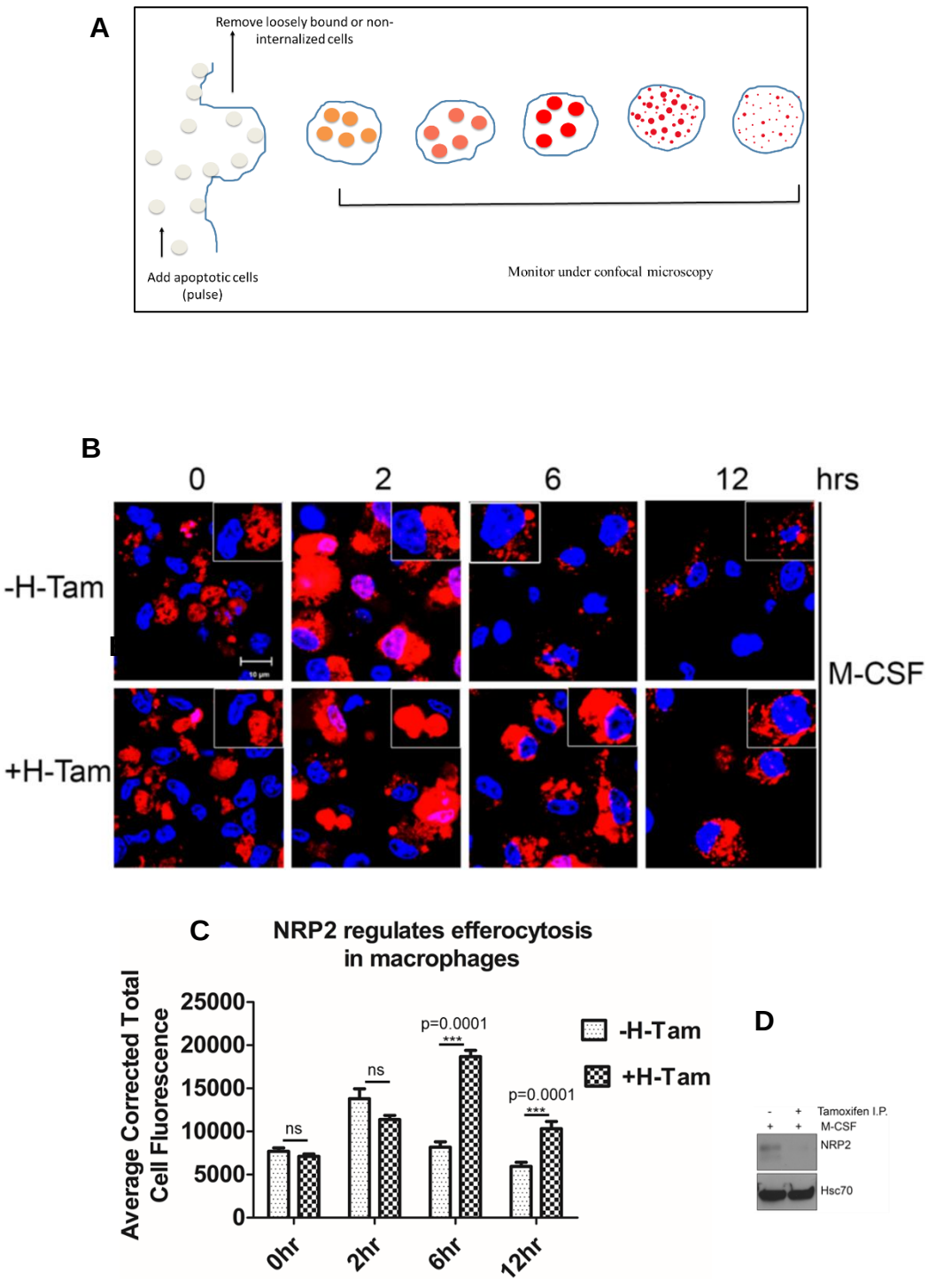
A
Remove loosely bound or non-internalized cells
Add apoptotic cells (pulse)
Monitor under confocal microscopy
B
0
2
6
12
hrs
-H-Tam
+H-Tam
M-CSF
C
NRP2 regulates efferocytosis in macrophages
Average Corrected Total Cell Fluorescence
25000
20000
15000
10000
5000
0
ns
ns
p=0.0001
***
p=0.0001
***
-H-Tam
+H-Tam
0hr
2hr
6hr
12hr
D
Tamoxifen I.P.
M-CSF
NRP2
Hsc70

Fig. 4.5 NRP2 regulates efferocytosis of apoptotic cells in peritoneal macrophages. Efferocytosis assay to assess the effect of NRP2 depletion on the ability of macrophages to mature the efferosomes and degrade the apoptotic cells. (A) Peritoneal macrophages isolated from NRP2$^{fl/fl}$CSF1R-iCre mice were cultured for 3 days with M-CSF. Macrophages were then challenged with apoptotic Jurkat cells for 1hr (pulse). Non-engulfed or loosely adherent apoptotic cells were removed and macrophages were then microscopically assessed for their ability to degrade the apoptotic cell cargo for the chase time points= 0hr, 2hr, 6hr, 8hr. Scale bars, 10μm. Magnified images within the insets show single cell containing apoptotic body at each indicated time point for the panels. (B) Intensity of cellular fluorescence (red) was analyzed using Image J software and used as a measure for the ability of the macrophages for efferosome maturation and to degrade the apoptotic cargo. Cells were analyzed at the time points indicated in the graph abscissa and results represented as bar graphs. Values are mean ± SEM. (C) Immunoblot to show knock out of NRP2 in peritoneal macrophages following addition of (Z)-4-Hydroxy Tamoxifen. Dapi was used for staining the nucleus in all experiments. Student *t* test was used for comparison between 2 groups of cells. **P* < .05; ***P* < .005; ****P* < .0005. ns=non-significant.

Fig. 4.5.

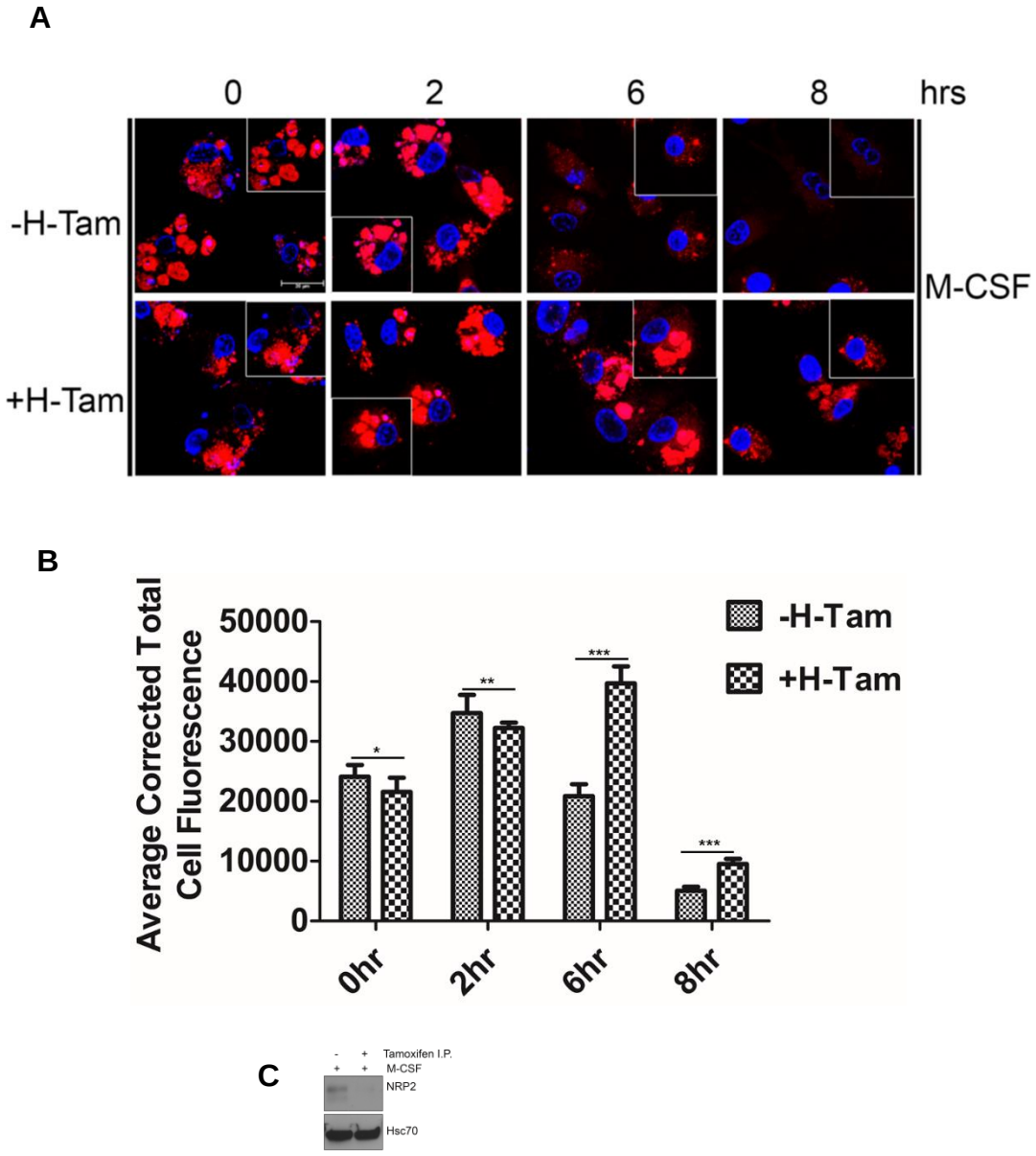
A
0
2
6
8
hrs
-H-Tam
+H-Tam
M-CSF
B
Average Corrected Total Cell Fluorescence
50000
40000
30000
20000
10000
0
-H-Tam
+H-Tam
*
**
***
***
0hr
2hr
6hr
8hr
C
- + Tamoxifen I.P.
+ + M-CSF
NRP2
Hsc70

Fig. 4.6 NRP2 regulates the clearance of apoptotic cells in TAMs *in vitro*. Efferocytosis assay to assess the effect of NRP2 depletion on the ability of TAMs to mature the efferosomes and degrade the apoptotic cells. (A) bone marrow cells isolated from $NRP2^{fl/fl}$CSF1R-iCre mice were cultured for 7 days with CM from UNKC-6141 cells. Macrophages were then challenged with apoptotic Jurkat cells for 1hr (pulse). Non-engulfed or loosely adherent apoptotic cells were removed and macrophages were then microscopically assessed for their ability to degrade the apoptotic cell cargo for the chase time points= 0hr, 2hr, 6hr, 12hr. Scale bars, 10µm. Magnified images within the insets show single cell containing apoptotic body at each indicated time point for the panels. (B) Intensity of cellular fluorescence (red) was analyzed using Image J software and used as a measure for the ability of the macrophages for efferosome maturation and to degrade the apoptotic cargo. Cells were analyzed at the time points indicated in the graph abscissa and results represented as bar graphs. Values are mean ± SEM. (C) Immunoblot to show knock out of NRP2 following addition of (Z)-4-Hydroxy Tamoxifen. Dapi was used for staining the nucleus in all experiments. Student *t* test was used for comparison between 2 groups of cells. **P* < .05; ***P* < .005; ****P* < .0005. ns=non-significant.

Fig. 4.6

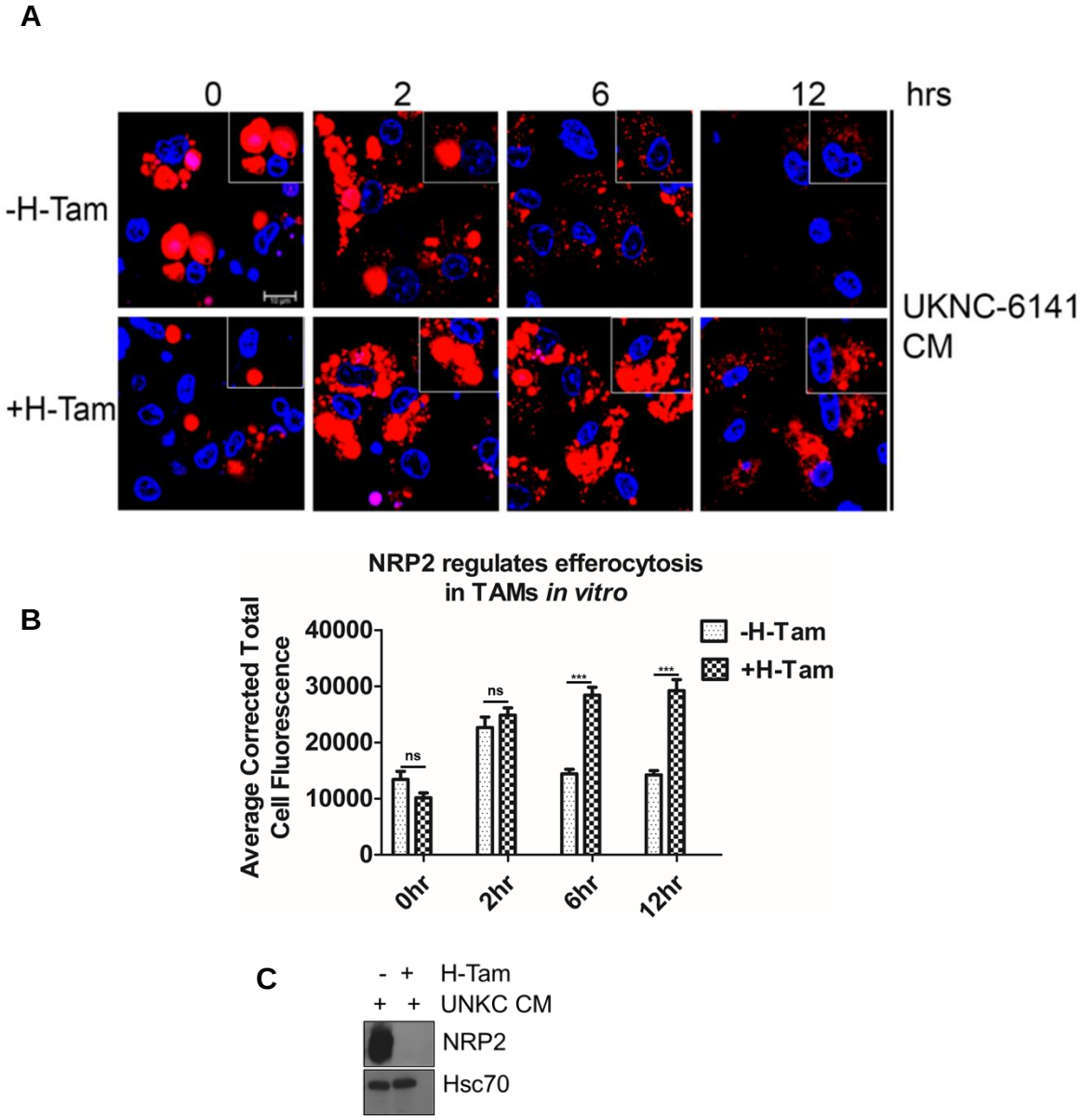
A
0
2
6
12
hrs
-H-Tam
+H-Tam
UKNC-6141 CM
B
NRP2 regulates efferocytosis in TAMs *in vitro*
Average Corrected Total Cell Fluorescence
40000
30000
20000
10000
0
-H-Tam
+H-Tam
ns
ns
***
***
0hr
2hr
6hr
12hr
C
- + H-Tam
+ + UNKC CM
NRP2
Hsc70

Fig. 4.7 Scheme of subcutaneous tumor growth model. Schematic diagram for subcutaneous tumor growth model. UNKC-6141 cells were mixed with Matrigel and subcutaneously implanted into the right flank of NRP2$^{fl/fl}$CSF1R-iCre mice. Once the tumors became palpable, animals were randomly divided into control and test groups (n=5). The test animals received daily intraperitoneal injection of Tamoxifen (20mg/kg body weight) to knock out NRP2 from the macrophages. Tumor growth was monitored for time periods indicated in Fig. 4.8 and Fig. 4.9.

Fig. 4.7

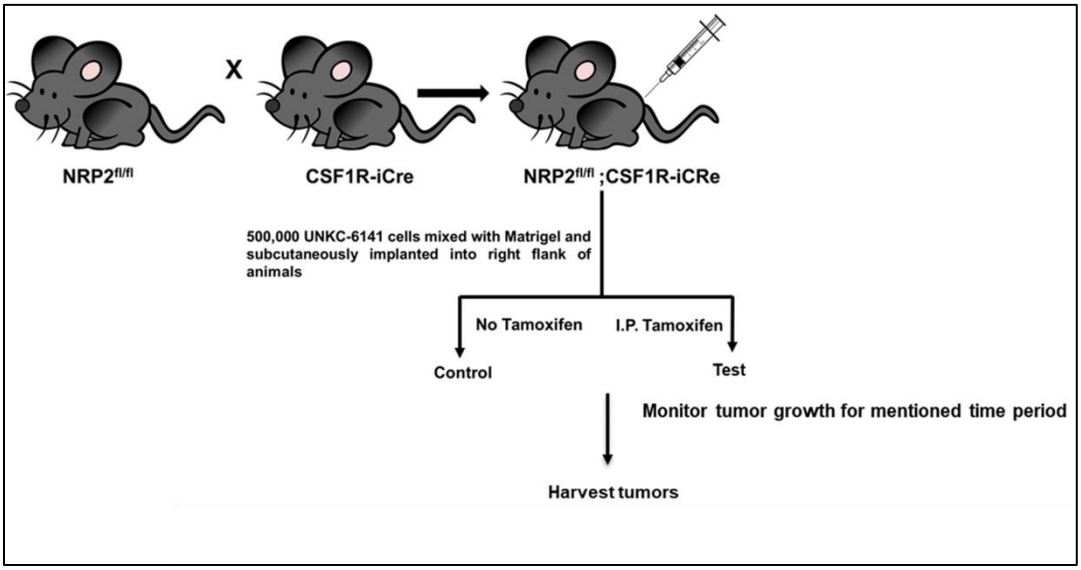
X
NRP2fl/fl
CSF1R-iCre
NRP2fl/fl;CSF1R-iCRe
500,000 UNKC-6141 cells mixed with Matrigel and subcutaneously implanted into right flank of animals
No Tamoxifen
I.P. Tamoxifen
Control
Test
Monitor tumor growth for mentioned time period
Harvest tumors

Fig. 4.8 NRP2 in macrophages affects tumor progression. (A) Representative image of the harvested tumors from the control and Tamoxifen treated mice, showing moderate decrease in the test group tumors following NRP2 depletion in macrophages. (B) Tumor growth was monitored regularly for the indicated time period and represented as a line graph. * indicates p=0.05. (C) Scatter plot comparing the volume of the control and test tumors after they were harvested. (D) Graphical representation of weight of harvested tumors. (E) Western Blot showing NRP2 was completely knocked out from the bone marrow macrophages following Tamoxifen injection into the test animals. (F) graph showing weight of animals before and at the end of the study.

Fig. 4.8

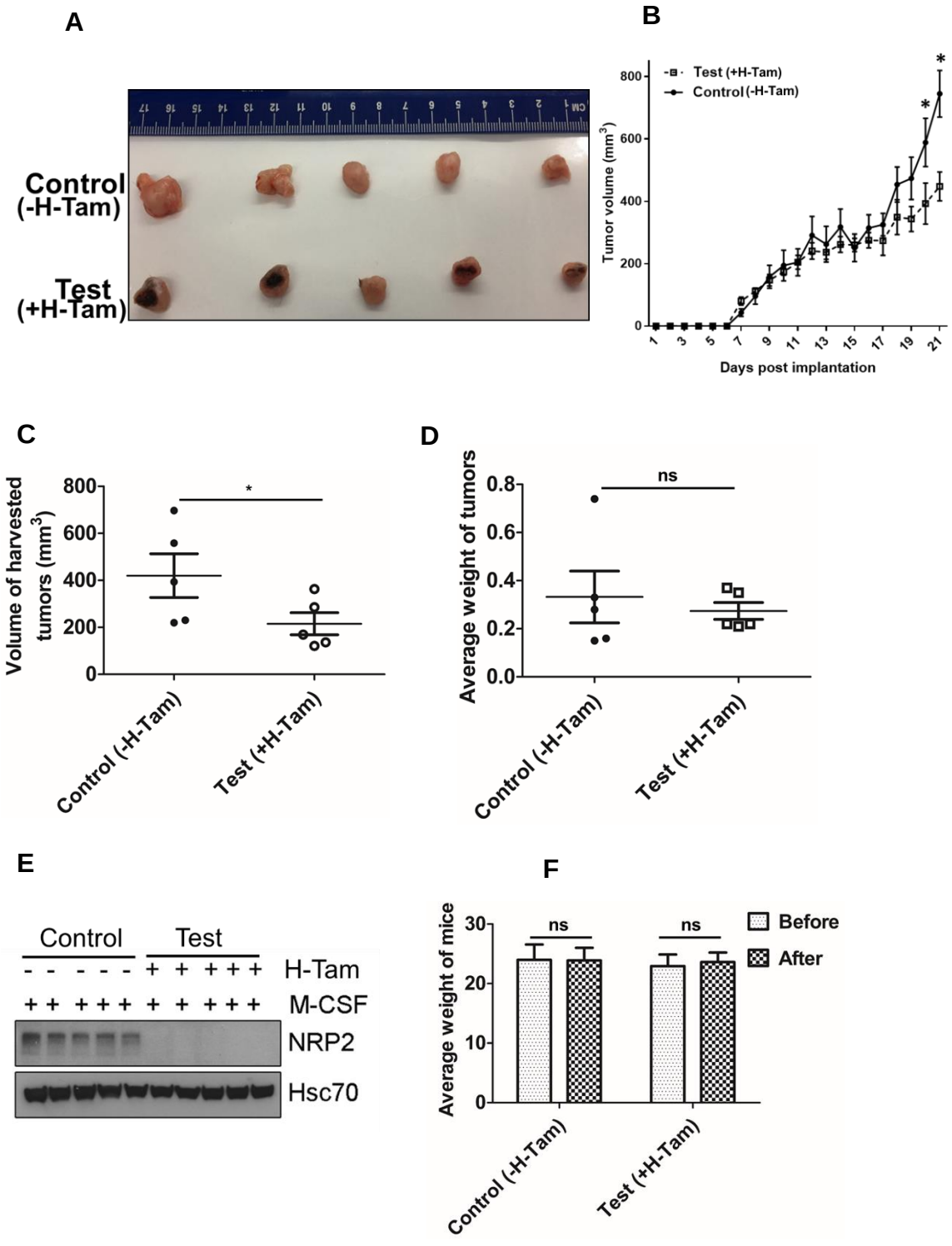
A
Control
(-H-Tam)
Test
(+H-Tam)
B
Test (+H-Tam)
Control (-H-Tam)
Tumor volume (mm3)
Days post implantation
C
Volume of harvested tumors (mm3)
Control (-H-Tam)
Test (+H-Tam)
D
Average weight of tumors
ns
Control (-H-Tam)
Test (+H-Tam)
E
Control
Test
H-Tam
M-CSF
NRP2
Hsc70
F
Average weight of mice
ns
ns
Before
After
Control (-H-Tam)
Test (+H-Tam)

Fig. 4.9 Depletion of NRP2 in macrophages increases the necrotic area in tumors. (A) Representative image H&E images from control and test tumors showing increase in necrotic area following NRP2 depletion in macrophages. (B) Necrotic areas were marked using Image J software and the areas calculated. Result represented as box plot. Values are mean ± SEM. * indicates p=0.05.

Fig. 4.9

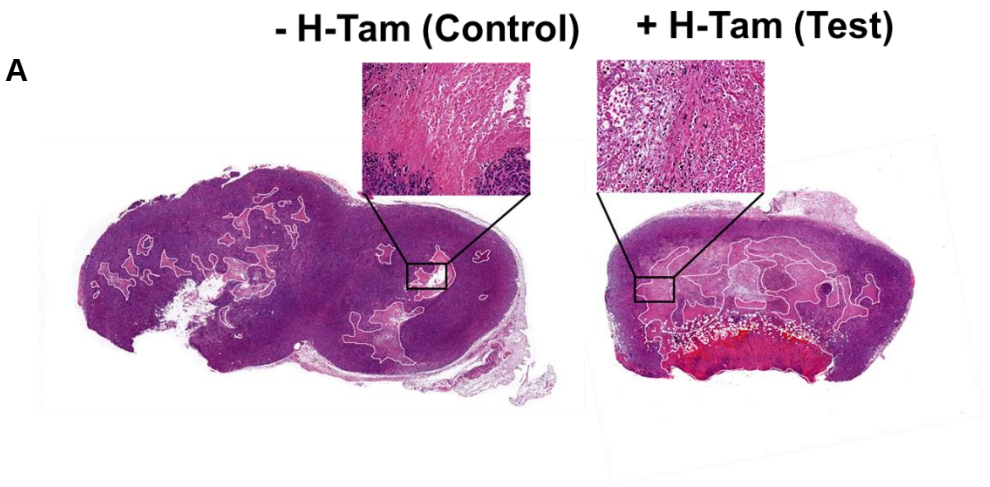
A
- H-Tam (Control)
+ H-Tam (Test)

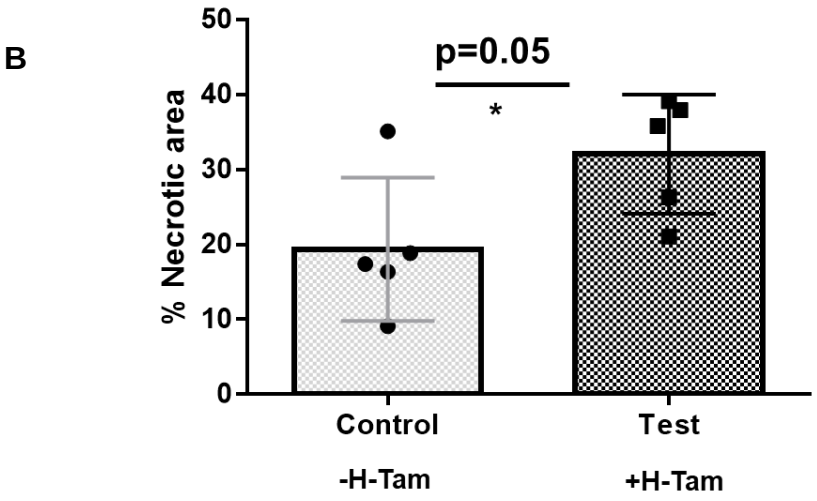
B
p=0.05
*
% Necrotic area
50
40
30
20
10
0
Control
-H-Tam
Test
+H-Tam

Fig. 4.10 Effect of macrophage NRP2 depletion on TAM recruitment, angiogenesis and CD8+ T cell infiltration. (A) representative confocal image of F4/80+ macrophages (red) infiltrating control (top) and test tumors (bottom). The first column shows only F4/80+ staining. The second column shows DAPI staining of the tissue. The third column represents merged picture for $F4/80^{+}$ cells in the tissue section. Images acquired at 20X magnification. Dapi was used for nuclear staining. Inset shows individual macrophage. (B) The number of $F4/80^{+}$ macrophages per field were counted for 10 random fields using Image J software and represented as a box plot. (C) Representative images of immunohistochemistry showing $CD8^{+}$ T cell infiltration (brown) in control and test tumors. Image scale, 20X magnification. (D) Number of CD8+ T cells per field was counted using Image J software, for 10 random fields and represented as a vertical scatter plot. (E) Representative immunohistochemistry image showing $CD31^{+}$ vessels in control and test tumor. Image scale, 20X magnification. (F) Number of $CD31^{+}$ vessels per field was counted (vessel density) using Image J software, for 10 random fields and represented as a vertical scatter plot. All values are mean± SEM. Student *t* test was used for comparison between control and test. $*P < .05$; $**P < .005$; $***P < .0005$. ns=non-significant.

Fig. 4.10

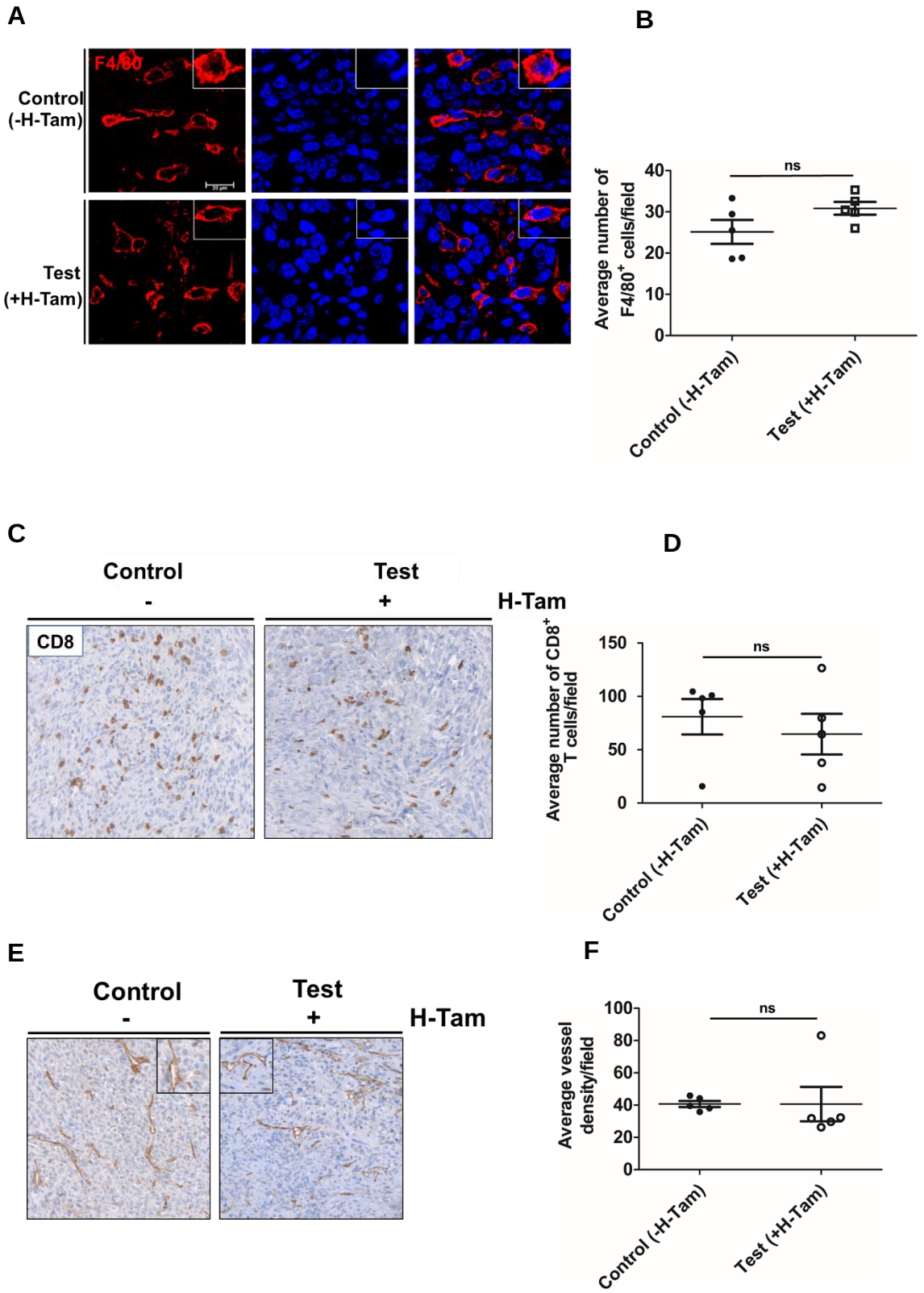
A
F4/80
Control
(-H-Tam)
Test
(+H-Tam)
B
Average number of F4/80+ cells/field
ns
40
30
20
10
0
Control (-H-Tam)
Test (+H-Tam)
C
Control
-
Test
+
H-Tam
CD8
D
Average number of CD8+ T cells/field
ns
150
100
50
0
Control (-H-Tam)
Test (+H-Tam)
E
Control
-
Test
+
H-Tam
F
Average vessel density/field
ns
100
80
60
40
20
0
Control (-H-Tam)
Test (+H-Tam)

Fig. 4.11 NRP2 in macrophages regulates tumor growth. 500,000 UNKC-6141 cells were mixed with Matrigel and subcutaneously implanted into the right flank of $NRP2^{fl/fl}$CSF1R-iCre mice. Once the tumors became palpable, animals were randomly divided into control and test groups (n=5). The test animals received daily intraperitoneal injection of Tamoxifen (20mg/kg body weight) to knock out NRP2 from the macrophages. Tumor progression was monitored for 25days. (A) Representative image of the harvested tumors from the control and Tamoxifen treated mice, showing moderate decrease in the test group tumors following NRP2 depletion in macrophages. (B) Tumor growth was monitored regularly for the indicated time period and represented as a line graph. * indicates p=0.05. (C) Scatter plot comparing the volume of the control and test tumors after they were harvested. (D) Graphical representation of weight of harvested tumors. (E) TUNEL staining showing increased number of apoptotic or necrotic cells in tumors following NRP2 depletion in myeloid cells. (F) Graphical representation of increased number of apoptotic or necrotic cells in tumors deficient in NRP2 in myeloid cells. (G) Western Blot showing NRP2 was completely deleted from macrophages following Tamoxifen administration. (H) graph showing NRP2 was knocked out from intratumoral TAMs following Tamoxifen administration.

Fig. 4.11

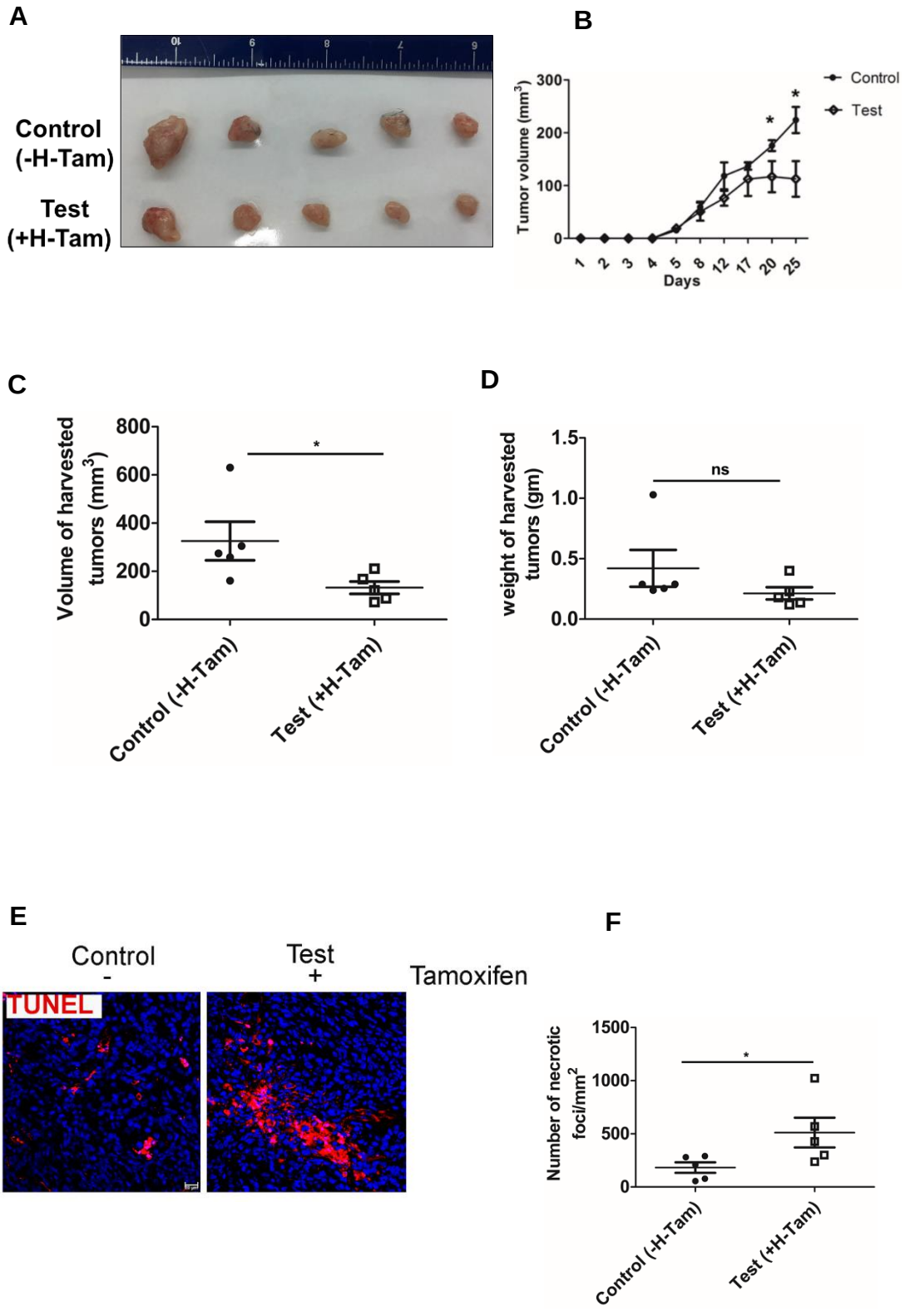
A
Control
(-H-Tam)
Test
(+H-Tam)
B
Tumor volume (mm3)
300
200
100
0
1
2
3
4
5
8
12
17
20
25
Days
Control
Test
*
*
C
Volume of harvested tumors (mm3)
800
600
400
200
0
*
Control (-H-Tam)
Test (+H-Tam)
D
weight of harvested tumors (gm)
1.5
1.0
0.5
0.0
ns
Control (-H-Tam)
Test (+H-Tam)
E
Control
-
Test
+
Tamoxifen
TUNEL
F
Number of necrotic foci/mm2
1500
1000
500
0
*
Control (-H-Tam)
Test (+H-Tam)

G

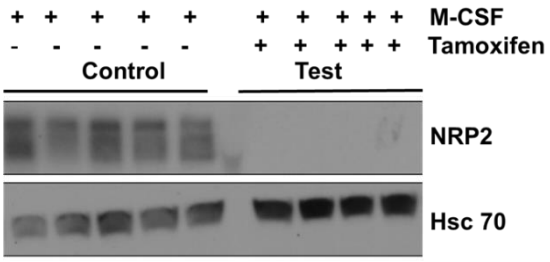
+ + + + + + + + + + M-CSF
- - - - - + + + + + Tamoxifen
Control
Test
NRP2
Hsc 70

H

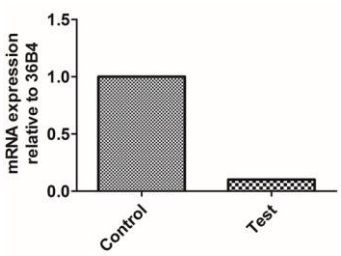
mRNA expression relative to 36B4
1.5
1.0
0.5
0.0
Control
Test

Fig. 4.12. Effect of NRP2 depletion in macrophages on TAM recruitment, angiogenesis and α-SMA. (A) Representative confocal microscopy image showing NRP2 does not have any role in the migration of macrophages (F4/80+, red) to the tumor. The first column shows only F4/80 staining in red, in control (upper) and test (bottom) tissue. The second column represents only DAPI staining for nucleus in control (upper) and test (bottom) tissue. The third column shows merged images with F4/80 and DAPI staining, for both control (upper) and test (bottom) tumors. Scale bar, 20µm. Inset shows magnified image of a single F4/80+ macrophage. (B) the number of F4/80+ cells per field (for 10 random field, 20X magnification) were counted using Image J software and represented graphically in a scatter plot. (C) Representative immunohistochemistry image showing CD31+ vessels in the control and test tumors. (D) The number of CD31+ vessels per field were counted (20X magnification, 10 random fields) using Image J software and represented as average vessel density in a vertical scatter plot. (E) Representative image showing α-SMA in control and test tumors. (F) Graphical representation of the result. All values are represented as mean± SEM. Student t test was used to compare between the control and test tumors. ns= not significant.

Fig. 4.12

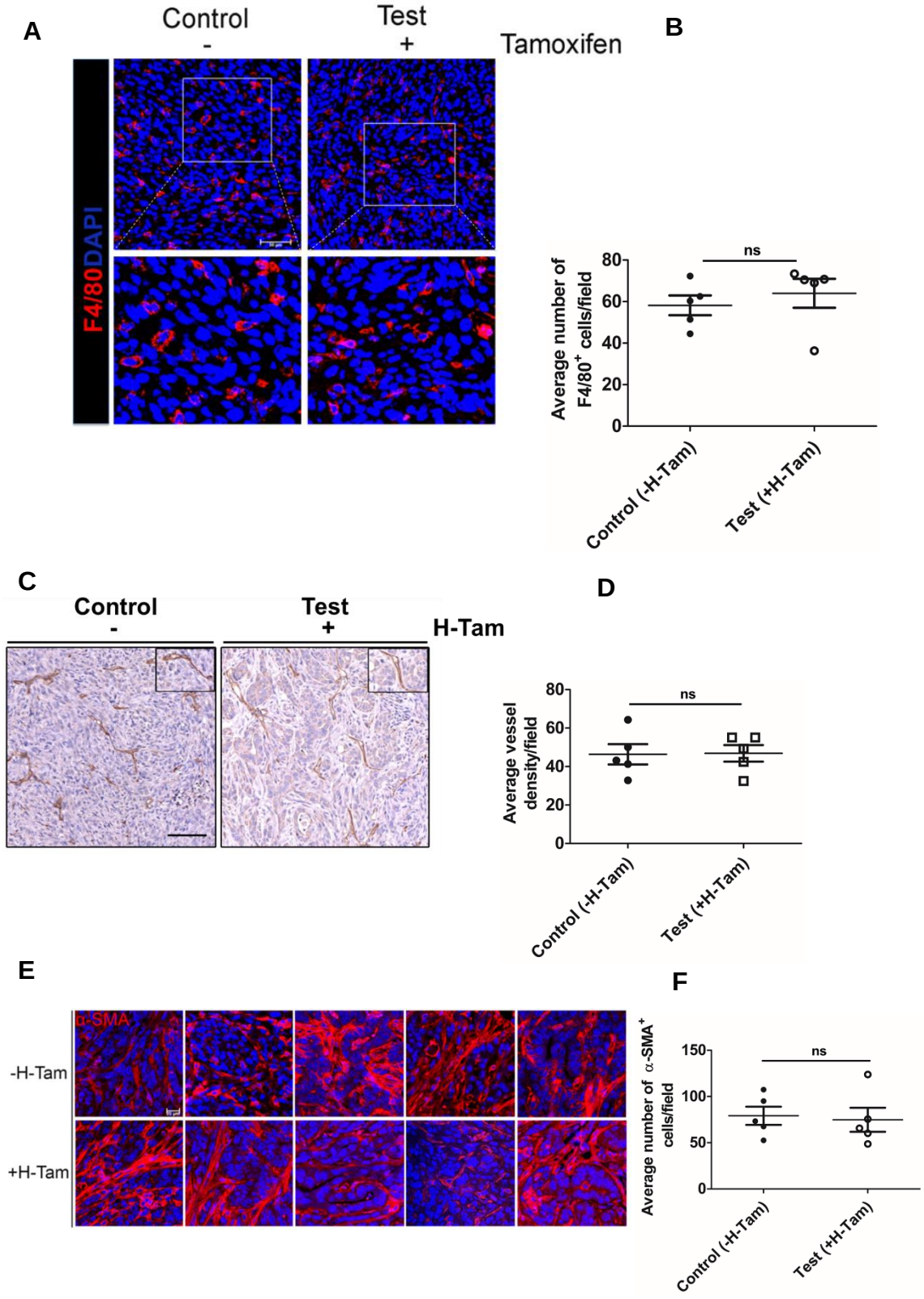
A
Control
-
Test
+
Tamoxifen
F4/80 DAPI
B
Average number of F4/80+ cells/field
ns
Control (-H-Tam)
Test (+H-Tam)
C
Control
-
Test
+
H-Tam
D
Average vessel density/field
ns
Control (-H-Tam)
Test (+H-Tam)
E
α-SMA
-H-Tam
+H-Tam
F
Average number of α-SMA+ cells/field
ns
Control (-H-Tam)
Test (+H-Tam)

Fig. 4.13 NRP2 depletion in macrophages affects T cell response in tumor. (A) Representative images of immunohistochemistry showing significantly higher CD8+ T cell infiltration in test tumors in comparison to control tumor. Image scale, 20X magnification. (B) Number of CD8+ T cells per field was counted using Image J software, for 10 random fields and represented as a vertical scatter plot. (C) Representative image showing Granzyme B positive cells in tumor. (D) Graphical representation of relative numbers of Granzyme positive cells per field in control and test tumors. (E) Representative confocal microscopy image for CD4+ T cell infiltration (red) in the control and test tumors. Scale bar 20µm. Inset shows magnified image of individual CD4+ T cell. Dapi was used to stain the nucleus. (F) Number of CD4+ T cells per field was counted using Image J software and represented in a scatter plot. All values are mean± SEM. Student *t* test was used for comparison between control and test. **P* < .05; ***P* < .005; ****P* < .0005. ns=non-significant.

Fig. 4.13

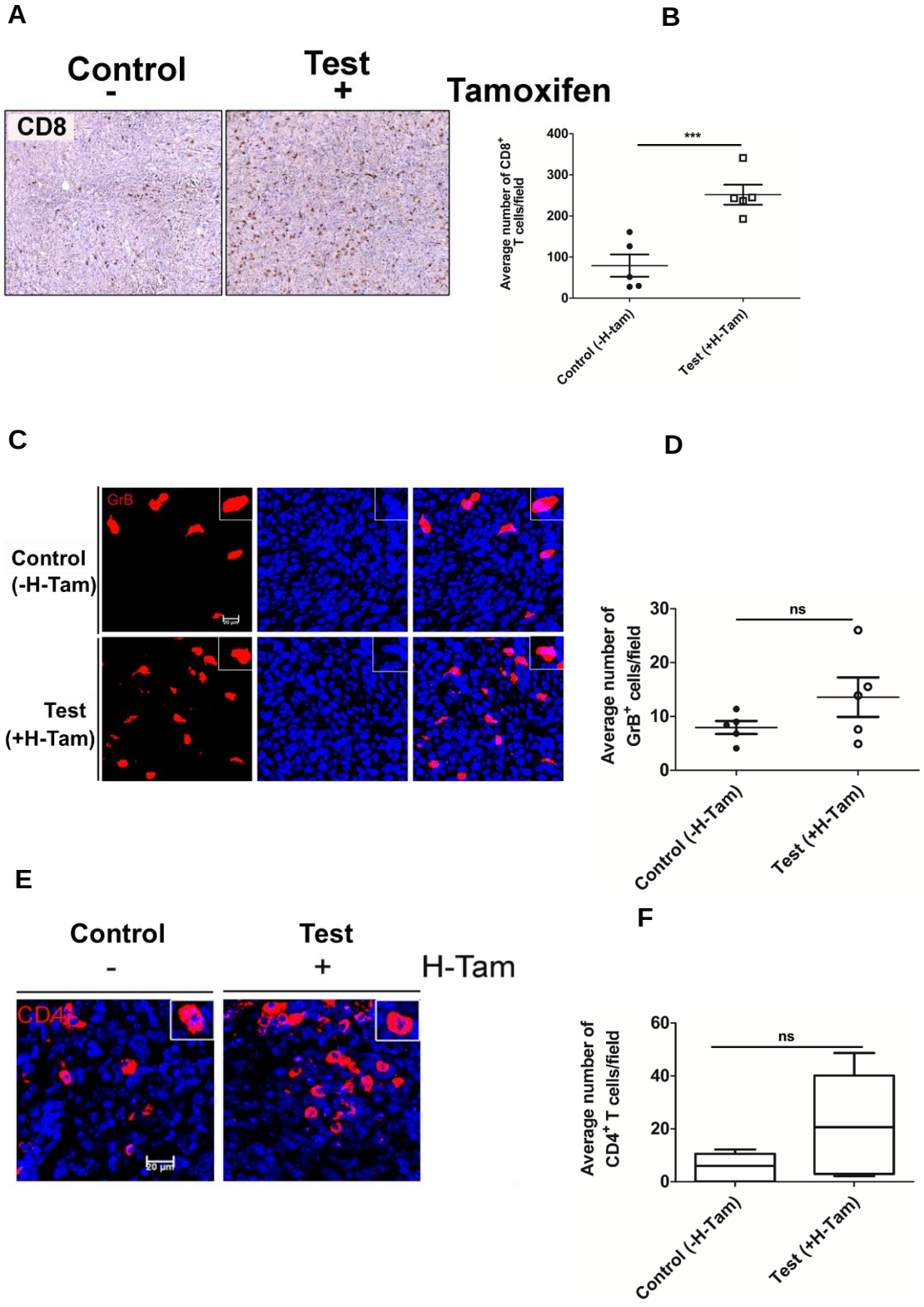
A
Control
-
Test
+
Tamoxifen
CD8
B
Average number of CD8+ T cells/field
400
300
200
100
0
***
Control (-H-tam)
Test (+H-Tam)
C
GrB
Control (-H-Tam)
Test (+H-Tam)
D
Average number of GrB+ cells/field
30
20
10
0
ns
Control (-H-Tam)
Test (+H-Tam)
E
Control
-
Test
+
H-Tam
CD4
20 µm
F
Average number of CD4+ T cells/field
60
40
20
0
ns
Control (-H-Tam)
Test (+H-Tam)

Fig. 4.14 Transcriptome analysis from CD11b+ cells by RNA-Sequencing analysis. (A) Schematic diagram showing the experimental design for the study. (B) Graphical representation of the volume of the harvested tumors. (C) Graphical representation of weight of excised tumors. (D) Pie chart showing number of genes (upregulated and downregulated) whose expression altered by atleast log_2 fold change 1 following NRP2 depletion in macrophages.

Fig. 4.14

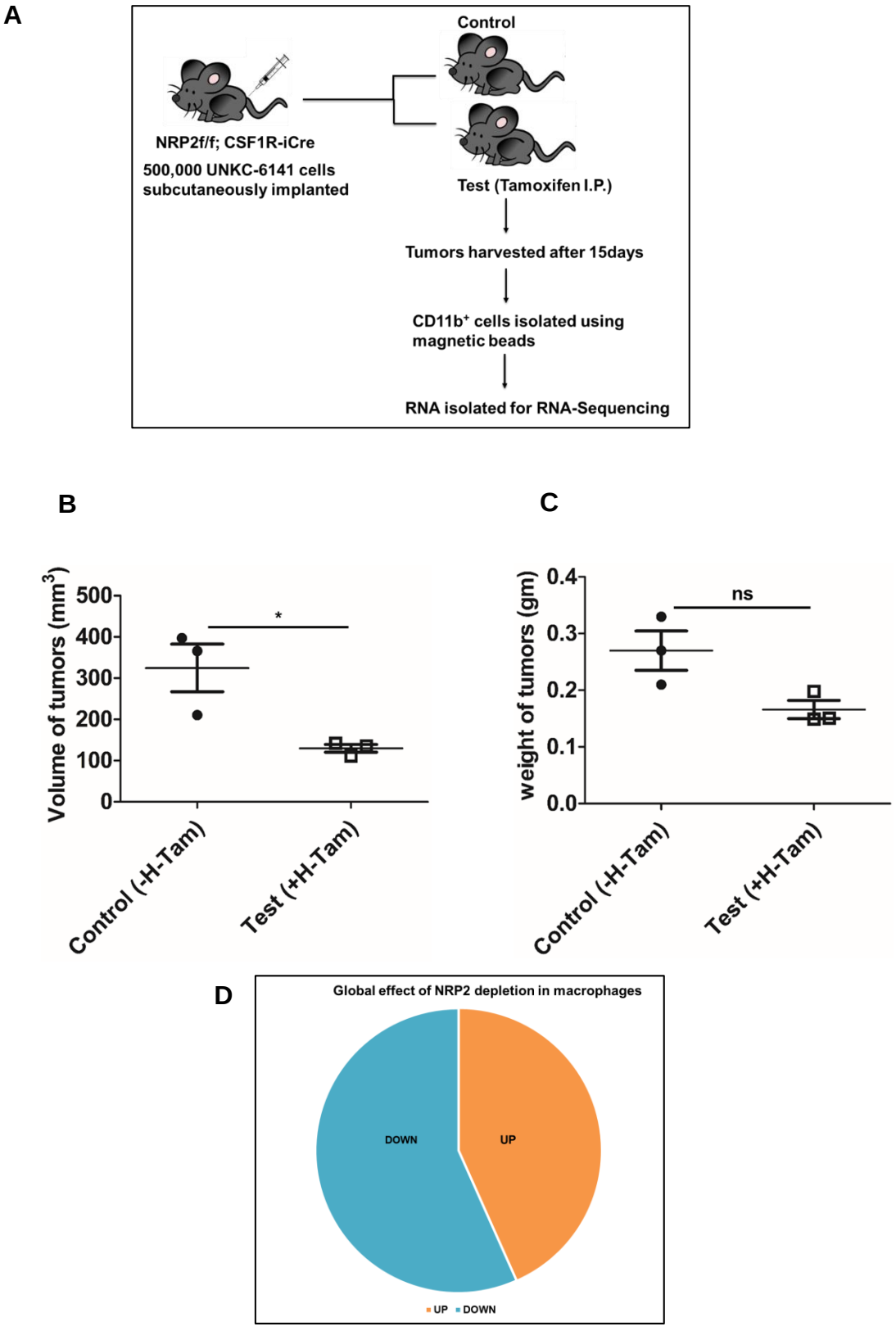
A
Control
NRP2f/f; CSF1R-iCre
500,000 UNKC-6141 cells
subcutaneously implanted
Test (Tamoxifen I.P.)
Tumors harvested after 15days
CD11b+ cells isolated using
magnetic beads
RNA isolated for RNA-Sequencing
B
Volume of tumors (mm3)
500
400
300
200
100
0
*
Control (-H-Tam)
Test (+H-Tam)
C
weight of tumors (gm)
0.4
0.3
0.2
0.1
0.0
ns
Control (-H-Tam)
Test (+H-Tam)
D
Global effect of NRP2 depletion in macrophages
DOWN
UP
UP
DOWN

Fig. 4.15 Analysis of differentially expressed genes using Ingenuity Pathway Analysis and DAVID functional annotation bioinformatics microarray analysis. (A) Representative canonical pathways enriched in IPA analysis. (B) Functional annotation clusters for the differentially expressed genes from DAVID database. (C) Representative functional annotation clusters related to immune response phagocytosis from DAVID database analyses.

A

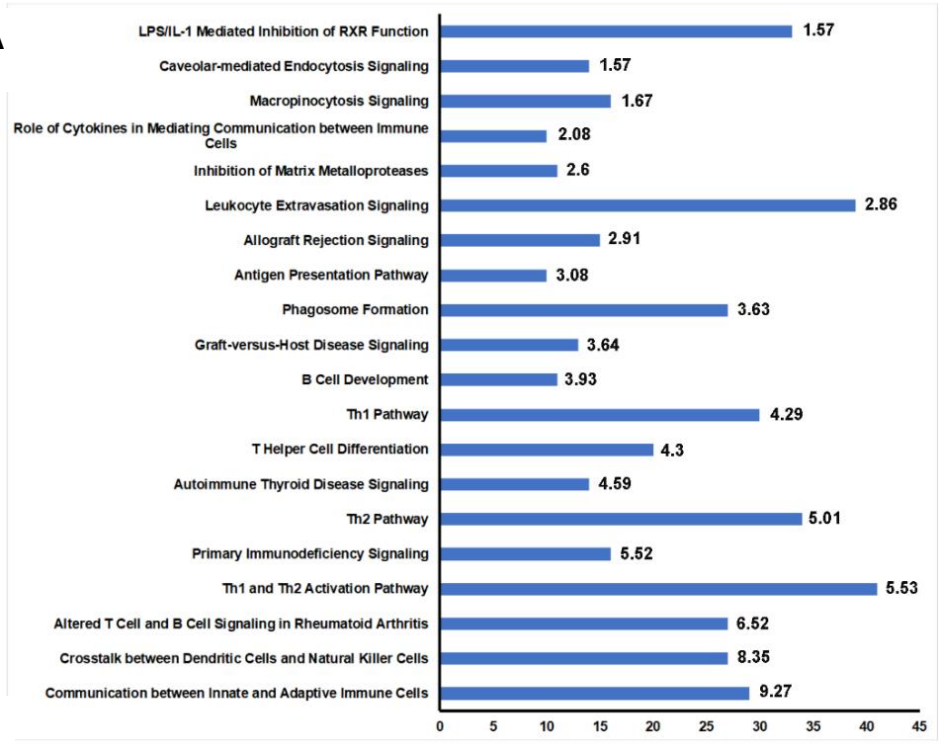
LPS/IL-1 Mediated Inhibition of RXR Function 1.57
Caveolar-mediated Endocytosis Signaling 1.57
Macropinocytosis Signaling 1.67
Role of Cytokines in Mediating Communication between Immune Cells 2.08
Inhibition of Matrix Metalloproteases 2.6
Leukocyte Extravasation Signaling 2.86
Allograft Rejection Signaling 2.91
Antigen Presentation Pathway 3.08
Phagosome Formation 3.63
Graft-versus-Host Disease Signaling 3.64
B Cell Development 3.93
Th1 Pathway 4.29
T Helper Cell Differentiation 4.3
Autoimmune Thyroid Disease Signaling 4.59
Th2 Pathway 5.01
Primary Immunodeficiency Signaling 5.52
Th1 and Th2 Activation Pathway 5.53
Altered T Cell and B Cell Signaling in Rheumatoid Arthritis 6.52
Crosstalk between Dendritic Cells and Natural Killer Cells 8.35
Communication between Innate and Adaptive Immune Cells 9.27
0 5 10 15 20 25 30 35 40 45

B

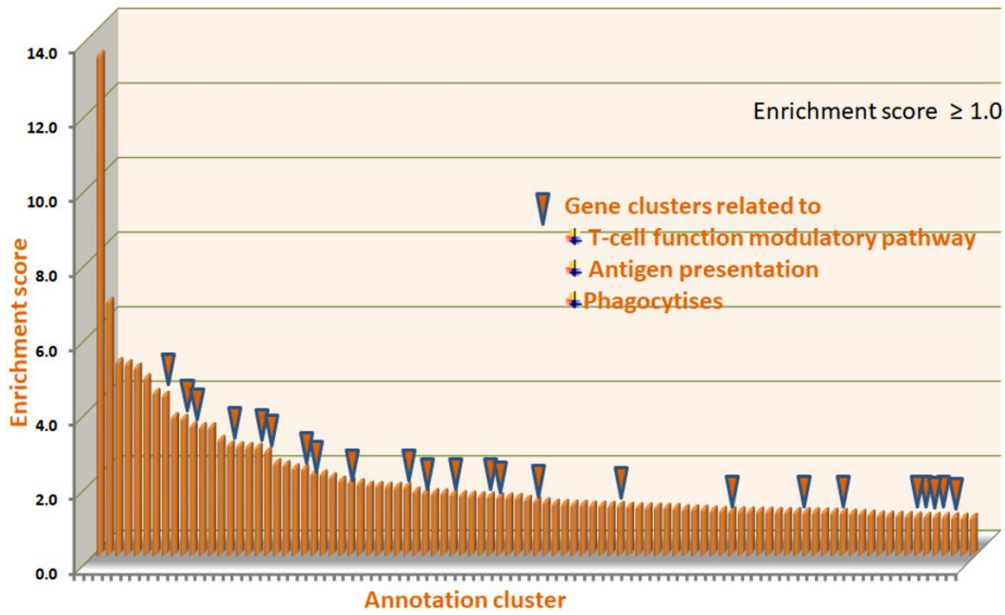
Enrichment score ≥ 1.0
Gene clusters related to
T-cell function modulatory pathway
Antigen presentation
Phagocytises
Enrichment score
14.0
12.0
10.0
8.0
6.0
4.0
2.0
0.0
Annotation cluster

C

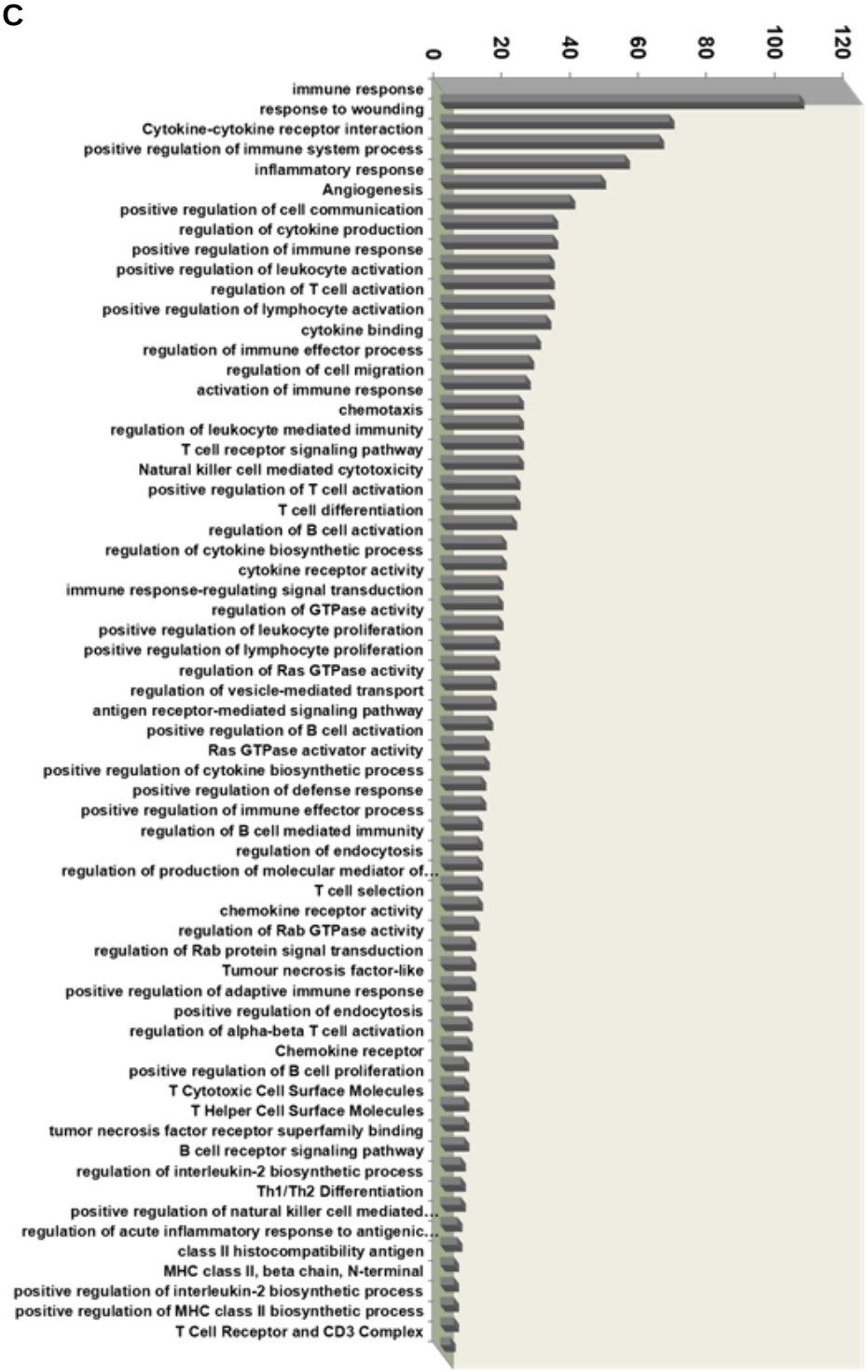
0
20
40
60
80
100
120
immune response
response to wounding
Cytokine-cytokine receptor interaction
positive regulation of immune system process
inflammatory response
Angiogenesis
positive regulation of cell communication
regulation of cytokine production
positive regulation of immune response
positive regulation of leukocyte activation
regulation of T cell activation
positive regulation of lymphocyte activation
cytokine binding
regulation of immune effector process
regulation of cell migration
activation of immune response
chemotaxis
regulation of leukocyte mediated immunity
T cell receptor signaling pathway
Natural killer cell mediated cytotoxicity
positive regulation of T cell activation
T cell differentiation
regulation of B cell activation
regulation of cytokine biosynthetic process
cytokine receptor activity
immune response-regulating signal transduction
regulation of GTPase activity
positive regulation of leukocyte proliferation
positive regulation of lymphocyte proliferation
regulation of Ras GTPase activity
regulation of vesicle-mediated transport
antigen receptor-mediated signaling pathway
positive regulation of B cell activation
Ras GTPase activator activity
positive regulation of cytokine biosynthetic process
positive regulation of defense response
positive regulation of immune effector process
regulation of B cell mediated immunity
regulation of endocytosis
regulation of production of molecular mediator of...
T cell selection
chemokine receptor activity
regulation of Rab GTPase activity
regulation of Rab protein signal transduction
Tumour necrosis factor-like
positive regulation of adaptive immune response
positive regulation of endocytosis
regulation of alpha-beta T cell activation
Chemokine receptor
positive regulation of B cell proliferation
T Cytotoxic Cell Surface Molecules
T Helper Cell Surface Molecules
tumor necrosis factor receptor superfamily binding
B cell receptor signaling pathway
regulation of interleukin-2 biosynthetic process
Th1/Th2 Differentiation
positive regulation of natural killer cell mediated...
regulation of acute inflammatory response to antigenic...
class II histocompatibility antigen
MHC class II, beta chain, N-terminal
positive regulation of interleukin-2 biosynthetic process
positive regulation of MHC class II biosynthetic process
T Cell Receptor and CD3 Complex

Fig. 4.16. Representative genes for phagocytosis pathway (A) and immune response related functions (B) are shown. (C) Representative genes encoding wound healing and immunosuppressive molecules in macrophages, that were altered following NRP2 depletion.

A

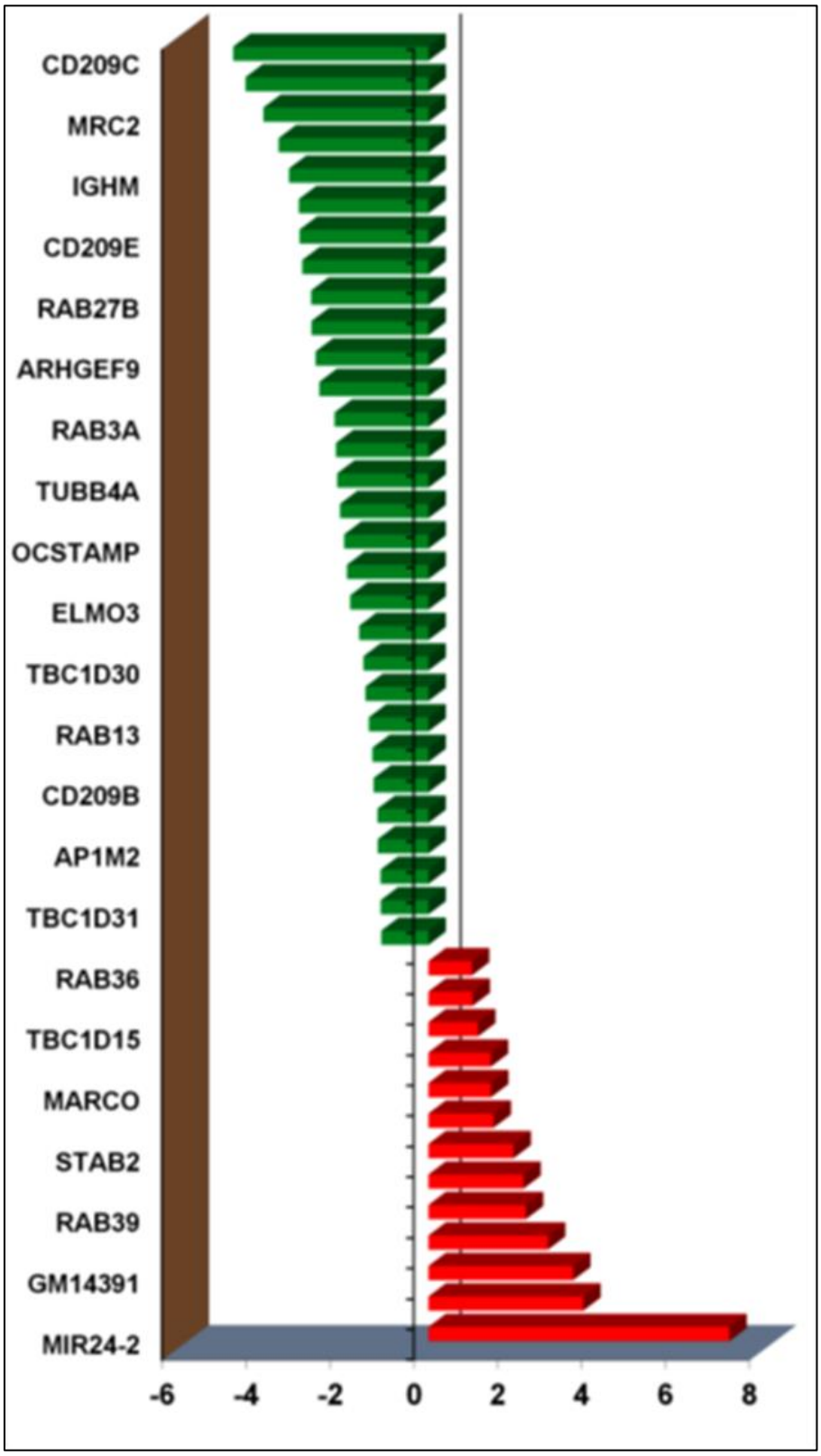
CD209C
MRC2
IGHM
CD209E
RAB27B
ARHGEF9
RAB3A
TUBB4A
OCSTAMP
ELMO3
TBC1D30
RAB13
CD209B
AP1M2
TBC1D31
RAB36
TBC1D15
MARCO
STAB2
RAB39
GM14391
MIR24-2
-6
-4
-2
0
2
4
6
8

B

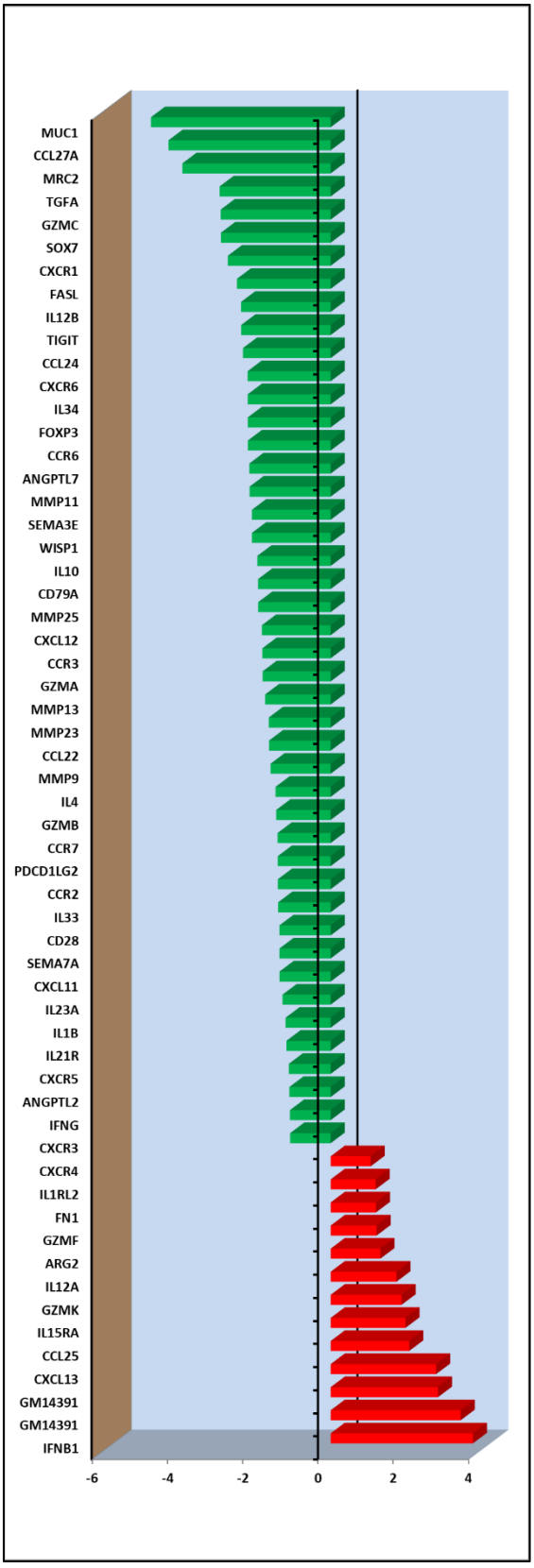
MUC1
CCL27A
MRC2
TGFA
GZMC
SOX7
CXCR1
FASL
IL12B
TIGIT
CCL24
CXCR6
IL34
FOXP3
CCR6
ANGPTL7
MMP11
SEMA3E
WISP1
IL10
CD79A
MMP25
CXCL12
CCR3
GZMA
MMP13
MMP23
CCL22
MMP9
IL4
GZMB
CCR7
PDCD1LG2
CCR2
IL33
CD28
SEMA7A
CXCL11
IL23A
IL1B
IL21R
CXCR5
ANGPTL2
IFNG
CXCR3
CXCR4
IL1RL2
FN1
GZMF
ARG2
IL12A
GZMK
IL15RA
CCL25
CXCL13
GM14391
GM14391
IFNB1
-6
-4
-2
0
2
4

C

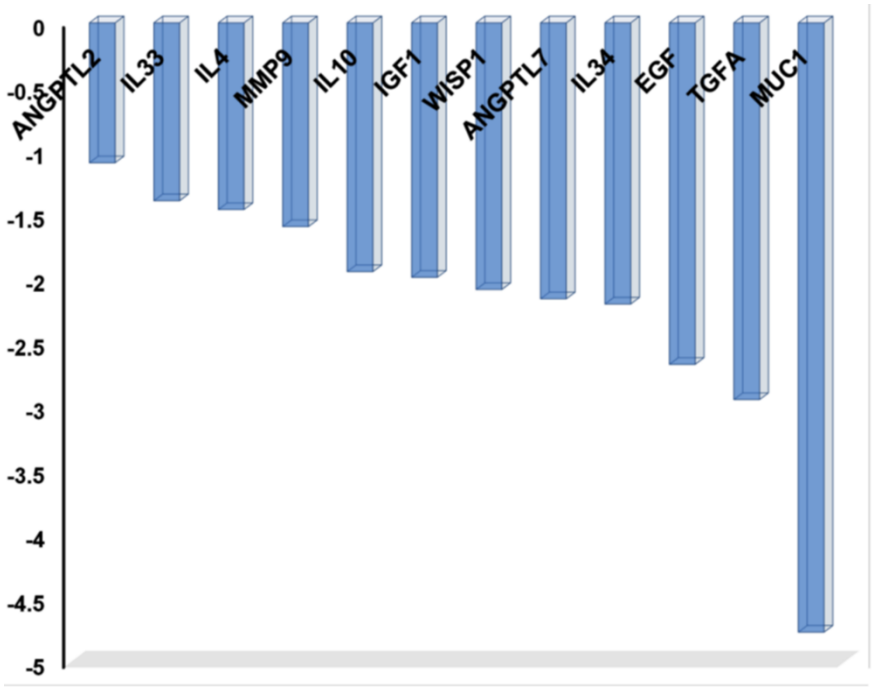
0
-0.5
-1
-1.5
-2
-2.5
-3
-3.5
-4
-4.5
-5
ANGPTL2
IL33
IL4
MMP9
IL10
IGF1
WISP1
ANGPTL7
IL34
EGF
TGFA
MUC1

Chapter V

Future Directions

5.1 Central theme of dissertation and approach

The central theme of the dissertation is to identify the role of NRP2 in macrophages and how it affects the pro-tumorigenic activities of TAMs in PC. Others and we have shown NRP2 is expressed in macrophages and TAMs. However, the exact function of NRP2 in macrophages and the signaling pathways it governs is still elusive. To clearly understand the effect of NRP2 in macrophages, we have used siRNA approach in human monocyte derived macrophages as well as genetically depleted NRP2 in inducible manner in mouse macrophages *in vitro* as well as *in vivo* studies. We also tested the effect of NRP2 depletion in TAMs in tumor progression, using a subcutaneous PC model, to identify the role of NRP2 in tumor progression and identify novel treatment modality for PC.

5.2 Current understanding

In summary, data presented in this dissertation indicate that the expression of NRP2 in macrophages is essential for phagocytosis. We show that NRP2 promotes the degradation and clearance of microbes (*E.coli*, zymosan) by promoting the maturation of early to late phagosomes. This was attributed to an increase in Rab5+ vesicles and a concomitant decrease in Rab7+ late endosomes/phagosomes in absence of NRP2. We further show that NRP2 is important for efferocytosis of apoptotic cells, a process although similar, but distinct from phagocytosis. The process of efficient cleaning up by macrophages is important for maintenance of physiological and immunological homeostasis,

however, it can also act as a double-edged sword in malignancies. Efferocytosis of dying tumor cells in the TME polarizes the macrophages towards an immunosuppressive phenotype and triggers non-inflammatory signaling cascades, such as, production of TGF-β, IL-10. This helps maintain an overall immunosuppressed environment in the TME by silencing effective T cell response, and creates a niche for tumor survival, growth and metastasis. Most of the patients undergoing treatment for cancer, including PC, receive either CT or RT as conventional treatment modalities. Intriguingly, these treatments result in increased recruitment of TAMs and trigger a TAM-mediated misdirected tissue repair response and immunosuppression by increasing efferocytosis of apoptotic tumor cells by TAMs. Pharmacological blockade of efferocytosis has been shown to reduce tumor burden by activating inflammatory responses in macrophages and activating T cell responses. We observed a slower tumor growth following depletion of NRP2 in macrophages. We attribute this to delayed clearance of dying tumor cells in the TME and subsequent activation of tumoricidal CD8+T cells in absence of NRP2 in TAMs. Thus, this study led to the identification of NRP2 in TAMs as a potential therapeutic strategy for treatment of PC and other cancers in the future.

5.3 Future Directions

There are a few open ends to this study that warrant further investigation. The next step for this work would be to understand the following:

How NRP2 regulates phagosome maturation at the molecular level: We have previously shown that NRP2 regulates maturation of early to late phagosomes and

that in its absence there is an increase in the number of Rab5+ early endosomes/phagosomes and a concomitant decrease in the number of Rab7+ late endosomes/phagosomes. This indicated a defect in the switch from Rab5 to Rab5, a step that is essential for phagosomes (and endosome) maturation. Although details about phagosome maturation is currently limited, it is believed that first Dynamin is recruited to the phagosome membrane, which then interacts with Vps34 (a PI3 Kinase) and helps recruit Rab5 to the phagosome surface. Rab5, is activated by Gapex-5 (Rab5 GEF), and further promotes Vps34 activation. Vps34 then generates PtdIns(3)P on the phagosome surface where the vacuolar fusion protein complex, Mon1A-Ccz1, is recruited. This complex recruits Rab7 and act as its effector. Rab7 next interacts with homotypic fusion and vacuole protein sorting (HOPS) complex to facilitate phagoslysosome generation. Since our data suggest NRP2 regulates the switch from Rab5 to Rab7, we hypothesize that NRP2 regulate the steps downstream of Rab5 recruitment, such as activation of Rab5, Vps34 or membrane recruitment of the Mon1a-Ccz1 complex. Additionally, differentially expressed genes from our RNA-Sequencing analyses revealed several molecules involved in either phagosome maturation, endocytic recycling, exocytosis were affected following NRP2 depletion. These need to be investigated to understand how NRP2 mechanistically regulate phagosome maturation.

Does NRP2 activate LAP pathway for clearance of apoptotic cells: LC3 associated phagocytosis has recently been shown to be important for clearance of fungal particles as well as engulfed apoptotic cellular debris in macrophages. We have previously reported that NRP2 regulates autophagy in cancer cells. Whether NRP2

promotes clearance of dead cells through activation of LAP pathway needs further investigation.

Does delayed phagosome maturation or efferocytic clearance in absence of NRP2 promote cross presentation: Our results indicated that NRP2 promotes the maturation of phagosomes. In NRP2 depleted conditions, phagosome maturation is delayed which subsequently results in significantly delayed clearance of phagocytosed cargo (*E.coli*, zymosan, apoptotic cells). It is now well understood that delayed phagosome maturation helps preserve antigenic peptides against degradative enzymes in the phagolysosome and favors antigen loading to the MHC complexes and subsequent presentation to the T cells. This is of particular importance in case of solid tumors where following NRP2 depletion in macrophages, we observed a robust infiltration of cytotoxic CD8+ T cells. It is plausible that delayed phagosome maturation in NRP2 depleted TAMs augmented cross presentation of tumor cell derived antigens to the CD8+ T cells. This needs to be tested in more details in the future.

Effect of NRP2 on PDAC metastasis: Previous studies have shown efferocytosis increases the risk for metastasis in a model of post-partum breast cancer (ppBC) by 10-fold. Pharmacologically blocking efferocytosis significantly reduced the metastasis in ppBC as well as therapy induced metastasis in tumor bearing animals. Since our current findings suggest a role for NRP2 in efferocytosis, and also it can affect tumor growth, the next step for the study would be to identify the role of NRP2 in TAMs on metastasis in PDAC. One of the limitations of the subcutaneous tumor progression model used in the current study is that it does

not mimic the natural PDAC TME. Orthotopically implanted tumors closely resemble the natural pattern of human PDAC development and progression. To test if blocking NRP2 mediated efferocytosis affects distant metastasis, we will orthotopically implant GFP- expressing UNKC-6141 clone into CSF1R-iCre;NRP2$^{f/f}$ mice. UNKC-6141 cells have previously been shown to develop metastatic lesions in the liver, spleen, small intestines and mesenteric lymph nodes within 1 month of implantation. We have observed in our mouse model, that tumors are established within 6-7 days of implantation. Once the tumors are established, NRP2 will be genetically knocked out from macrophages by daily intraperitoneal injection of Tamoxifen (75mg/kg body weight). Tumors will be allowed to grow for 1 month and then excised; spleen, liver, intestine and lungs will be harvested for metastatic foci. Metastasis was assessed by monitored by *in vivo* optical imaging for *GFP* expression using a Xenogen-IVIS cooled CCD optical system.

It is important to note that blockade of efferocytosis may increase inflammation that may potentially augment tumor progression and metastasis. Therefore, it is extremely important to optimize at what stage of the tumor NRP2 may be targeted for therapeutic efficacy.

<u>Correlation between NRP2 expression in TAMs and PDAC stage:</u>

In the current study, we tested a small cohort of patients (obtained from UNMC Pancreatic Cancer Rapid Autopsy Program), who died of PDAC with no prior history of treatment. We observed a high infiltration of NRP2 expressing macrophages in almost all of the tissues. Treatment with either radiation, chemotherapy or any other adjuvant therapy is known to modify the tissue

architecture and results in recruitment of myeloid cells to orchestrate tissue repair in response to therapy induced damage. Further, following any type of therapy, apoptotic index in the TME is high and the freshly recruited macrophages efficiently remove the dead tumor cells. This process has been reported to give rise to further immune suppression in post-partum breast cancer. Based on our current data that NRP2 regulates efferocytosis by macrophages as well as TAMs, and that it can regulate T cell responses, it will be interesting to see if there is any correlation between NRP2 expression in macrophages or their relative numbers in the TME with different stage of PDAC, metastasis or overall survival post therapy.

References

1. Ginhoux F, Jung S. Monocytes and macrophages: developmental pathways and tissue homeostasis. Nat Rev Immunol. 2014;14(6):392-404. Epub 2014/05/24. doi: 10.1038/nri3671. PubMed PMID: 24854589.
2. Ziegler-Heitbrock L, Ancuta P, Crowe S, Dalod M, Grau V, Hart DN, Leenen PJ, Liu YJ, MacPherson G, Randolph GJ, Scherberich J, Schmitz J, Shortman K, Sozzani S, Strobl H, Zembala M, Austyn JM, Lutz MB. Nomenclature of monocytes and dendritic cells in blood. Blood. 2010;116(16):e74-80. Epub 2010/07/16. doi: 10.1182/blood-2010-02-258558. PubMed PMID: 20628149.
3. Cros J, Cagnard N, Woollard K, Patey N, Zhang SY, Senechal B, Puel A, Biswas SK, Moshous D, Picard C, Jais JP, D'Cruz D, Casanova JL, Trouillet C, Geissmann F. Human CD14dim monocytes patrol and sense nucleic acids and viruses via TLR7 and TLR8 receptors. Immunity. 2010;33(3):375-86. Epub 2010/09/14. doi: 10.1016/j.immuni.2010.08.012. PubMed PMID: 20832340; PMCID: PMC3063338.
4. Haniffa M, Shin A, Bigley V, McGovern N, Teo P, See P, Wasan PS, Wang XN, Malinarich F, Malleret B, Larbi A, Tan P, Zhao H, Poidinger M, Pagan S, Cookson S, Dickinson R, Dimmick I, Jarrett RF, Renia L, Tam J, Song C, Connolly J, Chan JK, Gehring A, Bertoletti A, Collin M, Ginhoux F. Human tissues contain CD141hi cross-presenting dendritic cells with functional homology to mouse CD103+ nonlymphoid dendritic cells. Immunity. 2012;37(1):60-73. Epub 2012/07/17. doi: 10.1016/j.immuni.2012.04.012. PubMed PMID: 22795876; PMCID: PMC3476529.
5. Ingersoll MA, Spanbroek R, Lottaz C, Gautier EL, Frankenberger M, Hoffmann R, Lang R, Haniffa M, Collin M, Tacke F, Habenicht AJ, Ziegler-Heitbrock L, Randolph GJ. Comparison of gene expression profiles between human and mouse monocyte subsets. Blood. 2010;115(3):e10-9. Epub 2009/12/08. doi: 10.1182/blood-2009-07-235028. PubMed PMID: 19965649; PMCID: PMC2810986.
6. Shi C, Pamer EG. Monocyte recruitment during infection and inflammation. Nat Rev Immunol. 2011;11(11):762-74. Epub 2011/10/11. doi: 10.1038/nri3070. PubMed PMID: 21984070; PMCID: PMC3947780.
7. Auffray C, Fogg D, Garfa M, Elain G, Join-Lambert O, Kayal S, Sarnacki S, Cumano A, Lauvau G, Geissmann F. Monitoring of blood vessels and tissues by a population of monocytes with patrolling behavior. Science. 2007;317(5838):666-70. Epub 2007/08/04. doi: 10.1126/science.1142883. PubMed PMID: 17673663.
8. De Kleer I, Willems F, Lambrecht B, Goriely S. Ontogeny of myeloid cells. Front Immunol. 2014;5:423. Epub 2014/09/19. doi: 10.3389/fimmu.2014.00423. PubMed PMID: 25232355; PMCID: PMC4153297.
9. Krausgruber T, Blazek K, Smallie T, Alzabin S, Lockstone H, Sahgal N, Hussell T, Feldmann M, Udalova IA. IRF5 promotes inflammatory macrophage polarization and TH1-TH17 responses. Nat Immunol. 2011;12(3):231-8. Epub 2011/01/18. doi: 10.1038/ni.1990. PubMed PMID: 21240265.
10. Hu X, Ivashkiv LB. Cross-regulation of signaling pathways by interferon-gamma: implications for immune responses and autoimmune diseases. Immunity. 2009;31(4):539-50.

Epub 2009/10/17. doi: 10.1016/j.immuni.2009.09.002. PubMed PMID: 19833085; PMCID: PMC2774226.
11. Edwards JP, Zhang X, Frauwirth KA, Mosser DM. Biochemical and functional characterization of three activated macrophage populations. J Leukoc Biol. 2006;80(6):1298-307. Epub 2006/08/15. doi: 10.1189/jlb.0406249. PubMed PMID: 16905575; PMCID: PMC2642590.
12. Anderson CF, Mosser DM. A novel phenotype for an activated macrophage: the type 2 activated macrophage. J Leukoc Biol. 2002;72(1):101-6. Epub 2002/07/09. PubMed PMID: 12101268.
13. Ehrchen J, Steinmuller L, Barczyk K, Tenbrock K, Nacken W, Eisenacher M, Nordhues U, Sorg C, Sunderkotter C, Roth J. Glucocorticoids induce differentiation of a specifically activated, anti-inflammatory subtype of human monocytes. Blood. 2007;109(3):1265-74. Epub 2006/10/05. doi: 10.1182/blood-2006-02-001115. PubMed PMID: 17018861.
14. Park-Min KH, Antoniv TT, Ivashkiv LB. Regulation of macrophage phenotype by long-term exposure to IL-10. Immunobiology. 2005;210(2-4):77-86. Epub 2005/09/17. doi: 10.1016/j.imbio.2005.05.002. PubMed PMID: 16164014.
15. Wynn TA, Chawla A, Pollard JW. Macrophage biology in development, homeostasis and disease. Nature. 2013;496(7446):445-55. Epub 2013/04/27. doi: 10.1038/nature12034. PubMed PMID: 23619691; PMCID: PMC3725458.
16. Kawane K, Fukuyama H, Kondoh G, Takeda J, Ohsawa Y, Uchiyama Y, Nagata S. Requirement of DNase II for definitive erythropoiesis in the mouse fetal liver. Science. 2001;292(5521):1546-9. Epub 2001/05/26. doi: 10.1126/science.292.5521.1546. PubMed PMID: 11375492.
17. Jaiswal S, Jamieson CH, Pang WW, Park CY, Chao MP, Majeti R, Traver D, van Rooijen N, Weissman IL. CD47 is upregulated on circulating hematopoietic stem cells and leukemia cells to avoid phagocytosis. Cell. 2009;138(2):271-85. Epub 2009/07/28. doi: 10.1016/j.cell.2009.05.046. PubMed PMID: 19632178; PMCID: PMC2775564.
18. Gordy C, Pua H, Sempowski GD, He YW. Regulation of steady-state neutrophil homeostasis by macrophages. Blood. 2011;117(2):618-29. Epub 2010/10/29. doi: 10.1182/blood-2010-01-265959. PubMed PMID: 20980680; PMCID: PMC3031484.
19. Odegaard JI, Chawla A. Pleiotropic actions of insulin resistance and inflammation in metabolic homeostasis. Science. 2013;339(6116):172-7. Epub 2013/01/12. doi: 10.1126/science.1230721. PubMed PMID: 23307735; PMCID: PMC3725457.
20. Lumeng CN, Bodzin JL, Saltiel AR. Obesity induces a phenotypic switch in adipose tissue macrophage polarization. J Clin Invest. 2007;117(1):175-84. Epub 2007/01/04. doi: 10.1172/JCI29881. PubMed PMID: 17200717; PMCID: PMC1716210.
21. Weisberg SP, McCann D, Desai M, Rosenbaum M, Leibel RL, Ferrante AW, Jr. Obesity is associated with macrophage accumulation in adipose tissue. J Clin Invest. 2003;112(12):1796-808. Epub 2003/12/18. doi: 10.1172/JCI19246. PubMed PMID: 14679176; PMCID: PMC296995.
22. Xu H, Barnes GT, Yang Q, Tan G, Yang D, Chou CJ, Sole J, Nichols A, Ross JS, Tartaglia LA, Chen H. Chronic inflammation in fat plays a crucial role in the development of obesity-related insulin resistance. J Clin Invest. 2003;112(12):1821-30. Epub 2003/12/18. doi: 10.1172/JCI19451. PubMed PMID: 14679177; PMCID: PMC296998.
23. Weisberg SP, Hunter D, Huber R, Lemieux J, Slaymaker S, Vaddi K, Charo I, Leibel RL, Ferrante AW, Jr. CCR2 modulates inflammatory and metabolic effects of high-fat feeding. J Clin Invest. 2006;116(1):115-24. Epub 2005/12/13. doi: 10.1172/JCI24335. PubMed PMID: 16341265; PMCID: PMC1307559.
24. Eguchi K, Manabe I, Oishi-Tanaka Y, Ohsugi M, Kono N, Ogata F, Yagi N, Ohto U, Kimoto M, Miyake K, Tobe K, Arai H, Kadowaki T, Nagai R. Saturated fatty acid and TLR signaling link beta

cell dysfunction and islet inflammation. Cell Metab. 2012;15(4):518-33. Epub 2012/04/03. doi: 10.1016/j.cmet.2012.01.023. PubMed PMID: 22465073.
25. Ehses JA, Perren A, Eppler E, Ribaux P, Pospisilik JA, Maor-Cahn R, Gueripel X, Ellingsgaard H, Schneider MK, Biollaz G, Fontana A, Reinecke M, Homo-Delarche F, Donath MY. Increased number of islet-associated macrophages in type 2 diabetes. Diabetes. 2007;56(9):2356-70. Epub 2007/06/21. doi: 10.2337/db06-1650. PubMed PMID: 17579207.
26. Gordon S, Martinez-Pomares L. Physiological roles of macrophages. Pflugers Arch. 2017;469(3-4):365-74. Epub 2017/02/12. doi: 10.1007/s00424-017-1945-7. PubMed PMID: 28185068; PMCID: PMC5362657.
27. Rossignol M, Gagnon ML, Klagsbrun M. Genomic organization of human neuropilin-1 and neuropilin-2 genes: identification and distribution of splice variants and soluble isoforms. Genomics. 2000;70(2):211-22. Epub 2000/12/09. doi: 10.1006/geno.2000.6381. PubMed PMID: 11112349.
28. Gagnon ML, Bielenberg DR, Gechtman Z, Miao HQ, Takashima S, Soker S, Klagsbrun M. Identification of a natural soluble neuropilin-1 that binds vascular endothelial growth factor: In vivo expression and antitumor activity. Proc Natl Acad Sci U S A. 2000;97(6):2573-8. Epub 2000/02/26. doi: 10.1073/pnas.040337597. PubMed PMID: 10688880; PMCID: PMC15970.
29. Cackowski FC, Xu L, Hu B, Cheng SY. Identification of two novel alternatively spliced Neuropilin-1 isoforms. Genomics. 2004;84(1):82-94. Epub 2004/06/19. doi: 10.1016/j.ygeno.2004.02.001. PubMed PMID: 15203206; PMCID: PMC2868064.
30. Hendricks C, Dubail J, Brohee L, Delforge Y, Colige A, Deroanne C. A Novel Physiological Glycosaminoglycan-Deficient Splice Variant of Neuropilin-1 Is Anti-Tumorigenic In Vitro and In Vivo. PLoS One. 2016;11(10):e0165153. Epub 2016/11/01. doi: 10.1371/journal.pone.0165153. PubMed PMID: 27798666; PMCID: PMC5087894.
31. Gemmill RM, Nasarre P, Nair-Menon J, Cappuzzo F, Landi L, D'Incecco A, Uramoto H, Yoshida T, Haura EB, Armeson K, Drabkin HA. The neuropilin 2 isoform NRP2b uniquely supports TGFbeta-mediated progression in lung cancer. Sci Signal. 2017;10(462). Epub 2017/01/18. doi: 10.1126/scisignal.aag0528. PubMed PMID: 28096505.
32. Parker MW, Linkugel AD, Goel HL, Wu T, Mercurio AM, Vander Kooi CW. Structural basis for VEGF-C binding to neuropilin-2 and sequestration by a soluble splice form. Structure. 2015;23(4):677-87. Epub 2015/03/11. doi: 10.1016/j.str.2015.01.018. PubMed PMID: 25752543; PMCID: PMC4394031.
33. Shintani Y, Takashima S, Asano Y, Kato H, Liao Y, Yamazaki S, Tsukamoto O, Seguchi O, Yamamoto H, Fukushima T, Sugahara K, Kitakaze M, Hori M. Glycosaminoglycan modification of neuropilin-1 modulates VEGFR2 signaling. EMBO J. 2006;25(13):3045-55. Epub 2006/06/10. doi: 10.1038/sj.emboj.7601188. PubMed PMID: 16763549; PMCID: PMC1500974.
34. Frankel P, Pellet-Many C, Lehtolainen P, D'Abaco GM, Tickner ML, Cheng L, Zachary IC. Chondroitin sulphate-modified neuropilin 1 is expressed in human tumour cells and modulates 3D invasion in the U87MG human glioblastoma cell line through a p130Cas-mediated pathway. EMBO Rep. 2008;9(10):983-9. Epub 2008/08/16. doi: 10.1038/embor.2008.151. PubMed PMID: 18704117; PMCID: PMC2572126.
35. Rollenhagen M, Buettner FF, Reismann M, Jirmo AC, Grove M, Behrens GM, Gerardy-Schahn R, Hanisch FG, Muhlenhoff M. Polysialic acid on neuropilin-2 is exclusively synthesized by the polysialyltransferase ST8SiaIV and attached to mucin-type o-glycans located between the b2 and c domain. J Biol Chem. 2013;288(32):22880-92. Epub 2013/06/27. doi: 10.1074/jbc.M113.463927. PubMed PMID: 23801331; PMCID: PMC3743467.
36. Curreli S, Arany Z, Gerardy-Schahn R, Mann D, Stamatos NM. Polysialylated neuropilin-2 is expressed on the surface of human dendritic cells and modulates dendritic cell-T lymphocyte

interactions. J Biol Chem. 2007;282(42):30346-56. Epub 2007/08/19. doi: 10.1074/jbc.M702965200. PubMed PMID: 17699524.

37. Rey-Gallardo A, Delgado-Martin C, Gerardy-Schahn R, Rodriguez-Fernandez JL, Vega MA. Polysialic acid is required for neuropilin-2a/b-mediated control of CCL21-driven chemotaxis of mature dendritic cells and for their migration in vivo. Glycobiology. 2011;21(5):655-62. Epub 2011/01/05. doi: 10.1093/glycob/cwq216. PubMed PMID: 21199821.

38. Bhide GP, Fernandes NR, Colley KJ. Sequence Requirements for Neuropilin-2 Recognition by ST8SiaIV and Polysialylation of Its O-Glycans. J Biol Chem. 2016;291(18):9444-57. Epub 2016/02/18. doi: 10.1074/jbc.M116.714329. PubMed PMID: 26884342; PMCID: PMC4850285.

39. Kumanogoh A, Kikutani H. Immunological functions of the neuropilins and plexins as receptors for semaphorins. Nat Rev Immunol. 2013;13(11):802-14. Epub 2013/12/10. PubMed PMID: 24319778.

40. Prud'homme GJ, Glinka Y, Lichner Z, Yousef GM. Neuropilin-1 is a receptor for extracellular miRNA and AGO2/miRNA complexes and mediates the internalization of miRNAs that modulate cell function. Oncotarget. 2016;7(42):68057-71. Epub 2016/08/04. doi: 10.18632/oncotarget.10929. PubMed PMID: 27486976; PMCID: PMC5356539.

41. Kitsukawa T, Shimizu M, Sanbo M, Hirata T, Taniguchi M, Bekku Y, Yagi T, Fujisawa H. Neuropilin-semaphorin III/D-mediated chemorepulsive signals play a crucial role in peripheral nerve projection in mice. Neuron. 1997;19(5):995-1005. Epub 1997/12/09. PubMed PMID: 9390514.

42. Kawasaki T, Kitsukawa T, Bekku Y, Matsuda Y, Sanbo M, Yagi T, Fujisawa H. A requirement for neuropilin-1 in embryonic vessel formation. Development. 1999;126(21):4895-902. Epub 1999/10/16. PubMed PMID: 10518505.

43. Gerhardt H, Ruhrberg C, Abramsson A, Fujisawa H, Shima D, Betsholtz C. Neuropilin-1 is required for endothelial tip cell guidance in the developing central nervous system. Dev Dyn. 2004;231(3):503-9. Epub 2004/09/18. doi: 10.1002/dvdy.20148. PubMed PMID: 15376331.

44. Kitsukawa T, Shimono A, Kawakami A, Kondoh H, Fujisawa H. Overexpression of a membrane protein, neuropilin, in chimeric mice causes anomalies in the cardiovascular system, nervous system and limbs. Development. 1995;121(12):4309-18. Epub 1995/12/01. PubMed PMID: 8575331.

45. Giger RJ, Cloutier JF, Sahay A, Prinjha RK, Levengood DV, Moore SE, Pickering S, Simmons D, Rastan S, Walsh FS, Kolodkin AL, Ginty DD, Geppert M. Neuropilin-2 is required in vivo for selective axon guidance responses to secreted semaphorins. Neuron. 2000;25(1):29-41. Epub 2000/03/09. PubMed PMID: 10707970.

46. Chen H, Bagri A, Zupicich JA, Zou Y, Stoeckli E, Pleasure SJ, Lowenstein DH, Skarnes WC, Chedotal A, Tessier-Lavigne M. Neuropilin-2 regulates the development of selective cranial and sensory nerves and hippocampal mossy fiber projections. Neuron. 2000;25(1):43-56. Epub 2000/03/09. PubMed PMID: 10707971.

47. Yuan L, Moyon D, Pardanaud L, Breant C, Karkkainen MJ, Alitalo K, Eichmann A. Abnormal lymphatic vessel development in neuropilin 2 mutant mice. Development. 2002;129(20):4797-806. Epub 2002/10/04. PubMed PMID: 12361971.

48. Verlinden L, Kriebitzsch C, Beullens I, Tan BK, Carmeliet G, Verstuyf A. Nrp2 deficiency leads to trabecular bone loss and is accompanied by enhanced osteoclast and reduced osteoblast numbers. Bone. 2013;55(2):465-75. Epub 2013/04/20. doi: 10.1016/j.bone.2013.03.023. PubMed PMID: 23598046.

49. Takashima S, Kitakaze M, Asakura M, Asanuma H, Sanada S, Tashiro F, Niwa H, Miyazaki Ji J, Hirota S, Kitamura Y, Kitsukawa T, Fujisawa H, Klagsbrun M, Hori M. Targeting of both mouse neuropilin-1 and neuropilin-2 genes severely impairs developmental yolk sac and embryonic

angiogenesis. Proc Natl Acad Sci U S A. 2002;99(6):3657-62. Epub 2002/03/14. doi: 10.1073/pnas.022017899. PubMed PMID: 11891274; PMCID: PMC122579.

50. Aung NY, Ohe R, Meng H, Kabasawa T, Yang S, Kato T, Yamakawa M. Specific Neuropilins Expression in Alveolar Macrophages among Tissue-Specific Macrophages. PLoS One. 2016;11(2):e0147358. Epub 2016/02/24. doi: 10.1371/journal.pone.0147358. PubMed PMID: 26900851; PMCID: PMC4764655.

51. Lanahan A, Zhang X, Fantin A, Zhuang Z, Rivera-Molina F, Speichinger K, Prahst C, Zhang J, Wang Y, Davis G, Toomre D, Ruhrberg C, Simons M. The neuropilin 1 cytoplasmic domain is required for VEGF-A-dependent arteriogenesis. Dev Cell. 2013;25(2):156-68. Epub 2013/05/04. doi: 10.1016/j.devcel.2013.03.019. PubMed PMID: 23639442; PMCID: PMC3774154.

52. Fantin A, Vieira JM, Gestri G, Denti L, Schwarz Q, Prykhozhij S, Peri F, Wilson SW, Ruhrberg C. Tissue macrophages act as cellular chaperones for vascular anastomosis downstream of VEGF-mediated endothelial tip cell induction. Blood. 2010;116(5):829-40. Epub 2010/04/21. doi: 10.1182/blood-2009-12-257832. PubMed PMID: 20404134; PMCID: PMC2938310.

53. Fantin A, Vieira JM, Plein A, Denti L, Fruttiger M, Pollard JW, Ruhrberg C. NRP1 acts cell autonomously in endothelium to promote tip cell function during sprouting angiogenesis. Blood. 2013;121(12):2352-62. Epub 2013/01/15. doi: 10.1182/blood-2012-05-424713. PubMed PMID: 23315162; PMCID: PMC3606070.

54. Mantovani A, Sozzani S, Locati M, Allavena P, Sica A. Macrophage polarization: tumor-associated macrophages as a paradigm for polarized M2 mononuclear phagocytes. Trends Immunol. 2002;23(11):549-55. Epub 2002/10/29. PubMed PMID: 12401408.

55. Lewis CE, Pollard JW. Distinct role of macrophages in different tumor microenvironments. Cancer Res. 2006;66(2):605-12. Epub 2006/01/21. doi: 10.1158/0008-5472.CAN-05-4005. PubMed PMID: 16423985.

56. Noy R, Pollard JW. Tumor-associated macrophages: from mechanisms to therapy. Immunity. 2014;41(1):49-61. Epub 2014/07/19. doi: 10.1016/j.immuni.2014.06.010. PubMed PMID: 25035953; PMCID: PMC4137410.

57. Qian BZ, Pollard JW. Macrophage diversity enhances tumor progression and metastasis. Cell. 2010;141(1):39-51. Epub 2010/04/08. doi: 10.1016/j.cell.2010.03.014. PubMed PMID: 20371344; PMCID: PMC4994190.

58. Casazza A, Laoui D, Wenes M, Rizzolio S, Bassani N, Mambretti M, Deschoemaeker S, Van Ginderachter JA, Tamagnone L, Mazzone M. Impeding macrophage entry into hypoxic tumor areas by Sema3A/Nrp1 signaling blockade inhibits angiogenesis and restores antitumor immunity. Cancer Cell. 2013;24(6):695-709. Epub 2013/12/18. doi: 10.1016/j.ccr.2013.11.007. PubMed PMID: 24332039.

59. Rivera LB, Bergers G. Location, location, location: macrophage positioning within tumors determines pro- or antitumor activity. Cancer Cell. 2013;24(6):687-9. Epub 2013/12/18. doi: 10.1016/j.ccr.2013.11.014. PubMed PMID: 24332035; PMCID: PMC4243836.

60. Miyauchi JT, Chen D, Choi M, Nissen JC, Shroyer KR, Djordevic S, Zachary IC, Selwood D, Tsirka SE. Ablation of Neuropilin 1 from glioma-associated microglia and macrophages slows tumor progression. Oncotarget. 2016;7(9):9801-14. Epub 2016/01/13. doi: 10.18632/oncotarget.6877. PubMed PMID: 26755653; PMCID: PMC4891085.

61. Stamatos NM, Zhang L, Jokilammi A, Finne J, Chen WH, El-Maarouf A, Cross AS, Hankey KG. Changes in polysialic acid expression on myeloid cells during differentiation and recruitment to sites of inflammation: role in phagocytosis. Glycobiology. 2014;24(9):864-79. Epub 2014/05/29. doi: 10.1093/glycob/cwu050. PubMed PMID: 24865221; PMCID: PMC4116047.

62. Werneburg S, Muhlenhoff M, Stangel M, Hildebrandt H. Polysialic acid on SynCAM 1 in NG2 cells and on neuropilin-2 in microglia is confined to intracellular pools that are rapidly

depleted upon stimulation. Glia. 2015;63(7):1240-55. Epub 2015/03/11. doi: 10.1002/glia.22815. PubMed PMID: 25752299.

63. Werneburg S, Buettner FF, Erben L, Mathews M, Neumann H, Muhlenhoff M, Hildebrandt H. Polysialylation and lipopolysaccharide-induced shedding of E-selectin ligand-1 and neuropilin-2 by microglia and THP-1 macrophages. Glia. 2016;64(8):1314-30. Epub 2016/05/10. doi: 10.1002/glia.23004. PubMed PMID: 27159043.

64. Ojalvo LS, King W, Cox D, Pollard JW. High-density gene expression analysis of tumor-associated macrophages from mouse mammary tumors. Am J Pathol. 2009;174(3):1048-64. Epub 2009/02/17. doi: 10.2353/ajpath.2009.080676. PubMed PMID: 19218341; PMCID: PMC2665764.

65. Mantovani A, Marchesi F, Malesci A, Laghi L, Allavena P. Tumour-associated macrophages as treatment targets in oncology. Nat Rev Clin Oncol. 2017;14(7):399-416. Epub 2017/01/25. doi: 10.1038/nrclinonc.2016.217. PubMed PMID: 28117416; PMCID: PMC5480600.

66. Feng X, Szulzewsky F, Yerevanian A, Chen Z, Heinzmann D, Rasmussen RD, Alvarez-Garcia V, Kim Y, Wang B, Tamagno I, Zhou H, Li X, Kettenmann H, Ransohoff RM, Hambardzumyan D. Loss of CX3CR1 increases accumulation of inflammatory monocytes and promotes gliomagenesis. Oncotarget. 2015;6(17):15077-94. Epub 2015/05/20. doi: 10.18632/oncotarget.3730. PubMed PMID: 25987130; PMCID: PMC4558137.

67. Movahedi K, Laoui D, Gysemans C, Baeten M, Stange G, Van den Bossche J, Mack M, Pipeleers D, In't Veld P, De Baetselier P, Van Ginderachter JA. Different tumor microenvironments contain functionally distinct subsets of macrophages derived from Ly6C(high) monocytes. Cancer Res. 2010;70(14):5728-39. Epub 2010/06/24. doi: 10.1158/0008-5472.CAN-09-4672. PubMed PMID: 20570887.

68. Franklin RA, Liao W, Sarkar A, Kim MV, Bivona MR, Liu K, Pamer EG, Li MO. The cellular and molecular origin of tumor-associated macrophages. Science. 2014;344(6186):921-5. Epub 2014/05/09. doi: 10.1126/science.1252510. PubMed PMID: 24812208; PMCID: PMC4204732.

69. Shand FH, Ueha S, Otsuji M, Koid SS, Shichino S, Tsukui T, Kosugi-Kanaya M, Abe J, Tomura M, Ziogas J, Matsushima K. Tracking of intertissue migration reveals the origins of tumor-infiltrating monocytes. Proc Natl Acad Sci U S A. 2014;111(21):7771-6. Epub 2014/05/16. doi: 10.1073/pnas.1402914111. PubMed PMID: 24825888; PMCID: PMC4040600.

70. MacDonald KP, Palmer JS, Cronau S, Seppanen E, Olver S, Raffelt NC, Kuns R, Pettit AR, Clouston A, Wainwright B, Branstetter D, Smith J, Paxton RJ, Cerretti DP, Bonham L, Hill GR, Hume DA. An antibody against the colony-stimulating factor 1 receptor depletes the resident subset of monocytes and tissue- and tumor-associated macrophages but does not inhibit inflammation. Blood. 2010;116(19):3955-63. Epub 2010/08/05. doi: 10.1182/blood-2010-02-266296. PubMed PMID: 20682855.

71. Lehmann B, Biburger M, Bruckner C, Ipsen-Escobedo A, Gordan S, Lehmann C, Voehringer D, Winkler T, Schaft N, Dudziak D, Sirbu H, Weber GF, Nimmerjahn F. Tumor location determines tissue-specific recruitment of tumor-associated macrophages and antibody-dependent immunotherapy response. Sci Immunol. 2017;2(7). Epub 2017/08/08. doi: 10.1126/sciimmunol.aah6413. PubMed PMID: 28783667.

72. Lahmar Q, Keirsse J, Laoui D, Movahedi K, Van Overmeire E, Van Ginderachter JA. Tissue-resident versus monocyte-derived macrophages in the tumor microenvironment. Biochim Biophys Acta. 2016;1865(1):23-34. Epub 2015/07/07. doi: 10.1016/j.bbcan.2015.06.009. PubMed PMID: 26145884.

73. Lee HW, Choi HJ, Ha SJ, Lee KT, Kwon YG. Recruitment of monocytes/macrophages in different tumor microenvironments. Biochim Biophys Acta. 2013;1835(2):170-9. Epub 2013/01/05. doi: 10.1016/j.bbcan.2012.12.007. PubMed PMID: 23287570.

74. Chanmee T, Ontong P, Konno K, Itano N. Tumor-associated macrophages as major players in the tumor microenvironment. Cancers (Basel). 2014;6(3):1670-90. Epub 2014/08/16. doi: 10.3390/cancers6031670. PubMed PMID: 25125485; PMCID: PMC4190561.
75. Balkwill FR, Capasso M, Hagemann T. The tumor microenvironment at a glance. J Cell Sci. 2012;125(Pt 23):5591-6. Epub 2013/02/20. doi: 10.1242/jcs.116392. PubMed PMID: 23420197.
76. Balkwill F, Charles KA, Mantovani A. Smoldering and polarized inflammation in the initiation and promotion of malignant disease. Cancer Cell. 2005;7(3):211-7. Epub 2005/03/16. doi: 10.1016/j.ccr.2005.02.013. PubMed PMID: 15766659.
77. Coussens LM, Werb Z. Inflammation and cancer. Nature. 2002;420(6917):860-7. Epub 2002/12/20. doi: 10.1038/nature01322. PubMed PMID: 12490959; PMCID: PMC2803035.
78. Grivennikov SI, Karin M. Inflammation and oncogenesis: a vicious connection. Curr Opin Genet Dev. 2010;20(1):65-71. Epub 2009/12/29. doi: 10.1016/j.gde.2009.11.004. PubMed PMID: 20036794; PMCID: PMC2821983.
79. Brown ER, Charles KA, Hoare SA, Rye RL, Jodrell DI, Aird RE, Vora R, Prabhakar U, Nakada M, Corringham RE, DeWitte M, Sturgeon C, Propper D, Balkwill FR, Smyth JF. A clinical study assessing the tolerability and biological effects of infliximab, a TNF-alpha inhibitor, in patients with advanced cancer. Ann Oncol. 2008;19(7):1340-6. Epub 2008/03/08. doi: 10.1093/annonc/mdn054. PubMed PMID: 18325912.
80. Deng L, Zhou JF, Sellers RS, Li JF, Nguyen AV, Wang Y, Orlofsky A, Liu Q, Hume DA, Pollard JW, Augenlicht L, Lin EY. A novel mouse model of inflammatory bowel disease links mammalian target of rapamycin-dependent hyperproliferation of colonic epithelium to inflammation-associated tumorigenesis. Am J Pathol. 2010;176(2):952-67. Epub 2010/01/01. doi: 10.2353/ajpath.2010.090622. PubMed PMID: 20042677; PMCID: PMC2808099.
81. Lin EY, Pollard JW. Tumor-associated macrophages press the angiogenic switch in breast cancer. Cancer Res. 2007;67(11):5064-6. Epub 2007/06/05. doi: 10.1158/0008-5472.CAN-07-0912. PubMed PMID: 17545580.
82. Yeo EJ, Cassetta L, Qian BZ, Lewkowich I, Li JF, Stefater JA, 3rd, Smith AN, Wiechmann LS, Wang Y, Pollard JW, Lang RA. Myeloid WNT7b mediates the angiogenic switch and metastasis in breast cancer. Cancer Res. 2014;74(11):2962-73. Epub 2014/03/19. doi: 10.1158/0008-5472.CAN-13-2421. PubMed PMID: 24638982; PMCID: PMC4137408.
83. Mazzieri R, Pucci F, Moi D, Zonari E, Ranghetti A, Berti A, Politi LS, Gentner B, Brown JL, Naldini L, De Palma M. Targeting the ANG2/TIE2 axis inhibits tumor growth and metastasis by impairing angiogenesis and disabling rebounds of proangiogenic myeloid cells. Cancer Cell. 2011;19(4):512-26. Epub 2011/04/13. doi: 10.1016/j.ccr.2011.02.005. PubMed PMID: 21481792.
84. Coffelt SB, Hughes R, Lewis CE. Tumor-associated macrophages: effectors of angiogenesis and tumor progression. Biochim Biophys Acta. 2009;1796(1):11-8. Epub 2009/03/10. doi: 10.1016/j.bbcan.2009.02.004. PubMed PMID: 19269310.
85. Ran S, Montgomery KE. Macrophage-mediated lymphangiogenesis: the emerging role of macrophages as lymphatic endothelial progenitors. Cancers (Basel). 2012;4(3):618-57. Epub 2012/09/05. doi: 10.3390/cancers4030618. PubMed PMID: 22946011; PMCID: PMC3430523.
86. Biddle A, Mackenzie IC. Cancer stem cells and EMT in carcinoma. Cancer Metastasis Rev. 2012. Epub 2012/02/04. doi: 10.1007/s10555-012-9345-0. PubMed PMID: 22302111.
87. Su S, Liu Q, Chen J, Chen J, Chen F, He C, Huang D, Wu W, Lin L, Huang W, Zhang J, Cui X, Zheng F, Li H, Yao H, Su F, Song E. A positive feedback loop between mesenchymal-like cancer cells and macrophages is essential to breast cancer metastasis. Cancer Cell. 2014;25(5):605-20. Epub 2014/05/16. doi: 10.1016/j.ccr.2014.03.021. PubMed PMID: 24823638.
88. Fu XT, Dai Z, Song K, Zhang ZJ, Zhou ZJ, Zhou SL, Zhao YM, Xiao YS, Sun QM, Ding ZB, Fan J. Macrophage-secreted IL-8 induces epithelial-mesenchymal transition in hepatocellular

carcinoma cells by activating the JAK2/STAT3/Snail pathway. Int J Oncol. 2015;46(2):587-96. Epub 2014/11/19. doi: 10.3892/ijo.2014.2761. PubMed PMID: 25405790.

89. Bonde AK, Tischler V, Kumar S, Soltermann A, Schwendener RA. Intratumoral macrophages contribute to epithelial-mesenchymal transition in solid tumors. BMC Cancer. 2012;12:35. Epub 2012/01/26. doi: 10.1186/1471-2407-12-35. PubMed PMID: 22273460; PMCID: PMC3314544.

90. Quail DF, Joyce JA. Microenvironmental regulation of tumor progression and metastasis. Nat Med. 2013;19(11):1423-37. Epub 2013/11/10. doi: 10.1038/nm.3394. PubMed PMID: 24202395; PMCID: PMC3954707.

91. Sangaletti S, Di Carlo E, Gariboldi S, Miotti S, Cappetti B, Parenza M, Rumio C, Brekken RA, Chiodoni C, Colombo MP. Macrophage-derived SPARC bridges tumor cell-extracellular matrix interactions toward metastasis. Cancer Res. 2008;68(21):9050-9. Epub 2008/11/01. doi: 10.1158/0008-5472.CAN-08-1327. PubMed PMID: 18974151.

92. Wyckoff JB, Wang Y, Lin EY, Li JF, Goswami S, Stanley ER, Segall JE, Pollard JW, Condeelis J. Direct visualization of macrophage-assisted tumor cell intravasation in mammary tumors. Cancer Res. 2007;67(6):2649-56. Epub 2007/03/17. doi: 10.1158/0008-5472.CAN-06-1823. PubMed PMID: 17363585.

93. Rohan TE, Xue X, Lin HM, D'Alfonso TM, Ginter PS, Oktay MH, Robinson BD, Ginsberg M, Gertler FB, Glass AG, Sparano JA, Condeelis JS, Jones JG. Tumor microenvironment of metastasis and risk of distant metastasis of breast cancer. J Natl Cancer Inst. 2014;106(8). Epub 2014/06/05. doi: 10.1093/jnci/dju136. PubMed PMID: 24895374; PMCID: PMC4133559.

94. Condeelis J, Pollard JW. Macrophages: obligate partners for tumor cell migration, invasion, and metastasis. Cell. 2006;124(2):263-6. Epub 2006/01/28. doi: 10.1016/j.cell.2006.01.007. PubMed PMID: 16439202.

95. Biswas SK, Mantovani A. Macrophage plasticity and interaction with lymphocyte subsets: cancer as a paradigm. Nat Immunol. 2010;11(10):889-96. Epub 2010/09/22. doi: 10.1038/ni.1937. PubMed PMID: 20856220.

96. Ruffell B, Affara NI, Coussens LM. Differential macrophage programming in the tumor microenvironment. Trends Immunol. 2012;33(3):119-26. Epub 2012/01/27. doi: 10.1016/j.it.2011.12.001. PubMed PMID: 22277903; PMCID: PMC3294003.

97. Doedens AL, Stockmann C, Rubinstein MP, Liao D, Zhang N, DeNardo DG, Coussens LM, Karin M, Goldrath AW, Johnson RS. Macrophage expression of hypoxia-inducible factor-1 alpha suppresses T-cell function and promotes tumor progression. Cancer Res. 2010;70(19):7465-75. Epub 2010/09/16. doi: 10.1158/0008-5472.CAN-10-1439. PubMed PMID: 20841473; PMCID: PMC2948598.

98. Sharda DR, Yu S, Ray M, Squadrito ML, De Palma M, Wynn TA, Morris SM, Jr., Hankey PA. Regulation of macrophage arginase expression and tumor growth by the Ron receptor tyrosine kinase. J Immunol. 2011;187(5):2181-92. Epub 2011/08/04. doi: 10.4049/jimmunol.1003460. PubMed PMID: 21810604; PMCID: PMC4042865.

99. Rodriguez PC, Zea AH, DeSalvo J, Culotta KS, Zabaleta J, Quiceno DG, Ochoa JB, Ochoa AC. L-arginine consumption by macrophages modulates the expression of CD3 zeta chain in T lymphocytes. J Immunol. 2003;171(3):1232-9. Epub 2003/07/23. PubMed PMID: 12874210.

100. DeNardo DG, Barreto JB, Andreu P, Vasquez L, Tawfik D, Kolhatkar N, Coussens LM. CD4(+) T cells regulate pulmonary metastasis of mammary carcinomas by enhancing protumor properties of macrophages. Cancer Cell. 2009;16(2):91-102. Epub 2009/08/04. doi: 10.1016/j.ccr.2009.06.018. PubMed PMID: 19647220; PMCID: PMC2778576.

101. Shiao SL, Ruffell B, DeNardo DG, Faddegon BA, Park CC, Coussens LM. TH2-Polarized CD4(+) T Cells and Macrophages Limit Efficacy of Radiotherapy. Cancer Immunol Res.

2015;3(5):518-25. Epub 2015/02/27. doi: 10.1158/2326-6066.CIR-14-0232. PubMed PMID: 25716473; PMCID: PMC4420686.
102. Kratochvill F, Neale G, Haverkamp JM, Van de Velde LA, Smith AM, Kawauchi D, McEvoy J, Roussel MF, Dyer MA, Qualls JE, Murray PJ. TNF Counterbalances the Emergence of M2 Tumor Macrophages. Cell Rep. 2015;12(11):1902-14. Epub 2015/09/15. doi: 10.1016/j.celrep.2015.08.033. PubMed PMID: 26365184; PMCID: PMC4581986.
103. Mantovani A, Allavena P. The interaction of anticancer therapies with tumor-associated macrophages. J Exp Med. 2015;212(4):435-45. Epub 2015/03/11. doi: 10.1084/jem.20150295. PubMed PMID: 25753580; PMCID: PMC4387285.
104. Stanford JC, Young C, Hicks D, Owens P, Williams A, Vaught DB, Morrison MM, Lim J, Williams M, Brantley-Sieders DM, Balko JM, Tonetti D, Earp HS, 3rd, Cook RS. Efferocytosis produces a prometastatic landscape during postpartum mammary gland involution. J Clin Invest. 2014;124(11):4737-52. Epub 2014/09/25. doi: 10.1172/JCI76375. PubMed PMID: 25250573; PMCID: PMC4347249.
105. Gil-Bernabe AM, Ferjancic S, Tlalka M, Zhao L, Allen PD, Im JH, Watson K, Hill SA, Amirkhosravi A, Francis JL, Pollard JW, Ruf W, Muschel RJ. Recruitment of monocytes/macrophages by tissue factor-mediated coagulation is essential for metastatic cell survival and premetastatic niche establishment in mice. Blood. 2012;119(13):3164-75. Epub 2012/02/14. doi: 10.1182/blood-2011-08-376426. PubMed PMID: 22327225.
106. Qian BZ, Li J, Zhang H, Kitamura T, Zhang J, Campion LR, Kaiser EA, Snyder LA, Pollard JW. CCL2 recruits inflammatory monocytes to facilitate breast-tumour metastasis. Nature. 2011;475(7355):222-5. Epub 2011/06/10. doi: 10.1038/nature10138. PubMed PMID: 21654748; PMCID: PMC3208506.
107. Cortez-Retamozo V, Etzrodt M, Newton A, Rauch PJ, Chudnovskiy A, Berger C, Ryan RJ, Iwamoto Y, Marinelli B, Gorbatov R, Forghani R, Novobrantseva TI, Koteliansky V, Figueiredo JL, Chen JW, Anderson DG, Nahrendorf M, Swirski FK, Weissleder R, Pittet MJ. Origins of tumor-associated macrophages and neutrophils. Proc Natl Acad Sci U S A. 2012;109(7):2491-6. Epub 2012/02/07. doi: 10.1073/pnas.1113744109. PubMed PMID: 22308361; PMCID: PMC3289379.
108. Mantovani A, Allavena P, Sica A, Balkwill F. Cancer-related inflammation. Nature. 2008;454(7203):436-44. Epub 2008/07/25. doi: 10.1038/nature07205. PubMed PMID: 18650914.
109. Zhu XD, Zhang JB, Zhuang PY, Zhu HG, Zhang W, Xiong YQ, Wu WZ, Wang L, Tang ZY, Sun HC. High expression of macrophage colony-stimulating factor in peritumoral liver tissue is associated with poor survival after curative resection of hepatocellular carcinoma. J Clin Oncol. 2008;26(16):2707-16. Epub 2008/05/30. doi: 10.1200/JCO.2007.15.6521. PubMed PMID: 18509183.
110. Koh YW, Park C, Yoon DH, Suh C, Huh J. CSF-1R expression in tumor-associated macrophages is associated with worse prognosis in classical Hodgkin lymphoma. Am J Clin Pathol. 2014;141(4):573-83. Epub 2014/03/13. doi: 10.1309/AJCPR92TDDFARISU. PubMed PMID: 24619759.
111. Pyonteck SM, Akkari L, Schuhmacher AJ, Bowman RL, Sevenich L, Quail DF, Olson OC, Quick ML, Huse JT, Teijeiro V, Setty M, Leslie CS, Oei Y, Pedraza A, Zhang J, Brennan CW, Sutton JC, Holland EC, Daniel D, Joyce JA. CSF-1R inhibition alters macrophage polarization and blocks glioma progression. Nat Med. 2013;19(10):1264-72. Epub 2013/09/24. doi: 10.1038/nm.3337. PubMed PMID: 24056773; PMCID: PMC3840724.
112. Goswami S, Sahai E, Wyckoff JB, Cammer M, Cox D, Pixley FJ, Stanley ER, Segall JE, Condeelis JS. Macrophages promote the invasion of breast carcinoma cells via a colony-stimulating factor-1/epidermal growth factor paracrine loop. Cancer Res. 2005;65(12):5278-83. Epub 2005/06/17. doi: 10.1158/0008-5472.CAN-04-1853. PubMed PMID: 15958574.

113. Manthey CL, Johnson DL, Illig CR, Tuman RW, Zhou Z, Baker JF, Chaikin MA, Donatelli RR, Franks CF, Zeng L, Crysler C, Chen Y, Yurkow EJ, Boczon L, Meegalla SK, Wilson KJ, Wall MJ, Chen J, Ballentine SK, Ott H, Baumann C, Lawrence D, Tomczuk BE, Molloy CJ. JNJ-28312141, a novel orally active colony-stimulating factor-1 receptor/FMS-related receptor tyrosine kinase-3 receptor tyrosine kinase inhibitor with potential utility in solid tumors, bone metastases, and acute myeloid leukemia. Mol Cancer Ther. 2009;8(11):3151-61. Epub 2009/11/06. doi: 10.1158/1535-7163.MCT-09-0255. PubMed PMID: 19887542.

114. Ries CH, Cannarile MA, Hoves S, Benz J, Wartha K, Runza V, Rey-Giraud F, Pradel LP, Feuerhake F, Klaman I, Jones T, Jucknischke U, Scheiblich S, Kaluza K, Gorr IH, Walz A, Abiraj K, Cassier PA, Sica A, Gomez-Roca C, de Visser KE, Italiano A, Le Tourneau C, Delord JP, Levitsky H, Blay JY, Ruttinger D. Targeting tumor-associated macrophages with anti-CSF-1R antibody reveals a strategy for cancer therapy. Cancer Cell. 2014;25(6):846-59. Epub 2014/06/06. doi: 10.1016/j.ccr.2014.05.016. PubMed PMID: 24898549.

115. Tap WD, Wainberg ZA, Anthony SP, Ibrahim PN, Zhang C, Healey JH, Chmielowski B, Staddon AP, Cohn AL, Shapiro GI, Keedy VL, Singh AS, Puzanov I, Kwak EL, Wagner AJ, Von Hoff DD, Weiss GJ, Ramanathan RK, Zhang J, Habets G, Zhang Y, Burton EA, Visor G, Sanftner L, Severson P, Nguyen H, Kim MJ, Marimuthu A, Tsang G, Shellooe R, Gee C, West BL, Hirth P, Nolop K, van de Rijn M, Hsu HH, Peterfy C, Lin PS, Tong-Starksen S, Bollag G. Structure-Guided Blockade of CSF1R Kinase in Tenosynovial Giant-Cell Tumor. N Engl J Med. 2015;373(5):428-37. Epub 2015/07/30. doi: 10.1056/NEJMoa1411366. PubMed PMID: 26222558.

116. Butowski N, Colman H, De Groot JF, Omuro AM, Nayak L, Wen PY, Cloughesy TF, Marimuthu A, Haidar S, Perry A, Huse J, Phillips J, West BL, Nolop KB, Hsu HH, Ligon KL, Molinaro AM, Prados M. Orally administered colony stimulating factor 1 receptor inhibitor PLX3397 in recurrent glioblastoma: an Ivy Foundation Early Phase Clinical Trials Consortium phase II study. Neuro Oncol. 2016;18(4):557-64. Epub 2015/10/10. doi: 10.1093/neuonc/nov245. PubMed PMID: 26449250; PMCID: PMC4799682.

117. Quail DF, Bowman RL, Akkari L, Quick ML, Schuhmacher AJ, Huse JT, Holland EC, Sutton JC, Joyce JA. The tumor microenvironment underlies acquired resistance to CSF-1R inhibition in gliomas. Science. 2016;352(6288):aad3018. Epub 2016/05/21. doi: 10.1126/science.aad3018. PubMed PMID: 27199435; PMCID: PMC5450629.

118. Moughon DL, He H, Schokrpur S, Jiang ZK, Yaqoob M, David J, Lin C, Iruela-Arispe ML, Dorigo O, Wu L. Macrophage Blockade Using CSF1R Inhibitors Reverses the Vascular Leakage Underlying Malignant Ascites in Late-Stage Epithelial Ovarian Cancer. Cancer Res. 2015;75(22):4742-52. Epub 2015/10/17. doi: 10.1158/0008-5472.CAN-14-3373. PubMed PMID: 26471360; PMCID: PMC4675660.

119. Escamilla J, Schokrpur S, Liu C, Priceman SJ, Moughon D, Jiang Z, Pouliot F, Magyar C, Sung JL, Xu J, Deng G, West BL, Bollag G, Fradet Y, Lacombe L, Jung ME, Huang J, Wu L. CSF1 receptor targeting in prostate cancer reverses macrophage-mediated resistance to androgen blockade therapy. Cancer Res. 2015;75(6):950-62. Epub 2015/03/05. doi: 10.1158/0008-5472.CAN-14-0992. PubMed PMID: 25736687; PMCID: PMC4359956.

120. Colombo N, Peccatori F, Paganin C, Bini S, Brandely M, Mangioni C, Mantovani A, Allavena P. Anti-tumor and immunomodulatory activity of intraperitoneal IFN-gamma in ovarian carcinoma patients with minimal residual tumor after chemotherapy. Int J Cancer. 1992;51(1):42-6. Epub 1992/04/22. PubMed PMID: 1563843.

121. Pujade-Lauraine E, Guastalla JP, Colombo N, Devillier P, Francois E, Fumoleau P, Monnier A, Nooy M, Mignot L, Bugat R, Marques C, Mousseau M, Netter G, Maloisel F, Larbaoui S, Brandely M. Intraperitoneal recombinant interferon gamma in ovarian cancer patients with residual

disease at second-look laparotomy. J Clin Oncol. 1996;14(2):343-50. Epub 1996/02/01. doi: 10.1200/JCO.1996.14.2.343. PubMed PMID: 8636742.

122. Beatty GL, Chiorean EG, Fishman MP, Saboury B, Teitelbaum UR, Sun W, Huhn RD, Song W, Li D, Sharp LL, Torigian DA, O'Dwyer PJ, Vonderheide RH. CD40 agonists alter tumor stroma and show efficacy against pancreatic carcinoma in mice and humans. Science. 2011;331(6024):1612-6. Epub 2011/03/26. doi: 10.1126/science.1198443. PubMed PMID: 21436454; PMCID: PMC3406187.

123. Beatty GL, Torigian DA, Chiorean EG, Saboury B, Brothers A, Alavi A, Troxel AB, Sun W, Teitelbaum UR, Vonderheide RH, O'Dwyer PJ. A phase I study of an agonist CD40 monoclonal antibody (CP-870,893) in combination with gemcitabine in patients with advanced pancreatic ductal adenocarcinoma. Clin Cancer Res. 2013;19(22):6286-95. Epub 2013/08/29. doi: 10.1158/1078-0432.CCR-13-1320. PubMed PMID: 23983255; PMCID: PMC3834036.

124. Gunderson AJ, Kaneda MM, Tsujikawa T, Nguyen AV, Affara NI, Ruffell B, Gorjestani S, Liudahl SM, Truitt M, Olson P, Kim G, Hanahan D, Tempero MA, Sheppard B, Irving B, Chang BY, Varner JA, Coussens LM. Bruton Tyrosine Kinase-Dependent Immune Cell Cross-talk Drives Pancreas Cancer. Cancer Discov. 2016;6(3):270-85. Epub 2015/12/31. doi: 10.1158/2159-8290.CD-15-0827. PubMed PMID: 26715645; PMCID: PMC4783268.

125. Loberg RD, Ying C, Craig M, Day LL, Sargent E, Neeley C, Wojno K, Snyder LA, Yan L, Pienta KJ. Targeting CCL2 with systemic delivery of neutralizing antibodies induces prostate cancer tumor regression in vivo. Cancer Res. 2007;67(19):9417-24. Epub 2007/10/03. doi: 10.1158/0008-5472.CAN-07-1286. PubMed PMID: 17909051.

126. Fridlender ZG, Kapoor V, Buchlis G, Cheng G, Sun J, Wang LC, Singhal S, Snyder LA, Albelda SM. Monocyte chemoattractant protein-1 blockade inhibits lung cancer tumor growth by altering macrophage phenotype and activating CD8+ cells. Am J Respir Cell Mol Biol. 2011;44(2):230-7. Epub 2010/04/17. doi: 10.1165/rcmb.2010-0080OC. PubMed PMID: 20395632; PMCID: PMC3049234.

127. Moisan F, Francisco EB, Brozovic A, Duran GE, Wang YC, Chaturvedi S, Seetharam S, Snyder LA, Doshi P, Sikic BI. Enhancement of paclitaxel and carboplatin therapies by CCL2 blockade in ovarian cancers. Mol Oncol. 2014;8(7):1231-9. Epub 2014/05/13. doi: 10.1016/j.molonc.2014.03.016. PubMed PMID: 24816187; PMCID: PMC4801026.

128. Li X, Yao W, Yuan Y, Chen P, Li B, Li J, Chu R, Song H, Xie D, Jiang X, Wang H. Targeting of tumour-infiltrating macrophages via CCL2/CCR2 signalling as a therapeutic strategy against hepatocellular carcinoma. Gut. 2017;66(1):157-67. Epub 2015/10/11. doi: 10.1136/gutjnl-2015-310514. PubMed PMID: 26452628.

129. Pienta KJ, Machiels JP, Schrijvers D, Alekseev B, Shkolnik M, Crabb SJ, Li S, Seetharam S, Puchalski TA, Takimoto C, Elsayed Y, Dawkins F, de Bono JS. Phase 2 study of carlumab (CNTO 888), a human monoclonal antibody against CC-chemokine ligand 2 (CCL2), in metastatic castration-resistant prostate cancer. Invest New Drugs. 2013;31(3):760-8. Epub 2012/08/22. doi: 10.1007/s10637-012-9869-8. PubMed PMID: 22907596.

130. Sandhu SK, Papadopoulos K, Fong PC, Patnaik A, Messiou C, Olmos D, Wang G, Tromp BJ, Puchalski TA, Balkwill F, Berns B, Seetharam S, de Bono JS, Tolcher AW. A first-in-human, first-in-class, phase I study of carlumab (CNTO 888), a human monoclonal antibody against CC-chemokine ligand 2 in patients with solid tumors. Cancer Chemother Pharmacol. 2013;71(4):1041-50. Epub 2013/02/07. doi: 10.1007/s00280-013-2099-8. PubMed PMID: 23385782.

131. Brana I, Calles A, LoRusso PM, Yee LK, Puchalski TA, Seetharam S, Zhong B, de Boer CJ, Tabernero J, Calvo E. Carlumab, an anti-C-C chemokine ligand 2 monoclonal antibody, in combination with four chemotherapy regimens for the treatment of patients with solid tumors:

an open-label, multicenter phase 1b study. Target Oncol. 2015;10(1):111-23. Epub 2014/06/15. doi: 10.1007/s11523-014-0320-2. PubMed PMID: 24928772.

132. Halama N, Zoernig I, Berthel A, Kahlert C, Klupp F, Suarez-Carmona M, Suetterlin T, Brand K, Krauss J, Lasitschka F, Lerchl T, Luckner-Minden C, Ulrich A, Koch M, Weitz J, Schneider M, Buechler MW, Zitvogel L, Herrmann T, Benner A, Kunz C, Luecke S, Springfeld C, Grabe N, Falk CS, Jaeger D. Tumoral Immune Cell Exploitation in Colorectal Cancer Metastases Can Be Targeted Effectively by Anti-CCR5 Therapy in Cancer Patients. Cancer Cell. 2016;29(4):587-601. Epub 2016/04/14. doi: 10.1016/j.ccell.2016.03.005. PubMed PMID: 27070705.

133. Van Acker HH, Anguille S, Willemen Y, Smits EL, Van Tendeloo VF. Bisphosphonates for cancer treatment: Mechanisms of action and lessons from clinical trials. Pharmacol Ther. 2016;158:24-40. Epub 2015/12/01. doi: 10.1016/j.pharmthera.2015.11.008. PubMed PMID: 26617219.

134. Diel IJ, Solomayer EF, Costa SD, Gollan C, Goerner R, Wallwiener D, Kaufmann M, Bastert G. Reduction in new metastases in breast cancer with adjuvant clodronate treatment. N Engl J Med. 1998;339(6):357-63. Epub 1998/08/06. doi: 10.1056/NEJM199808063390601. PubMed PMID: 9691101.

135. Ishigami S, Natsugoe S, Tokuda K, Nakajo A, Okumura H, Matsumoto M, Miyazono F, Hokita S, Aikou T. Tumor-associated macrophage (TAM) infiltration in gastric cancer. Anticancer Res. 2003;23(5A):4079-83. Epub 2003/12/12. PubMed PMID: 14666722.

136. Welsh TJ, Green RH, Richardson D, Waller DA, O'Byrne KJ, Bradding P. Macrophage and mast-cell invasion of tumor cell islets confers a marked survival advantage in non-small-cell lung cancer. J Clin Oncol. 2005;23(35):8959-67. Epub 2005/10/13. doi: 10.1200/JCO.2005.01.4910. PubMed PMID: 16219934.

137. Forssell J, Oberg A, Henriksson ML, Stenling R, Jung A, Palmqvist R. High macrophage infiltration along the tumor front correlates with improved survival in colon cancer. Clin Cancer Res. 2007;13(5):1472-9. Epub 2007/03/03. doi: 10.1158/1078-0432.CCR-06-2073. PubMed PMID: 17332291.

138. DeNardo DG, Brennan DJ, Rexhepaj E, Ruffell B, Shiao SL, Madden SF, Gallagher WM, Wadhwani N, Keil SD, Junaid SA, Rugo HS, Hwang ES, Jirstrom K, West BL, Coussens LM. Leukocyte complexity predicts breast cancer survival and functionally regulates response to chemotherapy. Cancer Discov. 2011;1(1):54-67. Epub 2011/11/01. doi: 10.1158/2159-8274.CD-10-0028. PubMed PMID: 22039576; PMCID: PMC3203524.

139. Steidl C, Lee T, Shah SP, Farinha P, Han G, Nayar T, Delaney A, Jones SJ, Iqbal J, Weisenburger DD, Bast MA, Rosenwald A, Muller-Hermelink HK, Rimsza LM, Campo E, Delabie J, Braziel RM, Cook JR, Tubbs RR, Jaffe ES, Lenz G, Connors JM, Staudt LM, Chan WC, Gascoyne RD. Tumor-associated macrophages and survival in classic Hodgkin's lymphoma. N Engl J Med. 2010;362(10):875-85. Epub 2010/03/12. doi: 10.1056/NEJMoa0905680. PubMed PMID: 20220182; PMCID: PMC2897174.

140. Farinha P, Masoudi H, Skinnider BF, Shumansky K, Spinelli JJ, Gill K, Klasa R, Voss N, Connors JM, Gascoyne RD. Analysis of multiple biomarkers shows that lymphoma-associated macrophage (LAM) content is an independent predictor of survival in follicular lymphoma (FL). Blood. 2005;106(6):2169-74. Epub 2005/06/04. doi: 10.1182/blood-2005-04-1565. PubMed PMID: 15933054.

141. Taskinen M, Karjalainen-Lindsberg ML, Nyman H, Eerola LM, Leppa S. A high tumor-associated macrophage content predicts favorable outcome in follicular lymphoma patients treated with rituximab and cyclophosphamide-doxorubicin-vincristine-prednisone. Clin Cancer Res. 2007;13(19):5784-9. Epub 2007/10/03. doi: 10.1158/1078-0432.CCR-07-0778. PubMed PMID: 17908969.

142. Xu J, Escamilla J, Mok S, David J, Priceman S, West B, Bollag G, McBride W, Wu L. CSF1R signaling blockade stanches tumor-infiltrating myeloid cells and improves the efficacy of radiotherapy in prostate cancer. Cancer Res. 2013;73(9):2782-94. Epub 2013/02/19. doi: 10.1158/0008-5472.CAN-12-3981. PubMed PMID: 23418320; PMCID: PMC4097014.
143. Klug F, Prakash H, Huber PE, Seibel T, Bender N, Halama N, Pfirschke C, Voss RH, Timke C, Umansky L, Klapproth K, Schakel K, Garbi N, Jager D, Weitz J, Schmitz-Winnenthal H, Hammerling GJ, Beckhove P. Low-dose irradiation programs macrophage differentiation to an iNOS(+)/M1 phenotype that orchestrates effective T cell immunotherapy. Cancer Cell. 2013;24(5):589-602. Epub 2013/11/12. doi: 10.1016/j.ccr.2013.09.014. PubMed PMID: 24209604.
144. Cioffi M, Trabulo S, Hidalgo M, Costello E, Greenhalf W, Erkan M, Kleeff J, Sainz B, Jr., Heeschen C. Inhibition of CD47 Effectively Targets Pancreatic Cancer Stem Cells via Dual Mechanisms. Clin Cancer Res. 2015;21(10):2325-37. Epub 2015/02/27. doi: 10.1158/1078-0432.CCR-14-1399. PubMed PMID: 25717063.
145. Sockolosky JT, Dougan M, Ingram JR, Ho CC, Kauke MJ, Almo SC, Ploegh HL, Garcia KC. Durable antitumor responses to CD47 blockade require adaptive immune stimulation. Proc Natl Acad Sci U S A. 2016;113(19):E2646-54. Epub 2016/04/20. doi: 10.1073/pnas.1604268113. PubMed PMID: 27091975; PMCID: PMC4868409.
146. Noman MZ, Desantis G, Janji B, Hasmim M, Karray S, Dessen P, Bronte V, Chouaib S. PD-L1 is a novel direct target of HIF-1alpha, and its blockade under hypoxia enhanced MDSC-mediated T cell activation. J Exp Med. 2014;211(5):781-90. Epub 2014/04/30. doi: 10.1084/jem.20131916. PubMed PMID: 24778419; PMCID: PMC4010891.
147. Selby MJ, Engelhardt JJ, Quigley M, Henning KA, Chen T, Srinivasan M, Korman AJ. Anti-CTLA-4 antibodies of IgG2a isotype enhance antitumor activity through reduction of intratumoral regulatory T cells. Cancer Immunol Res. 2013;1(1):32-42. Epub 2014/04/30. doi: 10.1158/2326-6066.CIR-13-0013. PubMed PMID: 24777248.
148. Simpson TR, Li F, Montalvo-Ortiz W, Sepulveda MA, Bergerhoff K, Arce F, Roddie C, Henry JY, Yagita H, Wolchok JD, Peggs KS, Ravetch JV, Allison JP, Quezada SA. Fc-dependent depletion of tumor-infiltrating regulatory T cells co-defines the efficacy of anti-CTLA-4 therapy against melanoma. J Exp Med. 2013;210(9):1695-710. Epub 2013/07/31. doi: 10.1084/jem.20130579. PubMed PMID: 23897981; PMCID: PMC3754863.
149. Neoptolemos JP. Adjuvant treatment of pancreatic cancer. Eur J Cancer. 2011;47 Suppl 3:S378-80. Epub 2011/09/29. doi: 10.1016/S0959-8049(11)70210-6. PubMed PMID: 21944022.
150. Ying H, Dey P, Yao W, Kimmelman AC, Draetta GF, Maitra A, DePinho RA. Genetics and biology of pancreatic ductal adenocarcinoma. Genes Dev. 2016;30(4):355-85. Epub 2016/02/18. doi: 10.1101/gad.275776.115. PubMed PMID: 26883357; PMCID: PMC4762423.
151. Hruban RH, Maitra A, Kern SE, Goggins M. Precursors to pancreatic cancer. Gastroenterol Clin North Am. 2007;36(4):831-49, vi. Epub 2007/11/13. doi: 10.1016/j.gtc.2007.08.012. PubMed PMID: 17996793; PMCID: PMC2194627.
152. Kloppel G. Mixed exocrine-endocrine tumors of the pancreas. Semin Diagn Pathol. 2000;17(2):104-8. Epub 2000/06/06. PubMed PMID: 10839610.
153. Hruban RH, Takaori K, Klimstra DS, Adsay NV, Albores-Saavedra J, Biankin AV, Biankin SA, Compton C, Fukushima N, Furukawa T, Goggins M, Kato Y, Kloppel G, Longnecker DS, Luttges J, Maitra A, Offerhaus GJ, Shimizu M, Yonezawa S. An illustrated consensus on the classification of pancreatic intraepithelial neoplasia and intraductal papillary mucinous neoplasms. Am J Surg Pathol. 2004;28(8):977-87. Epub 2004/07/15. PubMed PMID: 15252303.
154. Sipos B, Frank S, Gress T, Hahn S, Kloppel G. Pancreatic intraepithelial neoplasia revisited and updated. Pancreatology. 2009;9(1-2):45-54. Epub 2008/12/17. doi: 10.1159/000178874. PubMed PMID: 19077454.

155. Basturk O, Hong SM, Wood LD, Adsay NV, Albores-Saavedra J, Biankin AV, Brosens LA, Fukushima N, Goggins M, Hruban RH, Kato Y, Klimstra DS, Kloppel G, Krasinskas A, Longnecker DS, Matthaei H, Offerhaus GJ, Shimizu M, Takaori K, Terris B, Yachida S, Esposito I, Furukawa T, Baltimore Consensus M. A Revised Classification System and Recommendations From the Baltimore Consensus Meeting for Neoplastic Precursor Lesions in the Pancreas. Am J Surg Pathol. 2015;39(12):1730-41. Epub 2015/11/13. doi: 10.1097/PAS.0000000000000533. PubMed PMID: 26559377; PMCID: PMC4646710.

156. Adsay NV, Adair CF, Heffess CS, Klimstra DS. Intraductal oncocytic papillary neoplasms of the pancreas. Am J Surg Pathol. 1996;20(8):980-94. Epub 1996/08/01. PubMed PMID: 8712298.

157. Furukawa T, Kloppel G, Volkan Adsay N, Albores-Saavedra J, Fukushima N, Horii A, Hruban RH, Kato Y, Klimstra DS, Longnecker DS, Luttges J, Offerhaus GJ, Shimizu M, Sunamura M, Suriawinata A, Takaori K, Yonezawa S. Classification of types of intraductal papillary-mucinous neoplasm of the pancreas: a consensus study. Virchows Arch. 2005;447(5):794-9. Epub 2005/08/10. doi: 10.1007/s00428-005-0039-7. PubMed PMID: 16088402.

158. Nakamura A, Horinouchi M, Goto M, Nagata K, Sakoda K, Takao S, Imai K, Kim YS, Sato E, Yonezawa S. New classification of pancreatic intraductal papillary-mucinous tumour by mucin expression: its relationship with potential for malignancy. J Pathol. 2002;197(2):201-10. Epub 2002/05/17. doi: 10.1002/path.1109. PubMed PMID: 12015744.

159. Metz DC, Jensen RT. Gastrointestinal neuroendocrine tumors: pancreatic endocrine tumors. Gastroenterology. 2008;135(5):1469-92. Epub 2008/08/16. doi: 10.1053/j.gastro.2008.05.047. PubMed PMID: 18703061; PMCID: PMC2612755.

160. Theocharis AD, Tsara ME, Papageorgacopoulou N, Karavias DD, Theocharis DA. Pancreatic carcinoma is characterized by elevated content of hyaluronan and chondroitin sulfate with altered disaccharide composition. Biochim Biophys Acta. 2000;1502(2):201-6. Epub 2000/10/21. PubMed PMID: 11040445.

161. Provenzano PP, Cuevas C, Chang AE, Goel VK, Von Hoff DD, Hingorani SR. Enzymatic targeting of the stroma ablates physical barriers to treatment of pancreatic ductal adenocarcinoma. Cancer Cell. 2012;21(3):418-29. Epub 2012/03/24. doi: 10.1016/j.ccr.2012.01.007. PubMed PMID: 22439937; PMCID: PMC3371414.

162. Jacobetz MA, Chan DS, Neesse A, Bapiro TE, Cook N, Frese KK, Feig C, Nakagawa T, Caldwell ME, Zecchini HI, Lolkema MP, Jiang P, Kultti A, Thompson CB, Maneval DC, Jodrell DI, Frost GI, Shepard HM, Skepper JN, Tuveson DA. Hyaluronan impairs vascular function and drug delivery in a mouse model of pancreatic cancer. Gut. 2013;62(1):112-20. Epub 2012/04/03. doi: 10.1136/gutjnl-2012-302529. PubMed PMID: 22466618; PMCID: PMC3551211.

163. Von Hoff DD, Ervin T, Arena FP, Chiorean EG, Infante J, Moore M, Seay T, Tjulandin SA, Ma WW, Saleh MN, Harris M, Reni M, Dowden S, Laheru D, Bahary N, Ramanathan RK, Tabernero J, Hidalgo M, Goldstein D, Van Cutsem E, Wei X, Iglesias J, Renschler MF. Increased survival in pancreatic cancer with nab-paclitaxel plus gemcitabine. N Engl J Med. 2013;369(18):1691-703. Epub 2013/10/18. doi: 10.1056/NEJMoa1304369. PubMed PMID: 24131140; PMCID: PMC4631139.

164. Stromnes IM, DelGiorno KE, Greenberg PD, Hingorani SR. Stromal reengineering to treat pancreas cancer. Carcinogenesis. 2014;35(7):1451-60. Epub 2014/06/09. doi: 10.1093/carcin/bgu115. PubMed PMID: 24908682; PMCID: PMC4076816.

165. Bachem MG, Schunemann M, Ramadani M, Siech M, Beger H, Buck A, Zhou S, Schmid-Kotsas A, Adler G. Pancreatic carcinoma cells induce fibrosis by stimulating proliferation and matrix synthesis of stellate cells. Gastroenterology. 2005;128(4):907-21. Epub 2005/04/13. PubMed PMID: 15825074.

166. Olive KP, Jacobetz MA, Davidson CJ, Gopinathan A, McIntyre D, Honess D, Madhu B, Goldgraben MA, Caldwell ME, Allard D, Frese KK, Denicola G, Feig C, Combs C, Winter SP, Ireland-Zecchini H, Reichelt S, Howat WJ, Chang A, Dhara M, Wang L, Ruckert F, Grutzmann R, Pilarsky C, Izeradjene K, Hingorani SR, Huang P, Davies SE, Plunkett W, Egorin M, Hruban RH, Whitebread N, McGovern K, Adams J, Iacobuzio-Donahue C, Griffiths J, Tuveson DA. Inhibition of Hedgehog signaling enhances delivery of chemotherapy in a mouse model of pancreatic cancer. Science. 2009;324(5933):1457-61. Epub 2009/05/23. doi: 10.1126/science.1171362. PubMed PMID: 19460966; PMCID: PMC2998180.

167. Diaz-Montero CM, Salem ML, Nishimura MI, Garrett-Mayer E, Cole DJ, Montero AJ. Increased circulating myeloid-derived suppressor cells correlate with clinical cancer stage, metastatic tumor burden, and doxorubicin-cyclophosphamide chemotherapy. Cancer Immunol Immunother. 2009;58(1):49-59. Epub 2008/05/01. doi: 10.1007/s00262-008-0523-4. PubMed PMID: 18446337; PMCID: PMC3401888.

168. Porembka MR, Mitchem JB, Belt BA, Hsieh CS, Lee HM, Herndon J, Gillanders WE, Linehan DC, Goedegebuure P. Pancreatic adenocarcinoma induces bone marrow mobilization of myeloid-derived suppressor cells which promote primary tumor growth. Cancer Immunol Immunother. 2012;61(9):1373-85. Epub 2012/01/05. doi: 10.1007/s00262-011-1178-0. PubMed PMID: 22215137; PMCID: PMC3697836.

169. Stromnes IM, Brockenbrough JS, Izeradjene K, Carlson MA, Cuevas C, Simmons RM, Greenberg PD, Hingorani SR. Targeted depletion of an MDSC subset unmasks pancreatic ductal adenocarcinoma to adaptive immunity. Gut. 2014;63(11):1769-81. Epub 2014/02/22. doi: 10.1136/gutjnl-2013-306271. PubMed PMID: 24555999; PMCID: PMC4340484.

170. Sanford DE, Porembka MR, Panni RZ, Mitchem JB, Belt BA, Plambeck-Suess SM, Lin G, Denardo DG, Fields RC, Hawkins WG, Strasberg SM, Lockhart AC, Wang-Gillam A, Goedegebuure SP, Linehan DC. A Study of Zoledronic Acid as Neo-Adjuvant, Perioperative Therapy in Patients with Resectable Pancreatic Ductal Adenocarcinoma. J Cancer Ther. 2013;4(3):797-803. Epub 2013/10/04. doi: 10.4236/jct.2013.43096. PubMed PMID: 24089656; PMCID: PMC3786568.

171. Hiraoka N, Onozato K, Kosuge T, Hirohashi S. Prevalence of FOXP3+ regulatory T cells increases during the progression of pancreatic ductal adenocarcinoma and its premalignant lesions. Clin Cancer Res. 2006;12(18):5423-34. Epub 2006/09/27. doi: 10.1158/1078-0432.CCR-06-0369. PubMed PMID: 17000676.

172. Liyanage UK, Goedegebuure PS, Moore TT, Viehl CT, Moo-Young TA, Larson JW, Frey DM, Ehlers JP, Eberlein TJ, Linehan DC. Increased prevalence of regulatory T cells (Treg) is induced by pancreas adenocarcinoma. J Immunother. 2006;29(4):416-24. Epub 2006/06/27. doi: 10.1097/01.cji.0000205644.43735.4e. PubMed PMID: 16799337.

173. Ino Y, Yamazaki-Itoh R, Shimada K, Iwasaki M, Kosuge T, Kanai Y, Hiraoka N. Immune cell infiltration as an indicator of the immune microenvironment of pancreatic cancer. Br J Cancer. 2013;108(4):914-23. Epub 2013/02/07. doi: 10.1038/bjc.2013.32. PubMed PMID: 23385730; PMCID: PMC3590668.

174. Johansson H, Andersson R, Bauden M, Hammes S, Holdenrieder S, Ansari D. Immune checkpoint therapy for pancreatic cancer. World J Gastroenterol. 2016;22(43):9457-76. Epub 2016/12/07. doi: 10.3748/wjg.v22.i43.9457. PubMed PMID: 27920468; PMCID: PMC5116591.

175. Le DT, Lutz E, Uram JN, Sugar EA, Onners B, Solt S, Zheng L, Diaz LA, Jr., Donehower RC, Jaffee EM, Laheru DA. Evaluation of ipilimumab in combination with allogeneic pancreatic tumor cells transfected with a GM-CSF gene in previously treated pancreatic cancer. J Immunother. 2013;36(7):382-9. Epub 2013/08/09. doi: 10.1097/CJI.0b013e31829fb7a2. PubMed PMID: 23924790; PMCID: PMC3779664.

176. Chmielewski M, Hahn O, Rappl G, Nowak M, Schmidt-Wolf IH, Hombach AA, Abken H. T cells that target carcinoembryonic antigen eradicate orthotopic pancreatic carcinomas without inducing autoimmune colitis in mice. Gastroenterology. 2012;143(4):1095-107 e2. Epub 2012/07/04. doi: 10.1053/j.gastro.2012.06.037. PubMed PMID: 22750462.
177. Maliar A, Servais C, Waks T, Chmielewski M, Lavy R, Altevogt P, Abken H, Eshhar Z. Redirected T cells that target pancreatic adenocarcinoma antigens eliminate tumors and metastases in mice. Gastroenterology. 2012;143(5):1375-84 e1-5. Epub 2012/07/24. doi: 10.1053/j.gastro.2012.07.017. PubMed PMID: 22819865.
178. Carpenito C, Milone MC, Hassan R, Simonet JC, Lakhal M, Suhoski MM, Varela-Rohena A, Haines KM, Heitjan DF, Albelda SM, Carroll RG, Riley JL, Pastan I, June CH. Control of large, established tumor xenografts with genetically retargeted human T cells containing CD28 and CD137 domains. Proc Natl Acad Sci U S A. 2009;106(9):3360-5. Epub 2009/02/13. doi: 10.1073/pnas.0813101106. PubMed PMID: 19211796; PMCID: PMC2651342.
179. Bellone G, Carbone A, Smirne C, Scirelli T, Buffolino A, Novarino A, Stacchini A, Bertetto O, Palestro G, Sorio C, Scarpa A, Emanuelli G, Rodeck U. Cooperative induction of a tolerogenic dendritic cell phenotype by cytokines secreted by pancreatic carcinoma cells. J Immunol. 2006;177(5):3448-60. Epub 2006/08/22. PubMed PMID: 16920987.
180. Hirooka S, Yanagimoto H, Satoi S, Yamamoto T, Toyokawa H, Yamaki S, Yui R, Inoue K, Michiura T, Kwon AH. The role of circulating dendritic cells in patients with unresectable pancreatic cancer. Anticancer Res. 2011;31(11):3827-34. Epub 2011/11/24. PubMed PMID: 22110205.
181. Yamamoto T, Yanagimoto H, Satoi S, Toyokawa H, Yamao J, Kim S, Terakawa N, Takahashi K, Kwon AH. Circulating myeloid dendritic cells as prognostic factors in patients with pancreatic cancer who have undergone surgical resection. J Surg Res. 2012;173(2):299-308. Epub 2011/01/05. doi: 10.1016/j.jss.2010.09.027. PubMed PMID: 21195425.
182. Tjomsland V, Sandstrom P, Spangeus A, Messmer D, Emilsson J, Falkmer U, Falkmer S, Magnusson KE, Borch K, Larsson M. Pancreatic adenocarcinoma exerts systemic effects on the peripheral blood myeloid and plasmacytoid dendritic cells: an indicator of disease severity? BMC Cancer. 2010;10:87. Epub 2010/03/11. doi: 10.1186/1471-2407-10-87. PubMed PMID: 20214814; PMCID: PMC2847547.
183. Hirooka Y, Itoh A, Kawashima H, Hara K, Nonogaki K, Kasugai T, Ohno E, Ishikawa T, Matsubara H, Ishigami M, Katano Y, Ohmiya N, Niwa Y, Yamamoto K, Kaneko T, Nieda M, Yokokawa K, Goto H. A combination therapy of gemcitabine with immunotherapy for patients with inoperable locally advanced pancreatic cancer. Pancreas. 2009;38(3):e69-74. Epub 2009/03/12. doi: 10.1097/MPA.0b013e318197a9e3. PubMed PMID: 19276867.
184. Kimura Y, Tsukada J, Tomoda T, Takahashi H, Imai K, Shimamura K, Sunamura M, Yonemitsu Y, Shimodaira S, Koido S, Homma S, Okamoto M. Clinical and immunologic evaluation of dendritic cell-based immunotherapy in combination with gemcitabine and/or S-1 in patients with advanced pancreatic carcinoma. Pancreas. 2012;41(2):195-205. Epub 2011/07/28. doi: 10.1097/MPA.0b013e31822398c6. PubMed PMID: 21792083.
185. Liou GY, Doppler H, Necela B, Krishna M, Crawford HC, Raimondo M, Storz P. Macrophage-secreted cytokines drive pancreatic acinar-to-ductal metaplasia through NF-kappaB and MMPs. J Cell Biol. 2013;202(3):563-77. Epub 2013/08/07. doi: 10.1083/jcb.201301001. PubMed PMID: 23918941; PMCID: PMC3734091.
186. Mielgo A, Schmid MC. Impact of tumour associated macrophages in pancreatic cancer. BMB Rep. 2013;46(3):131-8. Epub 2013/03/27. PubMed PMID: 23527856; PMCID: PMC4133870.
187. Hu H, Hang JJ, Han T, Zhuo M, Jiao F, Wang LW. The M2 phenotype of tumor-associated macrophages in the stroma confers a poor prognosis in pancreatic cancer. Tumour Biol.

2016;37(7):8657-64. Epub 2016/01/08. doi: 10.1007/s13277-015-4741-z. PubMed PMID: 26738860.

188. Kurahara H, Shinchi H, Mataki Y, Maemura K, Noma H, Kubo F, Sakoda M, Ueno S, Natsugoe S, Takao S. Significance of M2-polarized tumor-associated macrophage in pancreatic cancer. J Surg Res. 2011;167(2):e211-9. Epub 2009/09/22. doi: 10.1016/j.jss.2009.05.026. PubMed PMID: 19765725.

189. Meng F, Li C, Li W, Gao Z, Guo K, Song S. Interaction between pancreatic cancer cells and tumor-associated macrophages promotes the invasion of pancreatic cancer cells and the differentiation and migration of macrophages. IUBMB Life. 2014;66(12):835-46. Epub 2015/01/06. doi: 10.1002/iub.1336. PubMed PMID: 25557640.

190. Panni RZ, Linehan DC, DeNardo DG. Targeting tumor-infiltrating macrophages to combat cancer. Immunotherapy. 2013;5(10):1075-87. Epub 2013/10/04. doi: 10.2217/imt.13.102. PubMed PMID: 24088077; PMCID: PMC3867255.

191. Bayne LJ, Beatty GL, Jhala N, Clark CE, Rhim AD, Stanger BZ, Vonderheide RH. Tumor-derived granulocyte-macrophage colony-stimulating factor regulates myeloid inflammation and T cell immunity in pancreatic cancer. Cancer Cell. 2012;21(6):822-35. Epub 2012/06/16. doi: 10.1016/j.ccr.2012.04.025. PubMed PMID: 22698406; PMCID: PMC3575028.

192. Hermano E, Meirovitz A, Meir K, Nussbaum G, Appelbaum L, Peretz T, Elkin M. Macrophage polarization in pancreatic carcinoma: role of heparanase enzyme. J Natl Cancer Inst. 2014;106(12). Epub 2014/10/19. doi: 10.1093/jnci/dju332. PubMed PMID: 25326645; PMCID: PMC4334800.

193. Feig C, Gopinathan A, Neesse A, Chan DS, Cook N, Tuveson DA. The pancreas cancer microenvironment. Clin Cancer Res. 2012;18(16):4266-76. Epub 2012/08/17. doi: 10.1158/1078-0432.CCR-11-3114. PubMed PMID: 22896693; PMCID: PMC3442232.

194. Lewis CE, Hughes R. Inflammation and breast cancer. Microenvironmental factors regulating macrophage function in breast tumours: hypoxia and angiopoietin-2. Breast Cancer Res. 2007;9(3):209. Epub 2007/07/03. doi: 10.1186/bcr1679. PubMed PMID: 17601353; PMCID: PMC1929095.

195. Forget MA, Voorhees JL, Cole SL, Dakhlallah D, Patterson IL, Gross AC, Moldovan L, Mo X, Evans R, Marsh CB, Eubank TD. Macrophage colony-stimulating factor augments Tie2-expressing monocyte differentiation, angiogenic function, and recruitment in a mouse model of breast cancer. PLoS One. 2014;9(6):e98623. Epub 2014/06/04. doi: 10.1371/journal.pone.0098623. PubMed PMID: 24892425; PMCID: PMC4043882.

196. Jinushi M, Chiba S, Yoshiyama H, Masutomi K, Kinoshita I, Dosaka-Akita H, Yagita H, Takaoka A, Tahara H. Tumor-associated macrophages regulate tumorigenicity and anticancer drug responses of cancer stem/initiating cells. Proc Natl Acad Sci U S A. 2011;108(30):12425-30. Epub 2011/07/13. doi: 10.1073/pnas.1106645108. PubMed PMID: 21746895; PMCID: PMC3145680.

197. Mitchem JB, Brennan DJ, Knolhoff BL, Belt BA, Zhu Y, Sanford DE, Belaygorod L, Carpenter D, Collins L, Piwnica-Worms D, Hewitt S, Udupi GM, Gallagher WM, Wegner C, West BL, Wang-Gillam A, Goedegebuure P, Linehan DC, DeNardo DG. Targeting tumor-infiltrating macrophages decreases tumor-initiating cells, relieves immunosuppression, and improves chemotherapeutic responses. Cancer Res. 2013;73(3):1128-41. Epub 2012/12/12. doi: 10.1158/0008-5472.CAN-12-2731. PubMed PMID: 23221383; PMCID: PMC3563931.

198. Funamizu N, Hu C, Lacy C, Schetter A, Zhang G, He P, Gaedcke J, Ghadimi MB, Ried T, Yfantis HG, Lee DH, Subleski J, Chan T, Weiss JM, Back TC, Yanaga K, Hanna N, Alexander HR, Maitra A, Hussain SP. Macrophage migration inhibitory factor induces epithelial to mesenchymal transition, enhances tumor aggressiveness and predicts clinical outcome in resected pancreatic

ductal adenocarcinoma. Int J Cancer. 2013;132(4):785-94. Epub 2012/07/24. doi: 10.1002/ijc.27736. PubMed PMID: 22821831; PMCID: PMC3488363.
199. Kurahara H, Takao S, Maemura K, Mataki Y, Kuwahata T, Maeda K, Sakoda M, Iino S, Ishigami S, Ueno S, Shinchi H, Natsugoe S. M2-polarized tumor-associated macrophage infiltration of regional lymph nodes is associated with nodal lymphangiogenesis and occult nodal involvement in pN0 pancreatic cancer. Pancreas. 2013;42(1):155-9. Epub 2012/06/16. doi: 10.1097/MPA.0b013e318254f2d1. PubMed PMID: 22699204.
200. Gabrilovich DI, Nagaraj S. Myeloid-derived suppressor cells as regulators of the immune system. Nat Rev Immunol. 2009;9(3):162-74. Epub 2009/02/07. doi: 10.1038/nri2506. PubMed PMID: 19197294; PMCID: PMC2828349.
201. Sanford DE, Belt BA, Panni RZ, Mayer A, Deshpande AD, Carpenter D, Mitchem JB, Plambeck-Suess SM, Worley LA, Goetz BD, Wang-Gillam A, Eberlein TJ, Denardo DG, Goedegebuure SP, Linehan DC. Inflammatory monocyte mobilization decreases patient survival in pancreatic cancer: a role for targeting the CCL2/CCR2 axis. Clin Cancer Res. 2013;19(13):3404-15. Epub 2013/05/09. doi: 10.1158/1078-0432.CCR-13-0525. PubMed PMID: 23653148; PMCID: PMC3700620.
202. Cui R, Yue W, Lattime EC, Stein MN, Xu Q, Tan XL. Targeting tumor-associated macrophages to combat pancreatic cancer. Oncotarget. 2016;7(31):50735-54. Epub 2016/05/19. doi: 10.18632/oncotarget.9383. PubMed PMID: 27191744; PMCID: PMC5226617.
203. Zhu Y, Knolhoff BL, Meyer MA, Nywening TM, West BL, Luo J, Wang-Gillam A, Goedegebuure SP, Linehan DC, DeNardo DG. CSF1/CSF1R blockade reprograms tumor-infiltrating macrophages and improves response to T-cell checkpoint immunotherapy in pancreatic cancer models. Cancer Res. 2014;74(18):5057-69. Epub 2014/08/02. doi: 10.1158/0008-5472.CAN-13-3723. PubMed PMID: 25082815; PMCID: PMC4182950.
204. Borrow P, Tough DF, Eto D, Tishon A, Grewal IS, Sprent J, Flavell RA, Oldstone MB. CD40 ligand-mediated interactions are involved in the generation of memory CD8(+) cytotoxic T lymphocytes (CTL) but are not required for the maintenance of CTL memory following virus infection. J Virol. 1998;72(9):7440-9. Epub 1998/08/08. PubMed PMID: 9696840; PMCID: PMC109974.
205. Elliott MR, Ravichandran KS. Clearance of apoptotic cells: implications in health and disease. J Cell Biol. 2010;189(7):1059-70. Epub 2010/06/30. doi: 10.1083/jcb.201004096. PubMed PMID: 20584912; PMCID: PMC2894449.
206. Ravichandran KS. Find-me and eat-me signals in apoptotic cell clearance: progress and conundrums. J Exp Med. 2010;207(9):1807-17. Epub 2010/09/02. doi: 10.1084/jem.20101157. PubMed PMID: 20805564; PMCID: PMC2931173.
207. Juncadella IJ, Kadl A, Sharma AK, Shim YM, Hochreiter-Hufford A, Borish L, Ravichandran KS. Apoptotic cell clearance by bronchial epithelial cells critically influences airway inflammation. Nature. 2013;493(7433):547-51. Epub 2012/12/14. doi: 10.1038/nature11714. PubMed PMID: 23235830; PMCID: PMC3662023.
208. Elliott MR, Chekeni FB, Trampont PC, Lazarowski ER, Kadl A, Walk SF, Park D, Woodson RI, Ostankovich M, Sharma P, Lysiak JJ, Harden TK, Leitinger N, Ravichandran KS. Nucleotides released by apoptotic cells act as a find-me signal to promote phagocytic clearance. Nature. 2009;461(7261):282-6. Epub 2009/09/11. doi: 10.1038/nature08296. PubMed PMID: 19741708; PMCID: PMC2851546.
209. Ravichandran KS. Beginnings of a good apoptotic meal: the find-me and eat-me signaling pathways. Immunity. 2011;35(4):445-55. Epub 2011/11/01. doi: 10.1016/j.immuni.2011.09.004. PubMed PMID: 22035837; PMCID: PMC3241945.

210. Hochreiter-Hufford A, Ravichandran KS. Clearing the dead: apoptotic cell sensing, recognition, engulfment, and digestion. Cold Spring Harb Perspect Biol. 2013;5(1):a008748. Epub 2013/01/04. doi: 10.1101/cshperspect.a008748. PubMed PMID: 23284042; PMCID: PMC3579390.
211. Zhang M, Hutter G, Kahn SA, Azad TD, Gholamin S, Xu CY, Liu J, Achrol AS, Richard C, Sommerkamp P, Schoen MK, McCracken MN, Majeti R, Weissman I, Mitra SS, Cheshier SH. Anti-CD47 Treatment Stimulates Phagocytosis of Glioblastoma by M1 and M2 Polarized Macrophages and Promotes M1 Polarized Macrophages In Vivo. PLoS One. 2016;11(4):e0153550. Epub 2016/04/20. doi: 10.1371/journal.pone.0153550. PubMed PMID: 27092773; PMCID: PMC4836698.
212. Riento K, Ridley AJ. Rocks: multifunctional kinases in cell behaviour. Nat Rev Mol Cell Biol. 2003;4(6):446-56. Epub 2003/06/05. doi: 10.1038/nrm1128. PubMed PMID: 12778124.
213. Erwig LP, Henson PM. Clearance of apoptotic cells by phagocytes. Cell Death Differ. 2008;15(2):243-50. Epub 2007/06/16. doi: 10.1038/sj.cdd.4402184. PubMed PMID: 17571081.
214. Miki H, Suetsugu S, Takenawa T. WAVE, a novel WASP-family protein involved in actin reorganization induced by Rac. EMBO J. 1998;17(23):6932-41. Epub 1998/12/08. doi: 10.1093/emboj/17.23.6932. PubMed PMID: 9843499; PMCID: PMC1171041.
215. Castellano F, Montcourrier P, Chavrier P. Membrane recruitment of Rac1 triggers phagocytosis. J Cell Sci. 2000;113 (Pt 17):2955-61. Epub 2000/08/10. PubMed PMID: 10934035.
216. Wu YC, Horvitz HR. The C. elegans cell corpse engulfment gene ced-7 encodes a protein similar to ABC transporters. Cell. 1998;93(6):951-60. Epub 1998/07/11. PubMed PMID: 9635425.
217. Schrijvers DM, De Meyer GR, Kockx MM, Herman AG, Martinet W. Phagocytosis of apoptotic cells by macrophages is impaired in atherosclerosis. Arterioscler Thromb Vasc Biol. 2005;25(6):1256-61. Epub 2005/04/16. doi: 10.1161/01.ATV.0000166517.18801.a7. PubMed PMID: 15831805.
218. Park D, Han CZ, Elliott MR, Kinchen JM, Trampont PC, Das S, Collins S, Lysiak JJ, Hoehn KL, Ravichandran KS. Continued clearance of apoptotic cells critically depends on the phagocyte Ucp2 protein. Nature. 2011;477(7363):220-4. Epub 2011/08/23. doi: 10.1038/nature10340. PubMed PMID: 21857682; PMCID: PMC3513690.
219. Kinchen JM, Doukoumetzidis K, Almendinger J, Stergiou L, Tosello-Trampont A, Sifri CD, Hengartner MO, Ravichandran KS. A pathway for phagosome maturation during engulfment of apoptotic cells. Nat Cell Biol. 2008;10(5):556-66. Epub 2008/04/22. doi: 10.1038/ncb1718. PubMed PMID: 18425118; PMCID: PMC2851549.
220. Kinchen JM, Ravichandran KS. Phagosome maturation: going through the acid test. Nat Rev Mol Cell Biol. 2008;9(10):781-95. Epub 2008/09/25. doi: 10.1038/nrm2515. PubMed PMID: 18813294; PMCID: PMC2908392.
221. Kitano M, Nakaya M, Nakamura T, Nagata S, Matsuda M. Imaging of Rab5 activity identifies essential regulators for phagosome maturation. Nature. 2008;453(7192):241-5. Epub 2008/04/04. doi: 10.1038/nature06857. PubMed PMID: 18385674.
222. Kinchen JM, Ravichandran KS. Identification of two evolutionarily conserved genes regulating processing of engulfed apoptotic cells. Nature. 2010;464(7289):778-82. Epub 2010/03/23. doi: 10.1038/nature08853. PubMed PMID: 20305638; PMCID: PMC2901565.
223. Martinez J, Almendinger J, Oberst A, Ness R, Dillon CP, Fitzgerald P, Hengartner MO, Green DR. Microtubule-associated protein 1 light chain 3 alpha (LC3)-associated phagocytosis is required for the efficient clearance of dead cells. Proc Natl Acad Sci U S A. 2011;108(42):17396-401. Epub 2011/10/05. doi: 10.1073/pnas.1113421108. PubMed PMID: 21969579; PMCID: PMC3198353.

224. Martinez J, Malireddi RK, Lu Q, Cunha LD, Pelletier S, Gingras S, Orchard R, Guan JL, Tan H, Peng J, Kanneganti TD, Virgin HW, Green DR. Molecular characterization of LC3-associated phagocytosis reveals distinct roles for Rubicon, NOX2 and autophagy proteins. Nat Cell Biol. 2015;17(7):893-906. Epub 2015/06/23. doi: 10.1038/ncb3192. PubMed PMID: 26098576; PMCID: PMC4612372.
225. Henson PM. Cell Removal: Efferocytosis. Annu Rev Cell Dev Biol. 2017;33:127-44. Epub 2017/06/15. doi: 10.1146/annurev-cellbio-111315-125315. PubMed PMID: 28613937.
226. Erwig LP, McPhilips KA, Wynes MW, Ivetic A, Ridley AJ, Henson PM. Differential regulation of phagosome maturation in macrophages and dendritic cells mediated by Rho GTPases and ezrin-radixin-moesin (ERM) proteins. Proc Natl Acad Sci U S A. 2006;103(34):12825-30. Epub 2006/08/16. doi: 10.1073/pnas.0605331103. PubMed PMID: 16908865; PMCID: PMC1568932.
227. Desch AN, Randolph GJ, Murphy K, Gautier EL, Kedl RM, Lahoud MH, Caminschi I, Shortman K, Henson PM, Jakubzick CV. CD103+ pulmonary dendritic cells preferentially acquire and present apoptotic cell-associated antigen. J Exp Med. 2011;208(9):1789-97. Epub 2011/08/24. doi: 10.1084/jem.20110538. PubMed PMID: 21859845; PMCID: PMC3171085.
228. N AG, Bensinger SJ, Hong C, Beceiro S, Bradley MN, Zelcer N, Deniz J, Ramirez C, Diaz M, Gallardo G, de Galarreta CR, Salazar J, Lopez F, Edwards P, Parks J, Andujar M, Tontonoz P, Castrillo A. Apoptotic cells promote their own clearance and immune tolerance through activation of the nuclear receptor LXR. Immunity. 2009;31(2):245-58. Epub 2009/08/04. doi: 10.1016/j.immuni.2009.06.018. PubMed PMID: 19646905; PMCID: PMC2791787.
229. Schif-Zuck S, Gross N, Assi S, Rostoker R, Serhan CN, Ariel A. Saturated-efferocytosis generates pro-resolving CD11b low macrophages: modulation by resolvins and glucocorticoids. Eur J Immunol. 2011;41(2):366-79. Epub 2011/01/27. doi: 10.1002/eji.201040801. PubMed PMID: 21268007; PMCID: PMC3082320.
230. Martin CJ, Peters KN, Behar SM. Macrophages clean up: efferocytosis and microbial control. Curr Opin Microbiol. 2014;17:17-23. Epub 2014/03/04. doi: 10.1016/j.mib.2013.10.007. PubMed PMID: 24581688; PMCID: PMC3942671.
231. Behar SM, Divangahi M, Remold HG. Evasion of innate immunity by Mycobacterium tuberculosis: is death an exit strategy? Nat Rev Microbiol. 2010;8(9):668-74. Epub 2010/08/03. doi: 10.1038/nrmicro2387. PubMed PMID: 20676146; PMCID: PMC3221965.
232. Martin CJ, Booty MG, Rosebrock TR, Nunes-Alves C, Desjardins DM, Keren I, Fortune SM, Remold HG, Behar SM. Efferocytosis is an innate antibacterial mechanism. Cell Host Microbe. 2012;12(3):289-300. Epub 2012/09/18. doi: 10.1016/j.chom.2012.06.010. PubMed PMID: 22980326; PMCID: PMC3517204.
233. Vergne I, Chua J, Lee HH, Lucas M, Belisle J, Deretic V. Mechanism of phagolysosome biogenesis block by viable Mycobacterium tuberculosis. Proc Natl Acad Sci U S A. 2005;102(11):4033-8. Epub 2005/03/09. doi: 10.1073/pnas.0409716102. PubMed PMID: 15753315; PMCID: PMC554822.
234. Vergne I, Fratti RA, Hill PJ, Chua J, Belisle J, Deretic V. Mycobacterium tuberculosis phagosome maturation arrest: mycobacterial phosphatidylinositol analog phosphatidylinositol mannoside stimulates early endosomal fusion. Mol Biol Cell. 2004;15(2):751-60. Epub 2003/11/18. doi: 10.1091/mbc.E03-05-0307. PubMed PMID: 14617817; PMCID: PMC329390.
235. Linton MF, Babaev VR, Huang J, Linton EF, Tao H, Yancey PG. Macrophage Apoptosis and Efferocytosis in the Pathogenesis of Atherosclerosis. Circ J. 2016;80(11):2259-68. Epub 2016/10/28. doi: 10.1253/circj.CJ-16-0924. PubMed PMID: 27725526; PMCID: PMC5459487.
236. Colin S, Chinetti-Gbaguidi G, Staels B. Macrophage phenotypes in atherosclerosis. Immunol Rev. 2014;262(1):153-66. Epub 2014/10/17. doi: 10.1111/imr.12218. PubMed PMID: 25319333.

237. Gordon SR, Maute RL, Dulken BW, Hutter G, George BM, McCracken MN, Gupta R, Tsai JM, Sinha R, Corey D, Ring AM, Connolly AJ, Weissman IL. PD-1 expression by tumour-associated macrophages inhibits phagocytosis and tumour immunity. Nature. 2017;545(7655):495-9. Epub 2017/05/18. doi: 10.1038/nature22396. PubMed PMID: 28514441.
238. Cook RS, Jacobsen KM, Wofford AM, DeRyckere D, Stanford J, Prieto AL, Redente E, Sandahl M, Hunter DM, Strunk KE, Graham DK, Earp HS, 3rd. MerTK inhibition in tumor leukocytes decreases tumor growth and metastasis. J Clin Invest. 2013;123(8):3231-42. Epub 2013/07/23. doi: 10.1172/JCI67655. PubMed PMID: 23867499; PMCID: PMC3726162.
239. Yin Y, Huang X, Lynn KD, Thorpe PE. Phosphatidylserine-targeting antibody induces M1 macrophage polarization and promotes myeloid-derived suppressor cell differentiation. Cancer Immunol Res. 2013;1(4):256-68. Epub 2014/04/30. doi: 10.1158/2326-6066.CIR-13-0073. PubMed PMID: 24777853.
240. Birge RB, Boeltz S, Kumar S, Carlson J, Wanderley J, Calianese D, Barcinski M, Brekken RA, Huang X, Hutchins JT, Freimark B, Empig C, Mercer J, Schroit AJ, Schett G, Herrmann M. Phosphatidylserine is a global immunosuppressive signal in efferocytosis, infectious disease, and cancer. Cell Death Differ. 2016;23(6):962-78. Epub 2016/02/27. doi: 10.1038/cdd.2016.11. PubMed PMID: 26915293; PMCID: PMC4987730.
241. Roy S, Bag AK, Singh RK, Talmadge JE, Batra SK, Datta K. Multifaceted Role of Neuropilins in the Immune System: Potential Targets for Immunotherapy. Frontiers in Immunology. 2017;8(1228). doi: 10.3389/fimmu.2017.01228.
242. Dutta S, Roy S, Polavaram NS, Stanton MJ, Zhang H, Bhola T, Honscheid P, Donohue TM, Jr., Band H, Batra SK, Muders MH, Datta K. Neuropilin-2 Regulates Endosome Maturation and EGFR Trafficking to Support Cancer Cell Pathobiology. Cancer Res. 2016;76(2):418-28. Epub 2015/11/13. doi: 10.1158/0008-5472.CAN-15-1488. PubMed PMID: 26560516; PMCID: PMC4715955.
243. Carr RM, Fernandez-Zapico ME. Pancreatic cancer microenvironment, to target or not to target? EMBO Mol Med. 2016;8(2):80-2. Epub 2016/01/10. doi: 10.15252/emmm.201505948. PubMed PMID: 26747091; PMCID: PMC4734844.
244. Nielsen MF, Mortensen MB, Detlefsen S. Key players in pancreatic cancer-stroma interaction: Cancer-associated fibroblasts, endothelial and inflammatory cells. World J Gastroenterol. 2016;22(9):2678-700. Epub 2016/03/15. doi: 10.3748/wjg.v22.i9.2678. PubMed PMID: 26973408; PMCID: PMC4777992.
245. Waghray M, Yalamanchili M, di Magliano MP, Simeone DM. Deciphering the role of stroma in pancreatic cancer. Curr Opin Gastroenterol. 2013;29(5):537-43. Epub 2013/07/31. doi: 10.1097/MOG.0b013e328363affe. PubMed PMID: 23892539; PMCID: PMC4112589.
246. Cassetta L, Noy R, Swierczak A, Sugano G, Smith H, Wiechmann L, Pollard JW. Isolation of Mouse and Human Tumor-Associated Macrophages. Adv Exp Med Biol. 2016;899:211-29. Epub 2016/06/22. doi: 10.1007/978-3-319-26666-4_12. PubMed PMID: 27325269; PMCID: PMC5024544.
247. Martinez FO, Gordon S. The M1 and M2 paradigm of macrophage activation: time for reassessment. F1000Prime Rep. 2014;6:13. Epub 2014/03/29. doi: 10.12703/P6-13. PubMed PMID: 24669294; PMCID: PMC3944738.
248. Flannagan RS, Heit B, Heinrichs DE. Antimicrobial Mechanisms of Macrophages and the Immune Evasion Strategies of Staphylococcus aureus. Pathogens. 2015;4(4):826-68. Epub 2015/12/04. doi: 10.3390/pathogens4040826. PubMed PMID: 26633519; PMCID: PMC4693167.
249. Jakubzick CV, Randolph GJ, Henson PM. Monocyte differentiation and antigen-presenting functions. Nat Rev Immunol. 2017;17(6):349-62. Epub 2017/04/25. doi: 10.1038/nri.2017.28. PubMed PMID: 28436425.

250. Nair-Gupta P, Baccarini A, Tung N, Seyffer F, Florey O, Huang Y, Banerjee M, Overholtzer M, Roche PA, Tampe R, Brown BD, Amsen D, Whiteheart SW, Blander JM. TLR signals induce phagosomal MHC-I delivery from the endosomal recycling compartment to allow cross-presentation. Cell. 2014;158(3):506-21. Epub 2014/08/02. doi: 10.1016/j.cell.2014.04.054. PubMed PMID: 25083866; PMCID: PMC4212008.
251. Naqvi AR, Fordham JB, Nares S. miR-24, miR-30b, and miR-142-3p regulate phagocytosis in myeloid inflammatory cells. J Immunol. 2015;194(4):1916-27. Epub 2015/01/21. doi: 10.4049/jimmunol.1401893. PubMed PMID: 25601927; PMCID: PMC4323870.
252. Teng MW, Andrews DM, McLaughlin N, von Scheidt B, Ngiow SF, Moller A, Hill GR, Iwakura Y, Oft M, Smyth MJ. IL-23 suppresses innate immune response independently of IL-17A during carcinogenesis and metastasis. Proc Natl Acad Sci U S A. 2010;107(18):8328-33. Epub 2010/04/21. doi: 10.1073/pnas.1003251107. PubMed PMID: 20404142; PMCID: PMC2889517.
253. Anderson AC, Joller N, Kuchroo VK. Lag-3, Tim-3, and TIGIT: Co-inhibitory Receptors with Specialized Functions in Immune Regulation. Immunity. 2016;44(5):989-1004. Epub 2016/05/19. doi: 10.1016/j.immuni.2016.05.001. PubMed PMID: 27192565; PMCID: PMC4942846.
254. Devaud C, Yong CS, John LB, Westwood JA, Duong CP, House CM, Denoyer D, Li J, Darcy PK, Kershaw MH. Foxp3 expression in macrophages associated with RENCA tumors in mice. PLoS One. 2014;9(9):e108670. Epub 2014/09/30. doi: 10.1371/journal.pone.0108670. PubMed PMID: 25264896; PMCID: PMC4180934.
255. Rozali EN, Hato SV, Robinson BW, Lake RA, Lesterhuis WJ. Programmed death ligand 2 in cancer-induced immune suppression. Clin Dev Immunol. 2012;2012:656340. Epub 2012/05/23. doi: 10.1155/2012/656340. PubMed PMID: 22611421; PMCID: PMC3350956.
256. Greenlee-Wacker MC. Clearance of apoptotic neutrophils and resolution of inflammation. Immunol Rev. 2016;273(1):357-70. Epub 2016/08/26. doi: 10.1111/imr.12453. PubMed PMID: 27558346; PMCID: PMC5000862.
257. Meyer J, Arriaga Y, Anandam J, Karri S, Syed S, Verma U, Abdelnaby A, Raja G, Dong Y, Beg M, Balch G. A Phase I Clinical Trial of the Phosphatidylserine-targeting Antibody Bavituximab in Combination With Radiation Therapy and Capecitabine in the Preoperative Treatment of Rectal Adenocarcinoma. Am J Clin Oncol. 2017. Epub 2017/08/02. doi: 10.1097/COC.0000000000000401. PubMed PMID: 28763330.